Abbreviations

bR	bacteriorhodopsin
CD	circular dichroism
c.m.c.	critical micelle concentration
C.S.A.	chemical shift anisotropy (ppm)
Da	Dalton
$\Delta\nu_q$	deuterium quadrupole splitting (Hz)
DMPC	1,2-dimyristoyl-*sn*-glycero-3-phosphocholine
DMPE	1,2-dimyristoyl-*sn*-glycero-3-phosphoethanolamine
DMPG	1,2-dimyristoyl-*sn*-glycero-3-phospho-*rac*-glycerol
DSC	Differential scanning calorimetry
EDTA	diaminoethanetetra-acetic acid
ESR	Electron spin resonance
MeOH	methanol
MDP	methylene diphosphonate (^{31}P-NMR external shft standard)
M_r	molecular weight
NMR	Nuclear magnetic resonance
nsTP	non-specific lipid transfer protein
PC	phosphatidylcholine
PCSL	phosphatidylcholine spin-label
PG	phosphatidyl glycerol
PGP	*H.halobium* 2,3-di-O-phytanyl-*sn*-glycero-1-phosphoryl-3'-*sn*-glycerol-1'-phosphate
PGS	phosphatidylglycerol sulphate
PGSL	phosphatidylglycerol spin-label
PLSL	phospholipid spin-label
PMPL	purple membrane phospholipids
ppm	parts per million (NMR)
PS	phosphatidyl serine
SASL	stearic acid spin-label
SDS	Sodiun dodecyl sulphate
SUV	small unilamellar vesicle
T_c	lipid bilayer main gel-to-liquid crystalline phase transition temperature
T_q	temperature from which samples were quenched for freeze-fracture electron microscopy
TLC	thin layer chromatography
T_1	Spin-lattice relaxation time (NMR)
T_2	Spin-spin relaxation time (NMR)
TEMPO	2,2,6,6-tetramethyl-1-piperidinyloxy
UV/vis	ultra-violet/visible
ν_{ex}	exchange rate

Bacteriorhodopsin/Phospholipid Interactions.

- a study by ^{31}P- and ^{2}H-NMR

Thesis submitted to the

Board of the Faculty of Biological Sciences

in partial fulfilment of the requirements for the

Degree of Doctor of Philosophy

at the University of Oxford



Paul Gale

St Edmund Hall

Oxford

Michaelmas

1988

ABSTRACT.

Bacteriorhodopsin/phospholipid interactions - a ^{31}P and ^{2}H-NMR study.

Paul Gale
St. Edmund Hall.

D.Phil.,
Michaelmas Term, 1988.

Two methods were used to produce exogenous lipid/bR complexes. A detergent method (Huang *et al.*, 1980) reconstituted bR into DMPC or DMPG bilayers, free of all endogenous purple membrane lipids as shown by high resolution ^{31}P-NMR. A novel biological detergent-free method employed bovine liver non-specific lipid transfer protein (nsTP) to mediate addition of DMPC to purple membrane, while retaining 76 - 86% of the endogenous purple membrane phospholipids.

The variations with temperature of ^{2}H-NMR quadrupole splittings for the DMPC choline α- and β-methylene CD_2 segments were similar to those for protein-free lipid (Gally *et al.*, 1975) implying that temperature dependent changes in segmental amplitudes of motion within the choline group are preserved in the presence of bR. Incorporation of small quantities of bR increased the amplitudes of segmental motion within the choline headgroup relative to that of pure lipid, but increasing the bR content induced an ordering effect.

The choline α- and β-methylene segment quadrupole splittings showed a linear variation with protein content at constant temperature. This is consistent with freeze fracture electron microscopy data, which shows the bR particles to be dispersed at all lipid/protein ratios, when quenched from temperatures above the phase transition. Applying a fast two site exchange model to the ^{2}H-NMR data, values between 12 and 15 were calculated for the number of boundary lipids for bR (26,000 M_r) in DMPC bilayers free of purple membrane lipids.

From ESR data, for delipidated bR in DMPC and DMPG bilayers at temperatures above the phase transition, the number of boundary lipids calculated were 18 - 21, which is consistent with the bR being monomeric, as also observed in DMPC bilayers with all the purple membrane lipids retained (Cherry *et al.*, 1978). The purple membrane lipids thus appear to mediate crystallization of the bR particles into a hexagonal lattice at temperatures slightly below the exogenous lipid phase transition.

Contents.

Abstract. ii)

Acknowledgements. viii)

General Introduction ix)
Structure of bacteriorhodopsin and purple membrane from *H.halobium* ix)
Aggregation properties of bacteriorhodopsin in reconstituted lipid systems. x)
Nuclear Magnetic Resonance. xii)
Solid state deuterium NMR and phosphorus-31 NMR techniques for studying lipid bilayer membranes. xiv)
NMR studies of lipid/protein interactions. xvii)
Electron spin resonance of spin-labelled phospholipids. xx)
NMR and ESR timescales. xxii)

Chapter 1. Two methods for producing deuterated-DMPC bacteriorhodopsin lipo-protein complexes suitable for deuterium NMR studies.
1.I). Introduction. 1
1.II). Materials and Analytical Methods. 8
1.III). Methods for producing DMPC/bacteriorhodopsin complexes 10
Production of DMPC/bR complexes using conventional detergent methods. 10
Preparation of natural membranes labelled with deuterated lipids by nsTP. 12
1.IV). Results and Discussion. 14
Production of DMPC/bR complexes using detergents. 14
Analysis of bovine liver non-specific lipid transfer protein. 15
Production of DMPC/bR complexes by nsTP-mediated transfer of DMPC. 16
Mechanism of vesicle formation by nsTP-mediated DMPC transfer. 19
Spectroscopic properties of the chromophores in the two types of complexes. 19

Chapter 2. Characterisation of the DMPC/bR complexes.

2.I). Introduction. 21
2.II). Materials and Methods. 24
2.III). Results. 26
A). Size of vesicles. 26
B). Homogeneity of lipid/protein ratio 27

C). Phospholipid headgroup composition of purple membrane and DMPC/bR complexes by high resolution ^{31}P-NMR. 28
2.IV). Discussion. 35
Vesicle size. 35
Phospholipid headgroup composition of the vesicles. 37
Acquisition of ^{31}P-NMR spectra. 37
Assignment of phospholipid resonances. 38
Quantitative analysis of phospholipid headgroup composition of purple membrane and DMPC/bR complexes. 43
Summary of Chapters 1 and 2. 47

Chapter 3. Bacteriorhodopsin/DMPC interactions in vesicles from which all the endogenous purple membrane lipids have been removed - a 31P and 2H-NMR and electron spin resonance study.

3.I). Introduction. 48
3.II). Materials and Methods. 51
3.III). Results. 53
A). Deuterium NMR. 53
i) Deuterium NMR results for DMPC-d_9/bR complexes produced by the slow cholate removal technique. 54
ii) Deuterium NMR results for DMPC-d_9/bR complexes produced by the fast cholate removal technique. 55
iii) Temperature dependence of ^{2}H-NMR spectra for DMPC-d_9/bR complexes. 55
iv) Effect of temperature on deuterium NMR spectra obtained from the DMPC-d_4-d_9/bR complexes produced by the slow cholate removal procedure. 56
v) Effect of bR content on the choline α- and β-methylene segment powder patterns of DMPC-d_4. 58
vi) Stoichiometry of DMPC/bR interactions as seen by deuterium NMR. 60
B). Phosphorus-31 NMR. 62
i) Effect of small vesicle diameters on the spectral anisotropy of the phosphorus-31 NMR spectra. 62
ii) Effect of protein content on the ^{31}P-NMR spectra of large vesicle complexes. 63
iii) Effect of temperature on the measured ^{31}P-NMR c.s.a.s. 64
iv) Effects of bR on DMPC phosphorus-31 NMR relaxation rates 64
C). TEMPO partitioning. 67
D). ESR studies using spin-labelled phospholipids. 68
i) Effect of the presence of bR on the bulk phase bilayer lipids. 69
ii) Quantitative analysis of the number of boundary lipids per protein by spectral subtraction and simulation. 71
3.IV). Discussion. 74

Chapter 4 The effect of temperature and protein content on the dispersive properties of bR from H.halobium in reconstituted DMPC complexes free of endogenous purple membrane lipids: A freeze fracture electron microscopy study.

4.I) Introduction. 92
4.II). Materials and Methods. 93
4.III).Results. 93
Freeze fracture electron microscopy of DMPC/bR complexes quenched from temperatures below the main phase transition. 93
Freeze fracture electron microscopy of DMPC/bR complexes quenched from temperatures above the main phase transition using different quenching rates. 94
Effect of high ionic strength on the dispersion properties of the bR particles. 95
4.IV) Discussion. 95

Chapter 5. bR/DMPC interactions in vesicles produced by nsTP-mediated addition of DMPC to purple membrane.

5.I) Introduction. 99
5.II) Methods. 102
5.III) Results. 102
A). nsTP-labelled ghosts. 102
i)Deuterium NMR. 102
Broadline deuterium-NMR spectra of DMPC-d9 in erythrocyte ghosts. 102
Effect of temperature on the measured quadrupole splittings. 102
B).nsTP-labelled purple membrane. 104
i) Gel-to-liquid crystal phase transitions for nsTP-produced complexes as determined by TEMPO partitioning. 104
ii) Broadline phosphorus-31 NMR. 105
^{31}P-NMR spectra are two component but typical of phospholipids in a bilayer conformation. 105
Effect of the presence of saturated NaCl in the aqueous environment on ^{31}P-NMR spectra. 107
Effect of vesicle packing on the ^{31}P-NMR spectra. 107
Effect of protein content on the magnitude of the ^{31}P-NMR c.s.a.s. 107
Dynamics of the phosphate moieties in the nsTP-produced complexes. 108
iii) Broadline deuterium NMR. 109
Temperature dependencies of DMPC-d_9 quadrupole splittings as a means to investigate temperature-dependent aggregation dispersion of bacteriorhodopsin. 109
Effect of protein content on the DMPC-d_9 spectra at different temperatures. 111
Stoichiometry of DMPC/bR interactions. 111
Effect of saturated NaCl on the deuterium NMR DMPC-d^9 data. 114

Deuterium NMR spectra from DMPC-d_4 incorporated into purple membrane by nsTP. 115
Effect of temperature on the DMPC-d_4 quadrupole splittings. 116
Effect of bR content on the deuterium NMR spectra of DMPC-d_4 in nsTP-produced complexes. 117
Comparison of deuterium NMR spectra from DMPC-d_4-d_9/bR complexes produced by the nsTP technique with those of similar protein contents produced by detergent techniques. 118
Comparison of temperature sensitivities for DMPC-d_4 quadrupole splittings in complexes produced by the two different techniques. 119
iv) Freeze fracture electron microscopy. 119
5.IV) Discussion. 120

Chapter 6. Studies of bacteriorhodopsin dispersion properties in the synthetic phospholipid DMPG, with all endogenous purple membrane lipids removed.

6.I). Introduction. 127
6.II). Materials and Methods. 129
6.III). Results. 131
Visible absorption spectra. 131
Spin-labelled phospholipid ESR results. 132
Effect of bR on the main gel-to-liquid crystalline phase transition. 133
Effects of bR on broadline ^{31}P-NMR spectra at different temperatures. 134
Effect of bR on broadline deuterium NMR spectra at different temperatures. 135
Effect of bR on the dynamic properties of the glycerol headgroup. 136
Effect of lowering the ionic strength of the aqueous environment on solid state NMR spectra. 138
Freeze fracture electron microscopy. 138
6.IV). Discussion. 139

Chapter 7. Membrane electrostatics - effect of lipid headgroup composition and ionic strength on the retinal chromophore properties of bR.

7.I). Introduction. 147
7.II). Materials and Methods. 150
7.III). Results.
A). ^{31}P-NMR determination of apparent pK_as for synthetic lipids (DMPC and DMPG) in the bilayer environment of SUVs in aqueous detergent free media. 152
i) single lipid systems. 152
Effect of ionic strength on the titration properties of DMPG in SUVs. 152
Titration of DMPC SUVs. 153
Determination of the extent of phospholipid hydrolysis during the NMR

measurements at low pH points. 154
ii) Binary lipid systems. 155
Effect of the presence of PG on the properties of the PC headgroup as determined by high resolution ^{31}P-NMR. 155
Effect of salt in the aqueous medium on the phospholipid titration properties. 156
B). Membrane electrostatics and chromophore properties of the protein. 157
i) bR in detergent produced DMPC/bR systems with all the endogenous purple membrane lipids removed. 157
ii) bR in nsTP-produced complexes with most of the purple membrane lipids retained. 158
iii) Effect of salt in the aqueous environment on the chromophore titration properties for the high protein content nsTP-produced complex. 158
iv) bR in detergent produced DMPG bilayers with all the endogenous purple membrane lipids removed. 159
7.IV). Discussion. 160

References. 168

Acknowledgements.

I would like to thank my supervisors Dr. Tony Watts and Dr. Chris Dempsey for their advice, thoughtful criticism and encouragement. Financial support was provided by the Science and Engineering Research Council and I am grateful to Professor E.M.Southern for the opportunity to work in the Biochemistry Department.

I have very much enjoyed the last three years and would like to express my gratitude to all those people who contributed to this; Chris Dempsey, Jeremy Kemp, Joanne Douglas, Michael Edenborough, Jit Hayer, Nick Ryba, Phil Sizer, David Fraser, Jeremy Rowntree, Malkit Sami, Leon van Gorkom, Saira Malik, Lee Fielding and everbody else.

I am particlarly endebted to Dr. Brigitte Sternberg from Jena for the freeze fracture electron micrographs presented in Chapter 4.

I would like to thank Mrs. Barbara Luke for helping me with the negative stain electron microscopy, the Oxford Enzyme Group for allowing use of their Bruker WH300 and Nicolet 360 NMR spectrometers, and Peter Fisher for his excellent technical assistance.

Finally, I would like to thank my parents for their encouragement.

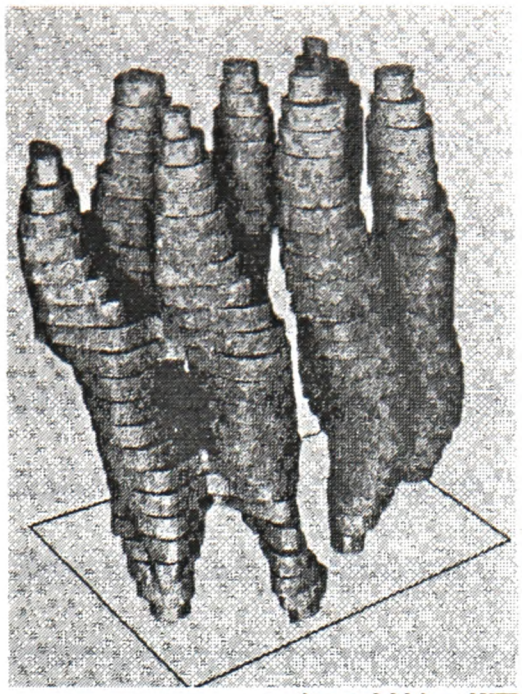
Paul Gale

Introduction.

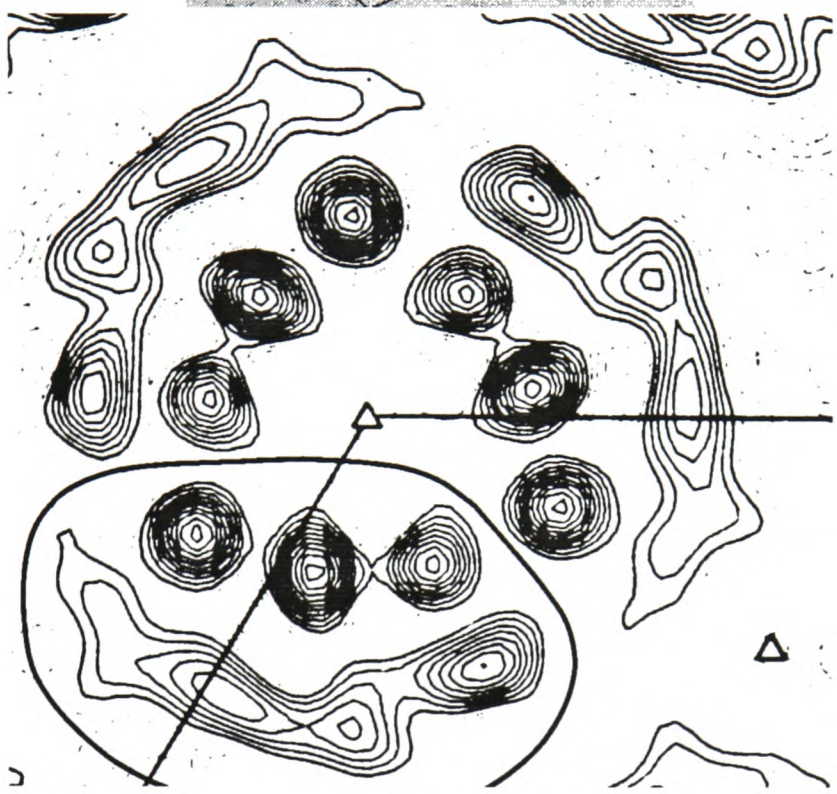
Bacteriorhodopsin is the sole integral membrane protein in the purple membrane patches of the extremely halophilic bacterium *H.halobium*. It has a molecular weight of 26,000Da and functions a light driven proton pump in the cytoplasmic membrane (Racker & Stoeckenius, 1974). Absorption of light is mediated via the prosthetic group, 11-*cis*-retinal, that is covalently bound to lys-41 by a Schiff base linkage (Bridgen & Walker, 1976).

Structure of bacteriorhodopsin and purple membrane from *H.halobium*. The complete amino acid sequence for bacteriorhodopsin has been determined (Ovchinnikov et al., 1979). The three-dimensional structure of the purple membrane protein bacteriorhodopsin is known to 7Å resolution (Henderson & Unwin, 1975). Each monomer contains seven closely packed α-helical segments which extend roughly perpendicular to the plane of the membrane (Fig.1.a). Seven segments of the amino acid sequence were selected as being probable trans-membrane α-helices (Engelman *et al.*, 1980) and the path of the polypeptide chain has been fitted to the three dimensional model. In purple membrane, each monomer is closely associated with two others to form trimers (Unwin & Henderson, 1975) as shown in Figs.1.b and c. Bacteriorhodopsin is an extreme example of a protein that self-associates within the plane of the bilayer to form specialised paracrystalline patches of hexagonal symmetry (Fig.1.b) in the purple membrane of *H. halobium* (Blaurock & Stoeckenius, 1971; Blaurock, 1975; Henderson & Unwin, 1975). Freeze fracture electron micrographs of purple membrane (Blaurock & Stoeckenius, 1971) reveal protein particles of 11.6 nm diameter (Fisher & Stoeckenius, 1977) which are organized into a hexagonal lattice. The polypeptide content for these particles has been determined to be 9 - 12 protein molecules i.e. 63 - 84 transmembrane a-helices (Fisher & Stoeckenius, 1977).

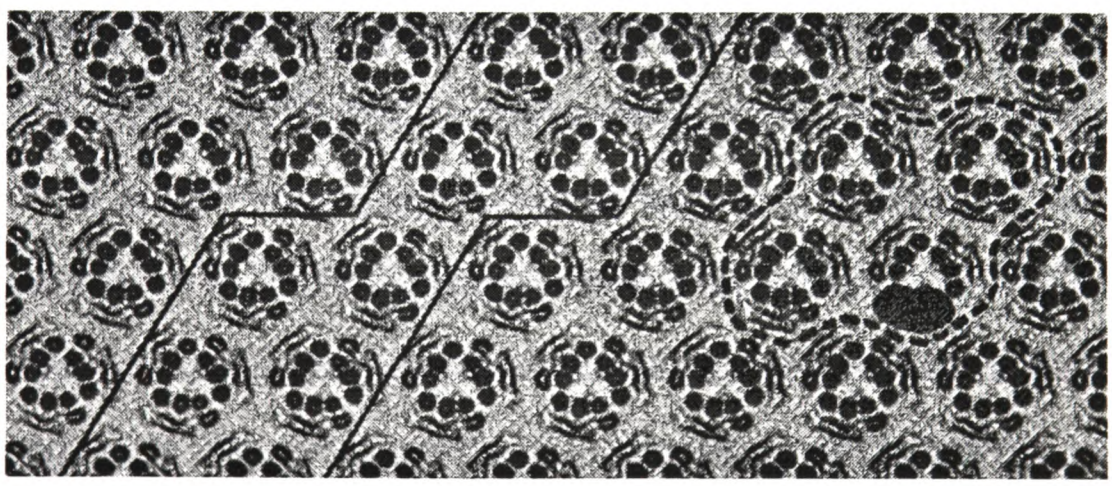
Whilst bacteriorhodopsin is exceptional, there are several examples of integral



a)



b)



c)

Introduction Fig.1. a) three-dimensional model of the seven α-helices constituting a single bacteriorhodopsin molecule, veiwed roughly parallel to the plane of the membrane (taken from Henderson & Unwin, 1975); b) Contour electron scattering map of the projected structure for the purple membrane showing a monomer (outlined) associated with two others to form a trimer (taken from Unwin & Henderson, 1975); c) Hexagonal arrangement of trimers in purple membrane and proposed structure of 11.6 nm diameter particles (outlined) seen in freeze fracture electron microscopy (taken from Fisher & Stoeckenius, 1977).

membrane proteins that form domains by lateral segregation within the plane of the membrane. Gap junction complexes are formed by association of a particular group of integral membrane protein units - connexons - with the exclusion of other proteins (Unwin & Zampighi, 1980). Similarly, at the post-synaptic junction, individual acetylcholine receptor molecules are self-associated (Kistler *et al.*, 1982).

How such proteins overcome the randomising effect of lateral diffusion in the fluid mosaic membrane and form domains depends on a variety of mechanisms. Some interact with peripheral membrane proteins, whilst others can interact with cytoskeletal components (Cherry, 1979). Evidence has been presented to show that the only components required to form hexagonal arrays of bacteriorhodopsin (bR) in the purple membrane are the endogenous purple membrane lipids and the bacteriorhodopsin molecules (Cherry *et al.*, 1978). Here, Triton X-100 solubilized purple membrane, i.e. micelles containing monomeric bacteriorhodopsin and endogenous lipids, reformed the hexagonal two-dimensional structures after removal of the detergent by dialysis. Various factors may be responsible for the association properties of bR. For example, the negatively charged headgroups of the bacterial membrane may order the monomers into hexagonal crystalline aggregates through electrostatic interactions. Alternatively, bacteriorhodopsin may be forced into aggregates because it is relatively insoluble in the negatively charged lipids of the purple membrane, especially at the very low lipid contents (25% w/w) of the purple membrane (Kates, 1978). One mechanism for insolubility of a protein in a bilayer could be imperfect matching of the hydrophobic surface of the protein to the bilayer core provided by the lipid acyl chains. In order to minimise exposure of the protein surface to the lipid, the protein particles may be forced to aggregate in the plane of the membrane (Israelachvili *et al.*, 1980). Alternatively, both factors (or even others) may influence the association of bacteriorhodopsin particles under different circumstances.

Aggregation properties of bacteriorhodopsin in reconstituted lipid systems. Numerous biophysical studies have been performed on bacteriorhodopsin (Cherry *et al.*, 1977, 1978, 1980; Cherry & Godfrey, 1981; Heyn *et al.*, 1981.a and b) relating to

the dispersion/aggregation properties of this integral membrane proteins in a variety of lipid environments. One method used to study the aggregation states of integral membrane proteins is to measure the rotational diffusion coefficients for the protein molecule, itself. The aggregation/dispersion properties of bacteriorhodopsin have been extensively studied by measuring rates of rotational diffusion of the protein and also by circular dichroism studies. CD was particularly useful as it distinguishes monomeric protein from aggregated bR. Transition charge interactions between retinal chromophores of adjacent molecules in the crystalline lattice give rise to exciton bands in the visible CD spectrum (Heyn *et al.*, 1975). These exciton bands disappear when the protein is in the monomeric state. In the paracrystalline lattice of purple membrane itself, rotational diffusion studies showed the bacteriorhodopsin to be immobilised as no decay of the absorption anisotropy was detected. When reconstituted by detergent techniques into DMPC and DPPC vesicles with all the endogenous purple membrane phospholipids retained (Cherry *et al.*, 1977, 1978; Heyn *et al.*, 1981a) bacteriorhodopsin was shown to exhibit a reversible temperature dependent aggregation/dispersion within the plane of the membrane. In DMPC, with all the endogenous purple membrane phospholipids present, the constant anisotropy revealed that bacteriorhodopsin was immobilised at temperatures below the main gel to liquid crystal phase transition. Furthermore, X-ray diffraction and freeze fracture electron microscopy studies revealed the protein particle aggregates to exhibit the same hexagonal two-dimensional para-crystalline array as in purple membrane itself. At temperatures above the DMPC phase transition CD results and the increased rate of rotational diffusion showed the protein to be monomeric, provided the lipid-protein ratio is greater than ~40:1 (Cherry *et al.*, 1978) or ~100:1 Cherry & Godfrey, 1981). Increasing the temperature from 12 to 25°C increased the rotational diffusion coefficient by more than three orders of magnitude. Furthermore, at 25°C, where CD results indicated the bacteriorhodopsin was monomeric (Heyn *et al.*, 1981a), the rotational diffusion constant is found to increase with increasing lipid/protein ratio. Increasing the lipid/protein content from 23:1 to 153:1 was found to increase the rate of

rotation by a factor of 50 (Cherry *et al.*, 1977) at 25°C. While CD measurements indicated some protein aggregation in the vesicles of very high protein contents, it was postulated that an increase in membrane viscosity may also contribute to the reduction in rate of rotation.

An alternative method to study the aggregation/solubility properties of integral membrane proteins is to measure the effect on the lipid molecules of the bilayer by solid state deuterium-NMR of membranes with deuterated lipids as probe. For DMPC systems reconstituted with band-3, the measured quadrupole splittings were found to decrease significantly on heating relative to those measured from the protein-free lipid dispersions (Dempsey, *et al.*, 1986). This was interpreted in terms of a reversible temperature dependent aggregation/dispersion of the band-3 dimers. In contrast the measured quadrupole splittings from DMPC/rhodopsin systems were found to be independent of temperature above the phase transition (Ryba, *et al.*, 1986), supporting no temperature dependent change in aggregation state of the rhodopsin. This is consistent with rhodopsin remaining monomeric (Downey 1985).

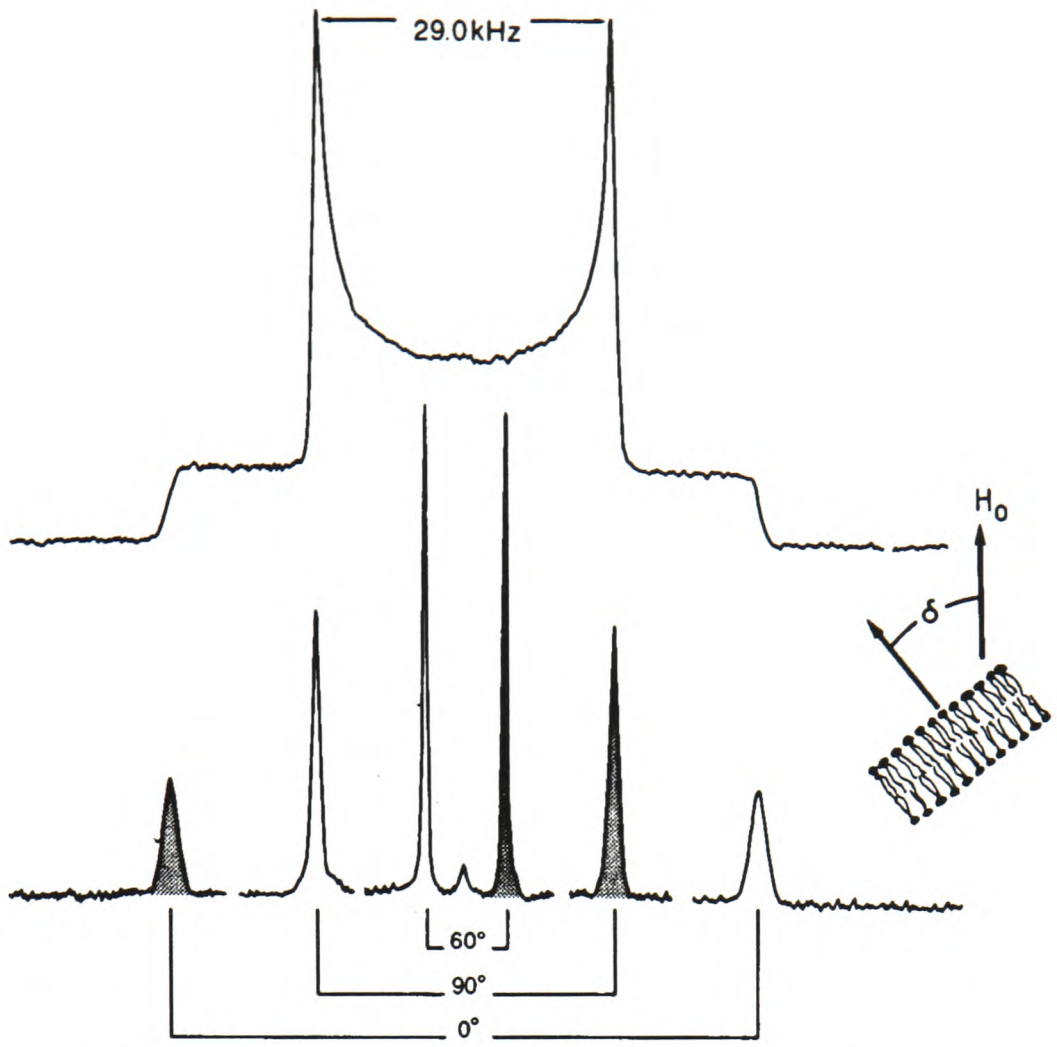
Nuclear Magnetic Resonance

Certain nuclei such as ^{1}H, ^{2}H, ^{13}C, ^{31}P possess a magnetic property known as spin. A nucleus with this magnetic property may have two or more spin states; the actual number of spin states in a nucleus being equal to $2I + 1$, where I is the spin quantum number. When placed in a magnetic field the nuclear spin states become degenerate and have slightly different energies. Transitions between these spin states occurs on absorption of electromagnetic radiation of the radiowave frequency. Modern NMR spectrometers operate in the Fourier transform mode, in which the magnetic field is fixed and the radiofrequency field is applied in short powerful pulses, the bandwidth of which is sufficient to excite all the resonances. Typically the radiofrequency pulse is applied for a time duration (~20μs) to tilt the net component of the nuclear magnetic moments in the z-axis into the xy plane (see Gadian, (1982) for description). Such a pulse is referred to as a 90° or Π pulse. In Fourier transform NMR, the signal in the form of a free induction decay (FID) is collected by the computer as a function of time

following the radiofrequency pulse. In order to obtain a conventional NMR spectrum (i.e. a variation of signal intensity as a function of frequency), the FID is manipulated by a mathematical device known as Fourier transformation. The FID is acquired by recording the intensity of the emitted radiofrequency signal at regular time intervals (the dwell time) over between 2K (2048) or 4K (4096) time points. The dwell time is equal to the inverse of the spectral sweep width (Hz) when using quadrature detection. After the acquisition of the FID, a certain time (the relaxation delay time) delay is observed before the applying the next 90° pulse and repeating the cycle. This time serves to allow return of the component magnetization along the z-axis to return to its equilibrium value of M_o.

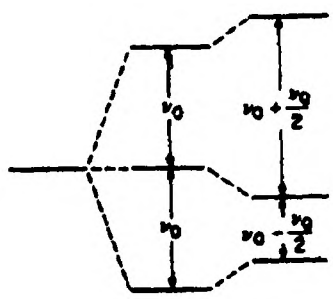
Two relaxation processes are important in effecting the return of the excited state to its equilibrium value. Following the application of the excitation pulse, the net magnetisation has a component in the xy-plane. When the pulse is switched off the component magnetisations in the z- and xy-planes return to their equilibrium values of M_o and zero respectively. The return of the magnetisation component in the z-axis to its equilibrium value is characterised by a time constant T_1, known as the spin-lattice or longitudinal relaxation time. The term spin-lattice is used because the processes involve an exchange of energy between the nuclear spins and their molecular framework. The return of the component magnetisation in the xy-plane (M_{xy}) to its equilibrium value of zero is termed spin-spin relaxation and is characterised by a time constant T_2. Knowledge of the T_1 and T_2 relaxation times is important when choosing the parameters for acquisition of NMR spectra (as discussed for acquisition of high resolution ^{31}P-NMR spectra for quantitative analysis of phospholipids in Chapter 2). Also T1 and T2 values provide information on the rates of molecular motion.

One technique used to measure T_1 values is the inversion-recovery method (pulse sequence shown in Fig.3.17). The application of a 180° pulse inverts the net magnetisation so that it is directed along the negative z-axis. The magnetisation component along the z-axis (M_z) relaxes back towards its equilibrium value with a time constant T_1 and a 90° pulse applied a time τ samples the value to which M_z has



Deuterium NMR spectra (at 46 MHz) of a selectively deuterated soap-like bilayer. Sample composition: sodium octanoate, 34 wt %; [1,1 – $^2H_2$]octanol, 30 wt %; water, 36 wt %. The lower part of the figure shows the ^{2}H-NMR spectra of planar oriented bilayers at various angles δ with respect to the magnetic field. The different shadings denote the two different transitions $-1 \leftrightarrow 0$ and $0 \leftrightarrow +1$. A crossover of the two resonances occurs at the "magic angle" with $\delta = 54.73°$. The quadrupole splitting $\Delta\nu_Q(\delta)$ is the frequency separation of the two transitions. The upper spectrum is the ^{2}H-NMR spectrum of a randomly dispersed sample of the same bilayer as was used for the orientation study. The two most intense peaks in the "powder-type" pattern correspond to the $\delta = 90°$ orientation, while the weak outer wings reflect the $\delta = 0°$ orientation.

Introduction Fig.2.a. Origin of deuterium-NMR powder patterns from lipid bilayers (taken from Seelig *et al* ., 1982).



Introduction Fig.2.b. Energy level diagram for spin $I = 1$ deuterium nucleus in C-D bond in the presence of Zeeman and first order quadrupolar interaction (taken from Kang, *et al* ., 1979).

relaxed after this time. Following signal detection the system is allowed to return to equilibrium by a relaxation delay time of at least $4T_1$. After Fourier transformation the T_1 can be obtained from a plot of $\ln(I_o - I_\tau)$ against τ which should give a straight line of gradient $1/T_1$, where I_o is the spectral intensity obtained for a τ time of $4T_1$ and I_τ is that obtained after a time τ. To measure T_2 relaxation times, the spin-echo pulse sequence is applied, which uses a 90° - τ - 180° - τ pulse sequence.

Solid state deuterium and phosphorus-31 NMR techniques for studying lipid bilayer membranes. Unlike ^{1}H- or ^{13}C-NMR, ^{2}H-NMR and phosphorus-31 NMR offer the advantages of providing unique structural and motional information allowing measurement of segmental molecular fluctuations quantitatively in terms of order parameters and correlation times. Both the deuterium and phosphorus-31 nuclei have the property of being anisotropic; that is, the orientation of the nucleus with respect to an applied magnetic field determines certain spectral properties, in particular the resonance position or chemical shift. The spin-spin relaxation times (T_2) and to a lesser extent the spin-lattice relaxation times (T_1) may also be dependent on orientation within the magnetic field (Torelisa & Szaba, 1982). In combination with ^{31}P-NMR, deuterium NMR of lipid systems in which the phospholipids are selectively deuterated at headgroup segments, can present a rather complete picture for the motions of the membrane lipids occurring and conformations occurring at the membrane surface.

Deuterium NMR. The natural abundance of deuterium is low; thus the phospholipids have to be synthesized with the deuterium atoms incorporated at selected sites on the molecule. This, however, facilitates assignment. Deuterium NMR spectra enable the deuterium quadrupole splitting to be measured, which provides information on segmental anisotropies, that is the amplitude of motion. The deuterium nucleus has a spin quantum number (I) of 1, (the number of energy levels or spin orientations being $2I + 1 = 3$) thus giving rise to two resonances and typical broadline deuterium NMR spectra (Fig.2.b) consist of two overlapping powder patterns. In an applied magnetic field, the three energy levels of the deuterium nucleus are no longer degenerate, and in the absence of quadrupolar effects, they are equally separated (Fig.2.b). Transitions are

only allowed between adjacent energy levels. In the absence of quadrupole effects the energy differences are equal so the two allowed transitions give rise to the same NMR signal. In addition to the magnetic moment, the deuteron nucleus also possesses an electric quadrupole moment. The interaction of the electric quadrupole with the electric field gradient of the surrounding bonding electrons modifies the magnetic energy levels (Fig.2.b) such that the two allowed transitions are no longer equal; consequently, the deuterium signal splits into two resonances. The frequency separation between the two signals is the residual deuterium quadrupole splitting ($\Delta\nu_q$). For a C-D bond in a perfectly ordered environment (e.g. a single crystal), the quadrupole splitting may reach a limiting value of 170kHz (Burnett & Muller, 1971), whereas in fluid membranes the value is usually between 1 and 60kHz, through partial averaging of the anisotropies through molecular motion.

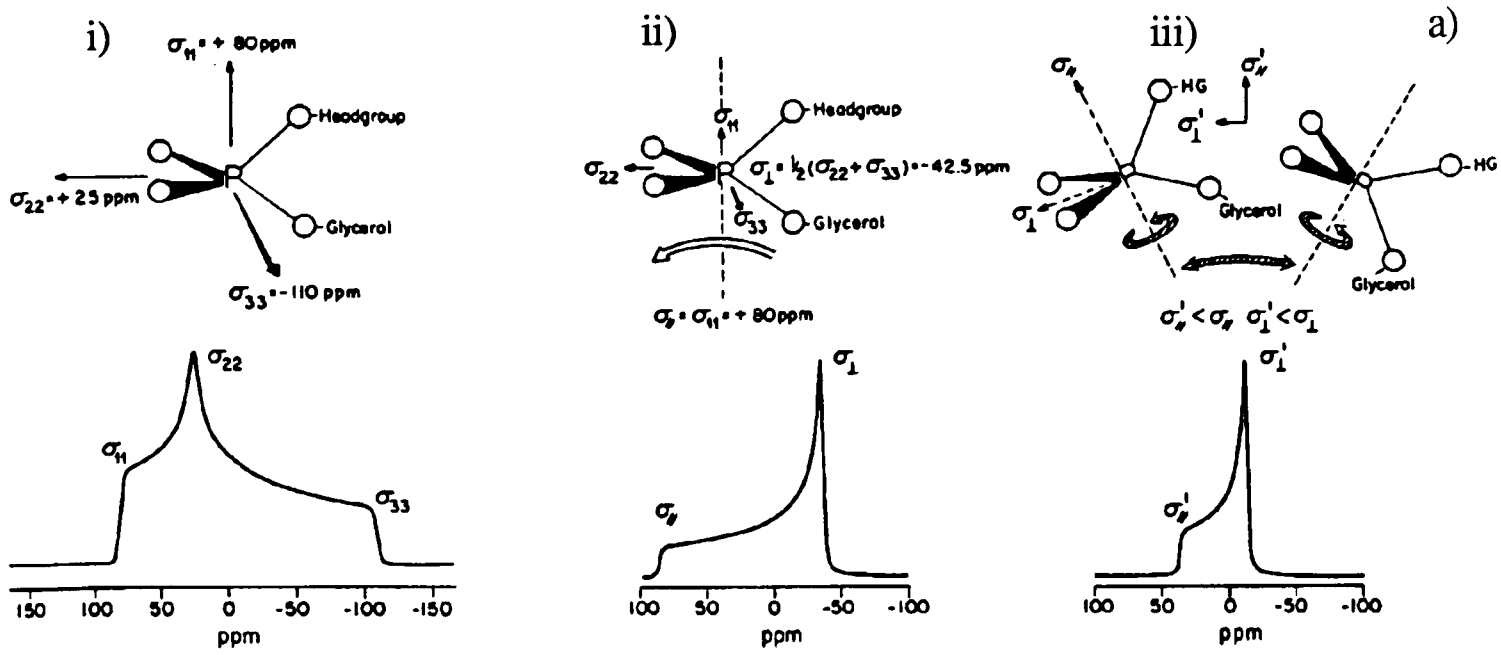
The deuterium quadrupole splitting of an oriented lipid bilayer is determined by:

$$\Delta\nu_q(\theta) = 3/2.e^2qQ/h.\, S_{CD}.(3\cos^2\theta - 1)/2$$

(Seelig, 1977) where e^2qQ/h is the static deuterium quadrupole coupling constant (~170kHz for a parafinic C-D bond), S_{CD} is the order parameter of the C-D bond vector and θ is the angle between the magnetic field and the bilayer normal.

The energy difference between three spin orientations of the deuteron is anisotropic i.e. dependent on the orientation of the deuterium nucleus with respect to applied magnetic field. It follows that the quadrupole splitting in the NMR spectrum will also vary depending on the orientation of the bilayer with respect to the external magnetic field. At the "magic angle" ($\theta = 54.73°$), $3\cos^2\theta - 1 = 0$, and the quadrupole splitting is collapsed. The quadrupole splitting is largest if the bilayer normal is parallel to the magnetic field ($\theta = 0°$).

In non-oriented samples, such as coarse liposomes and DMPC/bR vesicles, a spherically-averaged powder type spectrum (Fig.2.a) is obtained. This envelopes contains the resonances from all the possible bilayer orientations weighted by their



Introduction Fig.3. Origin and interpretation of broadline ^{31}P-NMR spectra of phospholipids; a) various possible motional states of the phosphodiester moiety of a membrane phospholipid and the expected spectrum (taken from Smith & Ekiel, 1984); i) static phosphodiester; ii) ordered phosphodiester with rapid axial motion; and iii) disordered phosphodiester with rapid axial motion.

$\sigma_\perp$ is the chemical shift for the applied magnetic field perpendicular ($\theta = 90°$) to the plane of the bilayer.

$\sigma_{//}$ is the chemical shift for the applied magnetic field parallel ($\theta = 0°$) to the plane of the bilayer

b) ^{31}P-NMR spectra of planar oriented multilayers of DMPE. (taken from Seelig & Gally, 1976); θ is the angle between the applied magnetic field and the normal to the plane of the bilayer. The chemical shift of the resonance is determined by θ.

corresponding geometrical probability. The most important feature of the "powder type" spectra is the frequency spacing of the two most intense peaks, which arise from bilayer microdomains oriented perpendicular to magnetic field ($\theta = 90°$). In isotropic situations the anisotropic effects are averaged out due to rapid tumbling of the molecules through all angles so that the NMR spectrum consists of a single line. The more restricted the amplitude of oscillation, however, the larger the measured quadrupole splitting becomes.

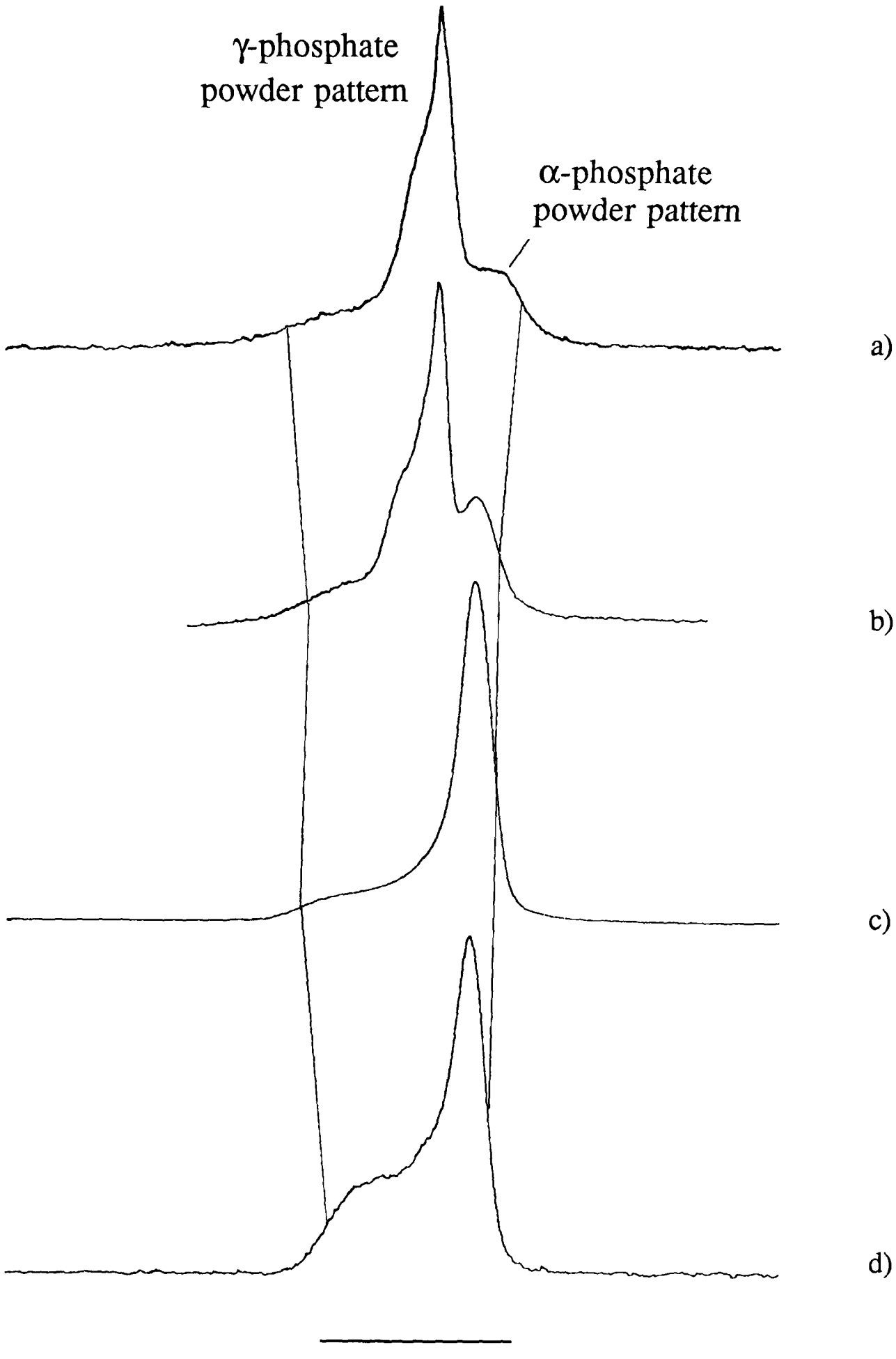
For a spherically averaged powder pattern, such as is obtained from coarse liposomes, the measured quadrupole splitting reports on the amplitude of motion of the C-D group. The ^{2}H-NMR quadrupole splitting can be related to the average lipid conformation (a structural property), whereas the deuterium spin- lattice (T_1) relaxation rate is determined by the rate of segmental motion (a dynamic property).

Phosphorus-31 NMR. The spin quantum number (I) for the phosphorus nucleus is 1/2, thus only a single resonance is observed. The ^{31}P-NMR chemical shift is anisotropic, i.e. depends on the orientation of the group with respect to the spectrometer magnetic field. This is represented in Fig.3.a.i, where the chemical shifts expected along the three directions are labelled σ_{11}, σ_{22} and σ_{33}. For orientations other than along the three principle axes, the chemical shifts will lie somewhere between σ_{11}, σ_{22} and σ_{33}. A powder pattern for completely immobilised ^{31}P-containing compound (e.g. anhydrous phospholipid) displays a very broad NMR spectrum, spanning some 190ppm, which is the sum of spectra for all possible orientations. The three principle chemical shielding tensors (σ_{11} = +80ppm, σ_{22} = +25ppm and σ_{33} = -110ppm) can then be measured. On hydration of anhydrous phospholipids, however, the formation of bilayer structures allows rapid axial motion of the phospholipid molecules which averages the tensor component such that a characteristic bilayer spectrum is obtained (Fig.3.a.iii). For the case of rapid axial motion around one axis but with a highly restricted amplitude of motion, thus averaging the σ_{22} and σ_{33}, a spherically averaged powder pattern (Fig.3.a.ii) with order parameter of one is recorded. In bilayer membranes, not only does rapid axial motion of the phospholipid about the normal to

the bilayer occur, but also the phosphodiester is allowed rapid motion of limited amplitude about the axis of motional averaging; which can be described by a cone. The resultant chemical shift anisotropy is thus reduced in the powder pattern and the amount by which it is reduced is related to the allowed amplitude of the motion, θ. The parameter measured from phosphorus-31 spectra is the chemical shift anisotropy (c.s.a.) in ppm and is measured between the half-heights of the intensities for the 0° and 90° absorptions (Fig.3.b). The observed c.s.a. reflects the degree of order of the phosphate moiety, i.e. the amplitude of angular oscillation during motional averaging. This, however, can only be related to the molecular order parameter if the axis for the phosphorus motion and molecular motion coincide, which they may not (Smith & Ekiel, 1984).

NMR studies of lipid/protein interactions. The bulk of ^{2}H-NMR experiments performed on reconstituted protein/lipid systems have been directed towards understanding the effects of the protein on the fatty acyl chains. Such studies have shown that proteins either disorder or have very little effect on the hydrocarbon chain order above the gel-to-liquid crystal phase transition of the bilayer (T_c). In contrast, cholesterol causes a very large ordering of the hydrocarbon chains above T_c, but both cholesterol and protein prevent chain crystallisation below T_c. Quadrupole splittings measured for the terminal methyl group of the acyl chains of DMPC display a linear decrease at 30°C as the amount of cytochrome *c* oxidase was increased (Kang *et al.*, 1979). Thus the methyl groups become more disordered in the boundary lipid. Cytochrome *c* oxidase, however, had no effect on the 28 kHz quadrupole splitting of DMPC deuterated in the C-6 methylene segment. Thus only the terminals of the fatty acyl chains appear to be influenced significantly by an integral protein. Similar effects were observed for sarcoplasmic reticulum Ca-ATPase reconstituted into DMPC (Rice *et al.*, 1979b).

Tamm & Seelig, (1983) report the first detailed ^{2}H-NMR study of the effects of an integral protein (cytochrome *c* oxidase) on the polar headgroup of a lipid bilayer using POPC labelled either in the choline α- or β-methylene segments. For both



Introduction; Fig. 4.

Phosphorus-31 NMR bilayer spectra (145.9 MHz.) display varying chemical shift anisotropies (c.s.a.) and lineshapes depending on the lipid or the protein/lipid system.

a) *H.halobium* purple membrane (10mM Tris/HCl, pH 7.5, 33°C)

b) *H.halobium* red membrane (1M NaCl, 100mM Tris/HCl, pH 7.5, 33°C)

c) DMPC dispersions (10mM Tris/HCl, pH 7.5, 33°C)

d) DMPG dispersions (150mM NaCl, 100mM Tris/HCl, 1mM EDTA, pH 7.6).

segments, the fluctuations in the reconstituted membranes resembled closely those observed in the pure lipid bilayer, even when a large percentage of the lipid molecules was in direct contact with the protein surface. Both the deuterium T_1s of the choline methylene segments and the ^{31}P T_1s were little effected by protein. The quadrupole splitting and T_1 data provided no evidence for any strong polar interactions between the PC headgroup and cytochrome *c* oxidase, neither in terms of a conformational change nor immobilisation. The only noticeable difference between deuterium NMR spectra of pure lipid and reconstituted systems was a distinct broadening by protein.

Phosphorus-31 NMR has been extensively used to study protein-lipid interactions. A decrease in measured c.s.a. (3 - 6 ppm) is reported (Seelig et al., 1981) for DOPC in reconstituted sarcoplasmic reticulum membrane vesicles. Cytochrome c oxidase also slightly decreases the apparent 31P-NMR c.s.a. of DMPC by 2.5 ppm (Rajan et al., 1981). Cytochrome c was found to increase the measured c.s.a. for acidic phospholipids by 4 - 6 ppm (Waltham et al., 1986). In purple membrane the c.s.a. is found to be increased from -40 ppm for pure PGP to -60.8 ppm (Ekiel et al., 1981). This is the most extreme case reported so far (Smith & Ekiel, 1984).

The measured c.s.a.s obtained from broadline ^{31}P-NMR spectra for phospholipids in bilayer conformations report on the motional properties of the diester phosphate segment; in particular the amplitude of motion. To illustrate some of the possible variations obtainable in measured c.s.a.s, the ^{31}P-NMR spectra of four different phospholipid containing systems at 33°C are displayed in Fig.4. All four systems exhibit a spectrum typical of fluid phospholipids in the bilayer conformation, although with different lineshapes and chemical shift anisotropies (c.s.a.). Substantial changes in c.s.a. are not generally observed even with large external perturbations. Thus, 50mol% cholesterol has no effect on the ^{31}P-NMR c.s.a. (Brown & Seelig, 1978). The spectra of *H.halobium* purple (10mM Tris/HCl, pH 7.5) (Fig.4.a) and red (Fig.4.b) membranes (1M NaCl) exhibit two component powder patterns. Both powder patterns are typical of bilayer conformations and arise from the two phosphate moieties in the PGP molecule, which is the major phospholipid species in H.halobium (Kates, 1978; Chapter 2 of this

thesis). The monoester g-phosphate moiety displays a much smaller c.s.a. (red membrane; -15 ppm) than the diester a-phosphate powder pattern (red membrane; -53.5 ppm). This is due to a greater restriction on the amplitude of motion (i.e. increased ordering) imposed on the a-phosphate group compared to the terminal g-moiety. Furthermore, the a-phosphate c.s.a. for purple membrane is significantly more (-60.8 ppm) than for red membrane (-53.5 ppm). For pure PGP, the measured c.s.a. for the diester moiety is even less (~-40 ppm) as reported in the literature (Ekiel et al., 1981). In purple membrane the protein content (bacteriorhodopsin) is twice as high as the protein content (halorhodopsin) in red membrane; purple membrane is 20% lipid (w/w) compared to 38% for red membrane (Kates, 1978). Thus, increasing the H.halobium protein content in PGP bilayers acts to increase the c.s.a.. This is interpreted in terms of a reduction in the amplitude (i.e. extent of motion) and rate of motion of the lipid headgroup due to interaction with the respective proteins, bacteriorhodopsin and halorhodopsin. This is consistent with the lipids being ordered and motionally restricted in the two dimensional hexagonal paracrystalline lattice of the purple membrane.

The measured c.s.a. for a phospholipid system also depends on the phospholipid headgroup type. Thus for DMPC (Fig.4.c) the c.s.a. is some 11 ppm larger than for DMPG (Fig.3.4.d). This may be interpreted in terms of ionic interactions between the zwitterionic choline headgroups in DMPC ordering the phosphate moieties more than the hydrogen bonds in DMPG. The measured c.s.a. for phosphatidylserine (PS) is reported as being even larger than that for PC (Browning & Seelig, 1980); again consistent with rigid headgroup ordering from electrostatic interactions.

The phosphorus-31 NMR spectra presented in Figs.4.a and c display opposite extremes of magnetic ordering. The acyl chains of the phospholipids exhibit diamagnetic anisotropy and tend to orientate themselves in applied magnetic fields, such that ^{31}P-NMR spectra of DMPC (Fig.4.c) show increased intensity for the 90 orientation relative to the low field 0 orientation. The net dipole moments of the seven a-helices comprising bacteriorhodopsin are arranged perpendicular to the plane of the membrane and serve to oppose the diamagnetic anisotropy of the lipid acyl chains, such

that in 31P-NMR spectra of purple membrane (Fig.4.a) the intensity of the 90 absorption is decreased relative to that for the 0 orientation. Increasing the lipid content tends to reduce this protein mediated orientation, as shown for red membrane (Fig.4.b). Similar effects are seen on the powder patterns for the g-PGP resonances.

Electron spin resonance of spin-labelled phospholipids. The ESR spectra of nitroxide spin-labelled lipids (sterols, fatty acids and phospholipids) in protein/lipid systems show a fluid component, typical of protein-free lipid systems and a broader spectral component (Jost *et al.*, 1973; Watts *et al.*, 1982; Marsh & watts, 1982 for review) the magnitude of which is directly related to protein content (Knowles *et al.*, 1979) and is attributed to boundary lipid that is motionally restricted by the protein. Information on stoichiometry (i.e. number of boundary lipids per protein) and specificity of integral membrane proteins for particular phospholipid headgroups is obtained from ESR spectra of distearoylphospholipids spin-labelled at the C-14 segment with a nitroxide spin-label group (reviewed in Marsh & Watts, 1982). To date, no ESR studies with spin-label phospholipids have been reported on DMPC/bR or DMPG/bR vesicles with all the endogenous purple membrane phospholipids removed. As reported for other protein systems (e.g. cytochrome *c* oxidase; Knowles *et al.*, 1979), the 14-PLSL spectra from bacteriorhodopsin-containing vesicles of high protein contents reveal two components. Spectral subtraction and simulation were used in this present work to determine the proportion of motionally restricted component in ESR spectra of 14-PCSL incorporated in a DMPC/bR complex of high protein content. From this the number of boundary lipids per 26,000Da bacteriorhodopsin monomer can be calculated. In addition, any selectivity of the bacteriorhodopsin for the phospholipid PG, with a net negative charge, relative to the zwitterionic PC is investigated. The only ESR studies reported on spin-labelled lipids in bacteriorhodopsin systems have used stearic acid spin-labels (SASL) incorporated into purple membrane itself. Chignell and Chignell (1975) demonstrated both 4- and 12-SASL to display highly immobilised spectra, with $2A_{max}$ values of 59 and 58.7 gauss at 37°C, respectively, consistent with a protein mediated ordering of the lipid acyl chains. The ESR spectrum, however, of

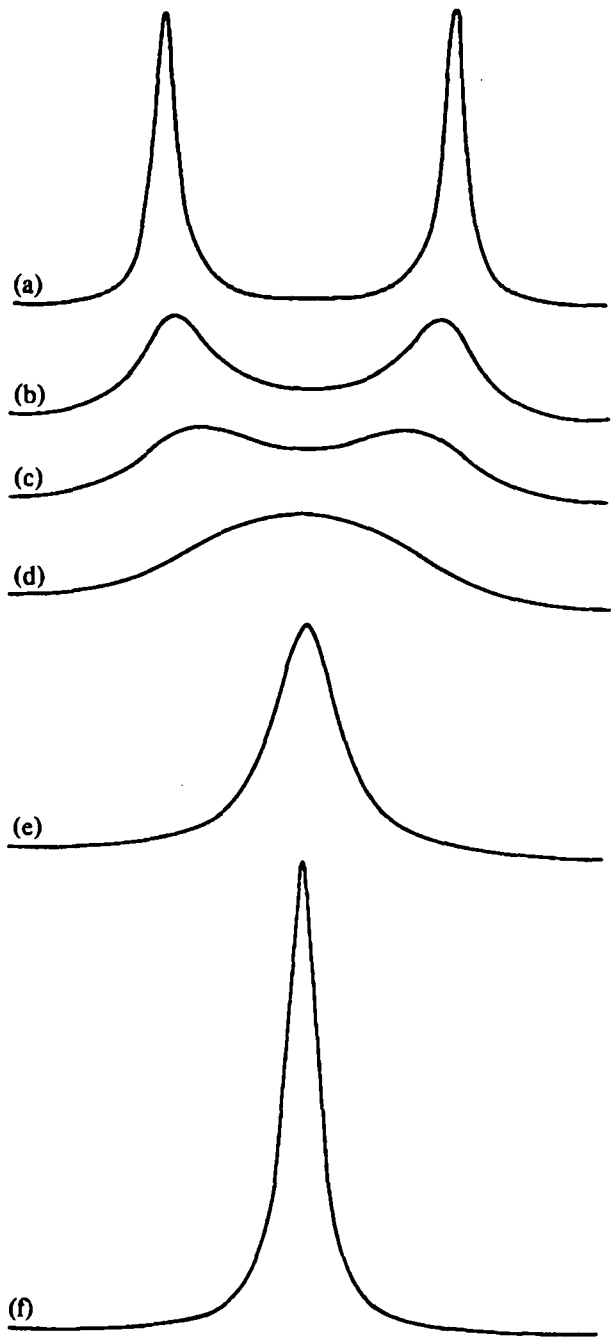


Diagram illustrating the effects of chemical exchange between two species A and B of equal concentration. The exchange rate gradually increases on moving down from spectrum (a) to (f). (a) represents slow exchange, (b)–(e) represent various types of intermediate exchange, and (f) represents fast exchange. The actual rate constants are as follows: (a) $k = \pi(\nu_A - \nu_B)/10$; (b) $k = 3\pi(\nu_A - \nu_B)/10$; (c) $k = \pi(\nu_A - \nu_B)/2$; (d) $k = 4\pi(\nu_A - \nu_B)/5$; (e) $k = 2\pi(\nu_A - \nu_B)$; (f) $k = 4\pi(\nu_A - \nu_B)$.

Introduction Fig.5 (taken from Gadian, 1982).

16-SASL revealed the presence of two populations of spin-label, one of which was more highly immmobilised than the other. This was interpreted in terms of a fluid and a boundary component. Hoffmann *et al.*, (1980) extended the work on 16-SASL in purple membrane and interpreted the two component spectra in terms of a temperature dependent protein conformational change, although no explanation regarding the nature of the change was offered.

NMR and ESR timescales. In contrast to ESR spectra from spin-labelled phospholipids, the deuterium and phosphorus-31 NMR spectra obtained from phospholipids in lipid/protein complexes display only a single component spectrum. The apparent discrepancy between the ESR and NMR results has caused much controversy (Kang *et al.*, 1979) but is reconciled in terms of the exchange rate between boundary and fluid lipid and the different time scales of the ESR and NMR experiments (Watts, 1981; Seelig *et al.*, 1982). Both ESR and NMR have their own dynamic timescales, which for magnetic resonance depends on the rate of motion required to average out the intrinsic anisotropy within the magnetic field. This is illustrated for NMR spectra in Fig.5, where ν_A is the frequency for the species in environment A and ν_B for environment B. In order to obtain a single component NMR spectrum the exchange rate between two distinct environments must faster than the difference (in Hz) between the frequencies (whether chemical shifts or quadrupole splittings) displayed by the species in the two separate environments. If as in spectrum (5.a) the exchange rate is 10 times slower than this frequency difference then two component spectra are observed. In NMR the maximum differences between deuterium NMR quadrupole splittings (or phosphorus-31 c.s.a.s) for lipids in contact with protein or in the free bilayer is 6,000 Hz, assuming values of zero for boundary lipids (Sixl *et al.*, 1985). Thus an exchange rate between lipids bound to the protein and bulk phase bilayer lipids of greater than 10^4 s^{-1} is sufficient to produce single component spectra. The ESR spin-labelled lipid studies the differences between the spectra from pure lipid bilayers and the more motionally restricted boundary lipids are between 2 and 10 gauss, corresponding to a frequency separation of 5 to 28 MHz. Thus the two-component

nature of ESR spectra of lipid/protein systems is consistent with an exchange rate slower than 5 x 10^7 s^{-1}.

It has been suggested (Yeagle, 1982, 1984 and Albert & Yeagle, 1983) that intrinsic membrane proteins are able to cause motional restriction or immobilisation of lipids on the NMR timescale leading to broad ^{31}P-NMR spectral components or to a reduction of lipid intensity due to the presence of an unobserved broad component. Ellena *et al.*, (1986) demonstrate two component phosphorus-31 NMR spectra for DSPC and DOPC binary mixtures at 22°C due to a co-existing solid and liquid-crystalline domains which are in slow exchange on the ^{31}P-NMR timescale. The phosphorus-31 NMR spectra of native rod outer segment and sarcoplasmic reticulum membranes, which contain integral proteins were found to consist only of a narrow component.

This thesis consists of seven chapters and reports on lipid/protein interactions in bacteriorhodopsin-containing vesicles. In the first chapter, two different methods are described for producing exogenous phospholipid/bR complexes, while in Chapter 2 the properties of these vesicles are reported. Of particular importance is the phospholipid composition of the vesicles with respect to the endogenous purple membrane phospholipids. This is investigated by high resolution ^{31}P-NMR of SDS-solubilized vesicles. One method for production of exogenous phospholipid/bR vesicles involves the use of detergents and successfully removes all the purple membrane lipids. The second is an as yet unpublished technique and employs a phospholipid transfer protein to add DMPC molecules to purple membrane. The advantage of this technique is that detergents are not used and the majority of the purple membrane phospholipids are retained. In chapters 3,4,5, and 6 the solubility properties of bacteriorhodopsin in a variety of lipid environments are investigated by ^{2}H-and ^{31}P-NMR, ESR and freeze-fracture electron microscopy. Also the effects of protein on the conformational and dynamic properties of the phospholipid headgroups are analysed. Finally Chapter 7 reports the effects of the lipid environment on the retinal chromophore properties of bacteriorhodopsin.

Chapter 1.

Two methods for producing deuterated-DMPC bacteriorhodopsin lipo-protein complexes suitable for deuterium NMR studies.

1.I) Introduction.

Numerous biophysical techniques are available to study the interactive effects of integral membrane proteins on the adjacent lipids in the bilayer. Preparation of the lipo-protein complexes for most of these studies at the very least requires the incorporation of a lipid probe molecule into the bilayer. Furthermore, if studies are to be performed on lipid-protein systems of a variety of lipid/protein ratios and comprising only a specific homogeneous synthetic lipid, then complex manipulation and reconstitution techniques are required. These techniques usually involve the use of one or more detergents at some stage in the sample preparation.

For electron spin resonance (ESR) studies, the probe is a nitroxide labelled lipid present at a molar ratio of 1:100 unlabelled lipids. One method to incorporate spin-labelled lipids into protein-lipid complexes is by ethanolic injection of the label (Watts *et al.* 1979). Another approach is to incorporate the label into the reconstitution mixture (Knowles *et al.*, 1979). Studying protein-lipid interactions by deuterium nuclear magnetic resonance (^{2}H-NMR) yields information on a slower time-scale than ESR (Watts, 1981). For ^{2}H-NMR, the probe is a lipid molecule in which non-exchangeable protons have been replaced by deuterons at specific sites. Such probes are non-perturbing for the membrane structure unlike the bulky nitroxide spin-labels. Due to the lower sensitivity of NMR, however, the deuterated lipid must be present at a much higher concentration in the bilayer, or even constitute the bilayer itself.

The most common method of making protein/exogenous lipid complexes is to solubilize the membrane protein and the (deuterated) exogenous lipid in a suitable detergent, and then remove the detergent by exhaustive dialysis. This detergent technique widely used to produce DMPC/bacteriorhodopsin complexes (with all the

endogenous purple membrane lipids retained) for biophysical studies is that described in Cherry *et al.*, (1978). Heyn & Dencher, (1983) have reviewed detergent techniques for other phospholipid types and van Dijck and van Dam (1983) review the various detergent and detergent free techniques for producing exogenous lipid/bacteriorhodopsin complexes. One detergent free process involves sonicating mixtures of lipids with purple membrane to yield very small vesicles which could be argued to be unsuitable models for natural membranes and such vesicles are frequently inappropriate for many biophysical techniques, including ^{2}H-NMR. Furthermore, sonication can denature proteins, although this does not appear to be a significant problem with bacteriorhodopsin.

The main advantage of solubilizing membranes in detergents is that it provides an additional step for purification of the proteins or removal of the membrane lipids, if desired. There are, however, several possible, practical disadvantages with a technique that involves the use of detergents.

i). A suitable detergent has to found that not only effectively solubilizes the membrane, but also does not irreversibly denature the protein, under optimal conditions of pH, temperature and ionic strength, which also have to be determined.

ii). Complete removal of every detergent molecule by exhaustive dialysis may not in practice be achieved. Residual cholate in a bilayer membrane has previously been shown to effect the measured deuterium quadrupole splittings (Rice, *et al.*, 1979; Ryba *et al.*, 1986). By using radioactive Triton X-100 it has been shown that about one detergent molecule remained per two bacteriorhodopsin molecules after removal by dialysis when producing bacteriorhodopsin/DMPC complexes (Heyn & Dencher, 1983; Cherry *et al.*, 1978). For octyl glucoside, with a relatively high c.m.c. of 23mM, 99.94% of the detergent may be removed in three days from reconstituted VSV glycoprotein (Petri and Wagner, 1979).

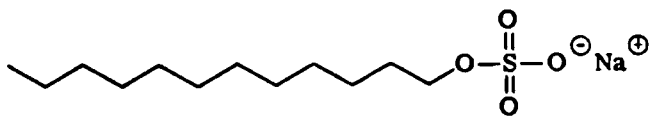
iii). The detergent dialysis technique may take a long time (up to three weeks with Triton X-100; Cherry *et al.*, 1978), during which the sample may deteriorate. This, however, does not appear to be a problem with the bacteriorhodopsin molecule which is

extremely stable. After one year at 4°C, the proton pumping activity of DMPC/bR vesicles prepared as described by Cherry *et al.*, (1979) is unaffected and the spectral properties unchanged (Heyn & Dencher, 1982).

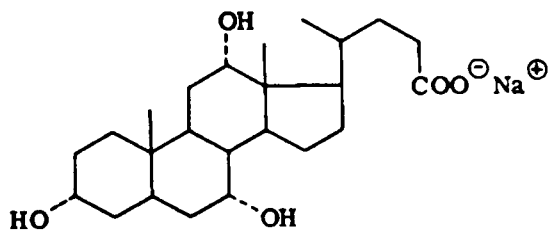
In this chapter, a novel non-detergent, biologically mediated method is presented for incorporating DMPC molecules into human erythrocyte ghost membranes and *H.halobium* purple membrane without the use of detergents. Furthermore, the DMPC used was selectively deuterated at the headgroup, allowing effects of protein on the motional and conformational properties of the choline headgroup to be investigated by solid state deuterium-NMR (Chapter 5). These two systems were chosen as models on which to test the method since they both contain a major integral protein - exclusively bacteriorhodopsin in the case of purple membrane and predominantly band-3 and glycophorin in the erythrocyte ghost. In addition, there is extensive literature coverage of the association/dispersion properties of band-3 (Cherry *et al.*, 1979; Dempsey *et al.*, 1986) and bacteriorhodopsin (Cherry *et al.*, 1978; Heyn *et al.*, 1981a) in detergent reconstituted DMPC systems.

The procedure, which is also much faster than detergent techniques, utilises a non-specific phospholipid transfer protein (nsTP) purified from bovine liver to promote transfer of DMPC from donor small unilamellar vesicles (SUVs) into purple membrane or erythrocyte ghosts. Previously, nsTP has been used to insert spin-labelled phospholipids into resealed erythrocyte ghost membranes (Gale, Part II Thesis, Biochemistry Dept. Oxford University). Order parameter and polarity profiles measured in that study demonstrated the incorporated phospholipids were in a bilayer conformation together with the protein.

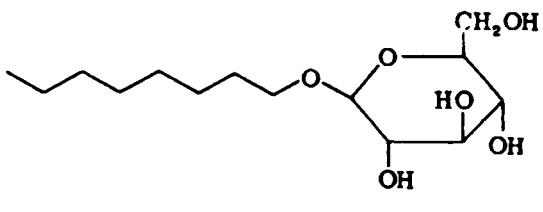
The types and properties of phospholipid transfer proteins are overviewed by Zilversmit (1983). Both bovine and rat liver cytosol contain a transfer protein (M_r 28,000), that is quite specific for the transfer of diacyl phosphatidyl choline. Non-specific transfer proteins have been isolated from rat and bovine liver. The bovine liver protein used here has a molecular weight of 13,600 Da (gel filtration) or 14,500 Da (SDS PAGE) and exists as two isozymes. It promotes the transfer not only of most



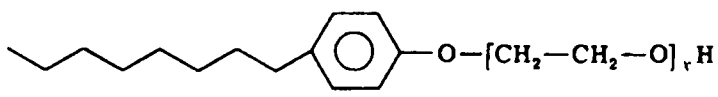
a)



b)



c)



d)

Fig.1.1.

The structures of the detergent molecules used in this present work (taken from Helenius *et al* ., 1979). Ionic detergents have ionisable groups and include sodium dodecyl sulphate - SDS (a) and sodium cholate, (b) which is a bile salt. The non-ionic detergents have no charged groups and include octyl-β-D-glucopyranoside - octyl glucoside (c) and alkyl phenylpoly-oxyethylene detergents e.g. Triton X-100 (d).

phospholipids, but also of a glycosphingolipid, ganglioside and cholesterol. The protein, however, does not transfer cardiolipin or triacylglycerol. The two isozymes are reported to exhibit identical mobilities on SDS PAGE, although the silver-stained PAGE gels clearly resolves two bands. Amino acid analysis shows a striking similarity between them and they are both basic proteins but with slightly different isoelectric points at pH 9.55 and 9.75 (Crain & Zilversmit, 1980a).

Bovine non-specific phospholipid transfer protein (nsTP) was chosen in preference to PC-specific exchange protein because it is capable of effecting a net transfer of phospholipid to the acceptor membrane (Crain & Zilversmit, 1980b), which is clearly desirable as purple membrane has only 6 - 12 polar lipids per bacteriorhodopsin (Kates *et al.*, 1983). If the acceptor membrane contains no PC, then PC-specific exchange protein will catalyse a net transfer until the acceptor vesicle contains 2mol% PC (Wirtz *et al.*, 1980). Once the acceptor membrane contains some PC, the PC- specific exchange protein catalyses a 1:1 exchange between donor and acceptor (Helmcamp, 1980). Incorporating DMPC to 2mol% in purple membrane, however, is of little use for producing DMPC/bacteriorhodopsin vesicles of a variety of lipid/protein ratios.

In this chapter is also described the production of thirteen different DMPC/bacteriorhodopsin complexes in which all the endogenous purple membrane phospholipids had been removed. These complexes were produced by a detergent technique similar to that first described by Huang *et al.*, (1980) but significantly different to produce complexes suitable for ^{2}H-NMR. The properties of the vesicles produced by the two methods are discussed and compared in Chapter 2.

The structures and properties of various detergents used for solubilization of membranes and as solvents for membrane proteins are reviewed in Helenius *et al.*, (1979). The molecular structures of the detergents used in this present work are shown in Fig. 1.1. Detergents, in their chemical properties, resemble the phospholipid and integral proteins of the membrane in that they are amphipathic molecules - they have a hydrophobic region and a polar region. In aqueous media, detergent molecules, when

present in numbers above the critical micelle concentration (c.m.c.), self-associate to form micellar structures. In detergent micelles, the hydrophobic regions are sequestered in the core, while the polar moieties are solvated in the aqueous medium at the surface. Thus, by providing both a hydrophobic region and a polar surface, a detergent micelle offers a suitable solvent medium for membrane components (phospholipid or integral protein).

Detergents may be broadly characterized into two groups depending on the nature of the polar moiety. The ionic detergents such as sodium dodecyl sulphate (SDS), sodium cholate and cetyl trimethylammonium bromide (CTAB) have charged groups in the polar headgroup. Nonionic detergents have no charged moieties in the polar headgroup and include octyl glucoside and Triton X-100. Much of the expertise in reconstitution technology is finding the optimal detergent, which maintains functional and conformational integrity for a particular membrane protein. Furthermore, different detergents may be better suited for the specific stages (solubilization, purification and reconstitution) of the procedure. The protocol employed here (initially developed by Huang *et al.*, 1980) exploits exchanging the solubilizing detergent during the delipidation procedure to one more suitable for reconstitution by dialysis.

In addition to choosing the most suitable detergent for a membrane protein, the correct ionic environment has to be attained. The integrity of protein/detergent micelles depends on the relative contributions of the amphipathic interactions, that is both hydrophobic interactions and polar contacts. The hydrophilic interactions at the micelle surface between charged moieties on the protein and the detergent polar groups are influenced by pH, ionic strength and specific ions. The properties of ionic detergents are strongly affected by the ionic strength and by the nature of the counterion. As the repulsion between headgroups is a limiting factor in micelle formation, increasing the counterion concentration lowers the c.m.c. and increases the micelle size. Furthermore, ionic detergents have a pK_a below which the detergent precipitates. For cholate the pK_a is at pH 5.2 (Carey & Small, 1972).

Alkyl ionic detergents, such as SDS, are nearly always denaturants. They usually

dissociate multisubunit proteins into their constituent polypeptide chains. SDS is used to analyse, isolate and characterize individual polypeptide chains of membrane proteins in their denatured state. London & Khorana (1979) report that on solubilization in SDS, bacteriorhodopsin undergoes denaturation with partial loss of the secondary structure and loss of retinal binding ability to give bacterio-opsin (bO). Thus SDS is considered a suitable solvent system for the high resolution ^{31}P-NMR studies to analyze the phospholipid composition of complexes as described in Chapter 2. Addition of phospholipid/cholate mixtures to bacterio-opsin denatured in SDS reforms the secondary structure. The protein is remarkable in that following complete denaturation it readily refolds, and upon the addition of retinal and a phospholipid/cholate mixture followed by dialysis it forms fully active vesicles. In contrast, delipidated bacteriorhodopsin in the ionic detergent deoxycholate retains its native structure and subsequent reconstitution with a variety of phospholipids forms vesicles that efficiently translocate protons (Huang, *et al.*, 1980; Lind *et al.*, 1981).

Nonionic detergents, with polyoxyethylene or sugar headgroups, do not usually denature proteins (Helenius, *et al.*, 1979). They can therefore be used for solubilization or characterisation of membrane proteins in the native state. Dencher & Heyn (1978), on the basis of the disappearence of the exciton CD bands, reported that solubilization of purple membrane in Triton X-100 or octyl-β,D-glucopyranoside leads to the formation of protein monomers. In Triton X-100, the kinetics of solubilization was found to be strongly pH dependent. Whereas at pH 6.88 and 20°C, complete solubilization is reached in 20 hours, at pH 5 it takes 48 hours to reach 60%. Bacteriorhodopsin solubilized in Triton-X-100 was stable for several days when stored in the dark at room temperature and showed no evidence of chromophore loss. Furthermore it was concluded that Triton X-100 solubilization did not lead to a major change in secondary structure with the protein still showing ~70% α-helix content. Reynolds and Stoeckenius, (1977), reported Triton X-100 solubilized bacteriorhodopsin to be monomeric, have a molecular weight 24,250 ± 2,000 Da and to bind one micelle of Triton X-100.

Octyl glucoside solubilization of purple membrane is reported to be markedly dependent on ionic strength. No solubilization occurs in the presence of 140mM NaCl and at room temperature progressive chromophore loss occurs after two days (Dencher & Heyn, 1978).

One advantage of using a detergent reconstitution method to produce protein/lipid complexes is that it presents the option of removing the natural membrane phospholipids from the detergent solubilized protein A number of methods are available to remove the endogenous lipids from a membrane protein extracted from a membrane and solubilized in detergent (bacteriorhodopsin, Happer & Overath 1976; Hwang & Stoeckenius, 1977; Wildenauer & Khorana, 1977; Huang *et al.* 1980; Bayley *et al.*, 1983; band 3, Dempsey *et al.*, 1986; bovine rhodopsin, Ryba *et al.*, 1986; Ca/Mg-ATPase, Warren *et al.*, 1974; East & Lee, 1982). This offers the opportunity to study the effect of a single chemically homogeneous synthetic lipid e.g. DMPC on the properties of an integral membrane protein. In the case of bacteriorhodopsin, (as described in further chapters) the presence of the endogenous purple membrane phospholipids markedly alters the aggregation/dispersion properties of the protein in DMPC. For detergent treated bacteriorhodopsin both gel-filtration and density gradient methods have been described for removing 80 - 99.9% of the endogenous purple membrane lipids from the protein micelles.

Hwang & Stoeckenius (1977) reported that 80% of the endogenous purple membrane lipids could be removed after applying deoxycholate treated purple membrane to a linear 20 - 60% sucrose gradient. Repeated delipidations using this technique (Kates *et al.*, 1983) removes 90% of the endogenous lipids. The membranes produced by this treatment, however, still retain the purple membrane lattice, as judged from X-ray diffraction patterns and electron microscopy data. The energy coupling between chromophores was also preserved in 10% deoxycholate treated purple membrane after 48 hrs, although the coupling disappears when the protein lattice dissociates into monomers (Heyn, *et al.*, 1975). This method was not adopted in this present study since it failed to produce bacteriorhodopsin monomers completely free of

purple membrane phospholipids.

Gel exclusion chromotography using a deoxycholate or cholate buffer removes 99.9% of the endogenous purple membrane lipids (Huang *et al.*, 1980; Bayley *et al.*, 1983). Furthermore the solubilizing detergent, Triton X-100, is replaced by cholate. Cholate has a higher c.m.c. (~10mM) than Triton X-100 (0.3mM) (Reynolds, 1982) and is thus removed far more rapidly by dialysis. This method not only produces bacteriorhodopsin monomers in a detergent suitable for dialysis, but also removes all the purple membrane lipids.

1.II. Materials and analytical methods.

Non-specific phospholipid transfer protein. The nsTP used for adding DMPC to natural membranes was purified from a 5kg bovine liver according to Bloj and Zilversmit, (1983). For most labelling experiments the final purification step - octyl agarose chromotography - was not performed and a partially purified nsTP extract was used.

Phospholipid synthesis. The phospholipid 1,2-dimyristoyl-*sn*-glycero-3-phosphocholine (DMPC) was specifically deuterated at the N,N,N-trimethyl moiety of the headgroup by methylation of 1,2-dimyristoyl-*sn*-glycero-3-phosphoethanolamine (DMPE) using deuterium enriched iodomethane to produce DMPC-d_9 (as described by Eibl, 1980). DMPC-d_4, specifically deuterated in the choline Cα and Cβ headgroup methylene segments (see Fig.3.1 for molecular structure), was produced using ethanolamine-d_4 in the phosphorylation step (as described by Eibl, 1978) followed by methylation of the DMPE-d_4 with iodomethane. Both lipids ran as a single spot on thin layer chromotography with $CHCl_3$/methanol/ammonia (65:30:3).

Lipid and protein analysis. For all DMPC/bacteriorhodopsin complexes produced, the final lipid/protein ratio was measured after its production and purification by density gradient centrifugation. nsTP-mediated incorporation of DMPC into purple membrane was estimated by lightly doping the deuterated DMPC with [^{3}H]-DMPC-t_9, in which the choline γ-methyl groups were radiolabelled with tritium. The final

amount of DMPC in the complex was determined by perchloric acid digestion and inorganic phosphate analysis according to the method of Rouser *et al.*, (1970). The amount of bacteriorhodopsin was determined by the modified Lowry method of Markwell *et al.* (1981). Before protein determination the vesicles were washed free of all remaining Tris buffer and EDTA by three centrifugations (100,000g; 20 min; 15°C). Lowry results were corrected for a systematic error in the case of bacteriorhodospin (Rehorek & Heyn, 1979); the final lipid/bR ratio being increased by 20%.

Purification of purple membrane. Purple membrane was isolated from cultures of *H.halobium* by the method of Oesterhelt and Stoeckenius (1974). Each five litre culture yielded around 50mg of bacteriorhodopsin as determined by absorbance at 560nm. Purple membrane was separated from any remaining red membrane on a 30 - 50% sucrose density gradient (100,000g; 17 hr; 4°C). The spectral ratio at 280 and 560 nm, $A_{280/560}$, of purified purple membrane was typically 2.

Assay of nsTP transfer activity. 15mg of egg PC (Lipid Products) in $CHCl_3$/MeOH was mixed with 0.5μCi of [^{3}H]-DMPC-t_9 and solvent removed with N_2 and then under vacuum (10^{-2} torr; 15hr). Lipid was resuspended in 3cm^3 of buffer (45mM NaCl; 25mM phosphate; 1mM mercaptoethanol; pH 7.4) and tip-sonicated. The small unilamellar vesicles were then centrifuged (25,000g; 15min; 4°C) and the supernatant used as donor vesicles. A separate assay sample was used for each assay time point (100μl of donor SUVs, 200μl of partially purified nsTP extract and 300μl of bovine ghosts). The assay was performed at 37°C. After time intervals between 15 min and 2hr the ghosts were pelleted (microfuge; 10,000rpm) and washed three times in 45mM NaCl, 25mM phosphate, 1mM mercaptoethanol, pH 7.4 before measuring incorporation of tritiated-DMPC.

Nomenclature of the nsTP-produced DMPC/bR complexes. Characterisation by high resolution ^{31}P-NMR of the 36:1, 85:1 and 123:1 total lipid phosphate mole ratio DMPC/bR complexes produced by nsTP-mediated DMPC incorporation (described in

Chapter 2) allowed accurate determination of the phospholipid headgroup compositions with regard to moles of exogenous DMPC and moles of endogenous purple membrane phospholipids (PMPL) per 26,000Da monomer of bacteriorhodopsin. These three complexes are thus labelled in terms of a DMPC/PMPL/bR (mol/mol/mol) ratio, that is 21:7.6:1, 72:7.3:1 and 109:7.8:1 for the 36:1, 85:1 and 123:1 total lipid phosphate/bR mole ratio complexes, respectively. For these complexes between 7.3 and 7.8 lipid α-phosphate groups were found to be retained per bacteriorhodopsin monomer. The complexes that were not analysed by high resolution ^{31}P-NMR are labelled in terms of the total phospholipid phosphate/bR mole ratio. Assuming the nsTP-labelling method to be reproducible, then between five and seven of these phosphates can be attributed to the PGP-γ phosphate and seven to eight to the purple membrane phospholipid α-phosphate moieties.

1.III. Methods for producing DMPC/bacteriorhodopsin complexes.

Production of DMPC/bacteriorhodopsin complexes using conventional detergent methods. Two different methods of detergent solubilization and reconstitution by dialysis were investigated for producing DMPC/bacteriorhodopsin complexes in which all the endogenous purple membrane lipids have been removed. All steps were performed in the dark or under dim-red light at 25°C.

The first method employed solubilization of purple membrane in the non-ionic detergent octyl glucoside (60mM octyl glucoside; 25mM sodium phosphate; pH 7.0; 48 hr), after which any unsolubilized or aggregated protein was pelleted (30min; 15°C; 100,000g). A sucrose density gradient method was developed to remove the endogenous purple membrane phospholipids from the bacteriorhodopsin/octyl glucoside micelles. The supernatant (doped with 0.1μCi exogenous [^{3}H]-DMPC) was layered onto a 10:12:20% sucrose step gradient pre-equilibrated with 60mM octyl glucoside (350,000g; 65,000 rpm; Beckman Type 70.1 Ti rotor; 4°C; 24hr). 0.5 cm^3 aliquots taken from the top of the gradient were analysed for [^{3}H]-DMPC (cpm) and bacteriorhodopsin micelles (as judged from purple colour). Aliquots containing

bacteriorhodopsin were pooled, mixed with deuterated DMPC that was solubilized in octyl glucoside (60mM octyl glucoside; 25mM phosphate; pH 7.0) and the mixture dialysed for three days. This method, however, had a number of disadvantages (discussed below) and was not employed for producing any of the DMPC/bR complexes discussed in this present work.

The second detergent method investigated is a modification of that described by Huang *et al.*, (1980) and consists of three stages:-

i) solubilization of the purple membrane to give bacteriorhodopsin micelles and endogenous purple membrane lipid micelles. A pellet of purple membrane (20 - 60mg) of bacteriorhodopsin (as determined by the absorbance at 560nm) was stirred overnight in the dark (25°C; 5cm^3 of 5% (v/v) Triton X-100; 100mM Tris/HCl; pH 7.0). The detergent:bacteriorhodopsin ratio (w/w) varied from 4.5:1 to 13.5:1. After 15 hours, the solubilized purple membrane was centrifuged (100,000g; 30 min; 15°C) to pellet any unsolubilized purple membrane or aggregated bacteriorhodopsin. This centrifugation is essential if complete removal of endogenous purple membrane phospholipids is to be achieved.

ii) separation of endogenous purple membrane lipid micelles from bacteriorhodopsin micelles by gel filtration (Huang *et al.* 1980; Bayley *et al.* 1983). The supernatant of the Triton X-100 solubilized purple membrane was loaded onto a Pharmacia 70 * 2.6 cm column packed with Sephadex G-75 (fine) beads pre-equilibrated with 1% cholate (w/v), 150 mM NaCl, 10 mM Tris/HCl, pH 8.0 at 25°C. The Sephadex slurry and cholate buffers were previously degassed. Bacteriorhodopsin/cholate micelles were eluted with the above buffer (flow rate 30cm^3 hr^{-1}) and collected in 10cm^3 fractions. The first six bacteriorhodopsin/cholate fractions (which accounted for ~75% of the protein) were pooled (~60 cm^3) and concentrated to 6 cm^3 using an Amicon pm10 ultrafiltration membrane.

iii) removal of the detergent by dialysis with concomitant reconstitution of the bacteriorhodopsin and added deuterated DMPC into protein /lipid bilayers. Deuterated DMPC was dried down with N_2 gas from chloroform/methanol in a glass vial and then

under vacuum (10^{-2} torr; 15hrs.) and resuspended in 1% cholate buffer. The mixture was tip-sonicated at 25°C for 1 - 2 minutes until the bilayer milkiness disappeared. The appropriate amount of bacteriorhodopsin/cholate micelles was added and stirred in the dark for 15 minutes and then dialysed against 2.5l buffer at 25°C in the dark. Dialysis buffer was changed 2 - 3 times a day.

Two different dialysis techniques were used that produced different rates of cholate removal. In the slow cholate removal procedure, the initial buffer contained 0.1 - 0.2% (w/w) sodium cholate in addition to 150mM NaCl, 10mM Tris/HCl, 1mM EDTA, pH 8.0, 0.025% azide. Vesicle formation was judged to have occurred from the increased turbidity in the dialysis tubing. Once vesicles had formed, usually after 4 - 5 days, the same buffer was used but without the cholate and Amberlite XAD-2 beads (B.D.H.) were added. These had previously been washed three times in acetone and then boiled in distiled water with frequent changes. After a week of dialysis, the buffer was changed to 10 mM Tris/HCl, pH 7.5 for 2 days. In the fast cholate removal technique the initial dialysis buffer (150mM NaCl, 10mM Tris/HCl, pH 8.0, 1mM EDTA) contained no cholate. Washed Amberlite XAD-2 beads were added after 2 - 3 days and dialysis continued for 4 - 5 days with twice daily changes of buffer. In both methods, the contents of the dialysis tubing (usually 10 - 12 cm^3) were loaded onto a 5 - 35% (for lipid/protein ratios greater than 100:1) or a 15 - 45% (for higher protein content vesicles) linear sucrose density gradient (250,000g; 4°C; 4hrs; Beckman Type SW40 rotor). The major band (if minor bands were present) was washed free of sucrose in 10 mM Tris/HCl, pH 7.5 (three centrifugations; 30min; 15°C; 100,000g) and then washed twice in the same buffer but made from deuterium depleted water for ^{2}H-NMR spectroscopy. The pellet (~2cm^3 containing 75mg DMPC) which was not found to be solidly packed was then loaded into a 10mm NMR tube using a Pasteur pipette.

Preparation of natural membranes labelled with deuterated lipids by nsTP. Deuterated DMPC, (with 0.1μCi [^{3}H]-DMPC-t_9 for some complexes), was dried down from $CHCl_3$/MeOH (2:1) first with nitrogen and then under heavy vacuum overnight on

the side of a glass vial. The lipid was resuspended in 3 cm^3 of 5mM phosphate/HCl buffer, pH 7.4 and tip sonicated at 25°C until the milkiness was replaced by an almost clear solution. The lipid suspension was then centrifuged (25,000g; 15 min; 15°C; Beckman Type 50 rotor) and the supernatnant used as the donor lipid vesicles.

To obtain different lipid/protein ratios in the final DMPC/PMPL/bR complexes, varying amounts of purple membrane were used. The desired amount of purple membrane was homogenised in 5 cm^3 of deionised water and mixed with the sonicated donor lipid vesicles. Partially purified nsTP extract (2cm^3) was added and the vial wrapped in silver foil and tape and incubated at 37°C for 60 hours with continual shaking.

Human erythrocyte ghosts were purified as described by Dodge *et al.*, (1963) and resealed by incubating at 37°C for one hour. 1 cm^3 of ghosts, 2cm^3 of nsTP extract and 3cm^3 of sonicated 3mg cm^{-3} DMPC-d_9 were mixed and shaken at 37°C for 48 hours.

Labelled membranes were washed twice by centrifuging (25,000g; 30min; 4°C for ghosts and 50,000g; 30min; 15°C for purple membrane complexes) to partially remove the remaining donor SUVs. Complete separation of unincorporated DMPC was achieved using a 10 - 45% linear sucrose gradients (in 10mM Tris/HCl, 1mM EDTA, pH 7.5) for purple membrane complexes (100,000g; 4°C; 18 hr; Beckman Type SW27 rotor) or a 10%, 20%, 30%, 40% sucrose step gradient for the ghosts. Membranes were then washed free of sucrose by three centrifugations, washed twice in buffer made from deuterium-depleted water and the pellet finally resuspended in 0.5cm^3 of buffer (made from deuterium-depleted water) and loaded into a 10mm NMR tube. For the 60:1 and 89:1 total lipid phosphate/bR mole ratio complexes and for the 21:7.6:1, 72:7.3:1 and 109:7.8:1 DMPC/PMPL/bR mole ratio complexes, after the final wash in 10mM Tris/HCl, 1mM EDTA, pH 7.5 (made in deuterium depleted water), the solid pellet was transferred into the NMR tube without resuspension in buffer.

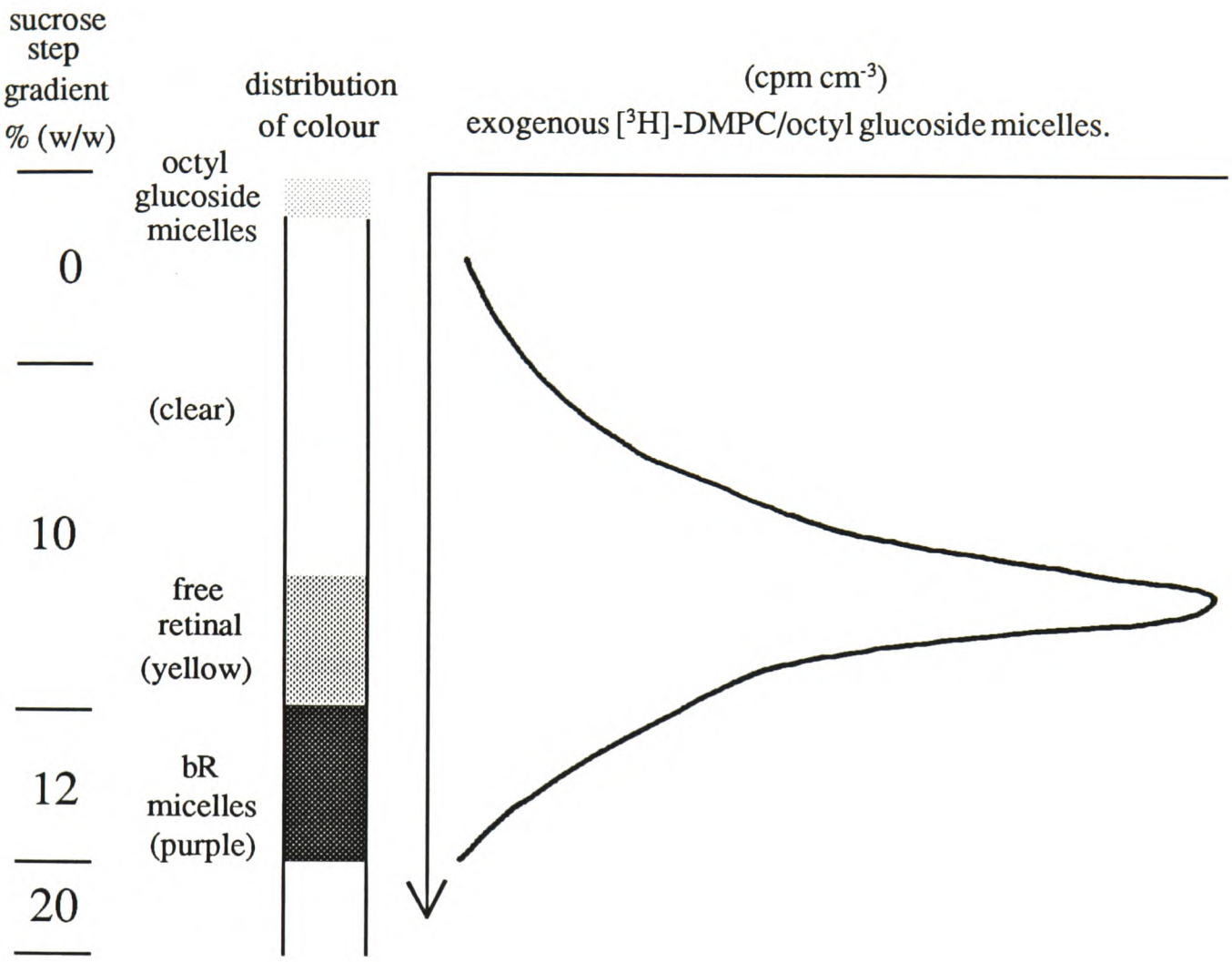


Fig. 1.2. Profile of distribution of lipid (DMPC) micelles (cpm) relative to that of bacteriorhodopsin micelles after sucrose step density gradient centrifugation (24 hr; 350,000g; 4 °C) of octyl glucoside-solubilized purple membrane and exogenous [^{3}H]-DMPC. 10/12/20% sucrose step gradient made using 60mM octyl glucoside buffer. Approximately 75% of the lipid micelles were separated from those containing bacteriorhodopsin.

1.IV. Results and Discussion.

Production of DMPC/bacteriorhodopsin complexes using detergents. It has been reported (Dencher and Heyn, 1978, 1983) that two non-ionic detergents, octyl-β-D-glucopyranoside and Triton X-100 efficiently solubilize purple membrane into bacteriorhodopsin monomers. Triton X-100 was used in preference to octyl glucoside for this present work since:-

i) bacteriorhodopsin proved rather unstable and susceptible to chromophore loss when solubilized in octyl glucoside particularly if exposed to the light.

ii) octyl glucoside was found to effect a less rapid and less complete solubilization of purple membrane when compared to Triton X-100. Typically, only 5 - 10% of the Triton X-100 treated purple membrane (as determined by A_{560nm}) was found to pellet after centrifugation (30 min; 100,000g); thus 90 - 95% of the purple membrane was considered to have been solubilized by Triton X-100 into bacteriorhodopsin monomers after 15 hr.

iii) octyl glucoside solubilized bacteriorhodopsin looses only 90% of the endogenous purple membrane lipid when passed down a gel-filtration column (Huang *et al.*, 1980), compared to 99.9% when using Triton X-100. The sucrose density gradient centrifugation method developed to separate endogenous purple lipid micelles from the bacteriorhodopsin micelles proved even less successful still (Fig. 1.2). The principle of this technique is that protein micelles being of higher density equilibrate further into the sucrose gradient than lipid micelles. Furthermore, endogenous purple membrane lipids would be expected to be displaced from protein/lipid micelles. A trail of yellow (free retinal form denatured bR) and brown (denatured bR) colouration was separated from the purple bacteriorhodopsin micelles at the 10%/12% sucrose boundary (Fig.1.2). The presence of denatured protein highlights the lability of bacteriorhodopsin solubilized in octyl glucoside. 75% of the exogenous [^{3}H]-DMPC, used as a tracer to detect lipid micelles occurred with the yellow retinal (Fig.1.2), while some 25% was inseparable from the purple bacteriorhodopsin micelles. Varying the sucrose concentrations in the step-gradient failed to improve the separation and the technique

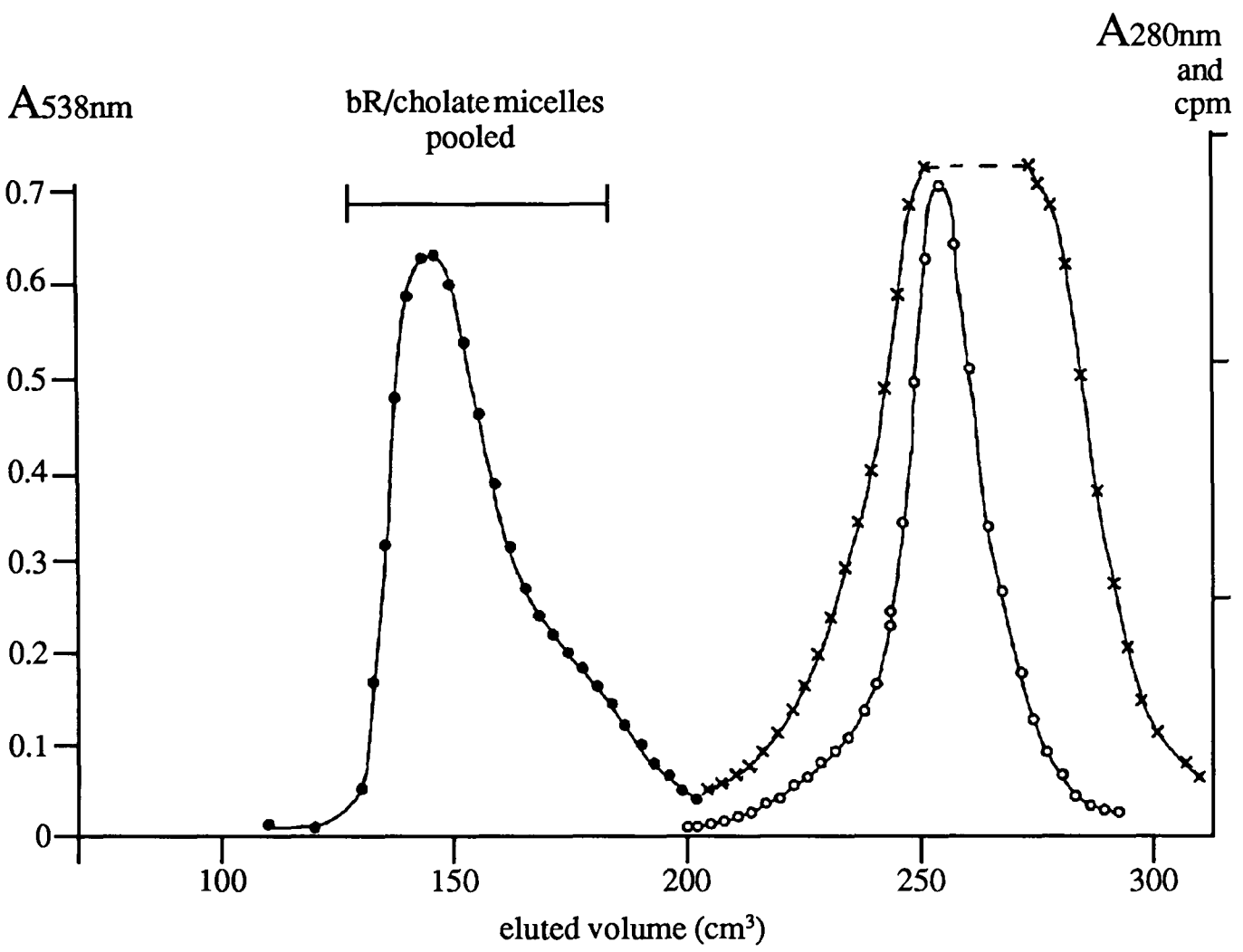


Fig.1.3.
Separation of Triton X-100 solubilized bacteriorhodopsin from Triton X-100 micelles and exogenous DMPC micelles using gel exclusion chromotography (as described by Huang, *et al* ., 1980).

- • bR/cholate micelles (Absorption at 538nm)
- • exogenous [^{3}H]-DMPC micelles (cpm)
- x Triton X-100 (Absorption at 280nm)

was abandoned in favour of gel-filtration methods.

In contrast, the gel filtration method of Triton X-100 solubilized-purple membrane was found to effect removal of all exogenous [^{3}H]-DMPC from the bacteriorhodopsin micelles and to displace the Triton X-100 with cholate. In order to monitor the efficiency of the gel-filtration column, 0.1μCi of exogenous [^{3}H]-DMPC tracer was mixed with 5 cm^3 of Triton X- 100 solubilized purple membrane before loading onto the column. 2.5cm^3 fractions were analysed. As shown in Fig.1.3, separation of the larger protein micelles (A_{max} 538nm) from the Triton X-100 (A_{max} 280nm) and exogenous [^{3}H]-DMPC tracer lipid micelles (cpm) is very efficient. It must be stressed, however, that elution of the [^{3}H]-DMPC micelles may not, but probably does, correspond exactly to the endogenous purple membrane lipid micelles.

Using this Triton X-100 solubilization and cholate gel-filtration method, seven DMPC-d_9/bacteriorhodopsin complexes of ratios (mol/mol) 68:1, 131:1, 141:1, 187:1, 242:1, 499:1 and 1,444:1, one DMPC-d_4/bacteriorhodopsin complex of ratio 379:1, and five DMPC-d_4-d_9/bacteriorhodopsin complexes of mole ratios 67:1, 95:1, 182:1, 218:1 and 222:1 were produced. Of these, the 187:1, 242:1, 499:1 and 1,444:1 DMPC-d_9/bR vesicles were produced by the fast cholate removal dialysis technique; all the others were produced by the slow cholate removal method.

Analysis of bovine liver non-specific lipid transfer protein. A silver stained 15% polyacrylamide gel in the presence of SDS of the partially purified nsTP preparation (used for labelling procedures), and a highly purified sample of nsTP after octyl agarose column (used for high resolution ^{1}H-NMR studies), is shown in Fig.1.4. The final step of the purification (octyl agarose column) displays two resolvable bands that are the two isozymes of nsTP. The low molecular weight of the protein - 14,500 Da - (Crain and Zilversmit, 1980a), makes nsTP an obvious choice for high resolution ^{1}H-NMR studies to investigate the membrane and lipid binding functions. At high concentrations, however, the protein had a tendency to aggregate. Under conditions of low ionic strength and acidic pH, aggregation appears to be prevented. A high resolution ^{1}H-NMR spectrum at 300 MHz of the two isozymes in 5mM phosphate, pH 3.5 was

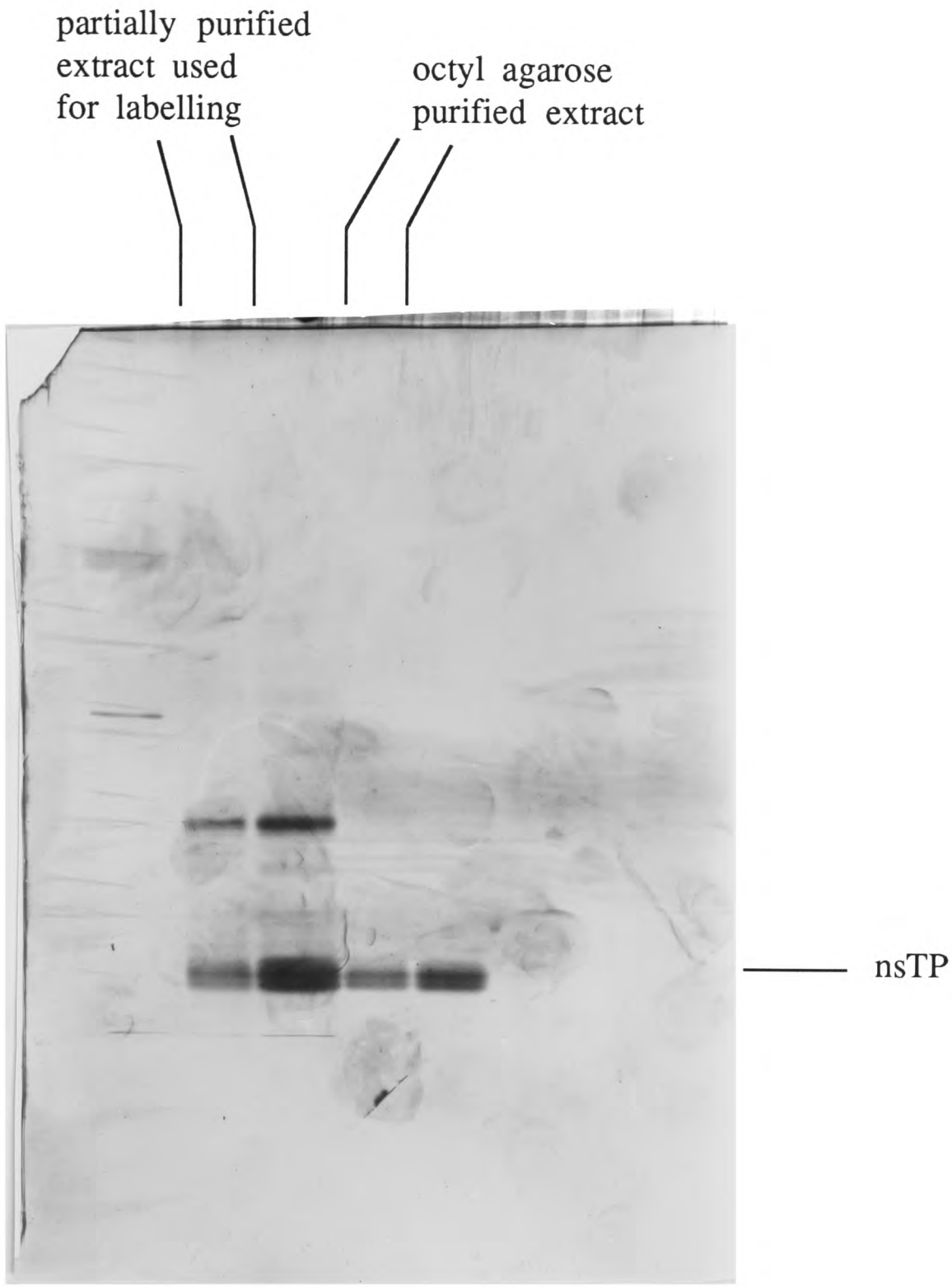


Fig.1.4. Silver stained SDS PAGE (15%) of bovine nsTP (25mg) purified as described by Crain & Zilversmit (1980a). The octyl-agarose chromatography step displays the two isozymes of nsTP as the only protein. The partially purified extract was used for incorporating DMPC into purple membrane.

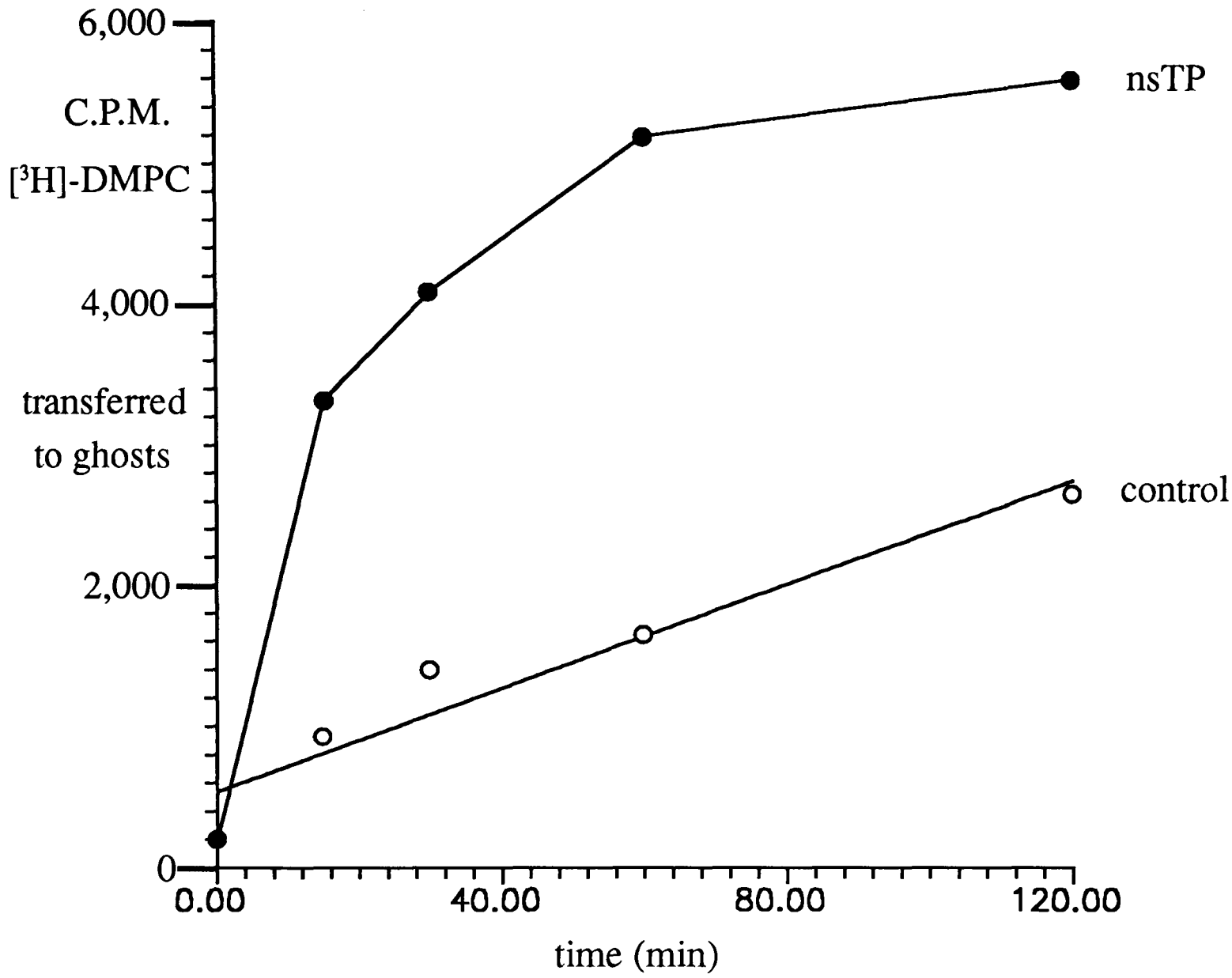


Fig.1.5.
Transfer of DMPC-t_9 from DMPC SUVs to resealed erythrocyte ghosts by partially purified nsTP extract and free diffusion. Buffer; 25mM sodium phosphate, 45mM NaCl, 5mM β-mercaptoethanol, pH 7.4.

obtained (not shown). Addition of 16-stearic acid spin-label (SASL) appeared to selectively broaden out the aromatic resonances implying a function of aromatic residues in the lipid binding site. The partially purified nsTP-extract used for the labelling of purple membrane displayed two major bands, one of which corresponded to nsTP. DMPC transfer activity in the partially purified nsTP extract as monitored by incorporation of [^{3}H]-DMPC into bovine red blood cell ghosts revealed active nsTP preparations (Fig. 1.5) and significant lipid transfer relative to nsTP-free controls.

Production of DMPC/bacteriorhodopsin complexes by nsTP-mediated transfer of DMPC. Phospholipid transfer proteins can only transfer lipids from the external leaflet of a membrane. They do not move lipids across bilayers. On suspending phospholipids in aqueous buffers, large multilamellar vesicles form spontaneously, in which most of the lipid would be unavailable to the nsTP and hence rendered unavailable for transfer by the outer vesicle. On tip sonication, however, these large concentric structures are broken into small unilamellar vesicles - SUVs (Watts *et al.*, 1979). Due to the high radius of curvature of the small unilamellar vesicle membrane more lipid (~66%) is accommodated in the outer leaflet (Berden *et al.*, 1975) than the inner leaflet. In addition, SUVs are unilamellar and there are no vesicles excluded from the exchange protein by an outer vesicle. Hence SUVs present the maximum amount of the donor lipid to the exchange protein for transfer to the erythrocyte ghosts or the purple membrane. The efficiency of sonication of the DMPC dispersions into SUVs was monitored by measuring the [^{3}H]-DMPC counts in solution, before and then after, centrifugation (25,000g; 15 min). Usually 95 - 98% of the radioactivity did not pellet as large multilamellar structures.

Four DMPC-d_9/bacteriorhodopsin complexes and one DMPC-d_4/bacteriorhodopsin complex were produced in which incorporation of DMPC was monitored using [^{3}H]-DMPC. Table 1 shows the amounts of lipid and purple membrane mixed, the calculated efficiency of incorporation and the final lipid/protein ratio obtained. In addition, four complexes of total lipid phosphate/bacteriorhodopsin mole ratios - 36:1, 85:1, 89:1 and 123:1 - were produced. For these 75mg of DMPC-d_4/-d_9

(4:1 w/w) mix was used.

Table 1. Analysis of nsTP-produced DMPC/bR complexes.

lipid type	lipid mixed (mg)	purple membrane (mg bR+)	% incorp-orated DMPC-t_9♣	final complex ratio (total moles P/bR)	mols PC added per mol bR*
DMPC-d_9	23.9	5	63	152:1	132
DMPC-d_9	70	20	55	88:1	68
DMPC-d_9	13.9	10	84	65:1	45
DMPC-d_9	17.5	20	69	31:1	11
DMPC-d_4	115	90	71	60:1	41
purple membrane	--	--		19.5:1	--

♣ c.p.m. recovered from purple band/total c.p.m. initially added to reaction x 100.
* calculated from total phosphate/protein ratio by assuming all 20 purple membrane phosphates were retained per bR monomer.
+ calculated from A_{max} using molar extinction coefficient of 54,000 M^{-1}.

The most important feature of these nsTP-produced complexes is that by varying the relative amounts of donor lipid SUVs and purple membrane, vesicles of a variety of total lipid phosphate/protein ratios from 31:1 to 152:1 (mol/mol) can be produced. Protein and lipid analysis of purple membrane reveals a total phosphate/protein ratio (mol/mol) of 19.5:1. From this, the nsTP must be catalyzing a net transfer of DMPC from the donor vesicles to the purple membrane. Indeed, assuming no exchange of endogenous purple membrane lipids, a minimum of from 11 to 132 DMPC molecules per bacteriorhodopsin molecule are seen to be successfully incorporated by nsTP. As reported previously (Crain and Zilversmit, 1980b), nsTP is not restricted to catalysing a

strict 1:1 exchange as PC specific transfer protein (PC-TP) (Helmkamp, 1980) does, but rather effects a net transfer.

From phosphate/protein analysis and high resolution phosphorus-31 NMR studies (presented in Chapter 2), each bacteriorhodopsin molecule in purple membrane appears to be associated with 10 purple phospholipids, although lower values are reported (Kates, *et al.*, 1983). In addition there are some glycosulphates and non-polar lipids (Kates, 1978; Kates, *et al.*, 1983). If, nsTP catalysed a strict 1:1 exchange with purple membrane phospholipids, then a maximum of around ten DMPC molecules could be incorporated. This is clearly not the case. Furthermore, if bacteriorhodopsin exerts a strong affinity for the endogenous purple membrane lipids, it is unlikely that nsTP will effectively exchange them for DMPC (as shown in Chapter 2).

The linear sucrose density gradient serves as a final purification step for each complex to remove any remaining donor DMPC SUVs, which would clearly add an undesirable isotropic signal to the ^{2}H-NMR spectra. For high protein/lipid ratio complexes the efficiency of transfer was very high - between 70 and 85% (Table 1). All the complexes equilibrated on a 10% to 45% linear sucrose gradient as a single sharp band implying the vesicles were of homogeneous lipid/protein ratio (discussed further in Chapter 2). For the three high protein/lipid ratio complexes, all the DMPC-t_9 occurred in the purple band; there being no trace of unincorporated DMPC near the top of the gradient. For the 88:1 and 152:1 total lipid phosphate/bR mole ratio complexes, however, some pure unincorporated lipid was found at the low density end of the gradient as a diffuse white band. This may be due to an instability of vesicles with relatively high amounts of lipid, resulting in their fragmentation on the density gradient at 4°C into pure lipid vesicles and complexes of higher protein/lipid ratio, or more likely due to incomplete removal of SUVs during the washes.

The two highest phosphate/protein ratios produced were 123:1 and 152:1, indicating a minimum net addition of 103 and 132 DMPC molecules per bacteriorhodopsin molecule. Even with excess donor SUVs (sufficient to produce complex ratios of 500:1), complexes of total lipid phosphate/protein ratio greater than

152:1 could not be produced. Clearly, this is one of the limitations of the technique and may reflect the mechanism of vesicles production.

Mechanism of vesicle formation by nsTP-mediated DMPC transfer. Negative stain electron microscopy revealed the nsTP produced complexes to consist of regularly sized (200-300nm diameter) vesicles which appear to be unilamellar. Purple membrane is different to other lipid bilayer membranes in that its rigid paracrystalline lattice structure prevents it from forming closed vesicles. Instead it exists as flat patches (Oesterhelt & Stoeckenius, 1974). So it is likely that nsTP adds lipids to both sides of these purple membrane sheets. As more DMPC is added, and at 37°C so the bacteriorhodopsin aggregates begin to disperse allowing the membranes to become more flexible and so seal to form vesicles. It is conceivable that vesicle formation may limit the size and lipid-protein ratio attainable with the technique. Once vesicles have formed, further net addition of DMPC may be slow and replaced by 1:1 nsTP-mediated exchange.

Spectroscopic properties of the chromophores in the two types of complexes. All complexes displayed the deep purple colour characteristic of purple membrane. UV/vis absorption spectra of the complexes against buffer blanks reveal increasing Rayliegh scattering at shorter wavelengths due to the liposomes. The determined A_{max} from such spectra is thus an apparent value. Actual values can be obtained using bacteriorhodopsin vesicles incubated with hydroxylamine, pH 7.5, as blanks. Hydroxylamine displaces the retinal chromophore from bacteriorhodopsin, effectively bleaching the sample. For the 21:7.6:1 and 72:7.3:1 mole ratio nsTP-produced complexes actual absorption maxima of 555nm and 554nm, respectively were measured at neutral pH. For the 67:1 DMPC/bR complex with all endogenous purple membrane lipids removed the actual A_{max} occurred at 562nm in vesicles at neutral pH (Fig.7.6.d). A value of 560nm is obtained for purple membrane in good agreement with published values (Oesterhelt & Stoeckenius, 1974). It would appear that the chromophore properties of the bacteriorhodopsin in complexes at neutral pH are not

disrupted by the techniques used to produce the vesicles. The chromophore properties are further studied in Chapter 7.

Chapter 2

Characterisation of the DMPC/bacteriorhodopsin complexes.

2.I) Introduction.

In the previous chapter, two very different methods were described for producing DMPC/bacteriorhodopsin lipo-protein complexes. While the vesicles produced according to Huang *et al.*, (1980) have been previously characterised with respect to endogenous purple membrane phospholipid content, the nsTP-mediated insertion of exogenous phospholipids into purple membrane is an as yet unpublished technique. Before interpretations and comparisons of solid-state ^{2}H-NMR data from complexes with different lipid/protein can be made, the vesicles must be characterised and their macroscopic properties shown to be consistent for all lipid/protein ratios. Two such properties of the vesicles that could considerably influence broadline ^{2}H-NMR spectra lineshapes and measured quadrupole splittings are the size of the lipid-protein complexes and the homogeneity in the same complex with respect to lipid protein ratio. It is possible to use linear sucrose density gradients to separate lipo-protein complexes according to protein content and also to assess the homogeneity of the vesicles with respect to lipid-protein ratio (Knowles *et al.*, 1979). Vesicle size can be determined by negative stain electron microscopy and although phospholipid bilayers do not contain enough electron dense atoms to be seen directly by electron microscopy the sample can be stained with an oxo-acid form of a large metal atom, usually tungsten, osmium or uranium.

Determination of the phospholipid composition (with respect to headgroup types) of the complexes produced by the two methods is also essential information which is required before conclusions on aggregation, packing and solubility can be assigned to lipid environment. Only a single exogenous phospholipid (DMPC) that is homogeneous and chemically well-defined was used in the present work to produce each complex.

The purple membrane itself is relatively protein-rich. The endogenous lipids present in the purple membrane, however, are unusual (Kates, 1978) and their presence or absence in exogenous lipid vesicles of egg PC and asolectin has been shown to influence the packing properties of the bacteriorhodopsin particles (Hwang and Stoeckenius, 1977) by freeze fracture electron microscopy.

It is reported that high resolution ^{31}P-NMR of phospholipids solubilized in detergent micelles (London and Feigenson 1979) or CHCl3/MeOH (Sotirhos *et al.*, 1986) is a powerful technique for analysing the phospholipid headgroup composition of phospholipid bilayer membranes (e.g. sarcoplasmic reticulum and hearts (Mogelson *et al.*, 1980)). Different headgroup phosphate nuclei exhibit characteristic chemical shifts. This method has been successfully used to identify and quantify the phospholipids in lipid-rich and lipid-depleted detergent solubilized cytochrome *c* oxidase (Seelig and Seelig, 1985). Furthermore the pK_a of the phosphate moiety in detergent solubilized phospholipids may be determined by pH titration. This method has allowed assignment of the PC and PE resonances in a mixture of the two phospholipids (London and Feigenson, 1979).

The chemical shift of the resonance for any one phospholipid depends in part on the ability of the phosphate group to form intra-molecular hydrogen bonds (Henderson, *et al* 1974). The phosphate of the PC headgroup, which is unable to form intramolecular hydrogen bonds, resonates at the highest magnetic field. Downfield shifts are consistent with deshielding of the ^{31}P nucleus by hydrogen bonding interactions of amine, amide or hydroxyl protons with a phosphate oxygen.

The proportion of lipid to protein in the purple membrane is very low and approximates 0.25:1 (w/w); there being some seven total lipids per bacteriorhodopsin monomer (Kates *et al.*, 1983). Blaurock (1975) estimated the composition of isolated purple membrane to correspond to ~10 total lipids per protein. The most comprehensive lipid analyses of halophilic bacteria reported so far were performed on the purple membrane of *Halobium cutirubrum* (Kates, 1978; Kates *et al.*, 1983). The lipid composition, however, of *H.halobium* purple membrane is reported to be essentially

identical to that of *H.cutirubrum* (Kushwaha *et al.*, 1976; Kates *et al*, 1983). *H.cutirubrum* purple membrane lipids are composed of 10% neutral lipids and 90% polar lipids. The polar lipids include the phospholipids and glycolipid sulphate. Glycolipid sulphate accounts for 28% total polar lipids. Purple membrane and red membrane from the extremely halophilic bacterium, *H.cutirubrum* display an unusual phospholipid composition, both in alkyl chains and headgroup (Kates 1978). The major phospholipid species is the ether linked diphytanyl phosphatidylglycerol phosphate (PGP). About 61 mol% of *H.cutirubrum* purple membrane polar lipids is PGP (Kates *et al.*, 1983). In addition in purple membrane 5 mol% of the polar lipids is phosphatidylglycerol sulphate (PGS) and another 6 mol% phosphatidylglcerol (PG). The exact mole ratios of lipid to bacteriorhodopsin reported varies. Kates *et al* (1983) report about seven total lipids (i.e. six polar lipid molecules) per 26,000M_r bacteriorhodopsin monomer, while Blaurock & Stoeckenius (1971) report double this amount i.e. 12 polar lipids per bR. Thus, since phospholipids account for 72% of the polar lipids then between 4 and 9 phospholipid molecules are present per bacteriorhodopsin monomer in the purple membrane.

Purple membrane lipids when extracted into chloroform, show two major resonances (Goni, *et al.*, 1982) by ^{31}P-NMR although chemical shift values were not reported. These authors on the basis of position of the monoester phosphate of phosphatidic acid relative to the diester phosphate of cardiolipin, assigned the low field peak as the PGP–γ-resonance and the other peak the PGP-α phosphorus. No definite assignment for the α- and γ-PGP resonances was thus made.

In this chapter, the phospholipid composition of detergent solubilized *H.halobium* purple membrane and also red membrane is studied by ^{31}P-NMR. Attempts to assign the PGP resonances were made by titrating against pH in an anionic detergent (SDS) and a non-ionic detergent (Triton X-100). Binding of Ca^{++} ions to the phosphate groups in Triton X-100 micelles was also investigated to aid assignment.

The resonances from the *H.halobium* phospholipids were sufficiently separated from that of DMPC for high resolution ^{31}P-NMR examination of SDS solubilized

complexes to be useful in quantifying the phospholipid headgroup composition of the DMPC/bR complexes produced as described in the previous chapter for solid state ^{2}H-nmr. Using ^{31}P-NMR the complete absence of *H.halobium* phospholipids could be confirmed in the complexes produced as described by Huang *et al.*, (1980) and a quantification of the number of moles of *H.halobium* PGP with each bacteriorhodopsin molecule retained after nsTP-mediated incorporation of DMPC could be made. Phospholipid analysis of nsTP-produced complexes by high resolution ^{31}P-NMR reveals the retention of the majority of endogenous purple membrane phospholipids.

2.II) Materials and Methods.

Vesicle size was determined by negative stain electron microscopy. Vesicle suspension (diluted in 10mM Tris/HCl, pH 7.4) was placed on a Formar coated grid and excess liquid removed with blotting paper. The sample was negatively stained with 2% aqueous uranyl acetate. Electron microscopy was preformed on a Philips scanning electron microscope. A magnification of 28,000 with normalisation for each photograph was used. Vesicle sizes were measured from the negative.

DMPC and DMPG (ammonium salt) were purchased from Sigma Chemical Co.. Sulphur trioxide-pyridine was obtained from Aldrich Chemical Co.. DMPG was sulphated as described by Hancock & Kates, (1973), only toluene was used instead of benzene. The reaction was terminated by adding 1M Na_2CO_3 to hydrolyse any remaining SO_3-pyridine. The pH was adjusted to 2 and the lipids extracted into chloroform/methanol.

Purple membrane was purified from cultures of *H.halobium* as described by Stoeckenius and Oesterhelt (1974). Red membrane was purified from *H.halobium* which had lost the ability to produce large amounts of purple membrane. Whole cell membrane was homogenised in 0.1M NaCl, and separated from trace amounts of purple membrane on a 30 - 50% linear sucrose gradient (0.1M NaCl). Red membrane was then washed in 1M NaCl, Tris/HCl by centrifugation (100,000g; 40min; 15°C).

A single DMPC/bR complex of total lipid phosphate/bR mole ratio ~60:1 was

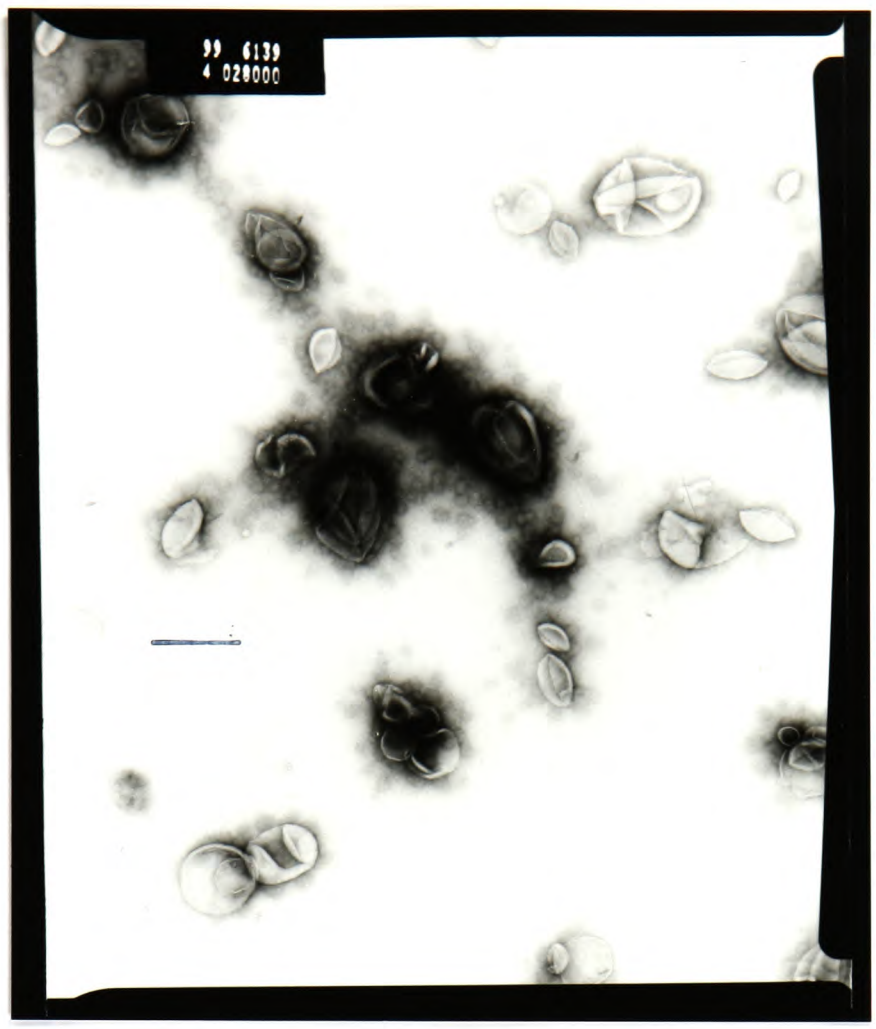
prepared with all the endogenous purple membrane phospholipids retained as described in Cherry *et al.*, (1978), but using octyl glucoside instead of Triton X-100.

In order to solubilize in detergents the purple membrane or DMPC/bR lipo-protein complex was pelleted and solubilization achieved with 4% SDS, 100mM Tris/HCl, pH 7.4 (20 min). Using Triton X-100 7.5% (w/w), 100mM Tris/HCl, pH 7.0, the purple membrane was allowed to stir for 15 hrs (Dencher & Heyn, 1978). Any unsolubilized material was pelleted (100,000g; 15 min; 25°C) and the supernatant (yellow/orange for SDS) used for high resolution ^{31}P-NMR. The detergent solutions were prepared in D_2O instead of water to provide a lock.

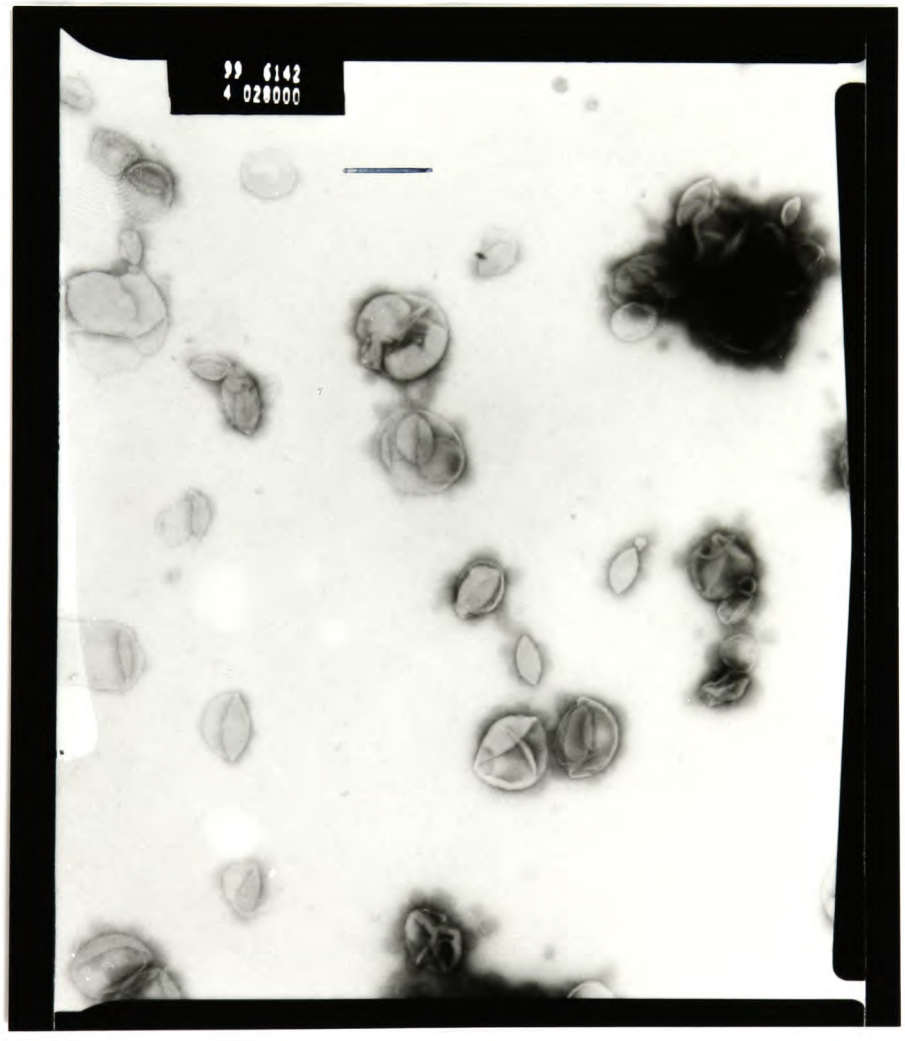
H.halobium polar lipids were extracted from lysed whole cell membranes as described by Kates, *et al.*, (1983) and separated from the non-polar lipids and retinal released from the two proteins by acetone precipitation. The precipitated lipids were collected on a 1μm filter and dissolved in $CHCl_3$/MeOH/HCl (2:1:0.1), and rotary evaporated. The extracted polar lipids were analysed by TLC ($CHCl_3$/MeOH/ 90% acetic acid; 30:4:10; v/v) staining with molybdenum blue spray to detect phosphate containing components. The lipid was suspended in 100mM Tris/HCl, pH 7.8 and tip-sonicated until a clear solution was obtained.

N.M.R. High resolution ^{31}P-NMR spectra were obtained using single 90° pulses (PW 16μs) at 145.9 MHz with a dedicated phosphorus probe and an Oxford Instruments 360 superconducting magnet. Spectra were collected into 4K points with a dwell time of 166μs (sweep width 6,000Hz) after a pre-acquisition delay of 50ms. A relaxation delay of 1 s was applied, although for quantitative spectra this was increased to 4s. For T_1 and T_2 determinations of isotropic phospholipids, a relaxation delay of 20s was used. T_1 measurements were made with the inversion recovery method and T_2 by the Carr-Purcell spin echo pulse sequence. 1mM Methylene diphosphonate - (MDP) in D_2O, 5mM Tris/HCl, pH 8.0 in a coaxial insert was used as a chemical shift reference. Phosphonates resonate well downfield (~17 ppm) of the phospholipid peaks.

Vesicles homogeneity with respect to lipid/protein ratio was assessed from the linear sucrose density gradient centrifugation (as described in Chapter 1) purification



a)

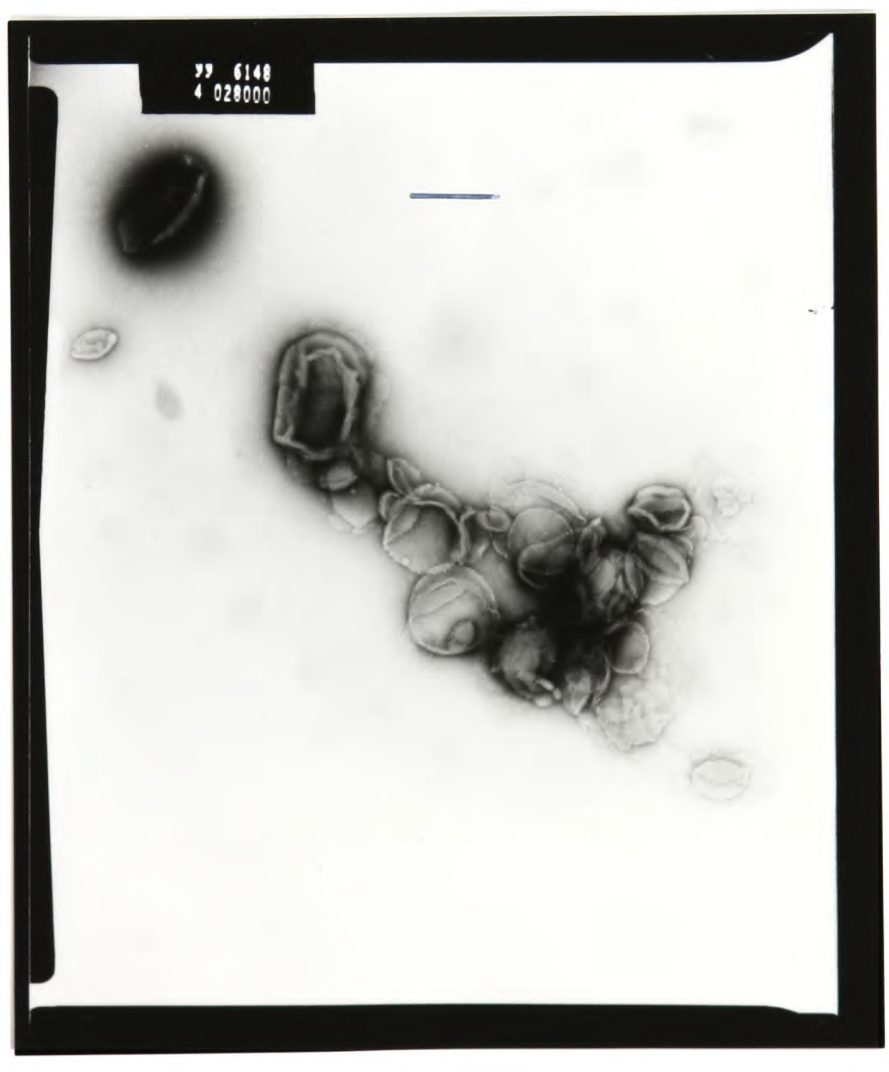


b)

Fig.2.1. Negative stain electron micrographs of DMPC/purple membrane vesicles produced by the nsTP method; a) and b) 72:7.3:1 DMPC/PMPL/bR mole ratio complex; c) 21:7.6:1 DMPC/PMPL/bR mole ratio complex; and d) 89:1 total lipid phosphate/bR mole ratio complex. Magnification = 28,000x. Bar = 300 nm.



c)

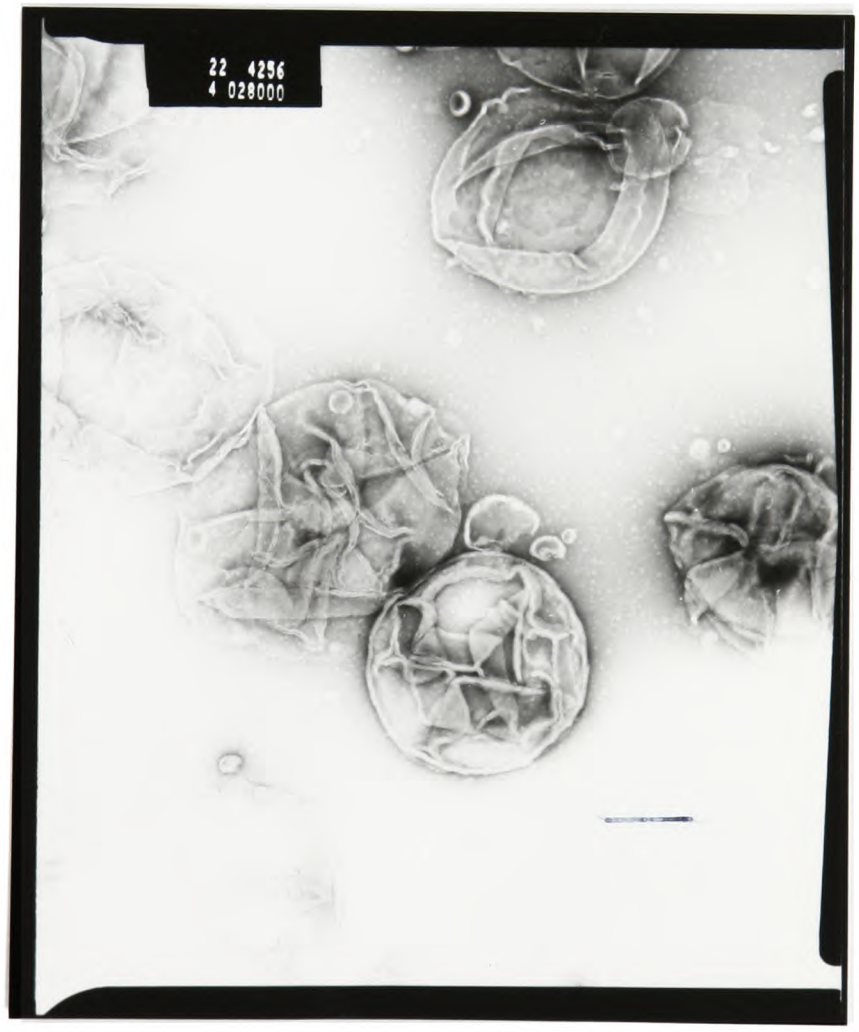


d)

Fig.2.1 (cont.)



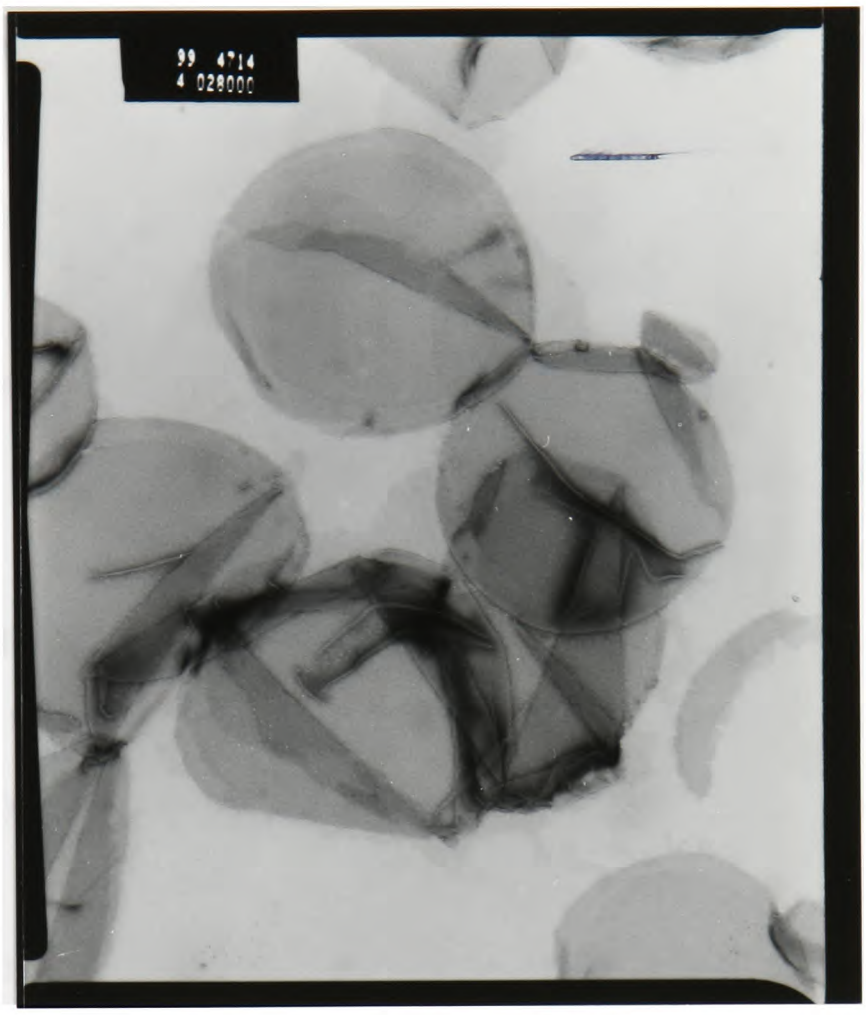
a)



b)

Fig.2.2. Negative stain electron micrographs of DMPC/bR complexes (all endogenous purple membrane lipids removed) of mole ratios; a) and b) 68:1; c) and d) 141:1 produced by the slow cholate removal technique. Magnification = 28,000x. Bar = 300 nm.

c)



d)

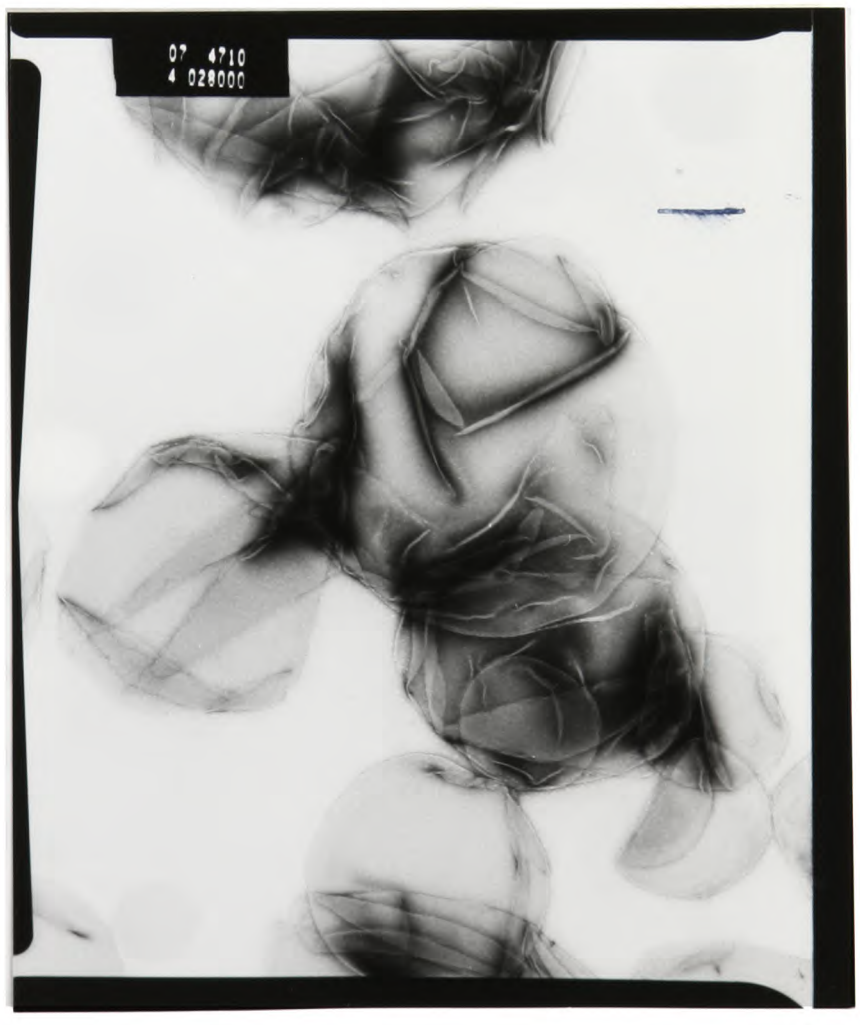


Fig.2.2 (cont.).

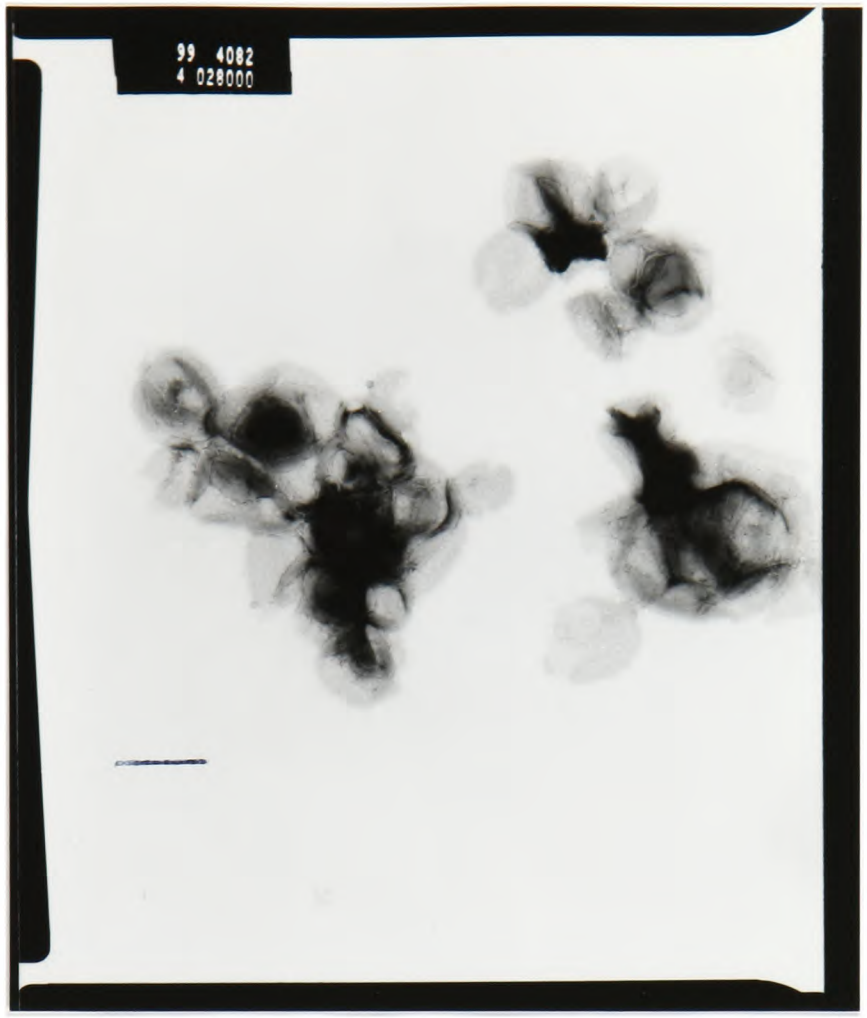
step. In addition, for the nsTP-produced complexes, small amounts of vesicles (~2mg bR) were loaded onto separate 10 - 40% gradients (made from 10mM Tris/HCl, 1mM EDTA, pH 7.5). To assess the limits of protein/lipid ratio homogeniety for the DMPC/bR complexes produced by the slow cholate removal technique, small quantities of the 222:1 and 182:1 DMPC/bR mole ratio complexes (~2mg lipid) were mixed and layered onto a linear 10 - 30% sucrose gradients (250,000g; 2hr; 4°C).

2.III) Results.

A). **Size of vesicles.**

i) DMPC/purple membrane complexes produced by nsTP-mediated DMPC transfer. Representative electron micrographs of the 72:7.3:1 and 21:7.6:1 mole ratio DMPC/PMPL/bR complexes and the 89:1 total lipid phosphate/bR mole ratio complexes produced by nsTP mediated lipid transfer are shown in Fig. 2.1. The vesicle sizes were found to vary with the complex. The 21:7.6:1 DMPC/PMPL/bR mole ratio complex (Fig.2.1.c) can be seen to be composed of a relatively uniform size of vesicle measuring between 150 and 200nm in diameter. For the 72:7.3:1 DMPC/PMPL/bR mole ratio complex, however, a more heterogeneous size distribution was observed. The majority of 72:7.3:1 mole ratio complex vesicles were found to be 200-350 nm in diameter, while some had diameters of up to 400nm and some as small as 150nm in diameter. The 89:1 total lipid phosphate mole ratio complex contained fewer small vesicles, with the majority being 200-350 nm in diameter and some being as large as 450nm.

ii) Reconstituted complexes produced by the slow cholate removal technique. Representative electron micrographs of the two DMPC/bR complexes with mole ratios of 68:1 and 141:1, and all endogenous purple membrane lipids removed, are shown in Fig.2.2. These vesicles were produced by slow removal of cholate detergent from the reconstitution mixture. For the 68:1 mole ratio complex the majority of the vesicles were between 700 and 1,100nm in diameter and several were larger at 1,500nm in diameter. Very few vesicles are less than 600nm in diameter and these may represent fragmented vesicles. The 141:1 mole ratio DMPC/bR complex also contained large



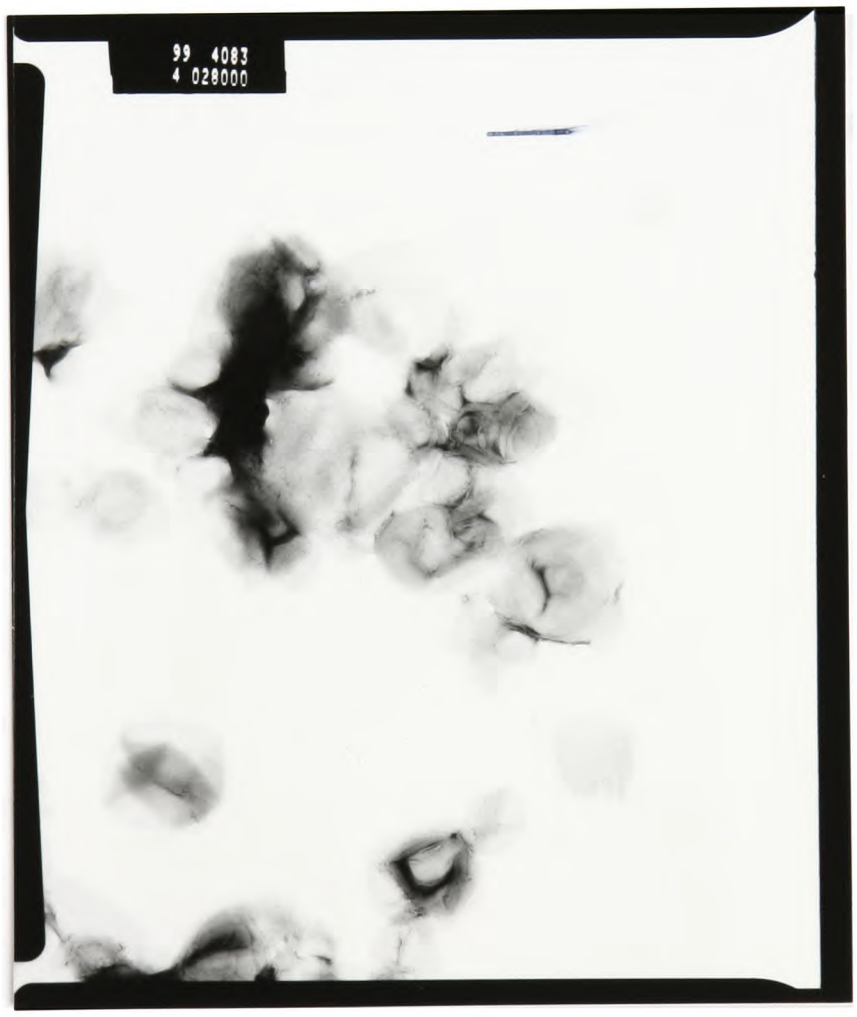


Fig.2.3. Negative stain electron micrographs of DMPC/bR complexes (all endogenous purple membrane lipids removed) of mole ratios; a) and b) 187:1; and c) 1,444:1 produced by the fast cholate removal technique. Magnification = 28,000x. Bar = 300 nm.

c)

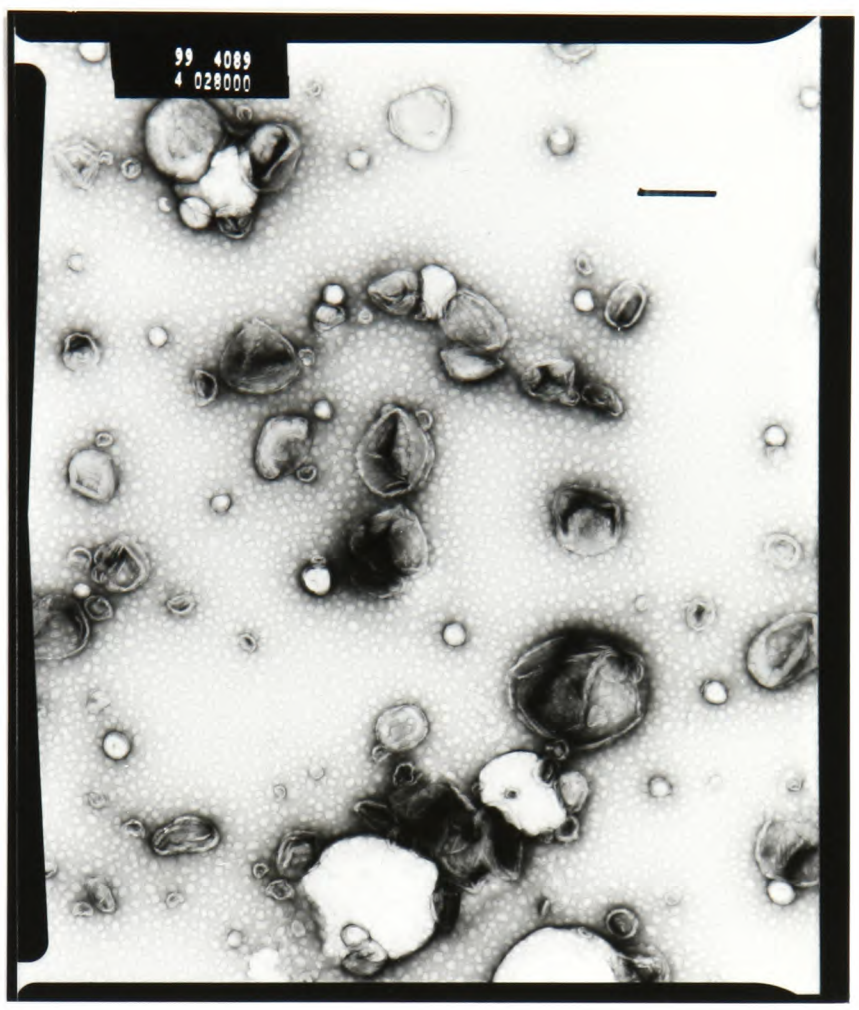


Fig.2.3. (cont.)

vesicles (1,000- 1,500nm diameter) of homogeneous distribution.

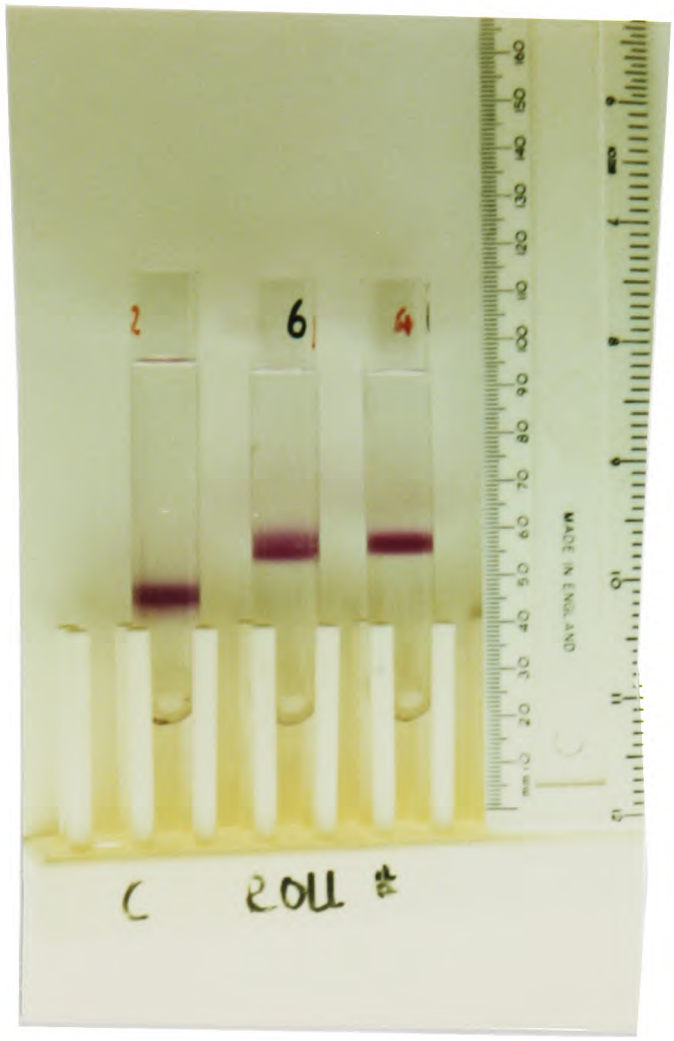
iii) Reconstituted complexes produced by the fast cholate removal technique. Representative micrographs of the 187:1 and 1,444:1 mole ratio DMPC/bR complexes, also with all purple membrane lipids removed, are presented in Fig.2.3. For the 187:1 mole ratio complex the vesicle size was found to be between 300 and 500nm in diameter. The 1,444:1 ratio exhibits even smaller vesicles. The largest vesicles are 200-300nm in diameter and many are smaller, being less than 100nm in diameter.

B). Homogeneity of lipid/protein ratio.

i). Complexes produced by detergent dialysis. Complexes produced by the fast cholate removal technique proved to be more prone to showing minor bands of significantly different lipid-protein ratio. Complexes, however, produced by slow cholate removal displayed a single sharp band. Indeed a mixture of the 182:1 and 222:1 complexes could be clearly resolved into two separate bands on a 10 - 30% linear gradient, while each complex alone revealed only a single sharp band (~1mm width). This demonstrates the slow cholate vesicles to be of very homogeneous protein/lipid content; the individual vesicles within the complex probably not varying by more than +/-5% with respect to DMPC/bR mole ratio for the complex.

ii). Complexes produced by nsTP-mediated DMPC transfer. During the vesicle purification, the complexes were loaded onto sucrose density gradients to remove any contaminating donor SUVs. For all complexes, all the purple colour (i.e. bacteriorhodopsin) was found to pre-equilibrate in a single band, indicating uniform homogeneity. The 21:7.6:1 and 72:7.3:1 mole ratio DMPC/PMPL/bR complexes and the 89:1 total lipid phosphate/bR mole ratio complex (see Chapter 5) were also loaded in small quantities onto 10 - 40% linear sucrose (10mM Tris/HCl, 1mM EDTA, pH 7.5) density gradients (250,000g; SW40 rotor; 4°C; 15hr) in order to assess more accurately the lipid content homogeneity of the vesicles. The gradients after centrifugation are shown in the photograph on the next page.

The 21:7.6:1 DMPC/PMPL/bR mole ratio complex has pre-equilibrated at higher sucrose densities as expected for higher protein content vesicles. The 72:7.3:1



Photograph to demonstrate lipid/bR homogeneity within vesicles produced by the nsTP method. 10 - 40% linear sucrose density gradients (250,000g; 4°C; 15 hr); left gradient, 21:7.6:1 DMPC/PMPL/bR mole ratio complex; centre gradient, 72:7.3:1 DMPC/PMPL/bR mole ratio complex; right gradient, 89:1 total lipid phosphate/bR mole ratio nsTP-produced complex.

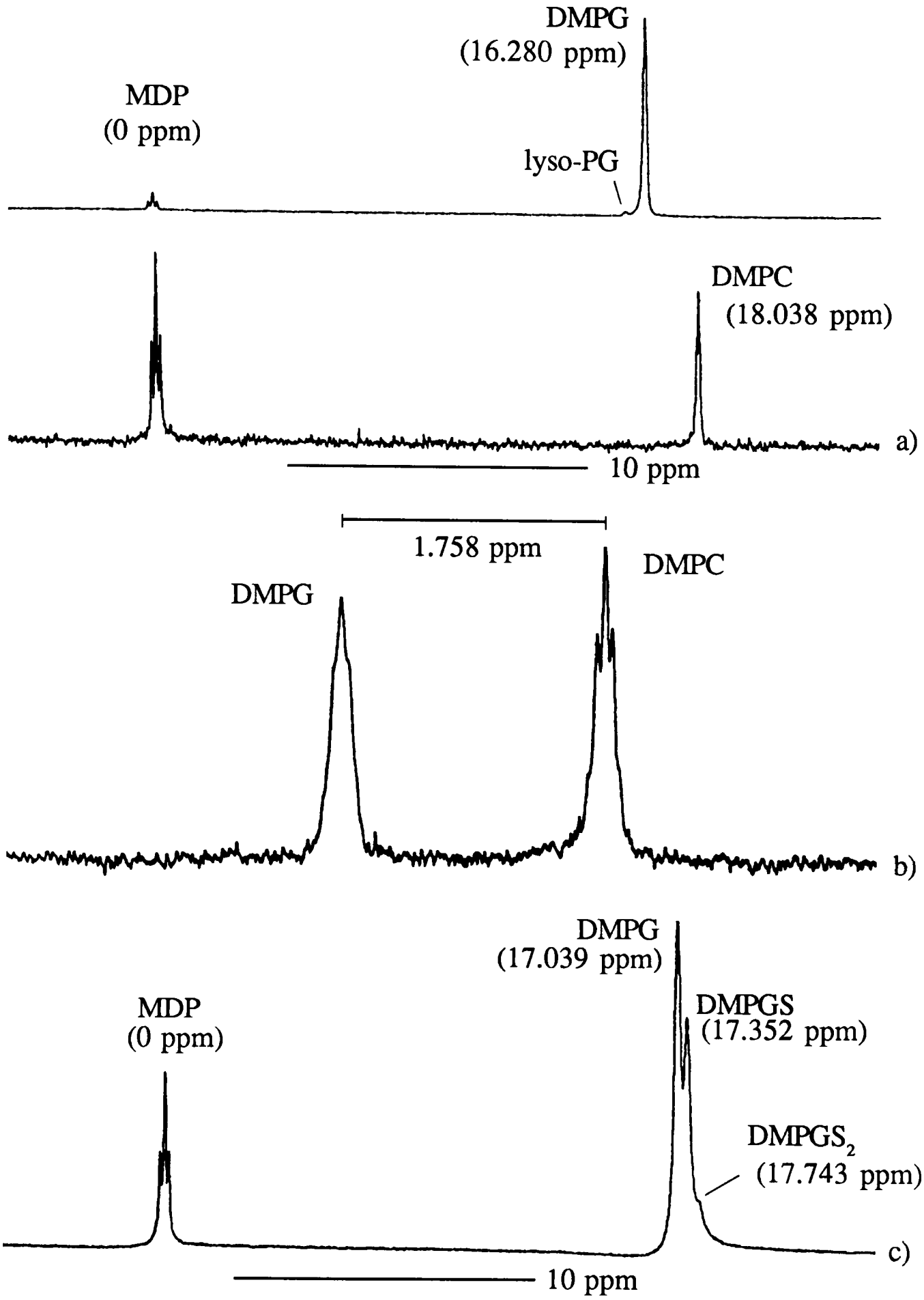


Fig.2.4. High resolution ^{31}P-NMR spectra (145.9 MHz) of synthetic phospholipids in $CHCl_3$/MeOH (2:1 vol/vol). The chemical shift depends on the headgroup type and the degree of protonation; a) spectra of DMPG and DMPC solubilzed from neutral pH with MDP as a chemical shift reference; b) DMPG and DMPC exhibit different J-coupling constants (lipids solubilized from neutral pH). The 1:4:6:4:1 quintet is more distinctive in DMPC; c) products of sulphation of DMPG with SO_3-pyridine solubilized from pH 2 (DMPGS; dimyristoyl phosphatidyl glycerol sulphate, $DMPGS_2$; dimyristoyl phosphatidylglycerol disulsulphate).

DMPC/PMPL/bR and 89:1 total lipid phosphate/bR mole ratio complexes, which have virtually identical lipid contents are seen to have pre-equilibrated at similar sucrose densities. The bands are very sharp indicating uniform lipid/protein ratio homogeneity within the vesicle populations for a given complex. Detailed inspection of the bands shows the 89:1 mole ratio complex to be a single component 3 mm in width. The 72:7.3:1 DMPC/PMPL/bR mole ratio complex consists of a major sharp band (2mm width) and in addition, just above, a much less intense sharp band. The 21:7.6:1 DMPC/PMPL/bR complex also displays a very homogeneous major band (1 mm width) and again an adjacent minor band (2mm width). These minor bands are of similar lipid/protein ratio to the major bands. Some indication of the vesicle size distribution could obtained by inspecting the gradient after 30min centrifugation. The 89:1 mole ratio total lipid phosphate/bR complex presented a single sharp band (5mm width), while the 21:7.6:1 DMPC/PMPL/bR complex gave a broad 10mm width band, not fully equilibrated.

C). **Phospholipid headgroup composition of purple membrane and DMPC/bR complexes by high resolution ^{31}P-N.M.R.**

The high resolution ^{31}P-NMR spectra (Fig.2.4a) of the synthetic phospholipids DMPG and DMPC dissolved in chloroform/methanol (2:1 vol/vol) each exhibit a single sharp well defined resonance, the chemical shift of which depends on the phospholipid headgroup. The DMPG resonance is 16.280 ppm upfield from MDP, while the DMPC phosphorus resonance is a further 1.758 ppm upfield from that of PG at 18.038 ppm. None of the spectra presented in Fig.2.4 were proton decoupled.

The MDP standard shows a triplet of intensities 1:2:1, while both the PG and PC phosphorus nuclei show J-coupling to the protons on the two adjacent CH_2 methylene segments (Fig.2.4.b). For the PC phosphorus nucleus, the J coupling constant is larger than for that of PG and the 1:4:6:4:1 quintet is distinct. The absolute chemical shifts (relative to external MDP) and the relative chemical shifts to each other are found to be dependent on the organic solvent. In chloroform alone the two phospholipid resonances are 1.300 ppm apart. On addition of methanol to one sample, the separation is found to

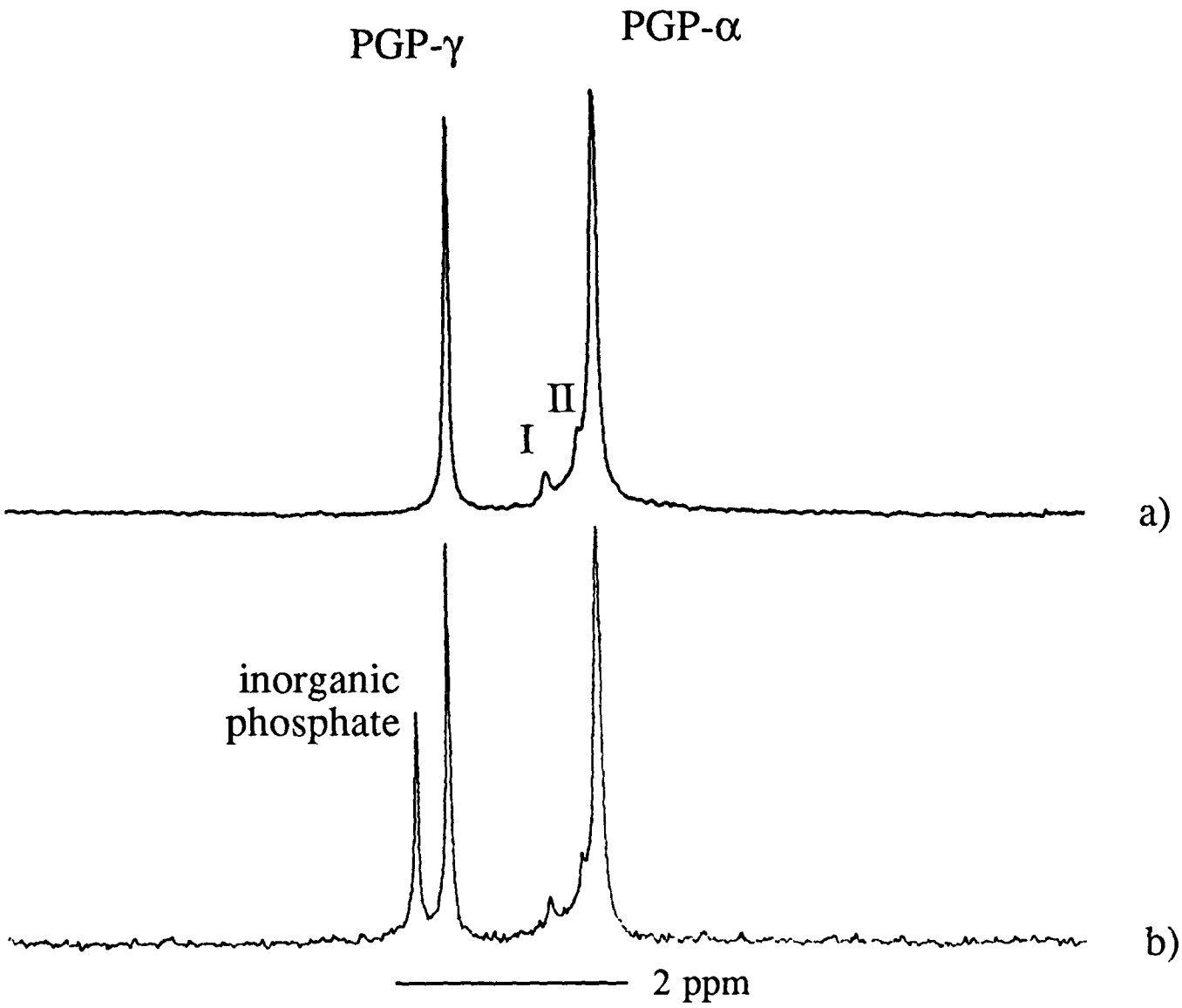


Fig.2.5. High resolution ^{31}P-NMR spectra of purple membrane solubilized in 4% SDS.
a) purple membrane alone, pH 7.8 (proton decoupled);
b) purple membrane with exogenous inorganic phosphate, pH 7.8 (proton decoupled);
c) purple membrane, pH 7.1 (not decoupled);
d) purple membrane, pH 12.7 (not decoupled) with spectrum integral above.
e) tip-sonicated aqueous polar lipids extracted from *H.halobium* whole cell membranes as described by Kates, *et al* ., (1983).

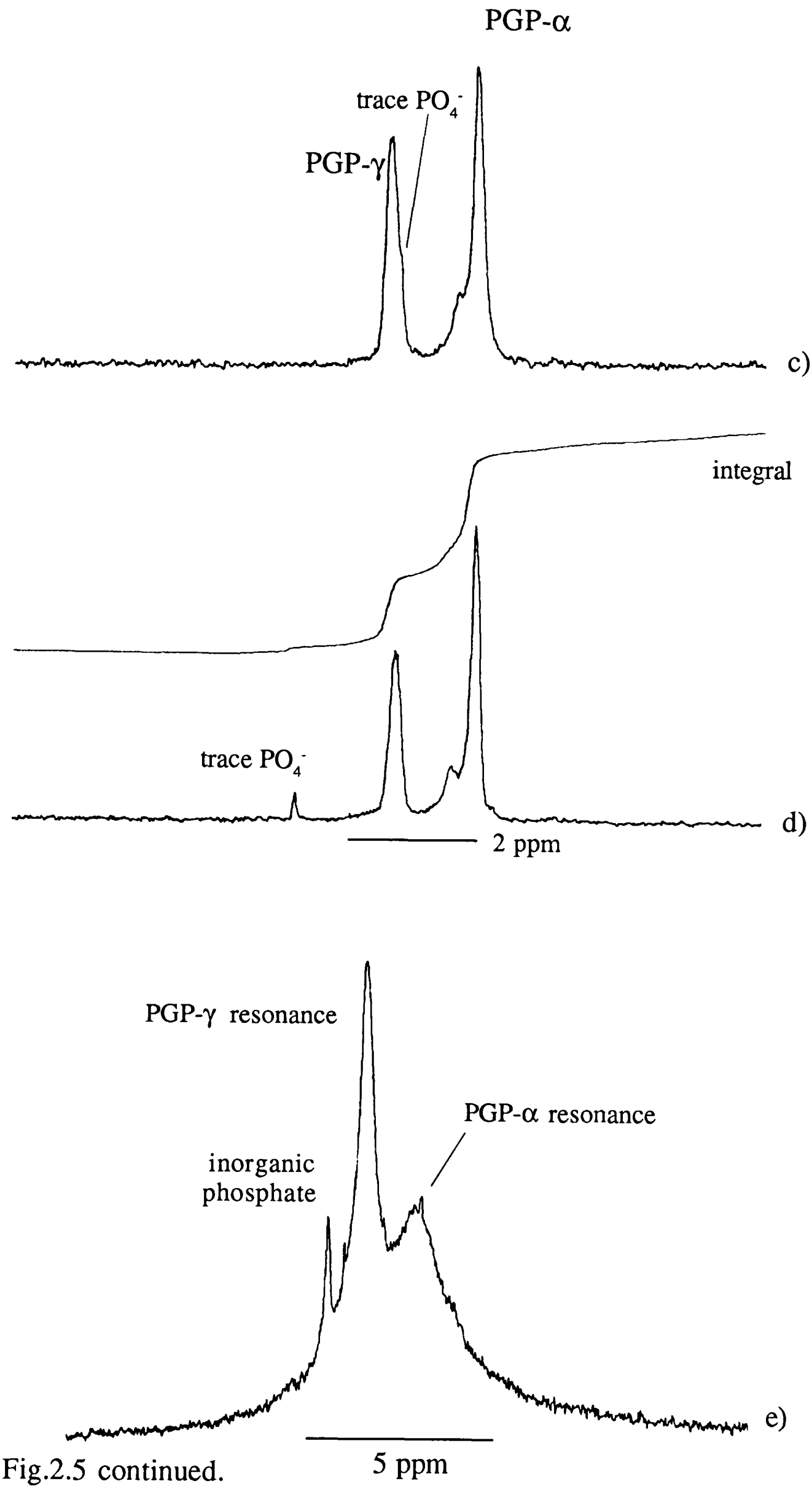


Fig.2.5 continued.

increase by 0.458ppm to 1.758 ppm. Furthermore both peaks shift downfield in the presence of methanol; in a second chloroform sample, the addition of methanol shifted the PC resonance downfield by 0.53ppm and the PG peak by 0.86 ppm.

The chemical shift of the phosphorus resonance of PG in $CHCl_3$/MeOH is sensitive to protonation and to chemical modification of the β- and γ-hydroxyl groups on the headgroup glycerol. Fig.2.4c shows the high resolution ^{31}P-NMR spectrum of the reaction mixture of DMPG with sulphur trioxide-pyridine after extraction from pH 2. The protonation of the phosphate shifts the resonance upfield by 0.76 ppm (compared to Fig. 2.4a). Sulphation at the γ-OH (to produce PGS) shifts the resonance a further 0.32 ppm upfield. In PGS_2, the β,γ-disulphated molecule, the phosphorus resonance is 0.7 ppm upfield from that in PG. The resonance assignments were made by comparison of the signal intensities with spot sizes on staining TLC with molybdate.

In Fig. 2.5a the noise decoupled ^{31}P spectrum of SDS solubilized purple membrane at pH 7.8 is presented. There are two major resonances and two minor resonances. The two main peaks (15.628 ppm and 16.891 ppm relative to MDP) coincide with the resonances from SDS solubilized *H.halobium* red membrane (Fig 2.7) and represent the two phosphorus nuclei from the major phospholipid species of *H.halobium* - namely 2,3-di-O-phytanyl-*sn*-glycero-1-phosphoryl-3'-*sn*-glycero-1'-phosphate (PGP). In the proton decoupled spectrum of the purple membrane (Fig.2.5.a), the lowfield PGP peak exhibits a narrower half-height line width than the upfield peak. In the absence of decoupling this is reversed, accounting for the decrease in height of the lowfield peak relative to the highfield peak, observed in the analytical spectra (described later). In the undecoupled spectra, the low field resonance exhibits a complex multiplet J-coupling pattern, which is responsible for the broadening of the resonance. For this reason determination of peak intensities in the analytical spectra (discussed later) is performed by integration rather than measurement of the line heights.

The two minor peaks (I at 16.490 ppm and II at 16.766 ppm) in the proton decoupled spectrum (Fig 2.5a), are demonstrated not to be inorganic phosphate. In Fig.

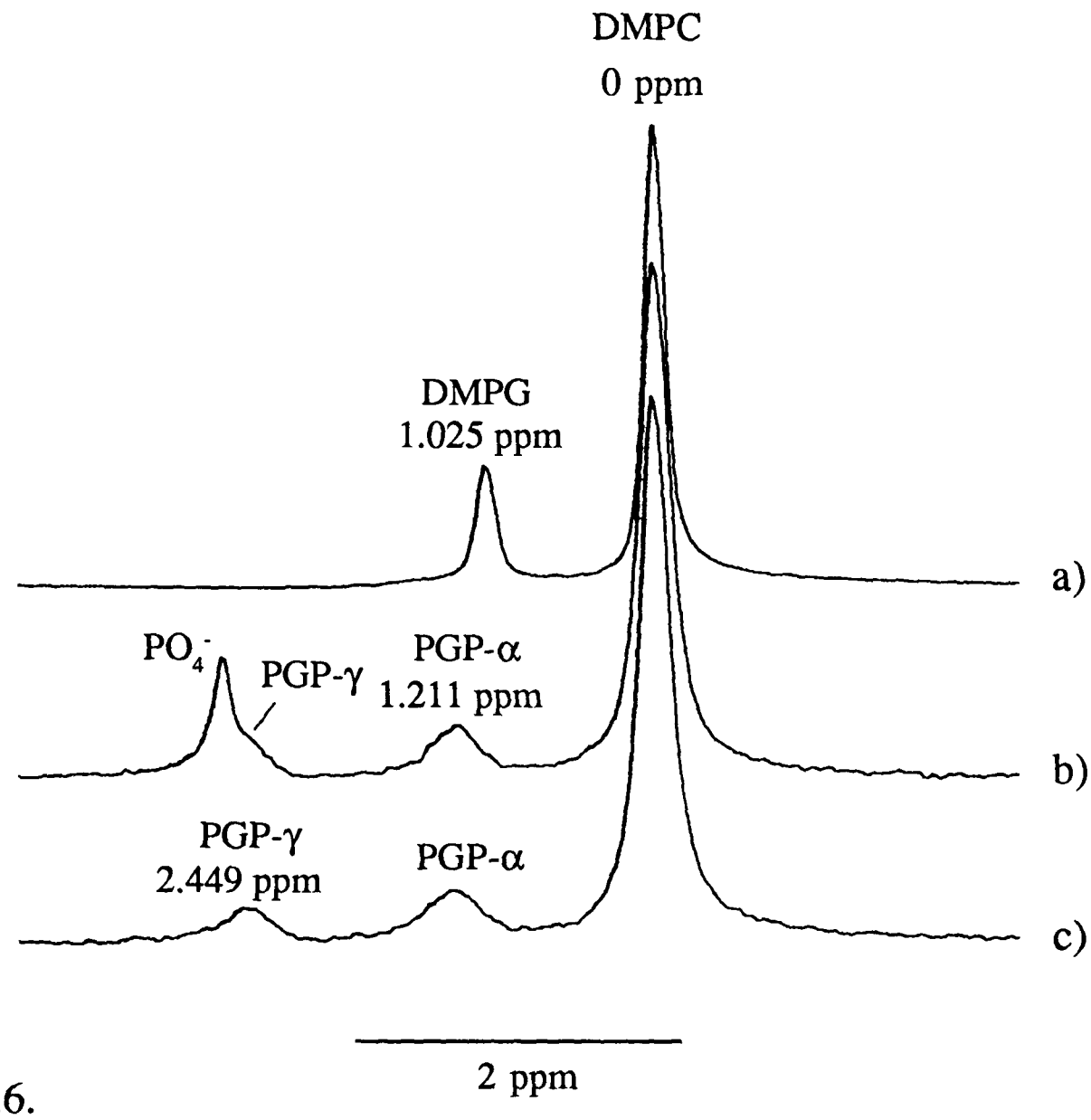


Fig.2.6.
High resolution ^{31}P-NMR spectra (proton decoupled) at 145.9 MHz of phospholipids solubilized in 4% SDS. Each phospholipid exhibits a chemical shift characteristic of the particular headgroup (ppm relative to DMPC resonance).
All spectra were recorded at pH 7.5 and 33°C.

a) DMPG and DMPC (Sigma)
b) *H.halobium* purple membrane with DMPC (Sigma) and inorganic phosphate
c) *H.halobium* purple membrane with DMPC (Sigma).

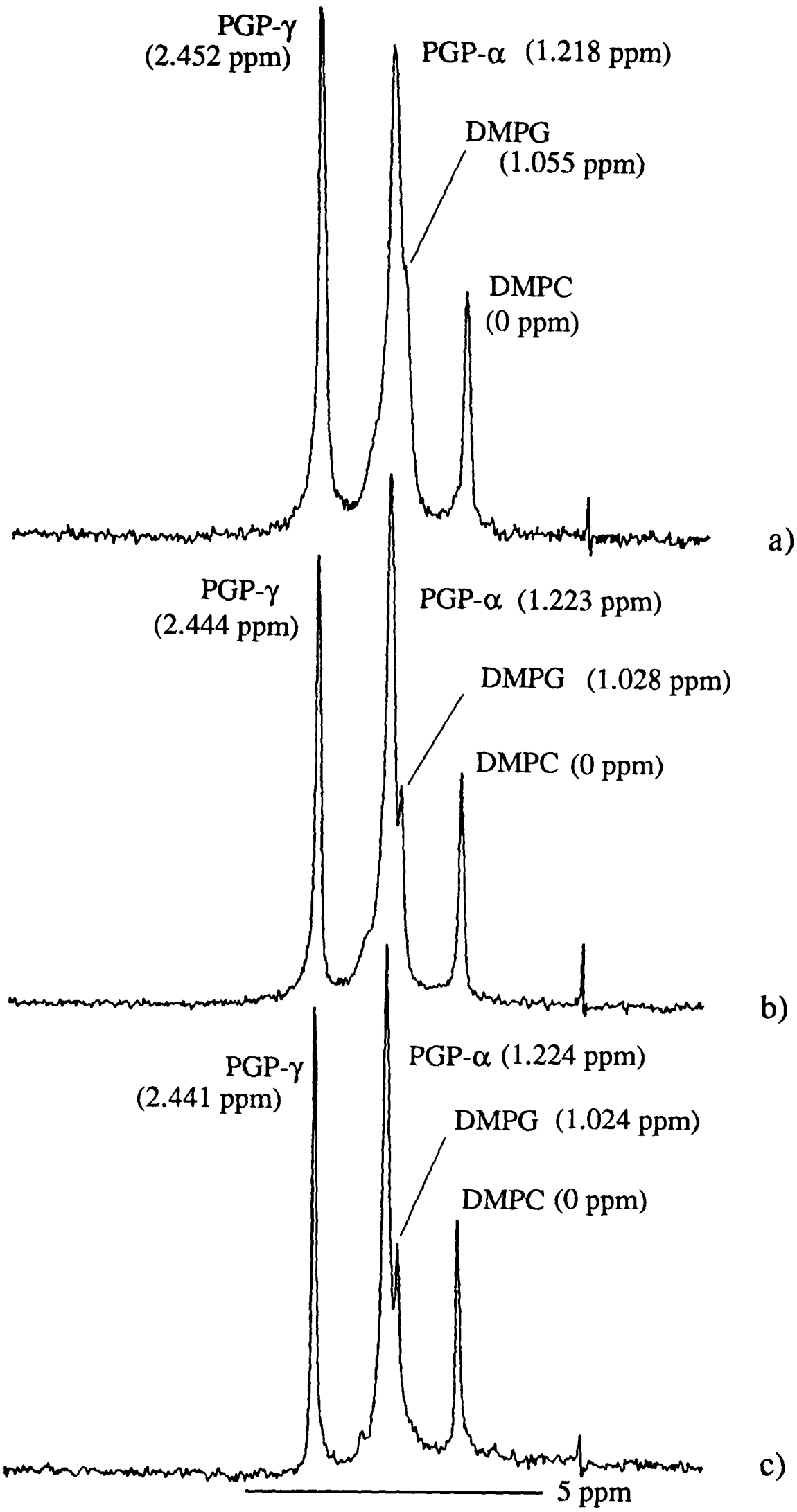


Fig.2.7. High resolution ^{31}P-NMR spectra (145.9 MHz) of SDS solubilized *H.halobium* red membrane with exogenous DMPG and DMPC. Spectra were proton decoupled and recorded at 33°C. The resolution of the resonances is enhanced with increasing pH; a) pH 7.3; b) pH 9.3; c) pH 9.8.

2.5b exogenous inorganic phosphate at pH 7.8 added (1mM) to the sample in Fig.2.5.a, exhibits a chemical shift of 15.360 ppm (relative to MDP). In the undecoupled spectra at pH 7.07 (Fig 2.5c) only one minor peak (I) is resolved (16.490ppm). Resolution from the upfield major peak can be enhanced by increasing the pH (Fig 2.5d). Thus high pH values assist quantitative analysis of the purple membrane phospholipid species by high resolution ^{31}P-NMR.

In Fig.2.5.e, the proton decoupled ^{31}P-NMR spectrum obtained from the polar lipids extracted from whole cell membranes by organic solvent and sonicated into small unilamellar vesicles after resuspension in aqueous buffer at pH 7.8 is presented. Three peaks are resolved. The low field peak (15.131 ppm from MDP) coincides with the resonance for inorganic phosphate at pH 7.8 (see Fig.2.9). The inorganic phosphate may originate from the degradation of PGP or PGS to PG on sonication or organic extraction. The two major peaks represent the signals from the PGP-g and the purple membrane phospholipid a-phosphates. The upfield resonance (17.307 ppm from external MDP) is broader with a larger half-hîeght peak width than the lowfield resonance (at 16.066 ppm). This implies a longer spin-spin (T_2) relaxation time for the lowfield peak, which is consistent with a faster rate of motion within the molecule.

Fig 2.6a shows the phosphorus-31 NMR resonances of DMPG and DMPC solubilized in SDS at pH 7.5. The DMPG peak is 1.023 ppm downfield from the DMPC phosphorus resonance and 17.010 ppm upfield from the MDP resonance. Figs 2.6b and c display the high resolution ^{31}P-NMR spectra of an SDS-solubilized DMPC/bacteriorhodopsin complex with all the purple membrane phospholipids retained. It can be seen that the two PGP resonances are well resolved from that of DMPC. At pH 7.5 the inorganic phosphate resonance (Fig 2.6b) overlaps with to the lowfield PGP resonance. Thus the SDS-solubilized DMPC/PMPL/bR samples must be free from inorganic phosphate for accurate quantitative analysis at pH 7.5.

Fig 2.7 shows the noise decoupled ^{31}P-NMR spectra of SDS solubilized DMPC and DMPG co-solubilized with *H.halobium* red membrane at three pH values. At pH 7.3 (Fig.2.7.a), the DMPC resonance is 1.055 ppm upfield from the DMPG. This

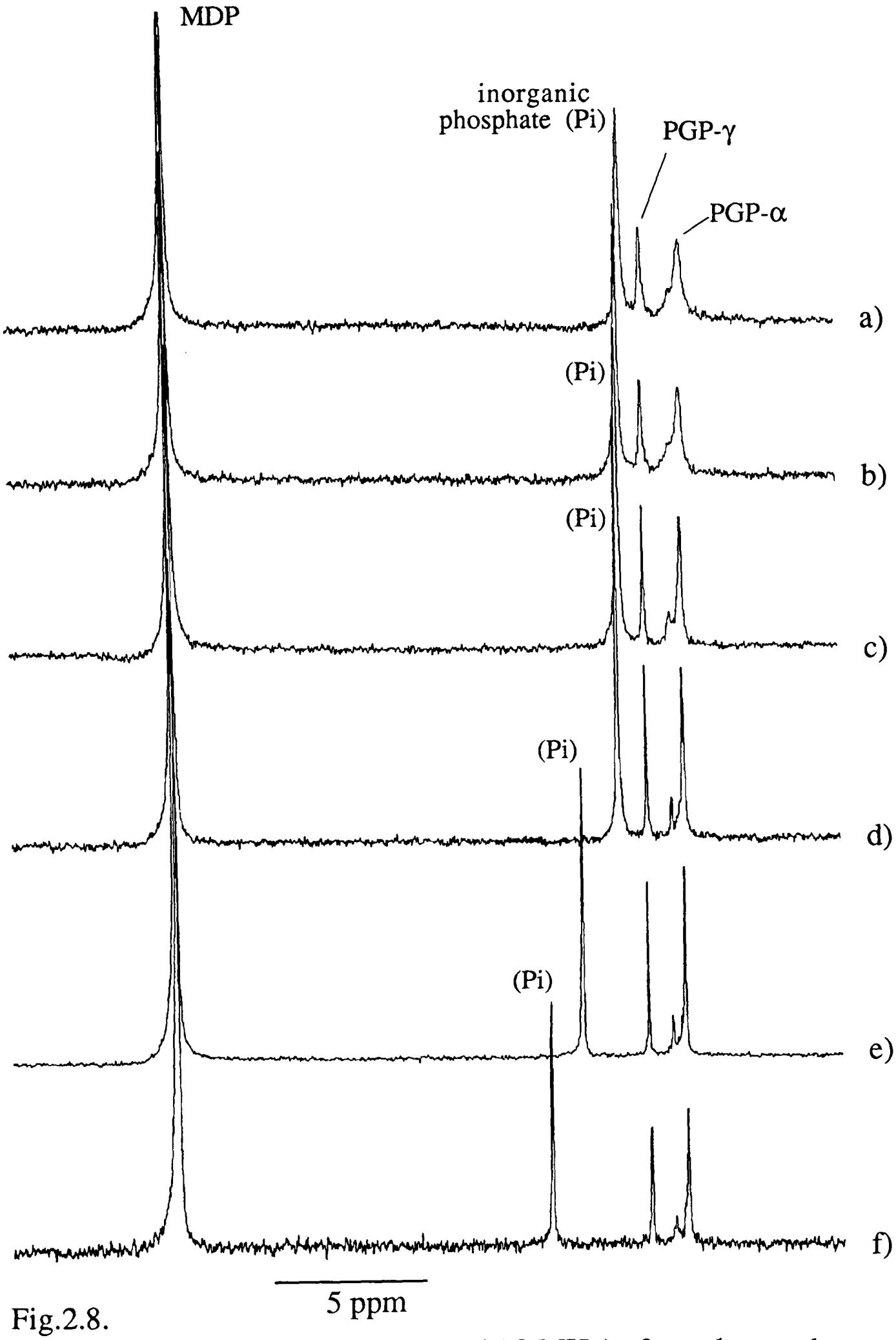


Fig.2.8.
High resolution ^{31}P-NMR spectra (145.9 MHz) of purple membrane solubilized in 4% SDS, 100mM Tris/HCl with exogenous inorganic phosphate at high pH values; a) pH 8.5; b) pH 9.3; c) pH 10.0; d) pH 10.7; e) pH 12.3; and f) pH 13.7. All spectra were proton decoupled and recorded at 33°C.

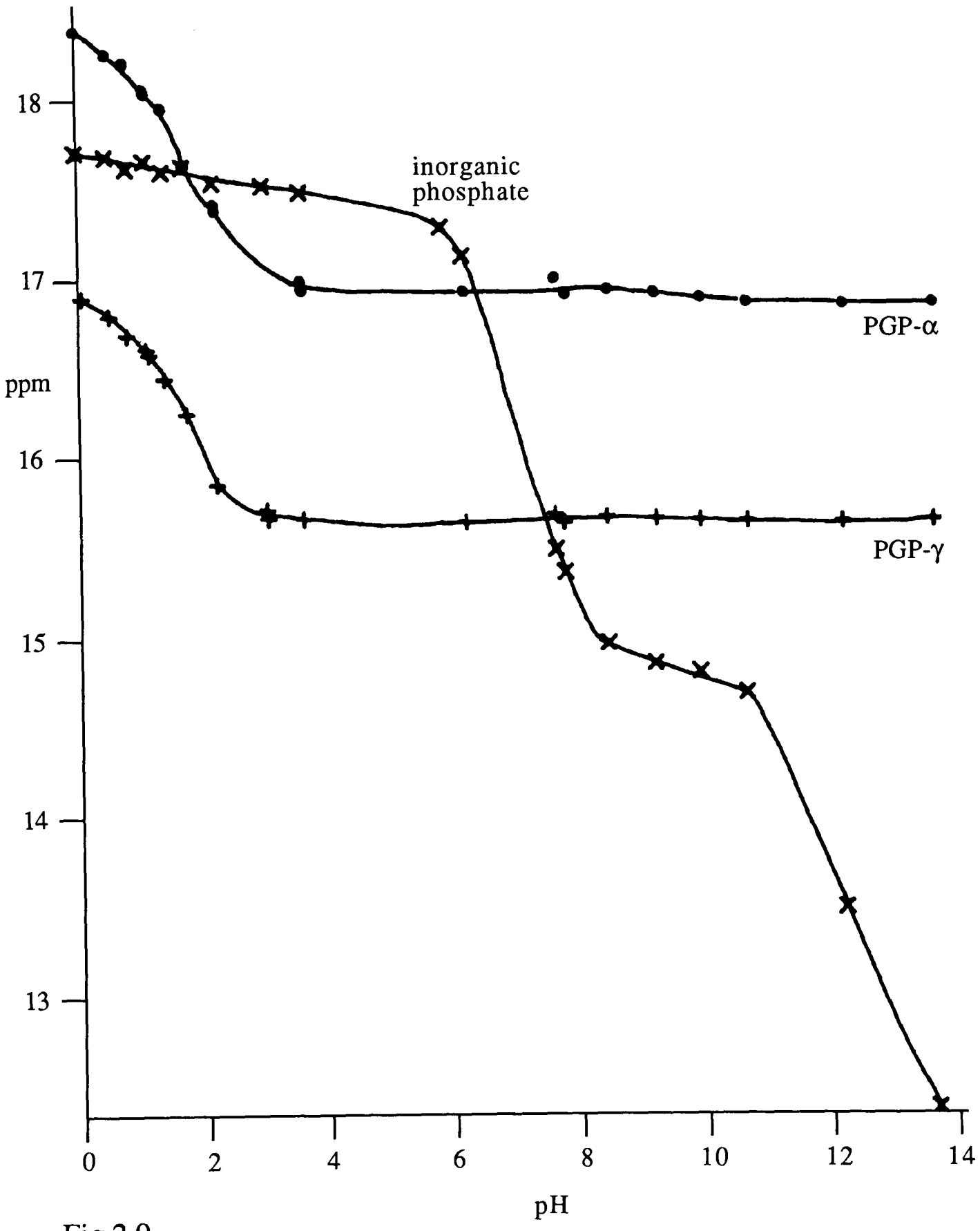


Fig.2.9
Chemical shifts (relative to MDP) of exogenous inorganic phosphate and *H.halobium* purple membrane PGP resonances from high resolution ^{31}P-NMR spectra plotted as a function of pH at 33°C. Purple membrane was solubilized in 4% SDS, 100mM Tris/HCl.

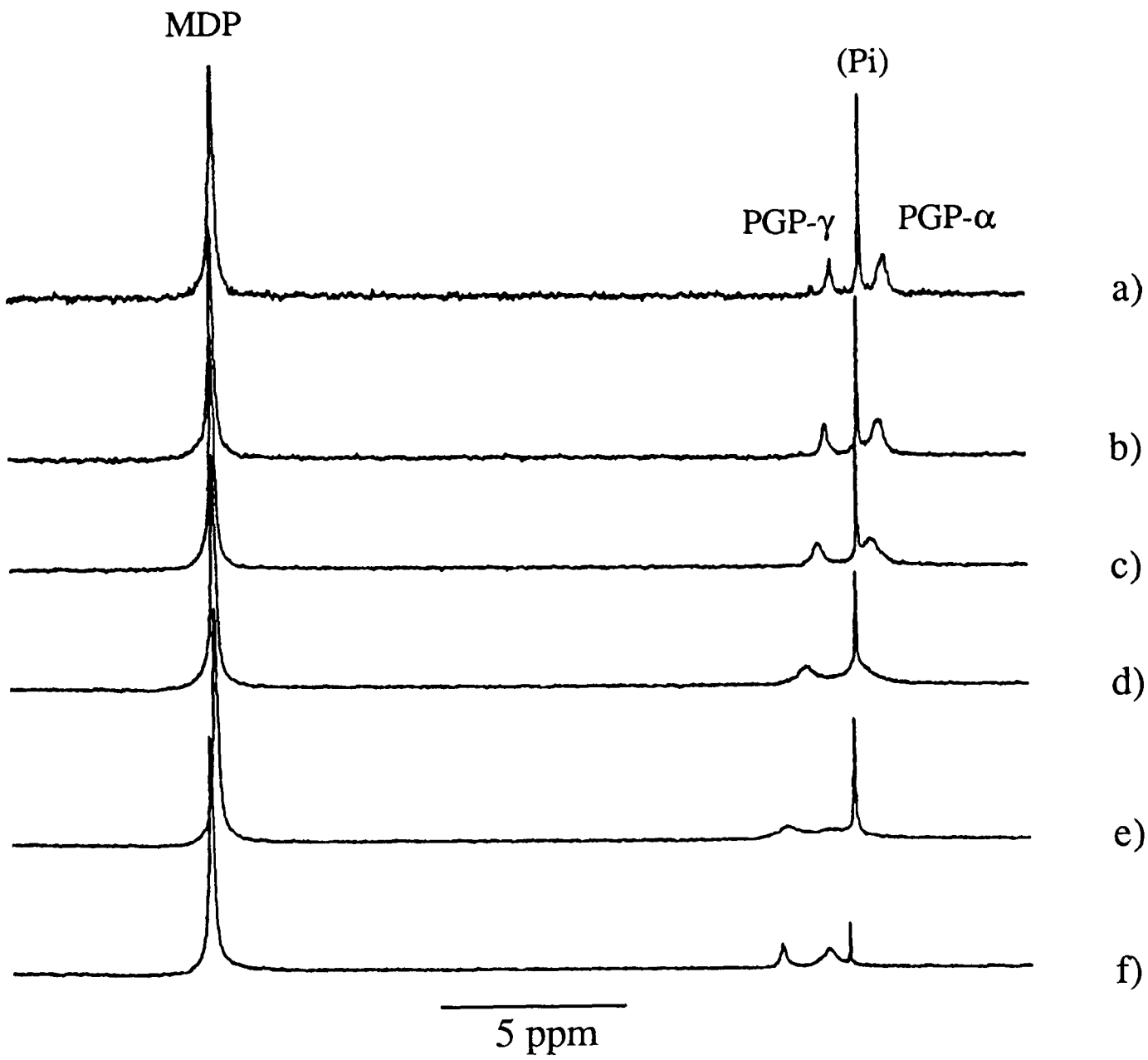


Fig.2.10. High resolution ^{31}P-NMR spectra (proton decoupled) of SDS solubilized purple membrane and exogenous inorganic phosphate (Pi) at low pH values; a) pH 0.06; b) pH 0.5; c) pH 1.1; d) pH 1.7; e) pH 3.0; and f) pH 3.6. Both PGP resonances are broadened and shift upfield, while the Pi peak remained unaffected. Spectra recorded at 33°C.

separation decreases to 1.028 ppm at pH 7.8 (Fig.2.7.b). At pH 7.3 (Fig.2.7.a) the DMPG peak is virtually indistinguishable from the red membrane PGP high field peak, being only 0.163 ppm upfield. Increasing the pH to above pH 9 (Fig. 2.7.b and c), however, improves the resolution due to a slight shift in both peaks and a narrowing of the lines. At pH 9.8, the DMPG resonance is 0.200 ppm upfield from the PGP-α and is clearly resolved.

Fig 2.8 shows the noise decoupled ^{31}P-NMR spectra of SDS solubilized purple membrane with added inorganic phosphate titrated over a pH range from 8.5 to 13.7. No trace of a resonance is evident that corresponds to that of DMPG headgroup. Although Fig. 2.7 demonstrates that increasing the pH to above 9 enhances the resolution of the DMPG resonance from the PGP-α resonance, none of the SDS solubilized purple membrane ^{31}P-NMR spectra at high pHs reveal a resonance 0.20 ppm upfield from PGP-α.

The chemical shifts (relative to MDP) for the two PGP resonances of *H.halobium* purple membrane solubilized in SDS and the exogenous inorganic phosphate titrated over the pH range 0.06 to 13.75 are plotted in Fig. 2.9. ^{31}P-NMR detects only a single titration for both the mono-ester α-phosphate moiety and the diester γ-group. In fact both resonances exhibit very similar titration patterns. Neither resonance exhibits a significant shift around pH 7 - 8, although the upfield PGP peak (which is assigned to the α-diester phosphate) appears weakly sensitive in this pH range changing its chemical shift by about 0.2 ppm with a pK_a around pH 9). Only below pH 3 does either resonance display significant sensitivity to pH titration. The upfield resonance shifts upfield by ~1 ppm with a pK_a of 1.75 while for the lowfield peak the observed pK_a is slightly lower. The upfield shift in resonance chemical shift observed on titrating at low pH values is also associated with a broadening of the resonances as shown in Fig.2.10. This effect is clearly not due to magnetic field inhomogeniety as the linewidth of the inorganic phosphate resonance is unaffected. For the exogenous inorganic phosphate, however, ^{31}P-NMR detects two titrations (pK_as 7 and 12); each imposing a change in chemical shift of ~2.5 ppm. The titration at pH 2 for inorganic phosphate results in a

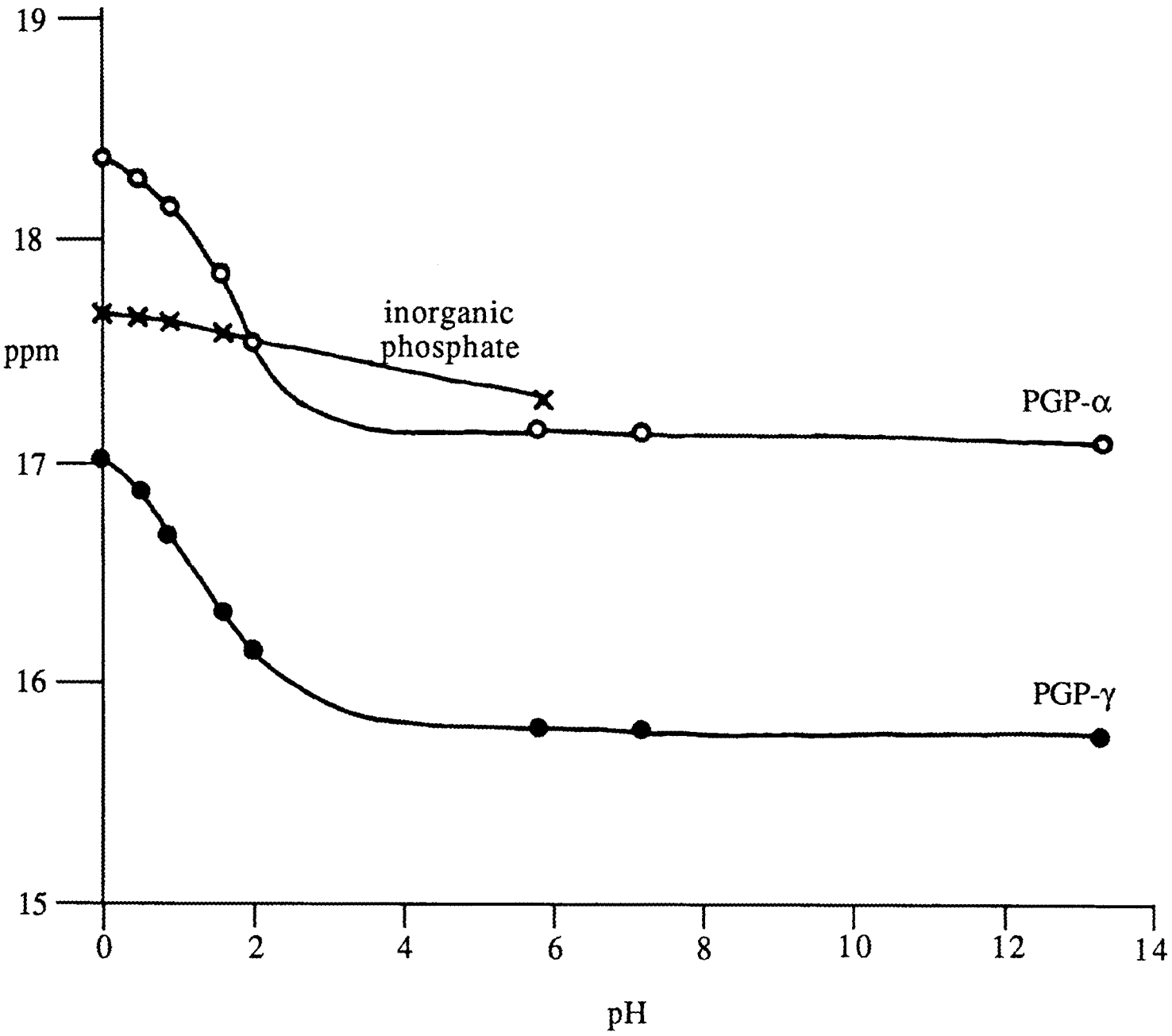


Fig.2.11.

^{31}P-NMR chemical shifts of exogenous inorganic phosphate and PGP resonances of *H.halobium* purple membrane solubilized in Triton X-100 micelles plotted as a function of pH (33°C). Purple membrane was solubilized in 7.5% Triton X-100, 100mM Tris/HCl, pH 7.0. Both the PGP-α and -γ resonances display only a single titration with pK_as of pH 1.8 and 1.5, respectively.

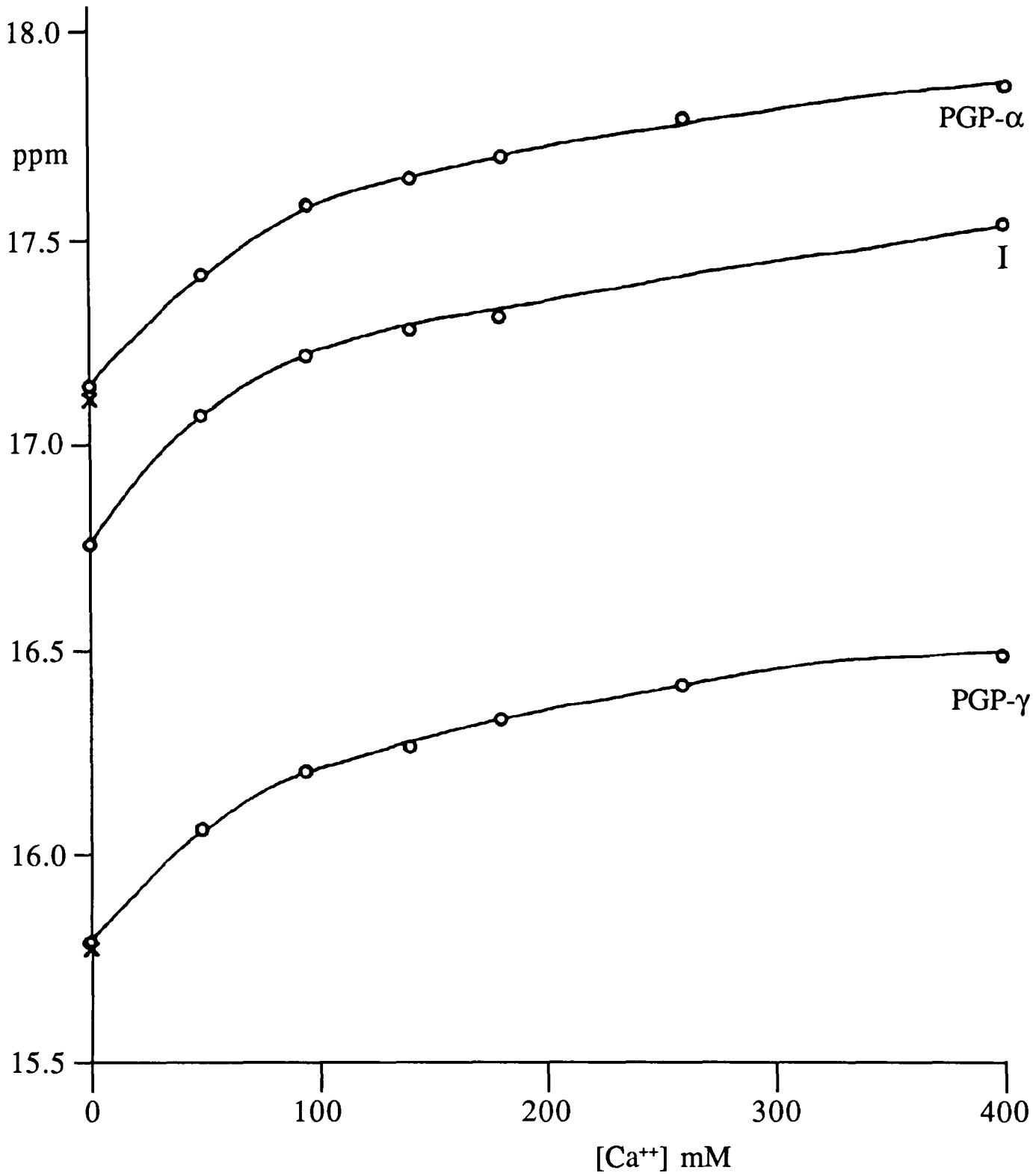


Fig.2.12. Binding of Ca^{++} ions to the α- and γ-phosphate groups of *H.halobium* PGP, solubilized in Triton X-100 micelles, as monitored by the shifts in ^{31}P-NMR resonances as a function of the Ca^{++} ion concentration. Also shown are the chemical shifts for the unassigned minor resonance (I). Addition of EDTA to 30mM in the absence of Ca^{++} ions (X) did not effect the chemical shift. Purple membrane was solubilized in 7.5% Triton X-100, 100mM Tris/HCl, pH 7.15 and spectra were recorded at 33°C.

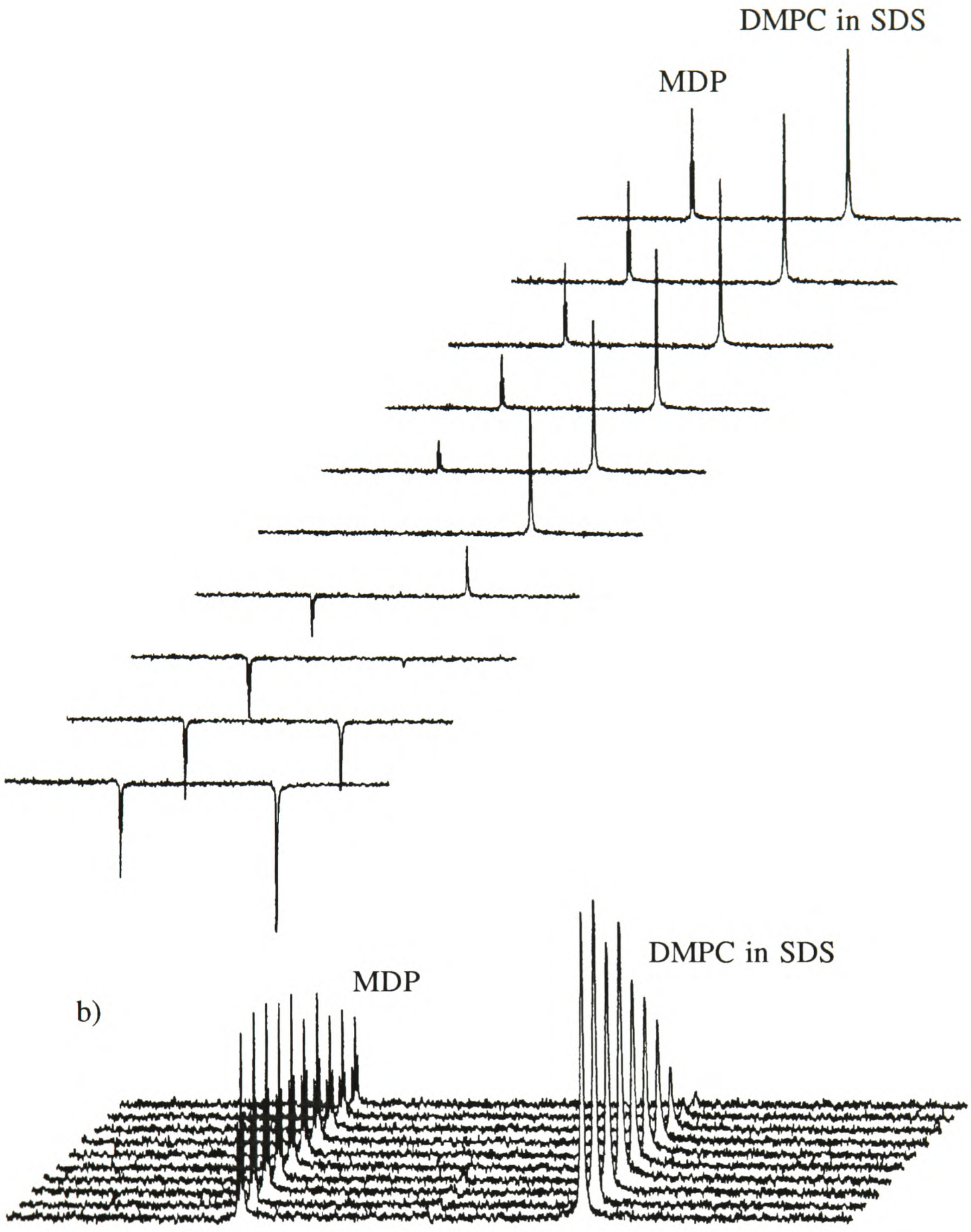


Fig. 2.13. High resolution ^{31}P-NMR relaxation time determination at 33°C for 222:1 mole ratio DMPC/bR complex after solubilization in 4% SDS, 100mM Tris/HCl, pH 7.5; a) spin-lattice relaxation time (T_1) by inversion recovery method with a relaxation delay of 20s and τ delay times (s) of 0.00002, 0.3, 0.6, 1.0, 2.0, 3.0, 4.0, 6.0, 10.0 and 20.0 (from bottom to top). A T_1 value of 3.035s was determined for MDP and 1.205s for DMPC. b) spin-spin relaxation time (T_2) by Carr-Purcell spin echo method with τ delay times (ms) of 0.2, 0.5, 1.0, 5.0, 10.0, 20.0, 30.0, 50.0, 80.0 and 100.0 (from bottom to top). A T_2 value of 68ms was determined for DMPC.

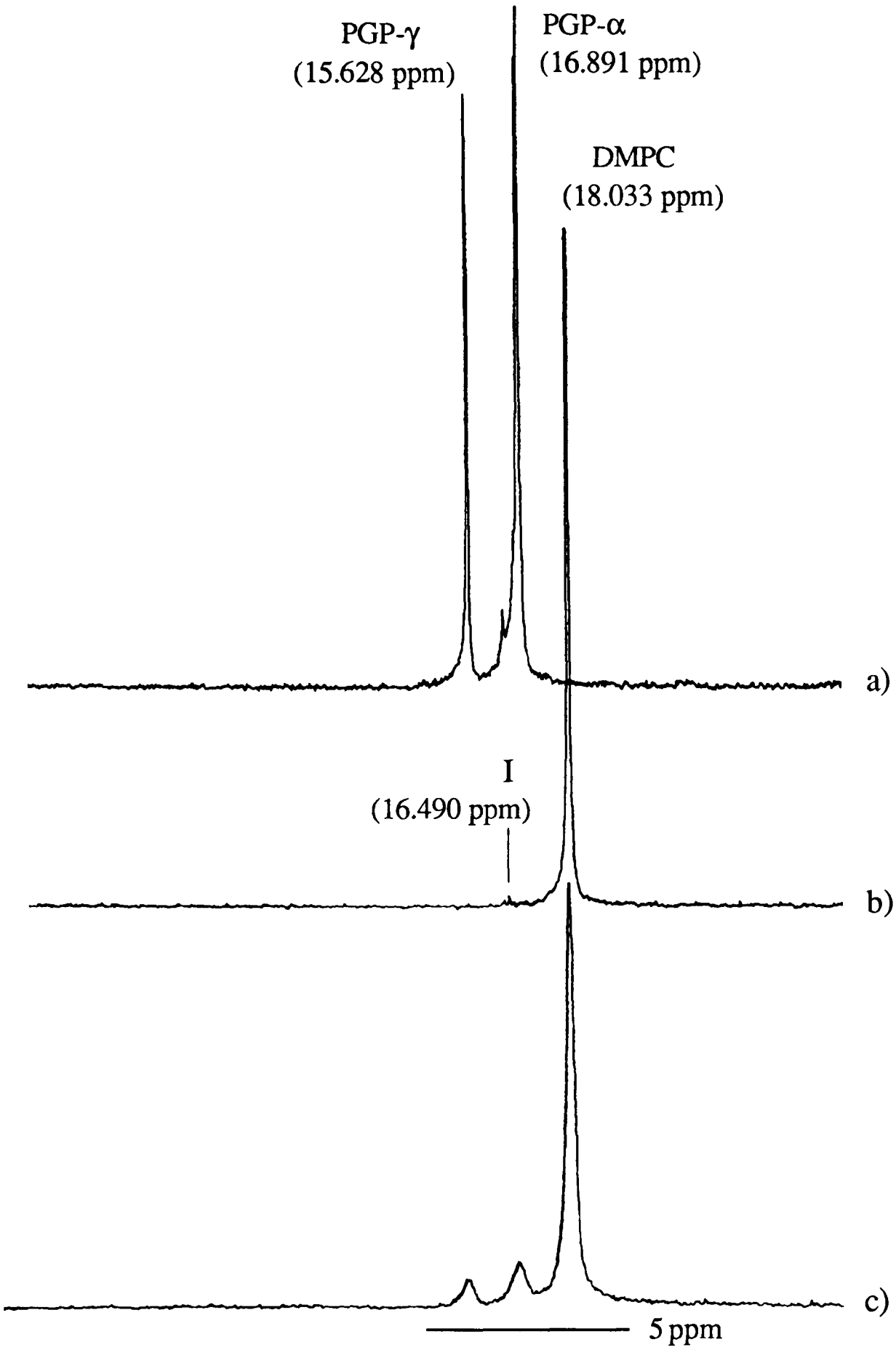


Fig. 2.14. High resolution phosphorus-31 NMR provides a method for analysis of phospholipid headgroup compositions of DMPC/bR complexes produced by detergent dialysis techniques. Complexes were solubilized in 4% SDS, 100mM Tris/HCl, pH 7.5. Spectra were recorded at 33°C with proton decoupling.

a) purple membrane alone.

b) 68:1 mole ratio DMPC/bR complex demonstrating removal of all purple membrane phospholipids.

c) DMPC/bR complex with all purple membrane lipids retained; produced as described by Cherry *et al* ., (1978) except using octyl glucoside.

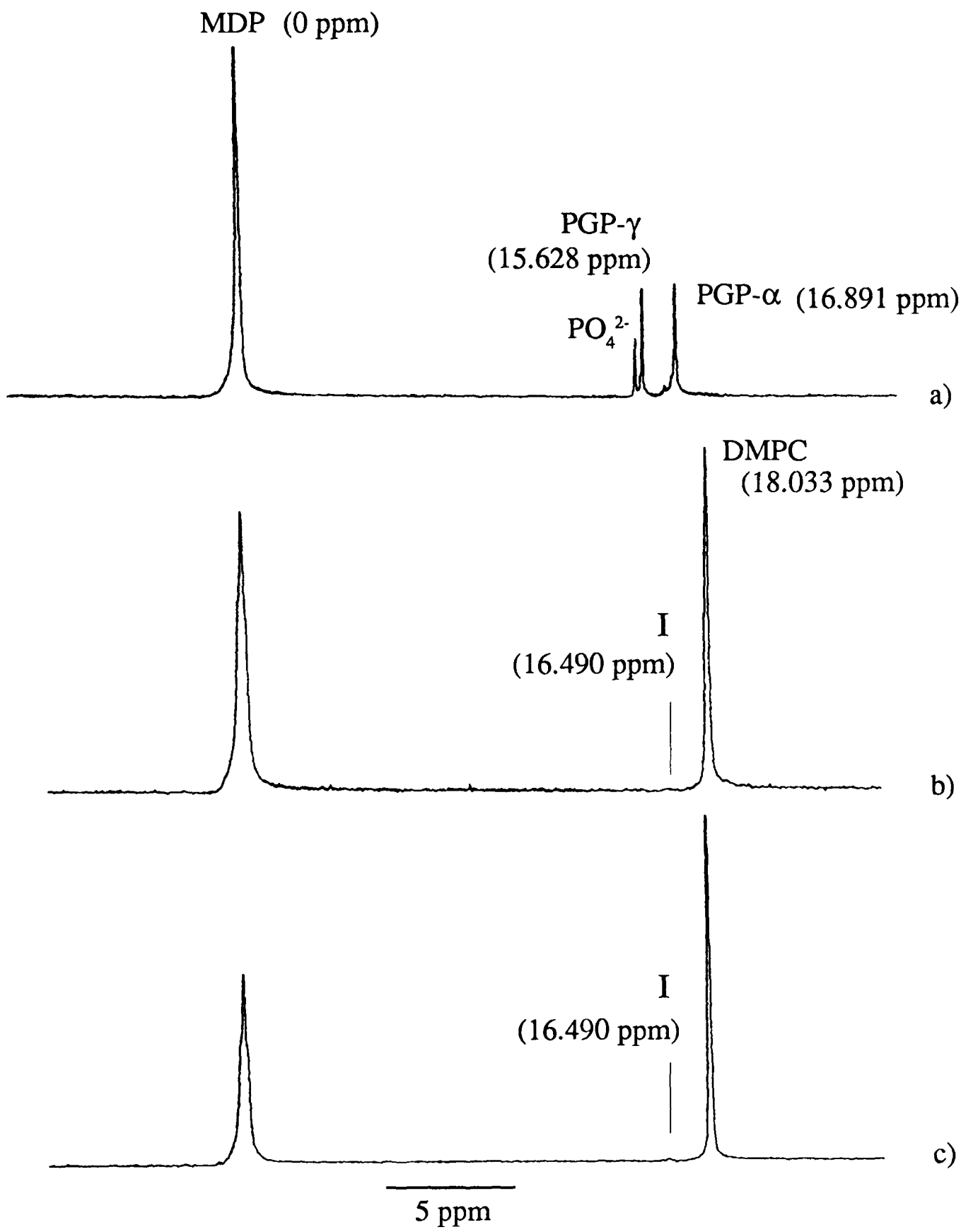


Fig. 2.15. Evidence from high resolution ^{31}P-NMR that all endogenous purple membrane PGP has been removed from the DMPC/bR complexes and that DMPC is the only phospholipid species present; although there appears to be a trace of the unassigned minor resonance (I) at 16.490 ppm. Complexes solubilized in 4% SDS, 100mM Tris/HCl and spectra recorded at 33°C.
a) purple membrane + exogenous inorganic phosphate, pH 7.8 (proton decoupled).
b) 67:1 mole ratio DMPC/bR complex, pH 7.5 (not proton decoupled).
c) 95:1 mole ratio DMPC/bR complex, pH 7.5 (not proton decoupled).

less significant change in chemical shift (Gadian *et al.*, 1979) and is not detected here.

The pH titration of the PGP phosphorus resonances was repeated for purple membrane solubilized in the non-ionic detergent Triton X-100. As for SDS, a plot of the chemical shifts (Fig. 2.11) over the pH range 0 - 13 exhibits only a single titration for each resonance with pK_as of pH~1.8 and 1.5 for the α- and γ-phosphates, respectively.

Triton X-100 solubilized purple membrane was titrated as a function of Ca^{++} ion concentration at pH 7.15. Fig. 2.12 shows the chemical shifts for the PGP-α and -γ phosphate resonances and the unassigned minor peak I (16.490 ppm from MDP in SDS) as a function of Ca^{++} ion concentration. Both the PGP resonances and the minor peak I appear to exhibit similar Ca^{++} ion binding properties. Addition of EDTA (to 30mM) to the sample in the absence of Ca^{++} ions did not significantly shift the resonances, implying that Ca^{++} and/or other alkaline earth metal ions were not already bound to the PGP-headgroup phosphate moieties. In view of the *H.halobium* growth medium, which contains both Ca^{++} and Mg^{++} ions, it was important to verify this

Stack plots of high resolution ^{31}P-NMR T_1 and T_2 experiments for the 222:1 mole ratio DMPC/bR complex after solubilization in SDS are shown in Fig.2.13. A T_1 value of 1.20 s and a T_2 of 68 ms was calculated for the DMPC resonance. The T_1 for MDP was 3.05 s.

Figs.2.14.b and 2.15.b and c show high resolution ^{31}P-NMR spectra of the SDS-solubilized 68:1, 67:1 and 95:1 mole ratio DMPC/bR reconstituted complexes, respectively, produced by the delipidation as described by Huang *et al.*, (1980). For each only a single major peak is observed 18.033 ppm from MDP. This peak corresponds to DMPC. There is also no evidence of a lyso-PC peak (0.41 ppm downfield from the PC resonance) in any of the samples. Also there are no traces of signal at 15.628 ppm and 16.891 ppm, where the purple membrane PGP-α and -γ phosphate moieties would resonate (Figs 2.14.a. and 2.15.a.). The gel filtration technique, however, does not appear to completely remove the phosphate species responsible for the minor purple membrane resonance I, 16.490 ppm from MDP.

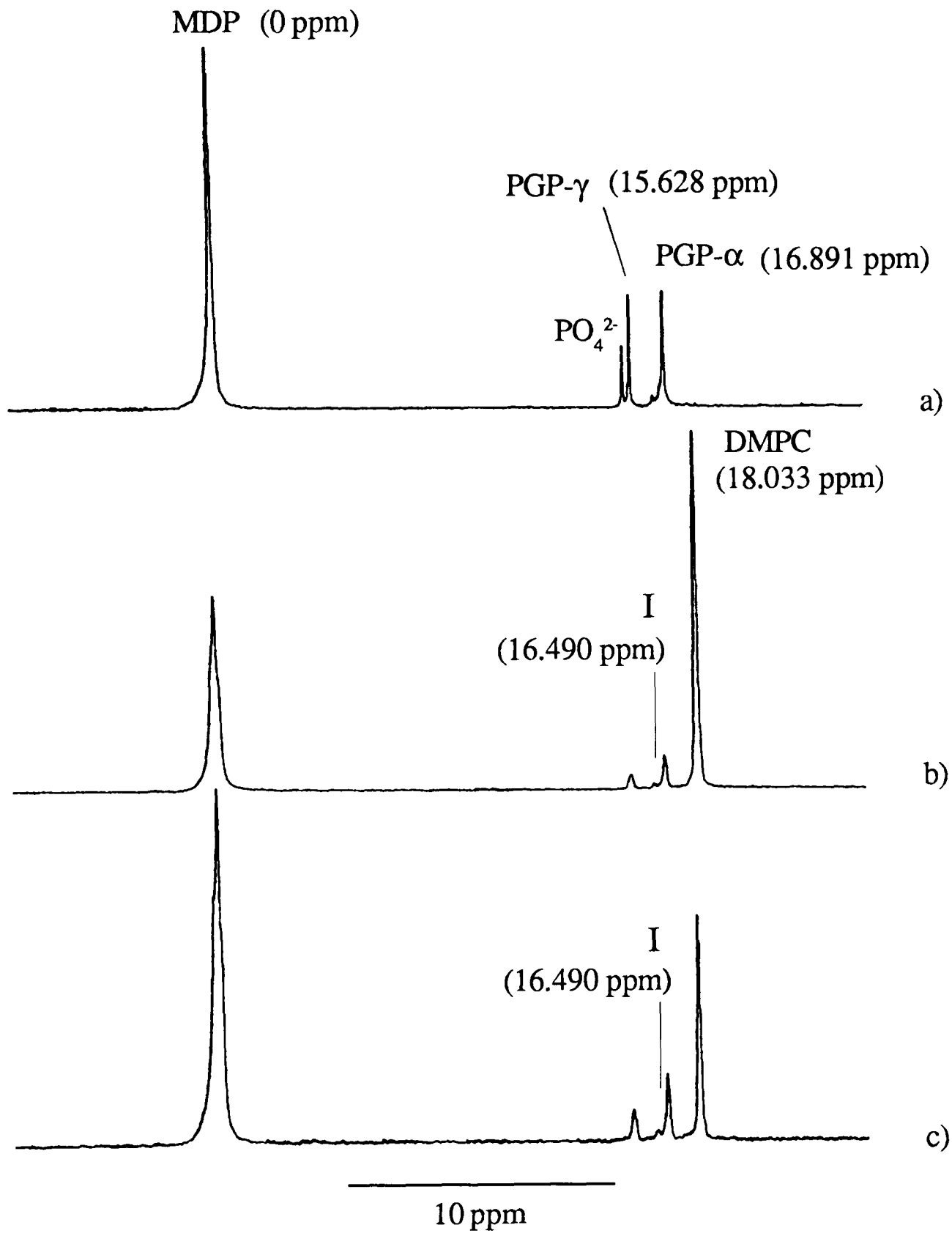


Fig. 2.16. Evidence from high resolution ^{31}P-NMR that nsTP-mediated addition of DMPC to purple membrane retains the endogenous purple membrane phospholipids. Spectra were recorded at 33°C from complexes after solubilization in 4% SDS, 100mM Tris/HCl, pH 7.5. A recycle time of 1.34 s was used.

a) purple membrane + exogenous inorganic phosphate, pH 7.8 (proton decoupled)

b) nsTP-produced complex; total phosphate:bR ratio 85:1, pH 7.5 (not proton decoupled).

c) nsTP-produced complex; total phosphate:bR ratio 36:1, pH 7.5 (not proton decoupled).

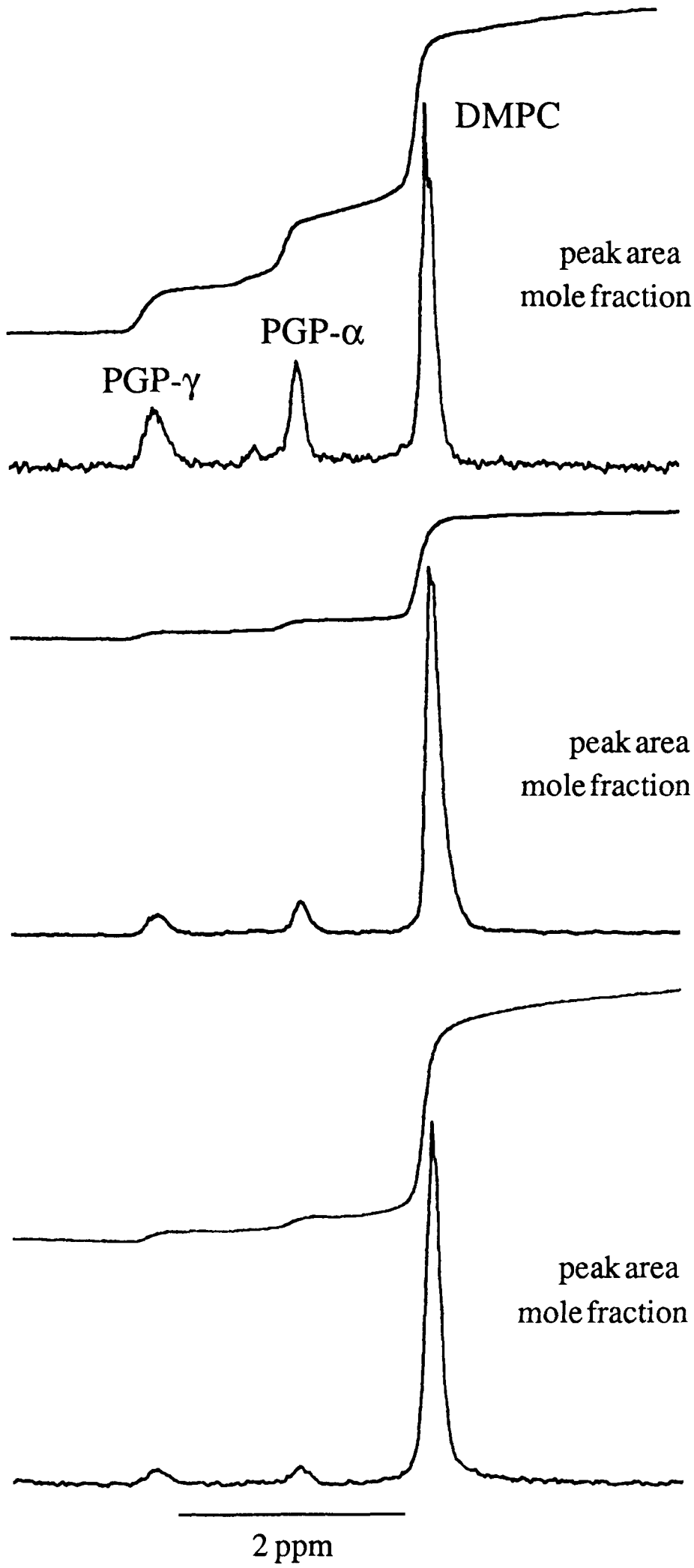


Fig.2.17. Quantitative high resolution ^{31}P-NMR spectra (recycle time 4.34 s) of nsTP-produced complexes of total lipid phosphate/bR mole ratios; a) 36:1; b) 85:1 and c) 123:1 after solubilization in 4% SDS, 100mM Tris/HCl, pH 7.5. Peak areas and mole fractions were calculated from spectrum integrals displayed above. Spectra were not proton decoupled.

To demonstrate the effectiveness of the high resolution ^{31}P-NMR technique in analysing the phospholipid composition, the spectrum of a DMPC/bR complex (total lipid phosphate/bR mole ratio ~60:1) in which all the endogenous purple membrane phospholipids were retained is presented (Fig.2.14.c). This complex was prepared as described by Cherry *et al.*, (1978), except that octyl glucoside was used as detergent instead of Triton X-100. No procedure was employed to remove the endogenous purple membrane lipids. The PGP phosphate resonances are clearly detected downfield of the DMPC resonance.

High resolution ^{31}P-NMR of SDS-solubilized nsTP-produced DMPC complexes (total phosphate/bR mole ratios 36:1; Fig.2.16b. and 85:1; Fig.2.16.c), reveal in addition to the main DMPC peak, the presence of resonances corresponding to the purple membrane phospholipids (Fig.2.16.a). The PGP-α and -γ phosphate resonances are distinct and the unassigned minor resonance, I, at 16.490 ppm is detectable in the spectra for the SDS-solubilized 36:1 and 85:1 total lipid phosphate/bR mole ratio complexes. Of particular importance is the confirmation of the complete absence of lyso-PC, which resonates 0.41 ppm downfield from the DMPC peak (see Fig.7.3).

For the phosphorus-31 spectra presented in Fig.2.16, a rather short recycle time of 1.34s was used. In order to allow for the possibility of different spin-lattice relaxation time (T_1) values for the three major phosphorus nuclei, the ^{31}P-NMR spectra used for the quantitative analyses were recorded with a much longer recycle time of 4.34s (Fig.2.17). The respective mole fractions of PGP-α, PGP-γ and DMPC phosphates in each nsTP-produced complex were calculated from the spectrum integrals (displayed in Fig.2.17) and not from the peak heights. Due to the different J-coupling multiplets of the PGP-γ, -α, and headgroup deuterated DMPC signals in the undecoupled spectra, the line-height does not accurately represent the signal intensity. The peak integrals and mole fractions of each phosphate group are presented in Fig.2.17. By multiplying the mole fractions calculated for the PGP-γ, -α and DMPC phosphate groups by the total lipid phosphate/protein (mol/mol) ratio (as determined by the methods of Rouser, *et al*,. 1970 and Markwell *et al.*, 1981 with correction for the 20% error; Rehorek & Heyn,

1979), the number of moles of each lipid phosphate per 26,000Da bacteriorhodopsin monomer is obtained (Table 1).

Lipid/protein analysis of *H.halobium* purple membrane itself, yielded a total lipid phosphate/bacteriorhodospin ratio of 19.5:1. From the integrals of the peaks in the high resolution ^{31}P-NMR spectrum of SDS-solubilized purple membrane recorded at high pH (12.7) (Fig.2.5d), mole fractions of 0.35, 0.51 and 0.13 were obtained for the PGP-γ, PGP-α and unassigned resonance at 16.498 ppm, respectively. These were used to calculate the number of moles of PGP-γ and -α phosphates (also presented in Table 1 for comparison) per 26,000Da bacteriorhodopsin molecule in purple membrane.

Table 1. Number of moles of purple membrane PGP-α and -γ phosphates and DMPC per 26,000Da bR monomer in nsTP-produced complexes and also in purple membrane as determined from high resolution ^{31}P-NMR spectroscopy.

total lipid P/bR ratio of complex*	PGP-γ	PGP-α	total PGP phosphate+	DMPC
36.0:1	6.05	7.63	13.68	21.2
85.2:1	5.54	7.33	12.87	72.2
123.6:1	6.67	7.79	14.46	109.1
purple membrane				
19.5:1	6.90	9.96	16.86	none

*protein determined as described by Markwell, *et al.*, (1981) and corrected as described by Rehorek & Heyn, (1979) and lipid phosphate as by Rouser, *et al.*, (1970).

+calculated by adding the number of moles of PGP-α and PGP-γ phosphates together.

The number of moles of phosphate determined for PGP-γ and -α moieties and the DMPC in the 36:1 total lipid phosphate/bR mole ratio complex, account for 34.8 moles of the total lipid phosphate. The unassigned minor peak, I, at 14.490 ppm (from

MDP) accounts for the remaining one mole of phosphate per protein. For the higher content vesicles the contribution from this resonance was ignored in the calculations because its peak area could not be determined from the spectrum integrals (shown in Figs.2.17.b and c).

In Table 2, the percentages of total purple membrane PGP phosphate, PGP-g and PGP-a phosphates that are retained in the nsTP-produced complexes compared to in the purple membrane itself are presented. It appears that during the nsTP-mediated addition of exogenous DMPC to purple membrane a major proportion of the purple membrane phospholipid, PGP, is retained; but between 14 and 24% of the total PGP phosphate being lost. The possible reasons for the observed discrepancies between the proportions of PGP-α and PGP-γ moieties retained per mole of protein are discussed below.

Table 2. Proportions (expressed as percentage) of endogenous purple membrane PGP retained in nsTP-produced DMPC/bR complexes analysed by high resolution ^{31}P-NMR.

total lipid P/bR ratio	% total	% PGP-γ	% PGP-α
36.0:1	81	87.6	76.6
85.2:1	76	80.3	73.5
123.6:1	86	96.6	78.2

2.IV). Discussion.

Vesicles Size. The size of the DMPC/bR vesicles can vary up to tenfold depending on the method of production as shown by electron micrographs in Figs.2.1 - 2.3. The vesicles produced by the nsTP method are consistently small and the higher the protein ratio, the smaller the vesicle size. The purple membrane isolated from

H.halobium is in the form of small rigid planar patches, (Oesterhelt & Stoeckenius, 1974) and not vesicles. Addition of DMPC at 37°C by nsTP may allow the hexagonal crystalline lattice of bacteriorhodopsin to disperse within the plane of the membrane (Cherry *et al.*, 1978) so facilitating the DMPC/purple membrane complex to fold over and seal itself into a vesicle. Clearly such unsealed patches would be unstable and likely to seal quickly and this may account for the small size of the final vesicle. Once sealed, addition of more DMPC to the vesicle may be restricted preventing any further increase in size. This would account for the fact that even with large excesses of DMPC SUVs, the highest total lipid phosphate/protein mole ratio produced using the nsTP method is 152:1 (mol/mol).

DMPC/bacteriorhodopsin complexes produced by the Triton X-100 dialysis method were shown to be unilamellar with diameters varying between 200 and 600 nm (Cherry *et al.*, 1978) and thus these compare in size with the vesicles produced by fast cholate removal method of Huang *et al.*, (1980).

The size of the detergent reconstituted vesicles appear to be influenced by the speed with which the cholate is removed. The slow cholate method is seen to increase the vesicle diameter by three to fivefold over the more rapid cholate removal procedure. The presence of 1 - 2% cholate in the dialysis buffer (until vesicles were judged to have formed from the turbidity) slows the rate of vesicle formation to 4 - 5 days. In the absence of cholate in the initial dialysis buffer, vesicles may be formed more quickly and within 2 days. As the cholate level in the reconstitution mixture approaches the c.m.c., DMPC and bR begin to form plates of bilayer structure. The exposed hydrophobic edges are shielded from the aqueous environment by the cholate molecules. If the cholate concentration decreases through the c.m.c slowly, then these plates will have time to interact with others, so forming larger plates before eventually sealing to form vesicles. Removal of cholate quickly through the c.m.c. will give the plates less opportunity to interact with each other and thus render them more likely to seal rapidly and so form smaller vesicles. Similar considerations explain the greater homogeneity with respect to lipid/protein ratio of the vesicles produced by slow cholate

removal.

It is interesting to note that the vesicles with a DMPC/bR mole ratio of 1,444:1 are smaller than the 187:1 mole ratio DMPC/bR vesicles, although both were formed by the same rapid cholate technique. One explanation is that bacteriorhodopsin may retain cholate with a greater affinity than the lipid does; relative retention rates, however, were not measured. Thus the eightfold excess of bR in the 187:1, DMPC/bR reconstitution mixture may slow cholate removal sufficiently to allow vesicles of a slightly larger diameter to form.

Phospholipid Headgroup compositions of the vesicles. High resolution ^{31}P-NMR spectroscopy is a powerful technique for analysing the headgroup compositions of phospholipid mixtures. Here the method has been applied to natural membranes, synthetic lipo-protein complexes and to analysing the products of lipid-synthesis. Lipid purity and degradation can also be monitored. The purchased preparation of DMPG (Fig. 2.4a), for example, reveals a trace of lyso-PG (downfield from the DMPG resonance).

Acquisition of high resolution ^{31}P-NMR spectra. A large sweep width of 6,000Hz (41 ppm) was applied in order to accommodate both the phospholipid and MDP resonances (separated by up to 18 ppm); if the sweep width is too short, then resonances outside the spectral width are folded back into the spectrum (Gadian, 1982). With quadrature detection, the dwell time (166 μs) equals the inverse of the spectral sweep width (6,000 Hz). Simultaneously collecting the real and imaginary FIDs each into 2048 points (total block size 4096 points) gives an acquisition time for the FID of 0.34 sec, which is equivalent to ~5T_2^* for DMPC in SDS micelles (Fig.2.13). T_2 is the actual spin-spin or transverse relaxation time and refers to the actual rate of decay of magnetisation in the xy plane. T_2^* is the apparent spin-spin relaxation time as measured by in an NMR experiment (e.g. the Carr-Purcell spin-echo sequence used in Fig.2.13.b). To ensure that the whole decay is collected, the FID should be collected for at least 4T_2^* (Gadian, 1982). The length of the T_2 is related to the motion of the nucleus. Liquid samples are characterised by longer T_2 times than solid samples (e.g for DMPC

solubilized in SDS, a T_2 of 68ms was determined; Fig.2.13). For solid state samples, the slower rate of motion effects much shorter T_2 values (e.g. 0.9ms for DMPC/bR bilayer; Chapter 3). Thus applying a pre-acquisition delay between the end of the excitation pulse and the start of recording the FID, results in distortion of solid state NMR spectra while liquid sample NMR spectra are relatively unaffected.

The T_1 value of 1.205 s obtained for DMPC in SDS micelles agrees well with that of 1.26 s for DMPC in cholate (Barrow *et al.*, 1983). The T_1 for MDP is much longer, being in the region of 3 s. For the qualitative NMR experiments, e.g. for pH titrations, the aim is to attain the maximum signal in the shortest time (particularly at low pH points). Applying a relaxation delay of 1 s gave a total recycle time of 1.34 s. To attain maximum signal from 90° pulse experiments, a recycle time of $1.35T_1$ is required. For the quantitative NMR experiments much longer relaxation times are required. To measure T_1 or T_2 values a relaxation time of $5T_1$ is recommended. A relaxation time of 20 s was used to accommodate the 3 s T_1 of MDP. To accurately determine the molar ratios of PGP to DMPC in the nsTP-produced complexes, a relaxation time of 4 s was applied giving a total recycle time of 4.34 s i.e. ~$4T_1$ of DMPC in SDS micelles.

Assignment of phospholipid resonances. Assignment of phospholipid resonances may be made by comparing the chemical shift with that of known standards. It is important to realise, however, that the chemical shift of a phospholipid is dependent on the nature of the organic solvent or detergent used. For this reason, assigning resonances from data in previous publications cannot be made. Furthermore, the chemical shift of one phospholipid headgroup resonance relative to another may be more sensitive to the particular solvent environment as shown in Table 3 for PG/PC mixes in chloroform and chloroform/methanol.

Table 3. Separation of ^{31}P-NMR resonances from DMPG and DMPC is dependent on the solvent system.

solvent system	DMPG/DMPC separation (ppm)
aqueous SDS, pH 7.5	1.025
chloroform alone (neutral pH)	1.300
chloroform/methanol (neutral pH)	1.758

The measured chemical shifts of the PGP phosphorus nuclei relative to MDP are found to depend on the detergent used (Table 4). The α-PGP and γ-PGP resonances shift 0.252 ppm and 0.166 ppm upfield, respectively, when removed from the ionic environment of the SDS micelle (pH 7.7) to the non-ionic environment of Triton X-100 (pH 7.2). The unassigned minor resonance (I) was observed to shift 0.221 ppm upfield.

Table 4. ^{31}P-NMR chemical shifts (ppm) of purple membrane phospholipids in different isotropic environments relative to MDP.

resonance	Triton X-100 pH 7.2	SDS pH 7.8	*H.halobium* polar lipid SUVs, pH 7.8.
PGP-γ	15.794	15.628	16.066
PGP-α	17.143	16.891	17.307
separation between α- and γ-	1.349	1.263	1.241
minor peak I	16.719	16.490	n. d.

Also, a phospholipid in detergent micelles exhibits a different chemical shift to that in small unilamellar vesicles (produced by sonication) in aqueous media. The chemical shift for DMPC in aqueous DMPC SUVs, pH 6.4 was measured at 18.392 ppm, compared to 18.033 ppm in SDS micelles; that is 0.359 ppm upfield. In *H.halobium* polar lipid extract SUVs in aqueous medium, pH 7.8 (Fig.2.5.e), the PGP-α and PGP-γ resonances are 0.416 ppm and 0.438 ppm upfield of their respective resonances in SDS micelles. The difference, however, between the α- and γ-resonances is preserved to within 2%; 1.263 ppm in SDS micelles and 1.241 ppm in SUVs at pH 7.8.

Another factor that effects the observed chemical shift, both in aqueous and organic media is the state of protonation of the phosphate group. Thus, in chloroform/methanol the chemical shift of DMPG depends on the pH of the aqueous solution from which the lipid was extracted.

If known standards are not available as is the case for the lipids of the *H.halobium* membrane (PGS and PGP), other methods of assignment have to be used. One method that is applicable to phospholipids solubilized in aqueous detergent solution is titration of the resonance chemical shift with pH. Thus, cholate solubilized PC was shown to exhibit a single titration (London & Feigenson, 1979), while the phosphorus resonance of PE shows two significant pH induced chemical shifts; one at low pH corresponding to protonation of the phosphate itself and a second at high pH due to titration of the neighbouring primary amine group.

Titration, however, of SDS solubilized purple membrane failed to yield evidence for positive assignment of the two resonances of PGP. The diester α-phosphate undergoes a single pH titration with a pK_a of 3.25 (Kates, 1978). The monoester γ-phosphate has two ionizable protons and thus has the potential to undergo two ionizations; one ionization with a pK_a of 3.25 and the second ionization with a pK_a between 7.5 and 8 (Kates, 1978). ^{31}P-NMR detects the low pH titrations for both the PGP resonances. Spectra at low pH reveal a broadening in the observed phospholipid resonances, while the inorganic phosphate is unaffected. This is most likely due to slow

exchange between the interconverting species. The second ionization of the PGP-γ resonance, however, is undetected. There are several possible explanations to account for this. First, changing the ionization state of the monoester γ-phosphate moiety between the double and single charged species may not result in a detectable chemical shift by ^{31}P-NMR. This is the case for the low pH ionization of inorganic phosphate (as shown in Fig.2.9). Although, the high pH ionizations (pK_a 7 and 12) result in large chemical shifts (~2.5 ppm), the low pH ionization of inorganic phosphate is virtually undetected (Gadian *et al.*, 1979). Second, complete ionization of the monoester phosphate at high pHs to produce the triple negatively charged species may be suppressed. One plausible reason is due to the formation of an intra-molecular ring involving a hydrogen bond. Also, the detergent headgroup may play a role in suppressing ionization. The high negative charge density at the surface of the SDS micelle may serve to oppose the formation of the triple negatively charged species of PGP. To investigate this, purple membrane was solubilized in the non-ionic detergent Triton X-100. As with SDS, however, each resonance only exhibited a single titration; each with a pK_a of 1.75.

Such pH titration behaviour would favour a structure containing a pyrophosphate bridge linking two PGP molecules via their γ-phosphate groups. Indeed, initial failure to detect the weak third ionization of PGP led to this proposal (Faure *et al.*, 1972). The presence of a pyrophosphate linkage, however, would give distinctive doublets in the undecoupled ^{31}P-NMR spectra (as observed for ATP α and γ-moieties; Cohn & Hughes, 1960) due to spin-spin coupling between neighbouring phosphorus nuclei. This is not observed (Fig.2.5.c).

The α- and γ-phosphate moieties of PGP may be expected to display differing alkaline earth metal ion binding properties, which may assist in the assignment of the two PGP ^{31}P-NMR resonances. The changes, however, observed in chemical shifts as a function of external Ca^{++} ion concentration for the two PGP resonances appeared similar, providing no further light on the assignment of the two peaks. At pH 7.15 (used for the Ca^{++} ion binding experiment) the monoester γ-PGP phosphate is unlikely to be

fully ionized (Kates, 1978). This may account for the similar Ca^{++} ion binding properties of the two phosphate moieties.

The lowfield PGP resonance is assigned as that from the γ-phosphate and the highfield peak to the α-phosphate by the following reasoning:

First, in the decoupled spectrum the half-height of the lowfield peak is less than that of the upfield peak (Fig.2.5.a), implying a longer spin-spin relaxation time (T_2). This is also observed in the high resolution phosphorus-31 spectra of organic solvent extracted PGP sonicated SUVs in aqueous buffers (Fig.2.5.e). A longer spin-spin (T_2) relaxation time is consistent with a faster rate of motion within a molecule. In a PGP molecule a terminal monoester phosphate moiety is less motionally restricted than a diester phosphate, particularly in a bilayer or micelle structure. This is also observed in the c.s.a.s measured from broad line phosphorus-31 powder patterns of red (Introduction Fig 4)) and purple membranes and PGP bilayers (Ekiel *et al.*, 1981).

Second, the upfield resonance is of very similar chemical shift to that from the diester phosphorus of DMPG. This assignment agrees with that postulated by Goni *et al.*, (1982) from comparison of the chemical shift exhibited by the monoester phosphate of phosphatidic acid relative to the diester moiety of cardiolipin.

None of the ^{31}P-NMR spectra of SDS solubilized purple membrane detect the presence of a resonance that corresponds to DMPG, although it is reported that 5mol% of the purple membrane polar lipids in *H.cutirubrum* is 2,3-O-diphytanyl-PG (Kates 1978 and Kates *et al.*, 1983). Furthermore TLC (30:4:10; $CHCl_3$:MeOH:90% acetic acid) of organic solvent extracted polar *H.halobium* lipids stained with molybdenum blue revealed three phosphate components; one of which showed much more intensely than the other two and corresponded to PGP (Kates, 1978). The faint spot of highest R_f value exhibited an similar mobility to DMPG, while the faint spot of slowest mobility was assigned as PGS. TLC thus confirms the presence of the three phospholipids described by Kates (1978) in the organic solvent polar lipid extract of *H.halobium* purple membrane. It is possible, however, that the PG detected by TLC originates from degradation of PGP or PGS during the organic solvent extraction procedure.

Solubilization of intact purple membrane in SDS at neutral pH may not cause such degradation, thus accounting for the absence of a resonance of chemical shift identical to DMPG. The assignments of two minor resonances (I and II) in SDS-solubilized purple membrane (Fig 2.5.a) has not yet been achieved, although it would not be unreasonable to suggest they are PGS and PG. If this were the case, the downfield shift of the *H.halobium* 2,3-O-diphytanyl-PG resonance relative to that of DMPG would be explained by the presence of O-alkyl ether linkages instead of the O-ester linkages in DMPG. A high resolution ^{31}P-NMR spectrum of the organic solvent extracted polar lipids is not available to confirm this.

An alternative assignment for the minor peak (I) 16.490 ppm upfield from MDP is phosphate bound to the bacteriorhodopsin molecule itself. Analysis of total phosphate and lipid phosphate in purple membrane (Kushwaha, *et al.*, 1975) suggest the presence of one or two moles of phosphate bound to the protein. Also Spudich & Spudich (1983) report a labelling with ^{32}P of a protein that comigrates with bacterio-opsin during SDS PAGE. This would account for its possible presence in the spectra of DMPC/bR complexes delipidated by gel exclusion chromatography.

Quantitative analysis of phospholipid headgroup composition of purple membrane and DMPC/bR complexes. It is reported (Kates, 1978) that in purple membrane, PGP accounts for some 60% of the polar lipids. Estimations of the number of polar lipids per bacteriorhodopsin monomer vary from 6 (Kates, *et al* 1983) to 12 (calculated from Blaurock & Stoeckenius, 1971); implying between four and eight PGP molecules per protein. From high resolution ^{31}P-NMR peak areas of SDS-solubilized purple membrane and using a total lipid phosphate/bR ratio of 19.5:1, it was calculated (Table 1) that there are 6.9 moles of PGP-γ phosphate, 9.96 moles of PGP-α and 2.5 moles of the unassigned phosphate species (16.490 ppm from MDP) per mole of bacteriorhodopsin (Table 1). These values thus agree well with those calculated from Blaurock & Stoeckenius, (1971), but are double those reported by Kates *et al.*, (1983).

The discrepancy observed between the molar ratios of PGP-α to -γ phosphate may be due to two reasons, which are not mutually exclusive.

First, the spin-lattice relaxation time (T_1) for the γ-phosphorus may be longer than that of the α-phosphorus. Spin-lattice relaxation times for detergent solubilized phospholipids are in the order of 1s. To obtain the spectra of SDS-solubilized purple membrane, a recycle time of 2.34 s was used which may impose a greater saturation on the γ-nucleus than the α-nucleus. This would cause a loss in intensity of the γ-resonance relative to the α-peak.

Second, the resonance assigned as the PGP-α phosphate may be superimposed on those from the as yet unassigned *H.halobium* PG and PGS phosphates. In the undecoupled ^{31}P-NMR spectrum of SDS-solubilized purple membrane (Fig.2.5.c), resolution of the minor resonance seen in noise decoupled spectra at 16.766 ppm (Fig 2.5a) from the PGP-α peak is not achieved. As discussed above this minor resonance may be 2,3-O-diphtanyl-PG or PGS. Thus the value of 9.9 moles PGP-α phosphate per bacteriorhodopsin monomer, may also include the PG and PGS components, which account for 15% of the phospholipids (calculated from Kates, 1978) i.e. 85 mol% of the phospholipids is PGP. If this is the case, the value of 8.5 PGP molecules per bR monomer is in better agreement with the number (7) of PGP-γ phosphate groups detected per protein.

High resolution ^{31}P-NMR is a particularly effective technique for quantitatively and quantitatively analysing the phospholipid headgroup compositions of SDS-solubilized DMPC/bacteriorhodopsin lipo-protein complexes (Fig.2.14). The presence of purple membrane PGP in detergent reconstituted DMPC/bR complexes, in which all the endogenous purple membrane phospholipids have been retained (using the reconstitution method of Cherry *et al.*, 1978) is clearly demonstrated (Fig.2.14.c). The DMPC resonance is well resolved from the purple membrane phospholipid resonances, being 1.2 ppm upfield, so facilitating determination of the peak areas from the spectrum integrals. Analysis of DMPG/bR lipo-protein complexes, for example, may not prove to be as successful because the purple membrane PGP-α resonance and DMPG resonance are not well separated (Figs. 2.6 and 2.7.), rendering accurate peak integral determination difficult.

Figs.2.13 (222:1 mole ratio DMPC/bR complex), 2.14.b (68:1 mole ratio DMPC/bR complex), 2.15.b (67:1 mole ratio DMPC/bR complex) and c (95:1 mole ratio DMPC/bR complex) present strong evidence that the gel filtration method of delipidating detergent solubilized bacteriorhodopsin (Huang *et al.*, 1980) does effectively remove all the endogenous purple membrane PGP and that DMPC is the only phospholipid species present. Furthermore, no trace of lyso-PC is detected in any of the complexes. The minor purple membrane phosphorus-31 resonance I, 16.490 ppm from MDP, however, may not be completely removed in any of the complexes, although it is difficult to distinguish the resonance from background noise. Accurate quantitative analysis for this phosphate species in the delipidated complexes could not be performed.

In contrast, high resolution ^{31}P-NMR spectra of the nsTP-produced complexes after SDS-solubilization reveal the presence of purple membrane phospholipids in addition to DMPC (Fig. 2.16). The nsTP labelling technique thus appears to retain purple membrane PGP and the phosphate species responsible for the minor resonance, I, at 16.490 ppm. Results presented in Table 2 indicate that between 76 and 86% of the total purple membrane PGP phosphate is retained after nsTP-mediated addition of DMPC. This implies that nsTP catalyses a transfer of DMPC into the purple membrane with little exchange of purple membrane phospholipids into the DMPC SUVs. The reason for this may be due to a high selectivity imposed by bacteriorhodopsin on the negatively charged purple membrane polar lipids.

For all three complexes quantitatively analysed by high resolution ^{31}P-NMR spectroscopy, the number of moles of PGP-α phosphate retained was found to be very consistent at between 7 and 8 moles per 26,000Da bR monomer (Table 1). The number of moles of PGP-γ phosphate group retained per bR monomer was in the order of one to two moles less than observed for the α-phosphate group. As discussed for purple membrane itself, this discrepancy may reflect the PGP-α resonance enveloping the signals from the other purple membrane phospholipid diester (α-) phosphate nuclei; namely those of PG and PGS. Determination of the number of moles of PGP-γ

phosphate present, thus reveals the actual number of moles of PGP retained per bR monomer. Comparing the number of moles of PGP-γ phosphate present in each complex with the value obtained for purple membrane itself, demonstrates between 80 and 97% of the purple membrane PGP to be retained in the nsTP-produced complexes (Table 2). The percentage retention of phospholipids contributing to the PGP-α resonance was not as high as for the PGP-γ phosphate, varying from 73 to 78%. Assuming the PGP-α resonance to include signals from PG and PGS, this may indicate a slight loss of PG or PGS from the vesicles relative to that of PGP during the nsTP-mediated addition.

High resolution ^{31}P-NMR, not only provides qualitative and quantitative information on the phospholipid headgroup composition of the vesicles, but also demonstrates the integrity of the DMPC in the vesicles. Detergent dialysis takes up to two weeks at 25°C. During this time, the DMPC could deteriorate. Confirmation of the absence of any lyso-PC is particularly important for the complexes prepared by nsTP-mediated transfer of DMPC to purple membrane; it would be conceivable to have traces of phospholipases present, particularly in the partially purified liver nsTP extracts. Any hydrolysis or rearrangement of the DMPC would be detected in the high resolution ^{31}P-NMR spectra. Lyso-PC, phosphatidic acid and phosphorylcholine exhibit different chemical shifts to DMPC (Henderson *et al.*, 1974). The high resolution ^{31}P-NMR spectra for the nsTP-produced complexes present evidence that the partially purified nsTP extracts used do not degrade the DMPC.

Summary of Chapters 1 & 2.

Two different methods are described for producing DMPC/bacteriorhodopsin vesicles of high homogeneity with respect to lipid/protein ratio as determined by sucrose density gradient centrifugation. The first method is a conventional detergent technique, that allows control of certain vesicle characteristics. Thus, by employing a gel-filtration step, all the endogenous purple membrane lipids can be removed, such that DMPC is the only lipid present. Furthermore, the vesicle size can be varied by the rate of cholate removal during dialysis. The second method employs a phospholipid transfer protein to incorporate DMPC from donor SUVs into the purple membrane. Its main advantages are that it is fast and detergents are not required. So far, no method has been explored to control vesicle size or phospholipid headgroup composition. For the complexes analysed, high resolution ^{31}P-NMR revealed a major proportion (76 - 86%) of the total purple membrane phospholipid phosphate to be retained by the method. Between 80 and 97% of the *H.halobium* PGP - the major phospholipid of purple membrane - was determined to remain. Two major disadvantages with the nsTP-technique are the small size of the vesicles produced and the limitation of the amount of DMPC that can be added per protein monomer.

Chapter 3

Bacteriorhodopsin/DMPC interactions in vesicles from which all the endogenous purple membrane lipids have been removed - a ^{31}P- and ^{2}H-NMR and electron spin resonance study.

3.I) Introduction.

In this chapter, protein-lipid interactions in the DMPC/bR vesicles, from which all the endogenous purple membrane phospholipids have been removed, are studied by magnetic resonance techniques - namely broadline deuterium and phosphorus-31 NMR and ESR. To date no biophysical studies have been reported on DMPC/bR complexes from which all the purple membrane lipids have been removed, although there is extensive literature coverage for such complexes with all the endogenous purple membrane lipids retained (reviewed in Introduction). The aim of this chapter is to obtain information on:

a) bacteriorhodopsin mediated changes in the dynamic and conformational properties within the DMPC phosphocholine headgroup moiety at the membrane surface;

b) temperature dependent changes in the aggregation state of the bacteriorhodopsin within the plane of the DMPC bilayer;

c) effect of bacteriorhodopsin on the main gel-to-liquid crystalline phase transition of the supporting DMPC bilayer; and

d) the number of boundary lipids per bacteriorhodopsin monomer and whether the protein exhibits any selectivity for negatively charged lipids (e.g.PG) over the zwitterionic PC.

The dimyristoyl phosphatidylcholine (DMPC) used to form bilayer complexes with bacteriorhodopsin was selectively deuterated at either the γ-methyl groups (DMPC-d_9) or the α- and β-CD_2 methylene segments (DMPC-d_4) of the choline

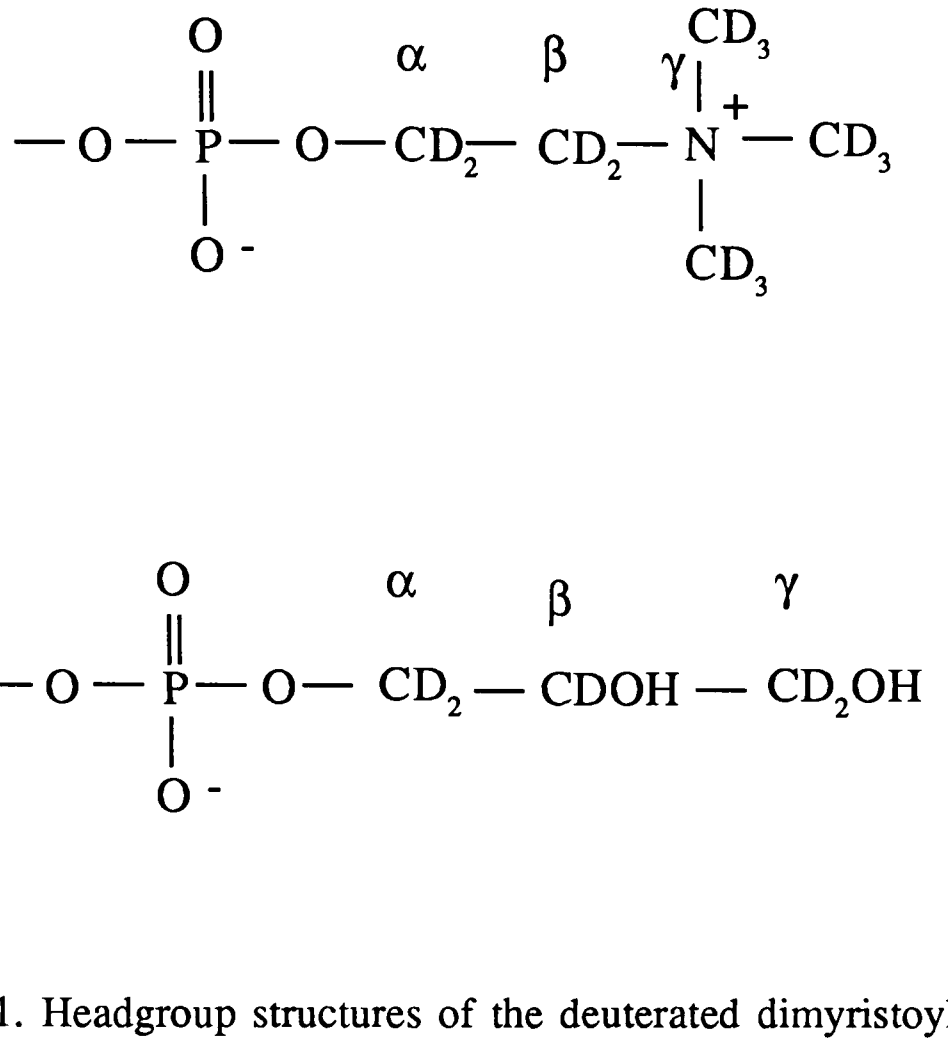


Fig. 3.1. Headgroup structures of the deuterated dimyristoyl phospholipids used in this thesis for deuterium NMR; a) PC. DMPC-d_4 with α- and β-methylene segments deuterated and DMPC-d_9 with γ-methyl groups deuterated; and b) PG-d_5.

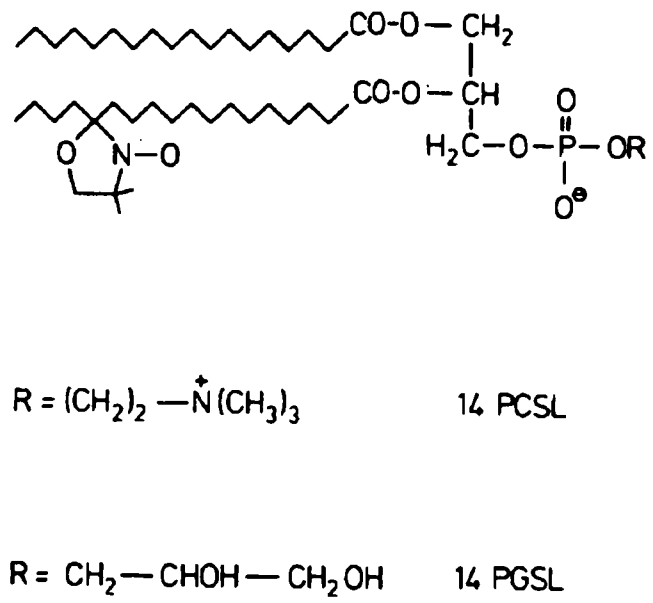


Fig. 3.2. Structures of the spin-labelled phospholipids, labelled with the doxyl moiety on the C-14 segment of the β-chain [β-14-(4',4'-dimethyl-oxazolidine-*N* - oxyl)stearoyl-γ-stearoyl-α-phospholipid (PLSL) used in this thesis; Two headgroups were used; 14-PCSL, phosphatidylcholine; 14-PGSL, phosphatidylglycerol.

headgroup (Fig.3.1.a). Solid state deuterium and phosphorus-31 NMR spectra thus provide information on all segments of the phosphocholine headgroup except that of the quaternary amine nitrogen. The parameters measured include the deuterium NMR quadrupole splittings and the phosphorus-31 c.s.a.s, spin-lattice (T_1) relaxation times and spin-spin (T_2) relaxation times, described in the Introduction to this work. The deuterium NMR quadrupole splittings and the phosphorus-31 chemical shift anisotropies (c.s.a.) measured from the NMR spectra provide information on the amplitude of motion of the particular segment of the headgroup. Phosphorus-31 spin-spin (T_2) and spin-lattice relaxation (T_1) times provide information on the effect of protein on the dynamics (i.e. rates of segmental motion) of the phosphate moiety. Thus from the deuterium and phosphorus-31 NMR data, a comprehensive picture of the effects of bacteriorhodopsin on the motional properties of the phosphocholine headgroup is attained. To date no broadline NMR studies on lipids reconstituted with bacteriorhodopsin have been reported. Indeed, the only literature available is a broadline ^{31}P-NMR study of bacteriorhodopsin in the purple membrane itself (Ekiel *et al.*, 1981).

The temperature dependence of the deuterium NMR quadrupole splittings as demonstrated for band-3 (Dempsey *et al.*, 1986), can be used to provide information on the state of protein aggregation. Bacteriorhodopsin is an integral membrane protein that in native purple membrane provides an extreme example of aggregation to form ordered para-crystalline two-dimensional hexagonal arrays within the bilayer. When reconstituted into DMPC bilayers with all the purple membrane lipids retained (Cherry *et al.*, 1978; Heyn *et al.*, 1981a) bacteriorhodopsin has been shown to crystallize into purple membrane like patches below the phase transition temperature of the lipid, but dissociate into monomers on warming to higher temperatures. Clearly, it is of interest to investigate the aggregation/dispersion properties of bacteriorhodopsin in DMPC bilayers without the endogenous purple membrane phospholipids present as this provides information on whether the temperature dependent association/dispersion properties of bacteriorhodopsin are mediated predominantly through protein-protein

interactions or alternatively dependent on the nature of the bilayer lipids.

In Chapter 2, it was found that the size of the DMPC/bR vesicles reconstituted by dialysis could be varied considerably by employing differential rates of cholate removal (described in Chapter 1). The quadrupole splittings and lineshapes of deuterium NMR spectra obtained from the choline γ-methyl groups are found to be particularly dependent on the rate of cholate removal used during the reconstitution procedure. Thus when interpreting the NMR data in terms of the effects of the protein on lipid headgroup conformational properties and temperature-dependent changes in the protein aggregation/dispersion properties, it is important to be aware of any contribution from averaging of the spectral anisotropy by tumbling of small vesicles (Burnell *et al.*, 1980).

Bilayers of synthetic phospholipids with homogeneous saturated fatty acyl chains undergo a highly co-operative main gel-to-liquid crystal phase transition. For protein-free DMPC bilayers this occurs sharply at 23°C (Marsh & Watts, 1981). Numerous biophysical techniques, including DSC (Mabrey-Gaud, 1981), fluorescence depolarisation and partitioning (Marsh & Watts, 1981) of the small nitroxide free radical (TEMPO) are available to investigate the phase transition of the lipids. In this present work, TEMPO partitioning is used to study the effect of changing the content of the integral protein bacteriorhodopsin on the mid-point and range of the main phase transition.

To date, no ESR studies with spin-label phospholipids (PLSL) have been reported on DMPC/bR vesicles with all the endogenous purple membrane phospholipids removed. The structures of the spin-labelled phospholipids - phosphatidylcholine spin-label (14-PCSL) and phosphatidylglycerol spin-label (14-PGSL) - used in this present study are shown in Fig.3.2. Both these spin-labelled phospholipids have stearoyl acyl chains the 2-position one of which bears the doxyl spin-label group at the C-14 segment. As reported for other protein systems (e.g. cytochrome *c* oxidase; Knowles *et al.*, 1979), the 14-PLSL spectra from bacteriorhodopsin-containing vesicles of high protein contents reveal two components. Spectral subtraction and simulation are used in this present work to determine the proportion of motionally restricted component in

ESR spectra of 14-PCSL incorporated in a DMPC/bR complex of high protein content. From this the number of boundary lipids per 26,000Da bacteriorhodopsin monomer can be calculated. In addition, any selectivity of the bacteriorhodopsin for phospholipids with the PG headgroup, with a net negative charge, relative to the zwitterionic PC is investigated. The only ESR studies reported on spin-labelled lipids in bacteriorhodopsin systems have used stearic acid spin-labels (SASL) incorporated into purple membrane itself. Chignell and Chignell (1975) demonstrated both 4- and 12-SASL to display highly motionally restricted spectra, with A_{max} values of 59 and 58.7 gauss at 37°C, respectively, consistent with a protein mediated ordering of the lipid acyl chains. The ESR spectrum, however, of 16-SASL revealed the presence of two populations of spin-label, one of which was more motionally restricted than the other. This was interpreted in terms of a *fluid* and a *boundary* component. Hoffmann *et al.*, (1980) extended the work on 16-SASL in purple membrane and interpreted the two component spectra in terms of a temperature dependent protein conformational change, although no explanation regarding the nature of the change was offered.

3.II). Materials and Methods.

Nuclear Magnetic Resonance. Broad line ^{2}H-NMR and ^{31}P-NMR spectra of phospholipid complexes were recorded on a Bruker WH300 (7.5 T) NMR spectrometer at 46.1 MHz and 121.4 MHz, respectively, or on a Nicolet 360 (8.4 T) magnet at 55.3 MHz and 145.9 MHz, respectively.

Deuterium NMR spectra were recorded into 2K points (1K real component and 1K imaginary component) after a pre-aquisition delay of 30μs (see Introduction) with a sweep width of 10,000 Hz (DMPC-d_9) or 40,000 Hz (DMPC-d_4). A relaxation delay of 250ms was used. The FIDs were zero-filled to 4 or 8K and a line broadening of 40 Hz applied with exponential multiplication. The apparent quadrupole splittings ($\Delta\nu_q$) were measured from the turning points of the powder pattern, as judged by the point of greatest height. For a spherically averaged powder pattern, the measured quadrupole splitting provides information on the amplitude of motion (Seelig *et al*, 1981).

Phosphorus-31 NMR spectra ($\Pi/_2$ pulse width; 18μs for dedicated ^{31}P probe; 21μs for broad band probe) were collected into 4K points after a pre-aquisition delay of 40μs with a sweep width of 40,000 Hz. The FIDs were zero filled to 8K and a line broadening of 80 Hz applied with exponential multiplication. A relaxation delay of 1s was used. The chemical shift anisotropy (c.s.a.) values (ppm) were measured from the half-heights of the upfield (90° orientation) and downfield (0° orientation) intensities. Phosphorus-31 spin-lattice (T_1) determinations were made using the inversion recovery method with a relaxation delay of 12s. Phosphorus-31 spin-spin (T_2) relaxation measurements were made with the Carr-Purcell (90 - τ - 180 - τ) spin echo pulse sequence with a relaxation delay of 6s. The pre-aquisition delay was set to a minimum value of 1μs to ensure that aquisition occurred very close to the top of the echo (Davies, 1983). Spin-spin (T_2) relaxation time (for the 90° resonance, high field spectral extreme) were calculated by plotting 2τ vs ln(I), where I is the absolute intensity, or by using a Nicolet curve fitting routine. ^{31}P-NMR spectra were not proton decoupled.

ESR of DMPC/bR complexes with spin-labelled phospholipids. Complexes were labelled with 14-PCSL or 14-PGSL by ethanolic injection as described previously (Watts *et al.*, 1979; Knowles *et al.*, 1979) to give approximately one spin-labelled lipid per 100 DMPC molecules. Free spin label and ethanol were removed by two washes in 10mM Tris/HCl, pH 7.5 (100,000g; 15°C; 20 min) and then a linear 5 - 35% (or 15 - 45%) sucrose density gradient (Beckman SW40 rotor; 250,000g; 4°C; 12 hr). Sucrose was removed by a further three washes in the same buffer and the pellet loaded into a sealed quartz tube, using a bench centrifuge. Spectra were recorded on a Bruker ESP300 spectrometer with a sweep width of 100 gauss, a modulation amplitude of 1 gauss. Spectra were collected into 1K points with a conversion time of 327.68ms (resulting scan time for spectrum; 335s) and a time constant of 2.56ms per point. A microwave power of 20mW was used at 9.3GHz (X band). The temperature was controlled with a Bruker liquid nitrogen variable temperature unit. The sample tube was temperature stabilized in silicone oil and the exact temperature measured by a

thermocouple placed in the oil. Spectra were recorded every 3°C.

Bilayer phase transition measurements using TEMPO partitioning. TEMPO (50µl 10^{-3}M in 10mM Tris/HCl, pH 7.5) was added to bacteriorhodopsin complex (~5mg lipid in 0.5cm^3 buffer) and the complex centrifuged (100,000g; 25°C; 15 min). After decanting the supernatant, the pellet was loaded into a sealed 100µl micropipette using a drawn out Pasteur pipette. The sealed sample tube was then placed in a 5mm NMR tube with silicone oil to stabilise the temperature. The exact temperature was determined by a thermocouple placed in the oil. ESR spectra were recorded on a Bruker ESP300 spectrometer using a conversion time of 164ms and a time constant of 82ms over 1K points. A sweep width of 100G with a modulation amplitude of 1G was used. Temperature was controlled by a Bruker liquid nitrogen VT unit. Spectra were recorded every 3°C and 5 min was allowed for temperature equilibration. The apparent partition coefficient (f) was calculated from the line heights as described in Marsh & Watts (1981).

3.III) Results.

A). **Deuterium-NMR**; In this section the solid state deuterium-NMR results obtained for the DMPC/bR complexes with all the endogenous purple membrane lipids removed are described. The effects of vesicle size (dependent on the speed of cholate removal used during the reconstitution procedure) on the deuterium NMR spectra and the temperature dependencies of the measured quadrupole splittings obtained from DMPC-d_9/bR complexes with the DMPC deuterated at the choline γ-methyl groups are reported first. For the large diameter vesicle complexes produced by the slow cholate removal procedure, averaging of the spectral anisotropy by tumbling effects is not significant, and the effects of bacteriorhodopsin content and temperature on the quadrupole splittings from the α- and β-methylene segment powder patterns are described. Finally, analysis in terms of a fast two site exchange model (Sixl *et al.*, 1984) allows quantification of the number of boundary lipids associated with each 26,000Da protein monomer.

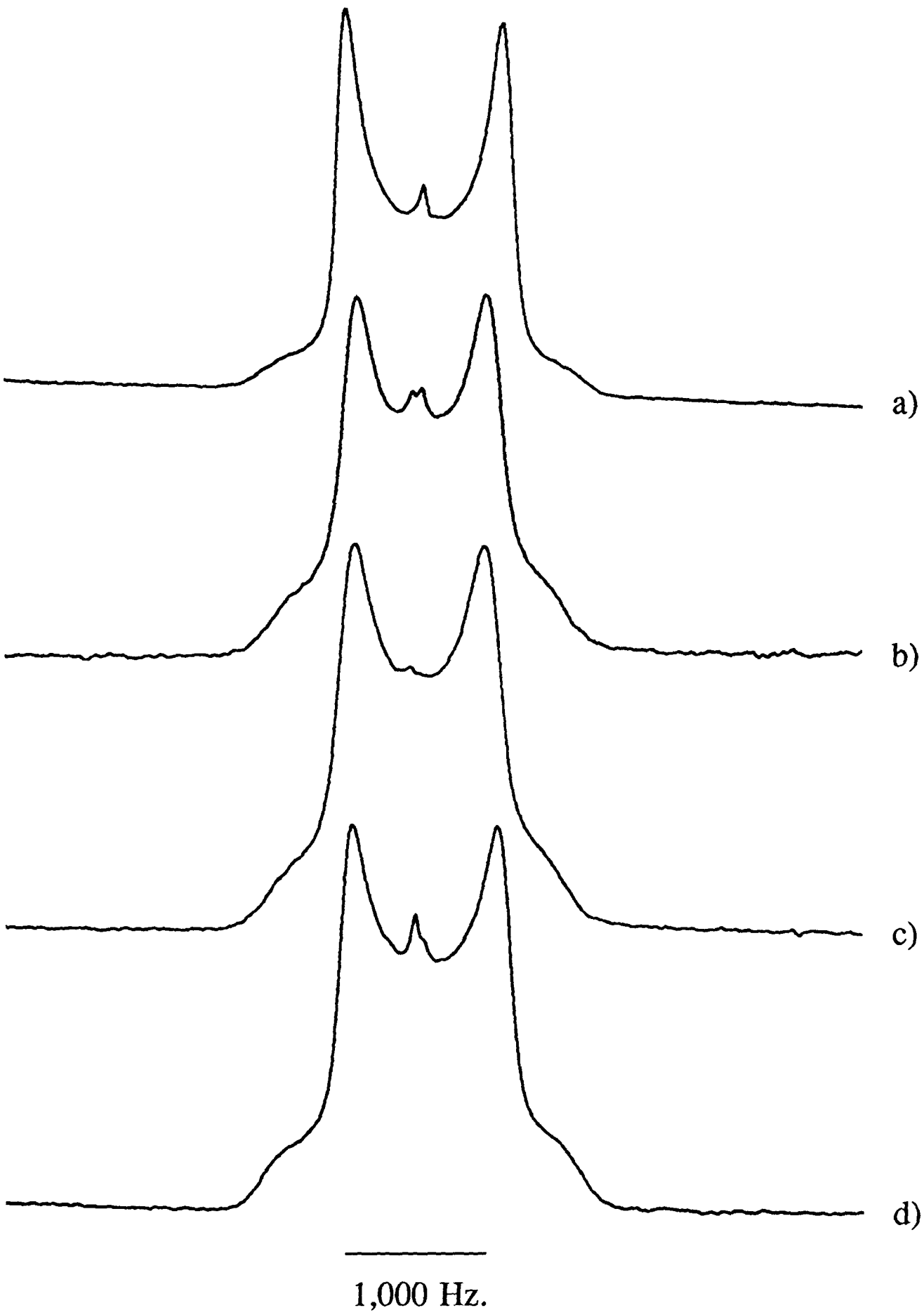


Fig.3.3

^{2}H-NMR spectra (46.1 MHz) recorded at 39°C of DMPC-d_9/bR complexes produced by the slow cholate removal method, with all endogenous purple membrane lipids removed. Vesicles in 10mM Tris/HCl, pH 7.5.
a) pure DMPC dispersion; b) 141:1 mole ratio DMPC/bR complex;
c) 131:1 mole ratio DMPC/bR complex; d) 68:1 mole ratio DMPC/bR complex.

For all bacteriorhodopsin/DMPC complexes only a single component deuterium powder pattern is observed for each set of equivalent deuterons. This is consistent with deuterium NMR spectra from other membrane protein/deuterated lipid systems and implies that lipids in contact with the protein are in fast exchange with bulk phase bilayer lipids. To obtain single component spectra the exchange rate between the two species must be greater than the difference in quadrupole splittings from each species. Thus, to obtain single component deuterium NMR spectra for DMPC-d_4 systems, where the quadrupole splitting (ν_f) for the α-methylene segment powder pattern in protein-free bilayer lipid is ~6,000 Hz and that for lipid in direct contact with the protein (ν_b) is small and approaching zero (Sixl *et al.*, 1984), then the exchange rate would have to be greater than $4\Pi(n_f - \nu_b)$ (see Introduction Fig.5) i.e. 75,000 s^{-1} in order to time average the quadrupole splittings. Thus exchange rates greater than the order of 10^4 s^{-1} will produce single component deuterium NMR spectra. The observed NMR spectra thus represent the time-averaged powder patterns from lipids in contact with the protein and from protein-free lipids in the bulk bilayer phase.

i) *Deuterium NMR results for DMPC-d_9/bR complexes produced by the slow cholate removal technique.* Representative ^{2}H-NMR spectra for the choline γ-methyl CD_3 groups of the DMPC-d_9/bR complexes of mole ratios of 141:1, 131:1 and 68:1, produced by the slow cholate removal technique and recorded at a temperature of 39°C, which is well above the main phase transition temperature of bR-containing DMPC bilayers (Fig.3.22) are shown in Figs. 3.3.b, c and d, respectively. Negative stain electron microscopy results (Chapter 2) show the vesicle diameters to be between 1,000 and 1,500 nm. These complexes give rise to well defined spherically averaged deuterium powder patterns with quadrupole splittings which could readily be determined to collapse by less than 20% when compared with protein-free DMPC bilayers (Fig.3.3.a). The quadrupole splitting measured for protein-free DMPC bilayers is 1,113 Hz at 39°C. The lower protein content complexes (131:1 and 141:1 DMPC/bR mole ratios) display similar quadrupole splittings to each other (923 Hz at 39°C) which are some 200 Hz smaller in magnitude than those for the protein-free DMPC

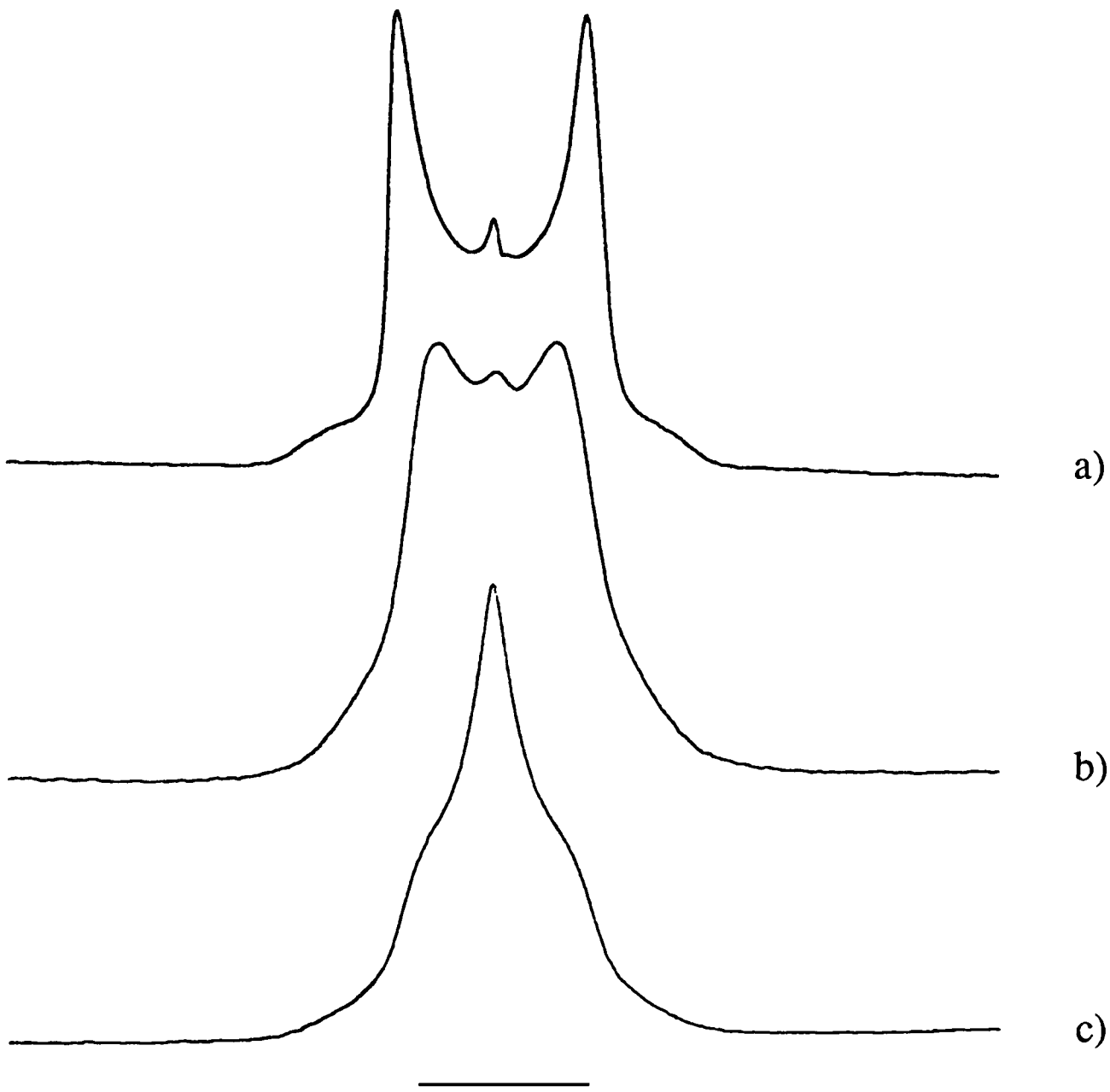


Fig.3.4

^{2}H-NMR spectra (46.1 MHz) recorded at 39°C for DMPC-d_9/bR vesicles of varying sizes, reconstituted by the fast cholate removal technique with all endogenous purple membrane lipids removed. Vesicles in 10 mM Tris/HCl, pH 7.5. a) pure DMPC dispersions with very large multilamellar vesicles; b) 187:1 mole ratio DMPC/bR complex with vesicles between 300 and 600nm in diameter; c) 1,444:1 mole ratio DMPC/bR complex with vesicles less than 300nm in diamter.

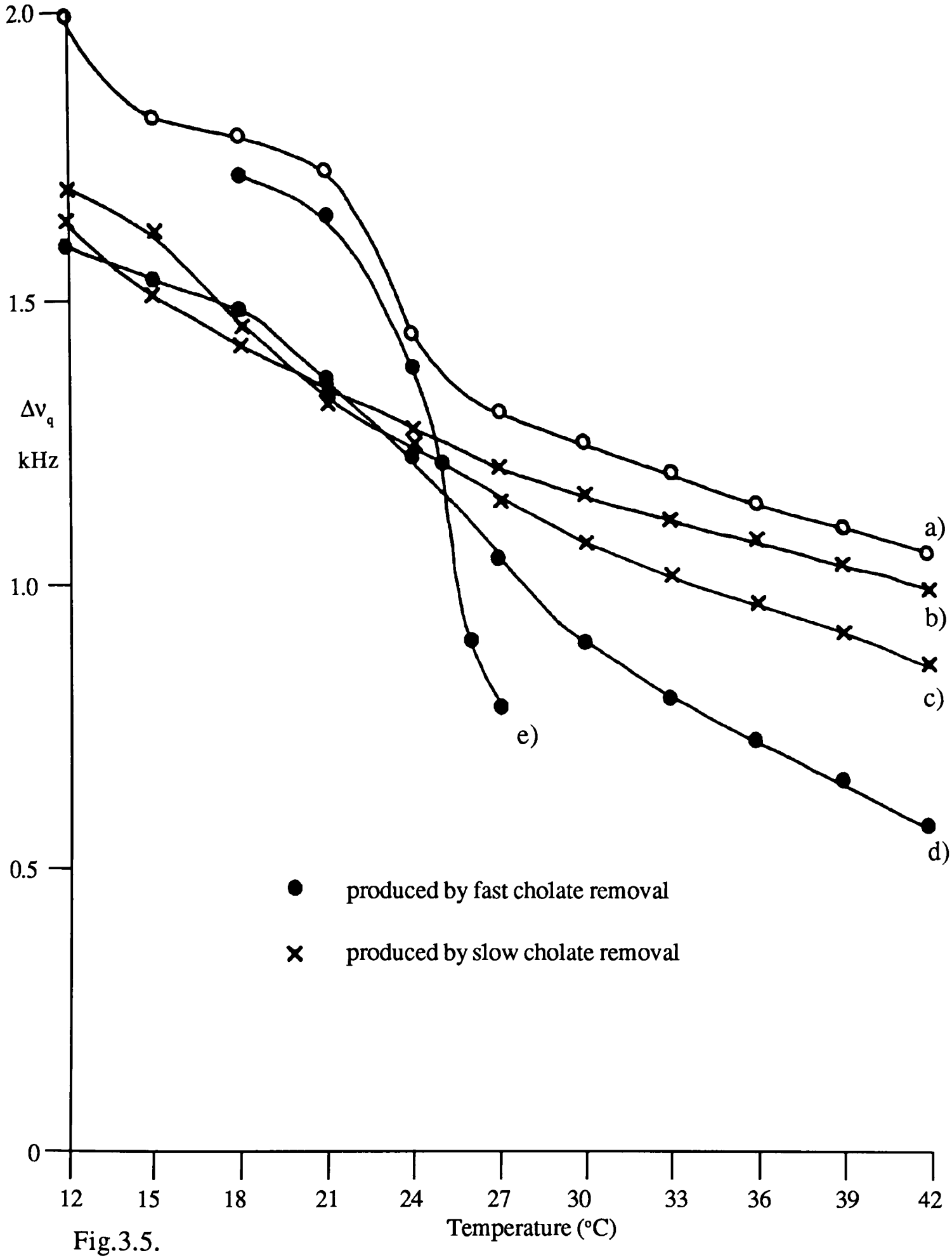


Fig.3.5.

^{2}H-NMR quadrupole splittings (46.1 MHz) measured for DMPC-d_9/bR complexes of different protein contents plotted as a function of temperature; a) protein-free lipid; b) 68:1 mole ratio complex; c) 141:1 mole ratio complex; d) 187:1 mole ratio complex; 1,444:1 mole ratio complex. The speed of cholate removal during dialysis appears to effect the temperature sensitivity of the quadrupole splitting.

sample. However, increasing the protein content from 131:1 to 68:1 DMPC/bR mole ratio was found to increase the magnitude of the quadrupole splitting (1,047 Hz for 68:1 mole ratio complex at 39°C), although this value is still smaller than for pure DMPC. For the protein complexes, the deuterium NMR spectra are seen to be broader than that for pure lipid. Furthermore the intensities of the 0° orientations are increased in the presence of protein. This may reflect magnetic ordering of the pure lipid (as is observed for the phosphorus-31 NMR spectra, discussed below).

ii) *Deuterium NMR results for DMPC-d_9/bR complexes produced by the fast cholate removal technique.* Fig.3.4.b and c show ^{2}H-NMR spectra, also recorded at temperatures above the main phase transition, from complexes produced by fast cholate removal during the reconstitution procedure, for which the vesicles are much smaller than those produced by slow cholate removal, as seen by negative stain electron microscopy (Chapter 2). The spectra for these complexes are different from those produced by the slow cholate removal technique; the measured quadrupole splittings being significantly reduced when compared to those of pure lipid dispersions or complexes produced by the slow cholate removal technique (described above). For example, the 187:1 mole ratio complex produced by fast cholate removal exhibits a quadrupole splitting of 664 Hz at 39°C, compared to 923 Hz measured for the similar protein content 141:1 mole ratio complex, produced by slow cholate removal. Indeed, spectra from the 1,444:1 mole ratio DMPC/bR complex, also produced by fast cholate removal, recorded at temperatures above 27°C appear completely collapsed and no quadrupole splitting is obtained. The intensities from the 0° orientations in spectra from both the 187:1 (Fig.3.4.b) and 1,444:1 (Fig.3.4.c) mole ratio complexes are almost smoothed out beyond detection compared to those displayed in the spectra of the protein-free lipid dispersions (Fig.3.4.a) or in those of the DMPC/bR complexes produced by slow cholate removal (Fig.3.).

iii) *Temperature dependence of ^{2}H-NMR spectra for DMPC-d_9/bR complexes.* In Fig.3.5., the quadrupole splittings ($\Delta\nu_q$) measured for the choline γ-methyl groups of DMPC-d_9 complexes are plotted as a function of temperature. The temperature profile

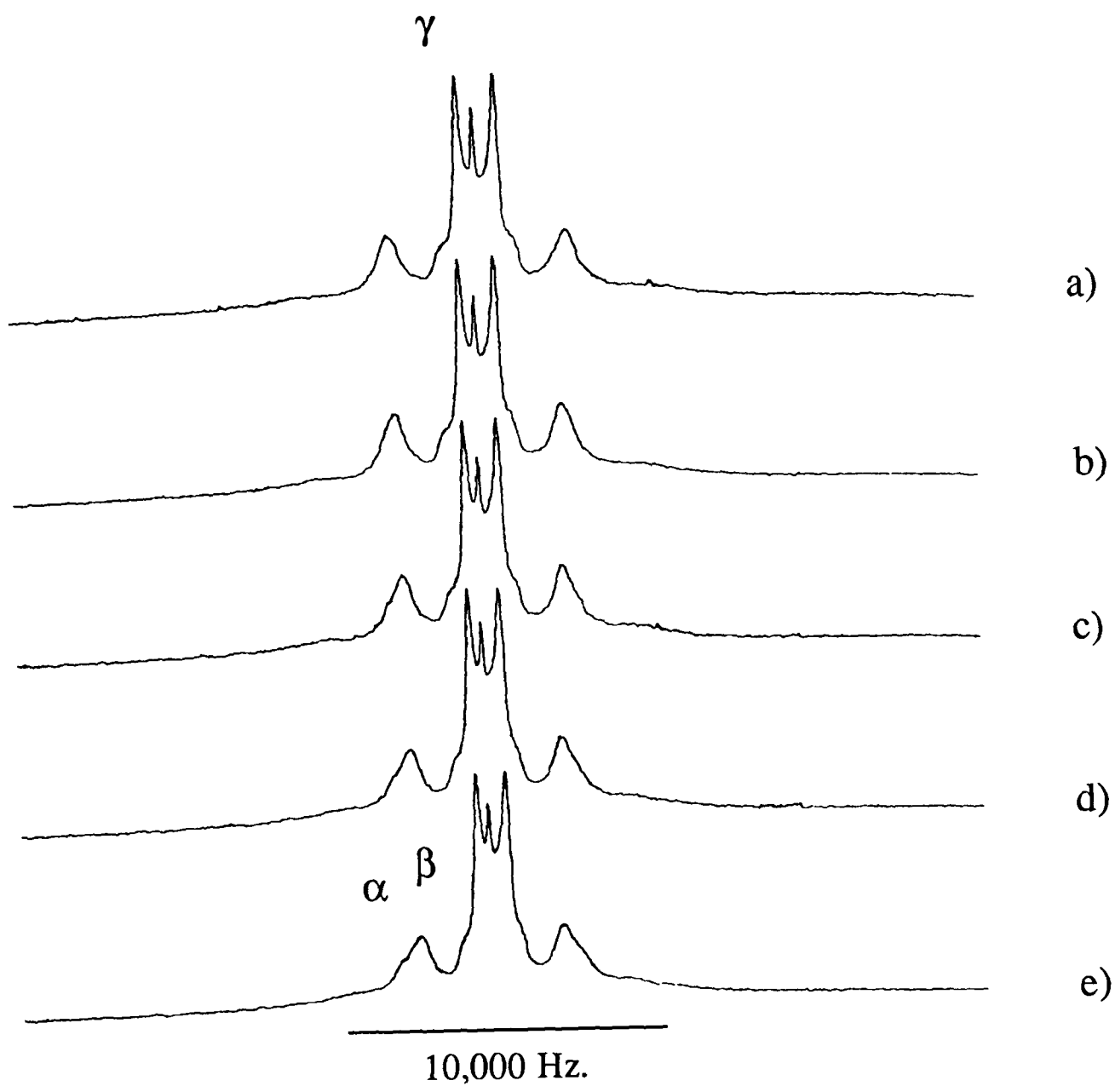


Fig.3.6. ^{2}H-NMR spectra (55.3 MHz) for the 67:1 mole ratio DMPC-d_4-d_9/bacteriorhodopsin complex produced by the slow cholate removal procedure with all purple membrane lipids removed. Vesicles in 10mM Tris/HCl, 1mM EDTA, pH 7.5. Spectra recorded at a) 25°C; b) 30°C; c) 35°C; d) 40°C; e) 45°C.

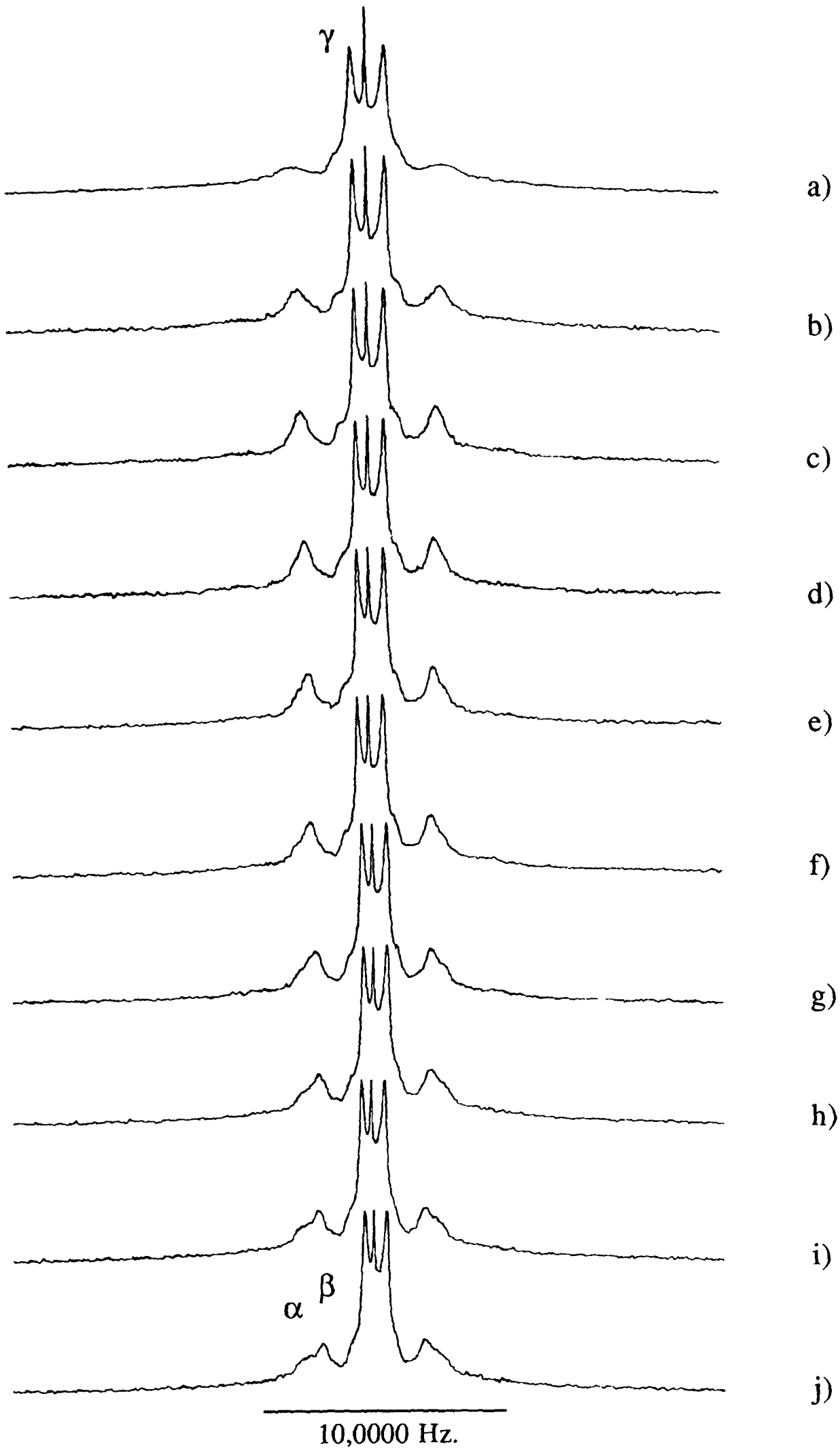


Fig.3.7. ^{2}H-NMR spectra (55.3 MHz) for the 95:1 mole ratio DMPC-d_4-d_9/bacteriorhodopsin complex reconstituted by the slow cholate removal procedure, with all purple membrane lipids removed. Vesicles in 10mM Tris/HCl, 1mM EDTA, pH 7.5. Spectra recorded at; a) 18°C; b) 21°C; c) 24°C; d) 27°C; e) 30°C; f) 33°C; g) 36°C; h) 39°C; i) 42°C; j) 45°C.

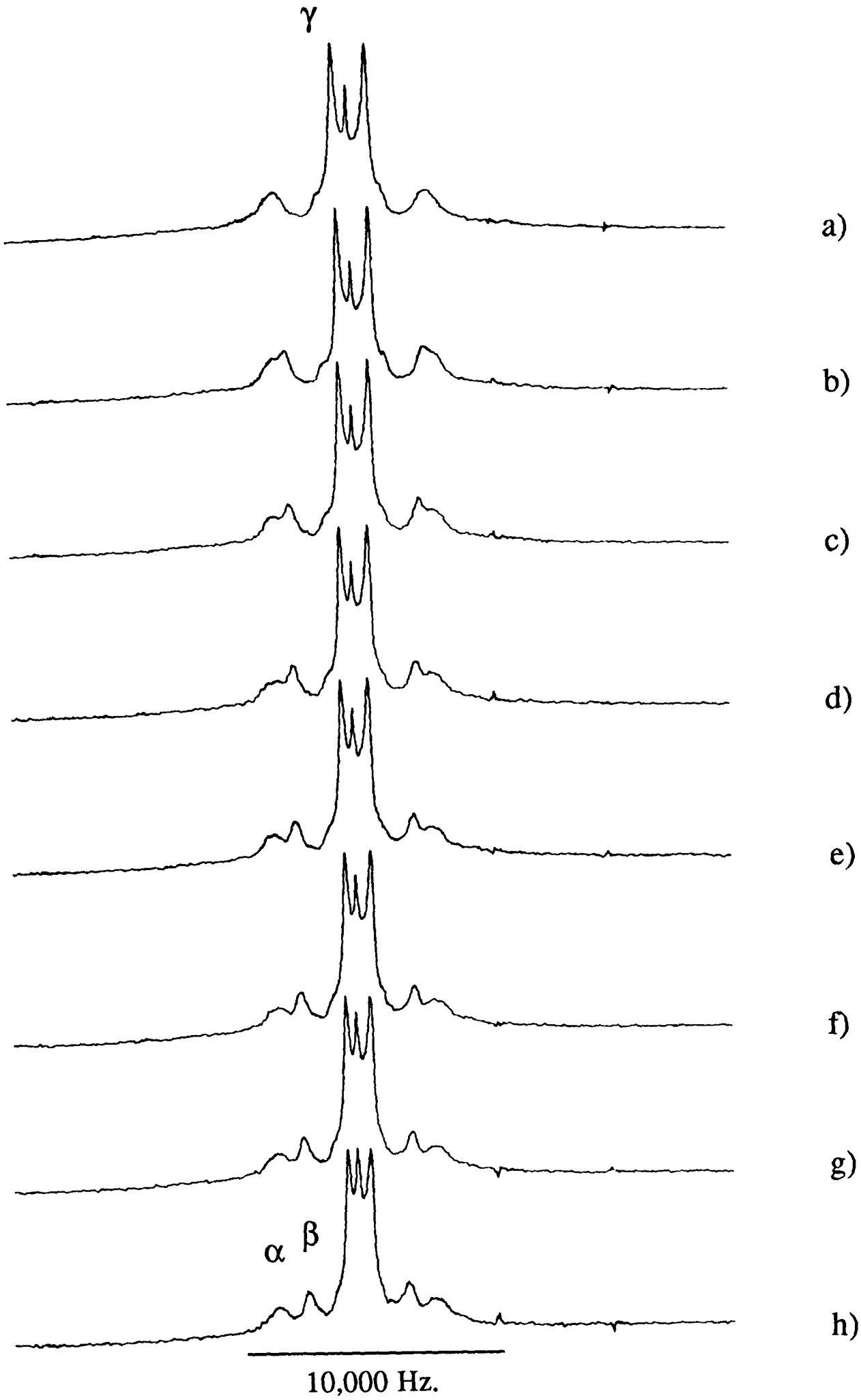


Fig.3.8. ^{2}H-NMR spectra (55.3 MHz) for the 182:1 mole ratio DMPC-d_4-d_9/bacteriorhodopsin complex, produced by the slow cholate removal procedure, with all purple membrane lipids removed. Vesicles in 10mM Tris/HCl, 1mM EDTA, pH 7.5. Spectra recorded at a) 21°C; b) 24°C; c) 27°C; d) 30°C; e) 33°C; f) 36°C; g) 39°C; and h) 45°C.

for protein-free DMPC displays two sharp changes at 10 and 23°C, corresponding to changes in the headgroup order associated with the pre-transition and the main gel-to-liquid crystal phase transition, respectively (Fig.3.22 this chapter; Sixl & Watts, 1982). Fig.3.5 is presented so as to emphasize the difference in temperature sensitivities displayed in the quadrupole splittings for complexes reconstituted by the two different rates of cholate removal.

The quadrupole splittings measured from the protein complexes (68:1 and 141:1 mole ratio DMPC/bR complexes) produced by slow cholate removal appear relatively insensitive to changes in temperature even at the phase transition. In contrast, the quadrupole splittings from complexes (187:1 and 1,444:1 mole ratio DMPC/bR complexes) produced by fast cholate removal display a greater sensitivity to temperature, particularly at the main phase transition temperature of pure lipid. This is most distinct for the quadrupole splittings measured from the 1,444:1 mole ratio DMPC/bR complex. On warming through the phase transition temperature (~23°C), the magnitude of the quadrupole splittings measured for this complex is seen to sharply decrease by the order of 1 kHz (Fig.3.5). Since the negative stain electron microscopy results (Chapter 2) showed a correlation between vesicle size and speed of cholate removal during DMPC/bR reconstitution (large vesicles with slow removal of cholate and small vesicles with fast detergent removal) it would appear that the deuterium NMR spectra from the choline γ-methyl groups of DMPC-d_9/bR vesicles may be reflecting this distribution in vesicle size.

iv) *Effect of temperature on deuterium NMR spectra obtained from the DMPC-d_4-d_9/bR complexes produced by the slow cholate removal procedure.* Figs.3.6, 3.7 and 3.8 show the deuterium-NMR spectra of the 67:1, 95:1 and 182:1 mole ratio DMPC-d_4-d_9/bR complexes, respectively, at increasing temperatures. All these complexes were produced by the slow cholate removal procedure and negative stain electron microscopy showed the vesicles to be larger than 600nm in diameter (Chapter 2). The powder patterns from the α- and β-methylene segments (DMPC-d_4) display larger splittings and are clearly resolved from that of the choline γ-methyl groups (DMPC-

d_9). On warming the component powder patterns from the α- and β-methylene segments become increasingly resolved although the extent depends on the protein content.

Gally *et al.*, (1975) assigned the component powder patterns from the α- and β-CD_2 choline methylene segments of protein-free DPPC using α-DPPC-d_2 and β-DPPC-d_2. The (outer) powder pattern with the larger quadrupole splitting was attributed to the α-CD_2 methylene segment, while the more temperature sensitive inner powder pattern represented the β-CD_2 methylene segments. For protein-free DMPC-d_4 (spectrum shown in Fig.3.11.f) the signal from the α-methylene CD_2 segment is seen to consist of two powder patterns of slightly different quadrupole splitting. The difference results from a small inequivalence in the motion of the two deuterons in the α-methylene CD_2 segment (as discussed by Wohlgemuth, *et al.*, (1980). In the presence of bacteriorhodopsin, however, their powder patterns become unresolvable due to a relaxation (T_2) broadening effect and the α-signal appears as a single broad powder pattern.

Increasing the temperature is seen to enhance resolution of the α- and β-methylene CD_2 segment powder patterns for all protein contents. This is particularly distinctive for the 182:1 mole ratio DMPC/bR complex (Fig.3.8); at 21°C, the two powder patterns are superimposed and only one quadrupole splitting is displayed. On warming to 27°C, the β-methylene segment powder pattern is clearly resolved from the broader α-methylene segment powder pattern, while at 45°C both powder patterns are entirely separate. Similar temperature dependent trends are displayed by the α- and β-methylene segment powder patterns for complexes of higher protein content on warming above the phase transition temperature; although as the protein content is increased so the resolution achieved between the α- and β-methylene segment powder pattern is reduced (discussed further below). Indeed for very high protein content vesicles (67:1 mole ratio DMPC/bR), the component α- and β-methylene segment powder patterns are virtually indistinguishable even at 45°C (Fig.3.6). For the 95:1 mole ratio complex (Fig.3.7) below 30°C the component α- and β-methylene segment

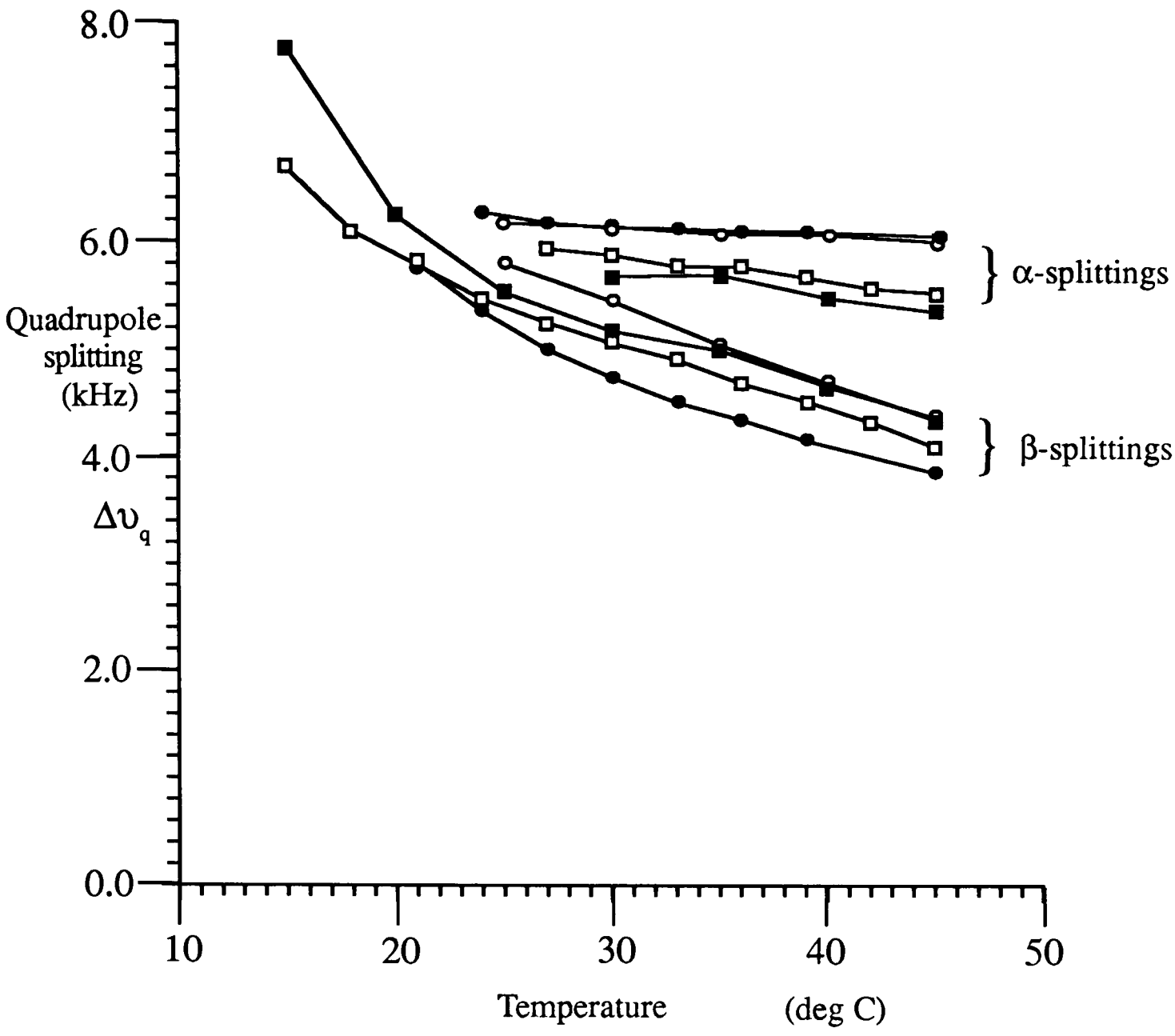


Fig.3.9. Effect of temperature on measured quadrupole splittings for the α- and β-methylene segments of DMPC-d_4 in the 67:1, 95:1 and 182:1 mole ratio DMPC/bR complexes with all endogenous purple membrane lipids removed, compared to those of protein-free DMPC dispersions. Vesicles in 10mM Tris/HCl, pH 7.5.

- ● pure lipid
- ○ 182:1 DMPC/bR complex
- □ 95:1 DMPC/bR complex
- ■ 67:1 DMPC/bR complex

powder patterns are not resolved. On heating to 45°C, partial resolution of the β-powder pattern from that of the α-methylene segment is displayed.

In Fig.3.9, the observed quadrupole splittings for the α- and β-methylene segments of DMPC-d_4 in complexes with bR at mole ratios of 67:1, 95:1 and 182:1 together with protein-free lipid are plotted as a function of temperature. The pure lipid value for the α-methylene quadrupole splitting is an average of the two component powder patterns. This was judged to approximate best the values obtained for the protein complexes, in which the two individual splittings are unresolved in the broad α-powder pattern. In the ^{2}H-NMR spectrum (not shown) of protein-free lipid at 25°C, the α- and β-powder patterns are barely resolved. On warming above the phase transition, the α-methylene segment quadrupole splittings remain constant at ~6kHz, while that of the β-methylene segment decrease (to 4,380Hz at 45°C); the β- powder pattern becoming clearly resolved from the α-powder pattern (spectrum shown in Fig.3.11.f). These results are consistent with those reported for DPPC above the phase transition temperature (Gally *et al.*, 1975). The α- and β-powder patterns in the presence of protein exhibit similar temperature dependent trends to the pure lipid, with the β-methylene segment quadrupole splittings being temperature sensitive and the α-splittings remaining virtually independent of temperature; although the absolute magnitudes of both α- and β- quadrupole splittings are influenced by the protein content of the vesicle (as described below).

v) *Effect of bacteriorhodopsin content on the choline α- and β-methylene segment powder patterns of DMPC-d_4.* Figs.3.10.a-e and 3.11.a-e display the ^{2}H-NMR spectra for DMPC-d_4-d_9/bR complexes ranging from lipid/protein mole ratios of 67:1 to 222:1 at 30°C and 45°C, respectively. All these complexes were produced by the slow cholate removal technique. The measured deuterium-NMR quadrupole splittings from the choline γ-methyl groups (DMPC-d_9) for these large vesicle complexes were found to be similar for all protein contents when measured at temperatures above the main phase transition, and their values when plotted as a function of temperature appeared between those of the 141:1 and 68:1 mole ratio DMPC/bR complexes, also

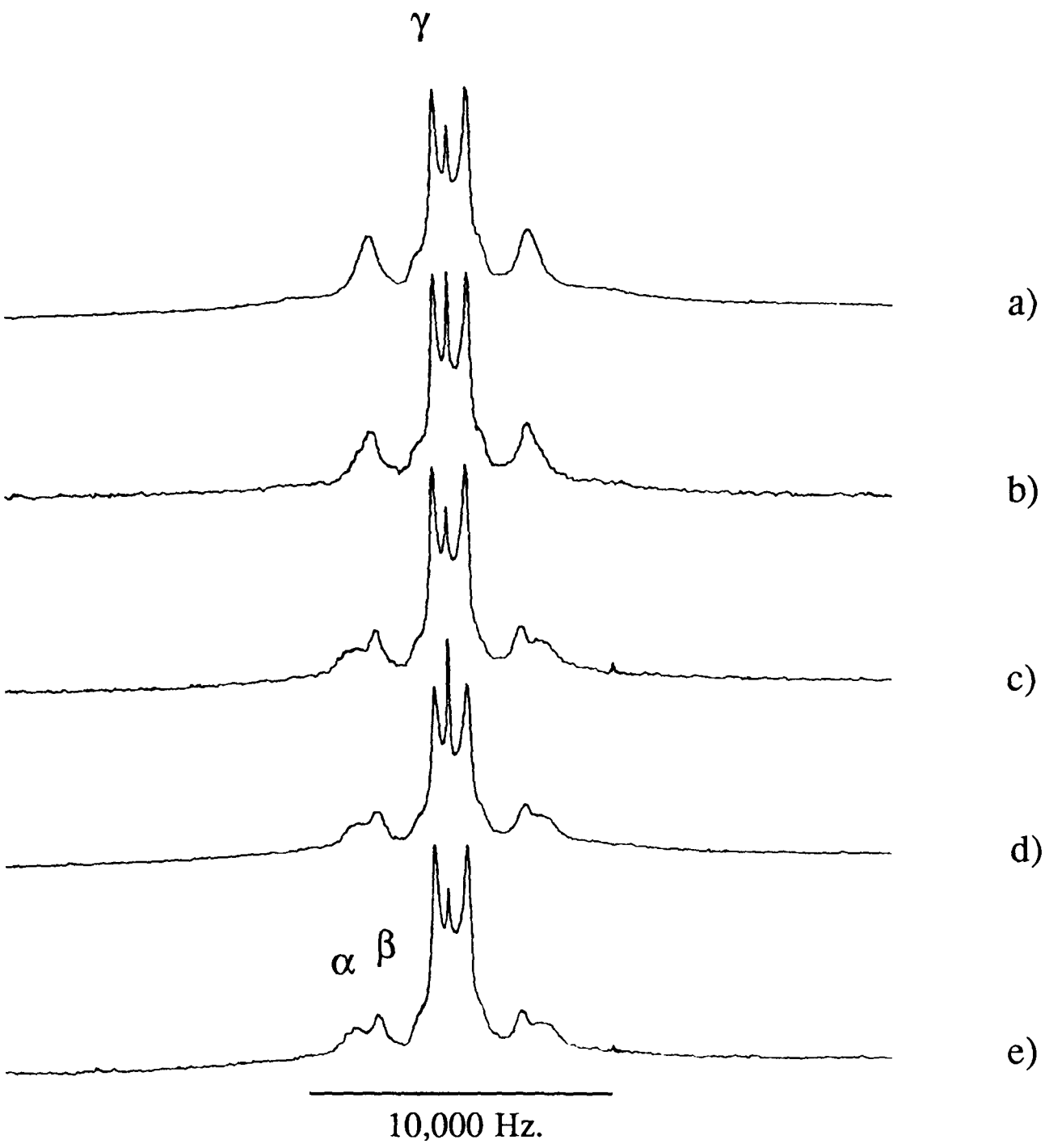


Fig.3.10. ^{2}H-NMR spectra (55.3 MHz) recorded at 30°C of DMPC-d_4-d_9/bacteriorhodopsin complexes of different protein contents produced by the slow cholate removal procedure, from which all endogenous purple membrane phospholipids have been removed. Vesicles in 10mM Tris/HCl, 1mM EDTA, pH 7.5. DMPC/bR mole ratios; a) 67:1; b) 95:1; c) 182:1; d) 218:1; e) 222:1.

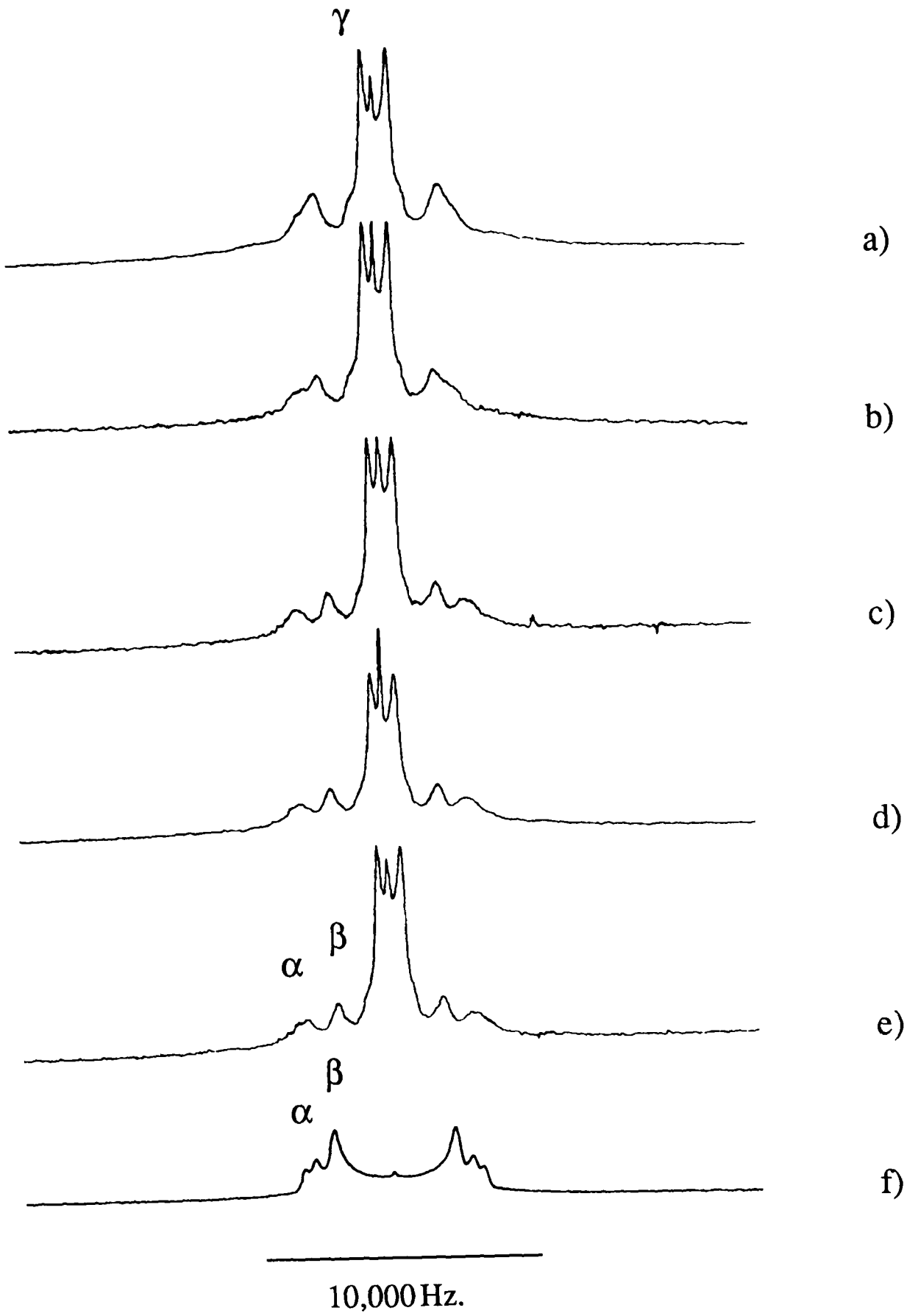


Fig. 3.11. ^{2}H-NMR spectra (55.3 MHz) recorded at 45°C of DMPC-d_4-d_9/bacteriorhodopsin complexes of different protein contents produced by the slow cholate removal procedure, from which all endogenous purple membrane phospholipids have been removed. Vesicles in 10mM Tris/HCl, 1mM EDTA, pH 7.5. DMPC/bR mole ratios; a) 67:1; b) 95:1; c) 182:1; d) 218:1; e) 222:1; and f) protein-free DMPC-d_4 dispersion for assignment comparison.

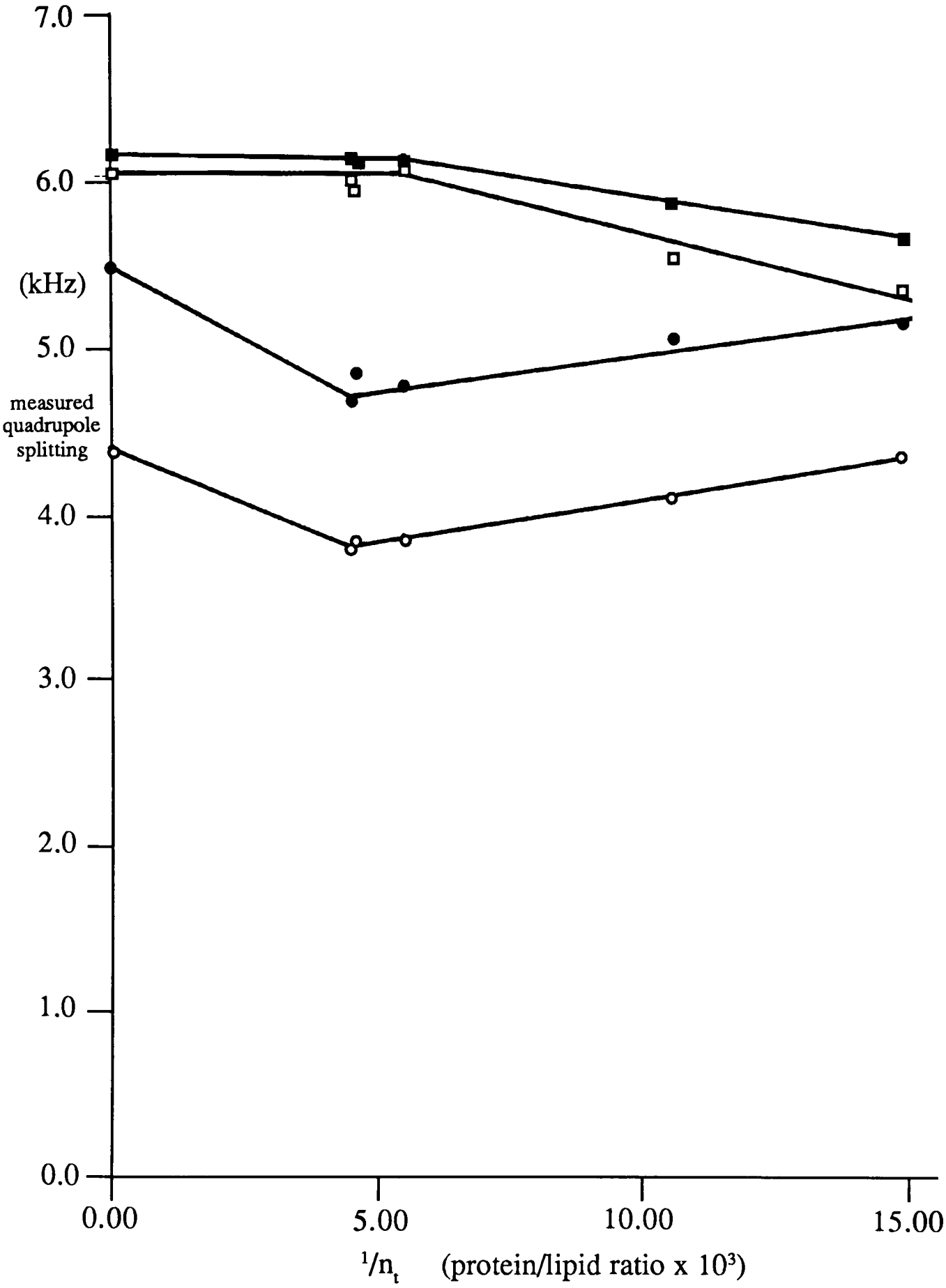


Fig.3.12. Deuterium-NMR quadrupole splittings of the α- and β-methylene segments for DMPC/bR complexes at 30°C and 45°C plotted as a function of inverse lipid/protein ratio (mol/mol).

- ■ α-methylene splitting at 30 °C
- □ α-methylene splitting at 45 °C
- ● β-methylene splitting at 30 °C
- ○ β-methylene splitting at 45 °C

produced by slow cholate removal, shown in Fig.3.5. However, the α- and β-CD_2 methylene segment deuterium-NMR powder patterns of DMPC-d_4 appeared to be significantly more sensitive to the protein content of the vesicles than the corresponding powder patterns for DMPC-d_9 choline γ-methyl group deuterons.

For temperatures above the main phase transition temperature, increasing the bacteriorhodopsin content of the vesicles is seen to result in the α- and β-methylene segment powder patterns becoming superimposed; reducing the resolution of the quadrupole splittings from the α- and β-methylene segments. Indeed at 30°C, the component powder patterns are virtually unresolvable for complexes with less than 95 DMPC lipids per protein molecule (Fig.3.10). At 45°C, for high protein content vesicles (DMPC/bR mole ratio 67:1), the α- and β-methylene powder patterns are just distinguishable, while increasing the lipid content to a mole ratio of 95:1 DMPC/bR, improves the resolution of these two powder patterns until at a DMPC/bR mole ratio of 182:1, a complete separation of the quadrupole splittings is observed as for protein-free lipid (Fig. 3.11.f). Complete separation is also displayed in spectra from the 218:1 and 222:1 mole ratio DMPC/bR complexes at 45°C (Fig.3.11.d and e).

Fig. 3.12 shows the quadrupole splittings for the α- and β-methylene deuterons measured from DMPC/bR complexes at two temperatures above the main phase transition (30 and 45°C), plotted as a function of the inverse of the lipid/protein ratio (that is the mole fraction of bacteriorhodopsin). At all temperatures above the main phase transition, incorporation of small amounts of bacteriorhodopsin (up to 0.55 mol% i.e the 182:1 mole ratio DMPC/bR complex) into DMPC bilayers is seen to have little effect on the magnitude of the quadrupole splitting measured for the α-methylene segments relative to those for pure lipid. In contrast, incorporation of small quantities of bacteriorhodopsin (0.45 to 0.55 mol% protein i.e. 222:1 to 182:1 DMPC/bR mole ratios) causes a significant decrease in magnitude (571 Hz) of the β-methylene segment quadrupole splittings relative to those of protein-free lipid. Indeed, for all temperatures above 30°C, the complexes of lower bacteriorhodopsin content (that is 222:1 to 182:1 mole ratios DMPC/bR) display the smallest magnitude quadrupole splittings for the β-

methylene segments, compared to pure lipid and the higher protein content complexes.

For the bacteriorhodopsin containing complexes, varying the protein content between 0.45 and 1.49 mol% (i.e. between DMPC/bR mole ratios of 222:1 to 67:1) appears to induce opposing effects on the magnitude of $\Delta\nu_q$ for the α- and β-methylene segment deuterons; for the α-methylene segments, the quadrupole splittings measured at 45°C, are reduced in magnitude by 645 Hz on increasing the bacteriorhodopsin content of the vesicles from 0.45 mol% (222:1 mole ratio DMPC/bR complex) to 1.49 mol% (67:1 mole ratio DMPC/bR complex) while a 585 Hz increase in the magnitude of the quadrupole splitting for the β-methylene segments is observed. Indeed, the increase in the β-methylene segment quadrupole splitting observed for the highest protein content (67:1 mole ratio DMPC/bR) complex makes it of similar magnitude to that displayed by the protein-free lipid, itself.

vi) *Stoichiometry of DMPC/bR interactions as seen by deuterium NMR.* From Fig.3.12, the magnitudes of the quadrupole splitting for the α- and β-methylene segments of DMPC in the protein-containing complexes, recorded at both 30 and 45°C, appear to exhibit a linear variation with the inverse of lipid/protein ratio. This is consistent with a fast two site exchange model between lipids in contact with the protein and free bulk phase bilayer lipids, as first shown in this lab (Sixl *et al.*, 1984; Dempsey, *et al.*, 1986; Ryba, *et al.*, 1986).

If the rate of exchange (ν_{ex}) of two deuterated lipid molecules between environments that give different quadrupole splittings e.g. a lipid associated with a protein surface with one in a protein-free pure lipid environment, is fast on the deuterium NMR quadrupole anisotropy averaging time scale,

$$\text{i.e. } \nu_{ex} > 10^4 \text{ sec}^{-1},$$

then the observed quadrupole splitting ($\Delta\nu_{q(obs)}$) is given by

$$\Delta\nu_{q(obs)} = \frac{[f]\nu_f + [b]\nu_b}{[f] + [b]}$$

where ν_f is the quadrupole splitting of protein-free lipid and ν_b is that for lipid bound to protein. [b] is the proportion of total lipid bound to protein and [f] is the proportion of total lipid free from protein contact.

Since [f] + [b] = 1, it follows that

$$\Delta\nu_{q(obs)} = [f].\nu_f \quad + \quad [b].\nu_b \qquad (1)$$

From Fig.3.12, a straight line can be drawn through the data points obtained from the bacteriorhodopsin complexes. Thus;

$$\Delta\nu_{q(obs)} = m.x \; + \; c \qquad (2)$$

where $x = 1/n_t$ (i.e. the inverse of the lipid protein ratio) and m is the gradient of the line. From eqn.1, when x = 0, i.e. pure protein free lipid, then

$$c = \nu_f \qquad (3)$$

Substituting equations (1) and (3) into (2)

$$n_b = m/(\nu_b - \nu_f)$$

If the quadrupole splitting ν_b for lipid in direct contact with protein has a small value approaching zero, that is the C-D bond orientation is completely disordered, as was proposed for DMPC-d_9 in band-3 and bovine rhodopsin studies (Dempsey *et al*, 1986; Ryba *et al*, 1986) and DMPG-d_5 with myelin basic protein (Sixl *et al.*, 1984), then the number of boundary lipids per 26,000Da bR monomer is given by:-

$$n_b = -m/\nu_f \qquad (4)$$

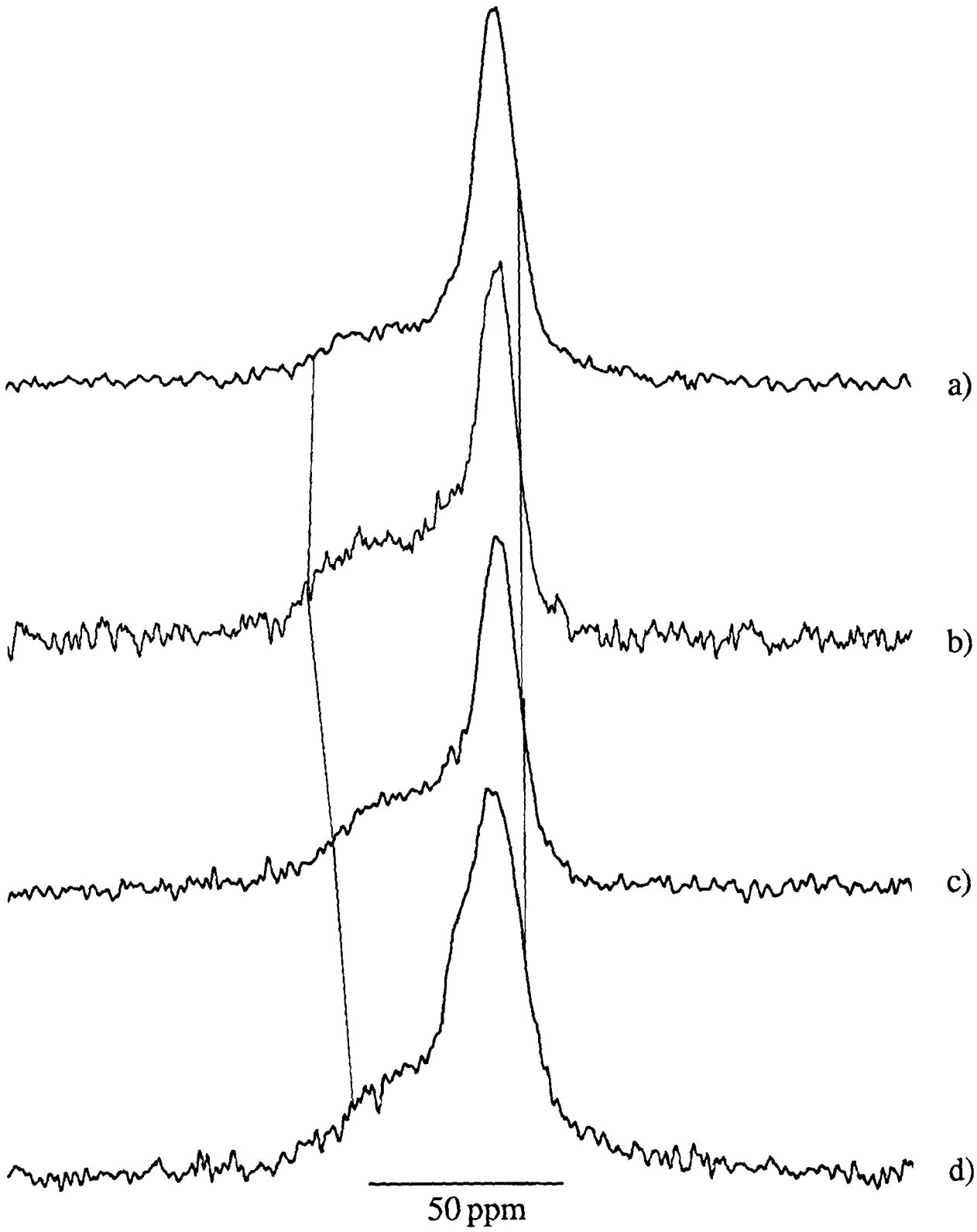


Fig. 3.13.
^{31}P-NMR spectra (121.4 MHz) for DMPC/bacteriorhodopsin complexes with vesicles of different sizes recorded at 33°C. a) protein-free dispersions of DMPC; b) 68:1 mole ratio complex with 1,000 - 1,500 nm diameter vesicles; c) 187:1 mole ratio complex with 300 - 600 nm diameter vesicles; d) 1,444:1 mole ratio complex with 100 - 300 nm diameter vesicles.

Best fit straight lines for the data points for the protein containing complexes at 45°C were calculated by the least squares fit in LOTUS 123 to determine values for n_b. For the α-splittings, the 182:1, 95:1 and 67:1 mole ratio data points were used for the best fit line and a value for n_b corresponding to a DMPC/bacteriorhodopsin mole ratio of 12:1 was obtained. For the β-splittings, all five DMPC/bR complex data points were used for the best fit line and n_b was determined to have a DMPC/bR mole ratio of -15:1. It should be noted, however, that the absolute values calculated for the number of boundary lipids per 26,000Da bacteriorhodopsin monomer are very similar.

From a comparison of spectra presented in Figs.3.8 and 3.11 it appears that increasing the temperature through the phase transition of the complex mimics the effect of increasing the lipid content at a fixed temperature above the phase transition. Both changes are seen to enhance the resolution of the component α- and β-methylene segment powder patterns.

B). **Phosphorus-31 NMR**; In this section the effects of vesicle size on the broadline phosphorus-31 NMR spectra are reported. For DMPC/bR complexes produced by the slow cholate removal procedure, in which averaging of spectral anisotropy by small vesicles is not a problem, the effects of protein content on the measured c.s.a.s are reported. Also the rates of motion for the phosphate moiety are investigated by measuring the spin-lattice (T_1) and spin-spin (T_2) phosphorus-31 relaxation times.

The broadline phosphorus-31 NMR spectra for DMPC, reconstituted by either method of cholate removal, with the integral protein bacteriorhodopsin are characteristic for fluid phospholipids organised into bilayer structures, irrespective of the protein content. There is no evidence for the existence of hexagonal H_{II} phase components (Cullis & de Kruijff, 1979).

i) *Effect of small vesicle diameters on the spectral anisotropy of the phosphorus-31 NMR spectra.* The phosphorus-31 NMR spectra for the DMPC-d_9/bR complexes, comprising of vesicles of a variety of diameters produced by different rates of cholate

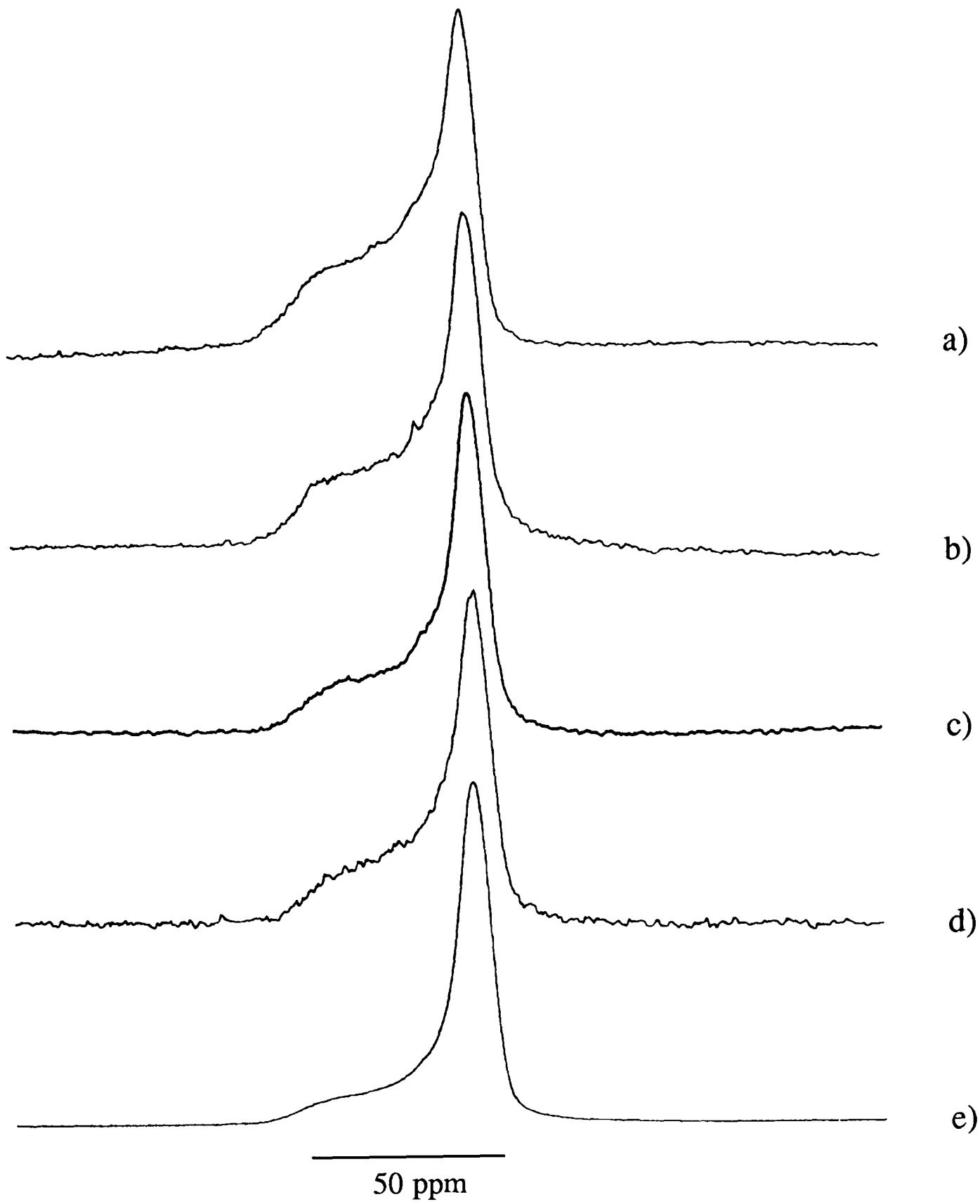


Fig.3.14.
^{31}P-NMR spectra (145.9 MHz) for DMPC/bacteriorhodopsin complexes, of mole ratios; a) 67:1; b) 95:1; c) 182:1; d) 218:1; and e) protein free DMPC dispersions. Protein complexes were reconstituted by the slow cholate removal procedure, with all endogenous purple membrane lipids removed. Spectra recorded at 33°C.

removal during dialysis are presented in Fig.3.13. The c.s.a. displayed by the 68:1 mole ratio complex (Fig.3.13.b) with vesicles between 1,000 and 1,500 nm in diameter (Chapter 2) produced by slow removal of cholate, is similar to that obtained from the spectrum for dispersions of protein-free DMPC, which contain very large vesicles (Fig.3.13.a). The phosphorus-31 NMR lineshape of the spectrum (Fig.3.13.c) displayed by vesicles of 300-600 nm in diameter (187:1 mole ratio complex, produced by fast cholate removal) is less sensitive to the tumbling effects of vesicle size than the corresponding deuterium-NMR spectrum (Fig 3.4.b) from the choline γ-methyl groups. The magnitude of the c.s.a., however, is reduced relative to that of the 68:1 mole ratio complex (Fig.3.13.b), although this may reflect the effect from variation in protein content (see below). Only the spectrum (Fig.3.13.d) obtained from the high lipid content 1,444:1 mole ratio complex, which comprised vesicles with diameters from 300nm to less than 100nm (Chapter 2), is seen to exhibit a significant reduction in measured chemical shift anisotropy and a noticeable second, possibly isotropic component.

ii) *Effect of protein content on the phosphorus-31 NMR spectra of large vesicle complexes*. Broadline phosphorus-31 NMR spectra recorded for bacteriorhodopsin containing complexes of DMPC/bR mole ratios ranging from 67:1 to 218:1 and with vesicles of 1,000 - 1,500 nm diameter, produced by the slow cholate removal technique, are presented in Fig.3.14 together with that for protein-free aqueous dispersions of DMPC (Fig.3.14.e). All the spectra, irrespective of protein content are seen to be single component and characteristic for phospholipids in a bilayer conformation. There is no evidence of an isotropic component. The intensity from the 90° orientation (upfield) is significantly increased relative to that of the 0° orientation (downfield) in the phosphorus-31 spectrum for pure DMPC bilayers (Fig.3.14.e) suggesting magnetic ordering of the vesicles in the magnetic field (8.4 T) due to diamagnetic anisotropy of the fatty acyl chains (Seelig *et al.*, 1985; Griffin *et al.*, 1981). Increasing the bacteriorhodopsin content (Figs.3.14.d to a) tends to reverse this ordering as judged by the increase in contribution to the spherically averaged powder pattern from lipids in

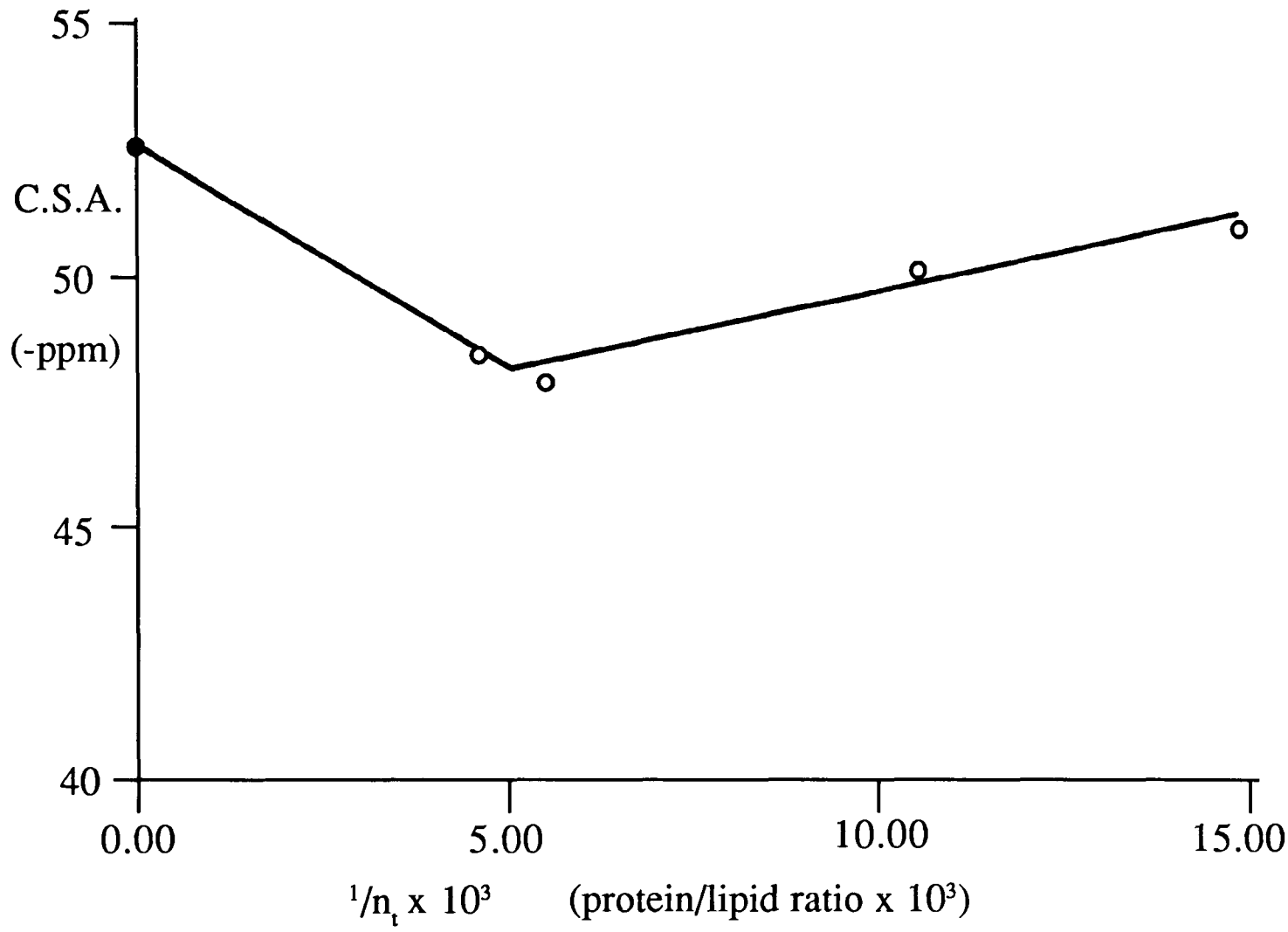


Fig.3.15. Measured chemical shift anisotropies from ^{31}P-NMR spectra of protein-free DMPC dispersion (filled symbol) and DMPC/bR complexes (open symbols) recorded at 33°C plotted as a function of the inverse lipid :protein ratio (mol/mol).

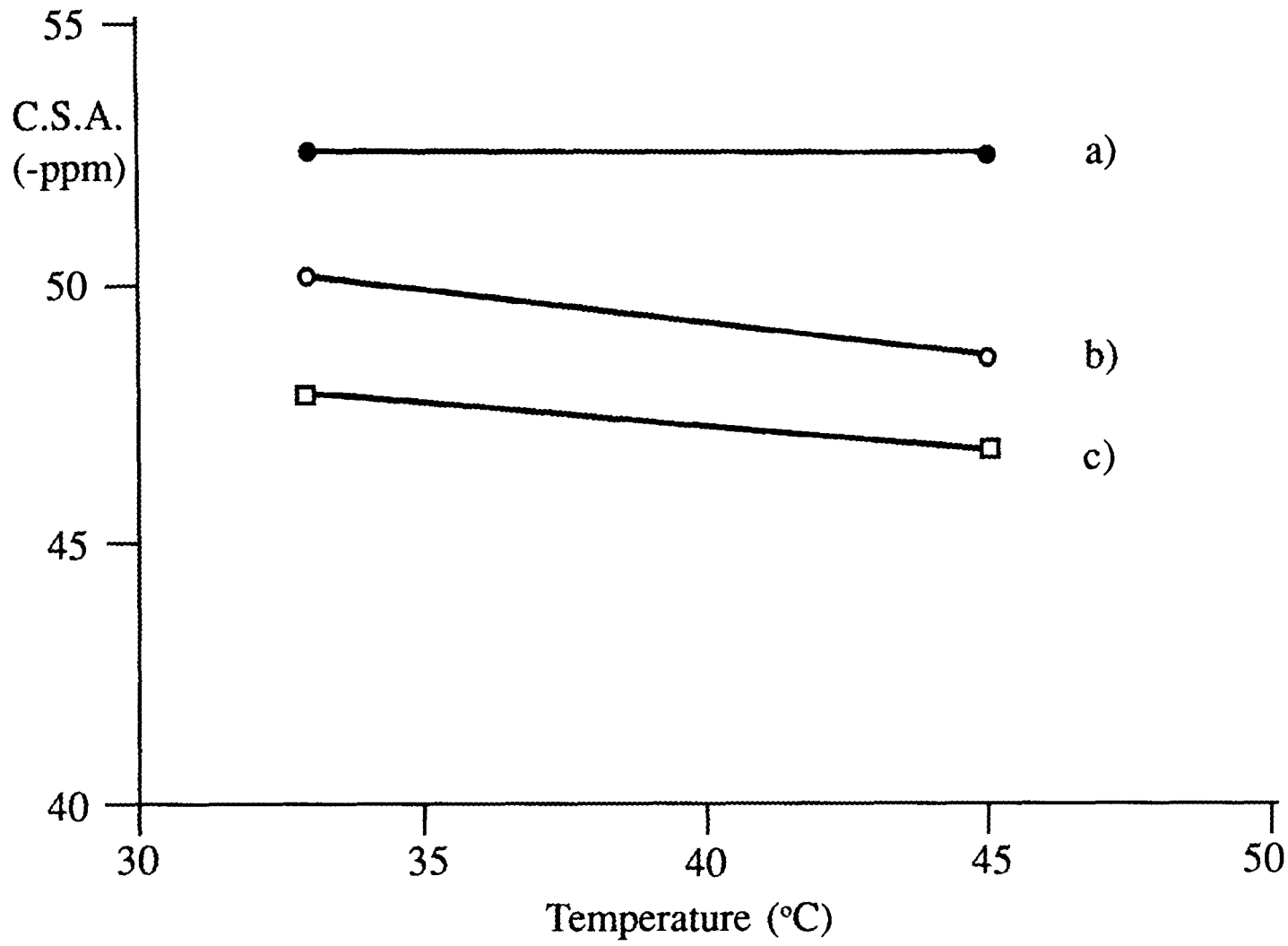


Fig.3.16. Phosphorus-31 chemical shift anisotropies (C.S.A.) plotted as a function of temperature for protein-free DMPC dispersions (a) and DMPC/bacteriorhodopsin complexes of mole ratios, 95:1 (b) and 182:1 (c), with all endogenous purple membrane lipids removed.

the 0° orientation to the applied magnetic field.

Plotting the ^{31}P-NMR c.s.a.s measured at 33°C for the bacteriorhodopsin-containing complexes, produced by the slow cholate removal technique, as a function of the inverse of lipid/protein ratio (Fig.3.15) reveals a linear increase in the magnitude of the c.s.a. with increasing protein content. The value, however, of -52.5 ppm obtained for protein-free dispersions of lipid does not share this linear dependence, being larger in magnitude than those displayed by any of the bacteriorhodopsin-containing complexes. Incorporation of small amounts of bacteriorhodopsin (up to 0.55 mol% bacteriorhodopsin; i.e.182:1 DMPC/bR mole ratio) into DMPC bilayers is thus seen to effect the most significant reduction in magnitude (~4.5 ppm) of the phosphate moiety c.s.a. relative to that of protein-free DMPC. Further incorporation of bacteriorhodopsin, however, increases the measured c.s.a. and the value (-51.4 ppm) for 67:1 mole ratio complex is similar in magnitude to that for protein-free lipid. Similar trends are observed for the deuterium NMR quadrupole splittings measured for the β-methylene segments (Fig.3.12) and the choline γ-methyl groups.

iii) *Effect on temperature on the measured ^{31}P-NMR c.s.a.s.* In Fig.3.16, the measured c.s.a.s for the 95:1 and 182:1 mole ratio DMPC/bR complexes, produced by the slow cholate removal technique, and those for pure DMPC are plotted as a function of temperature. While the measured c.s.a. for the pure lipid spectrum appears to be insensitive to warming from 33°C to 45°C, those for both the bacteriorhodopsin-containing complexes exhibit a slight decrease (~2 ppm).

iv) *Effects of bacteriorhodopsin on DMPC phosphorus-31 NMR relaxation rates.* ^{31}P-NMR spin-lattice (T_1) relaxation times at 33°C, were in the order of 1s and appeared to be little affected by addition of protein. Representative T_1 inversion-recovery stack plots for a protein-free dispersion of DMPC at 33°C is displayed in Fig.3.17.a. The inversion recovery pulse sequence used for the experiment is shown in (b). Stack plot for phosphorus-31 T_1 determinations for protein-containing complexes of DMPC/bR mole ratios 67:1 and 95:1 at 33°C are presented in Figs. 3.18.a and b, respectively. A null point for phosphorus T_1 spectra was obtained at τ values slightly

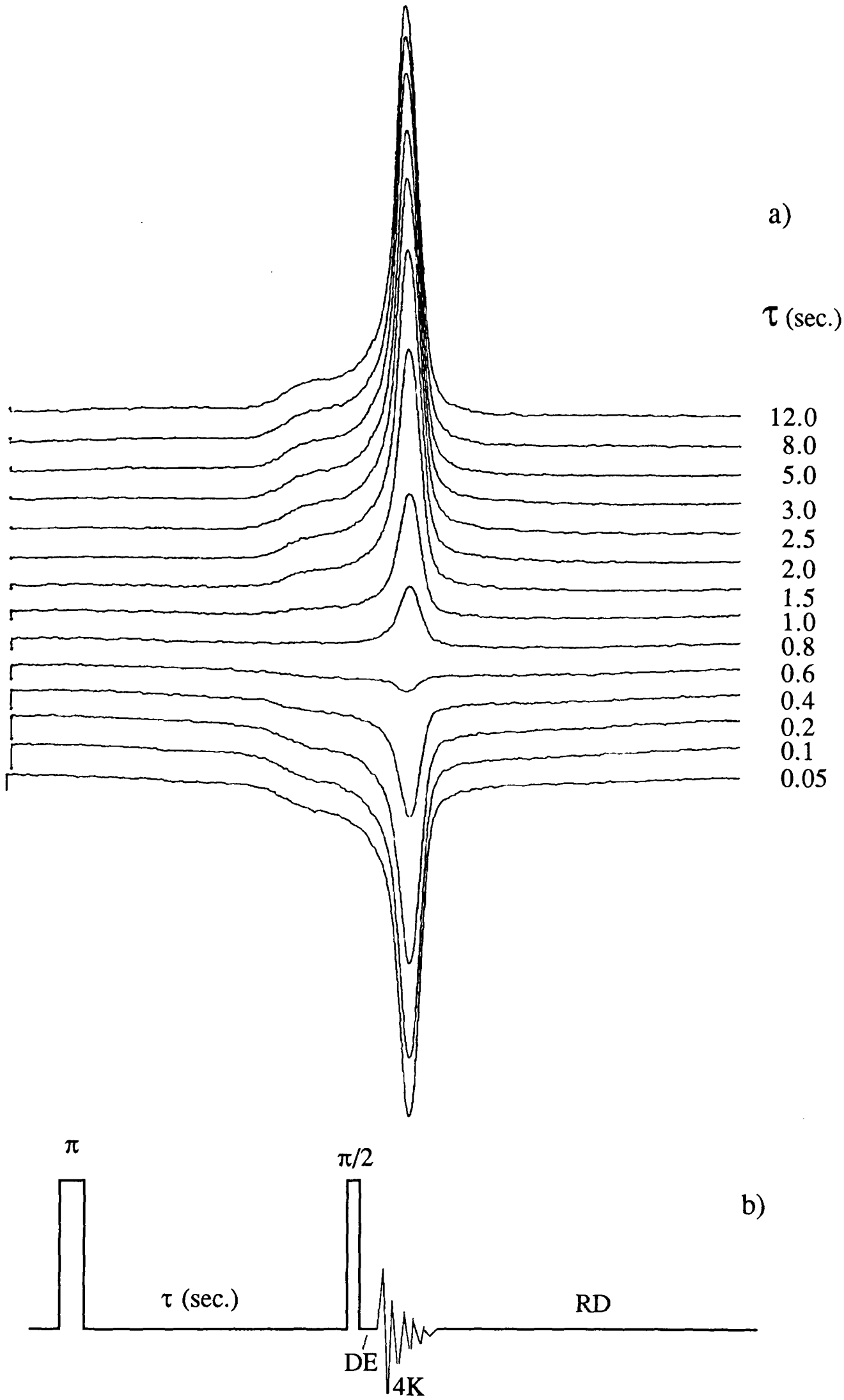


Fig.3.17.
^{31}P-NMR spin-lattice (T_1) time determination for pure DMPC dispersion at 33°C. a) stack plot of spectra obtained for different τ values; b) the inversion recovery pulse sequence used.

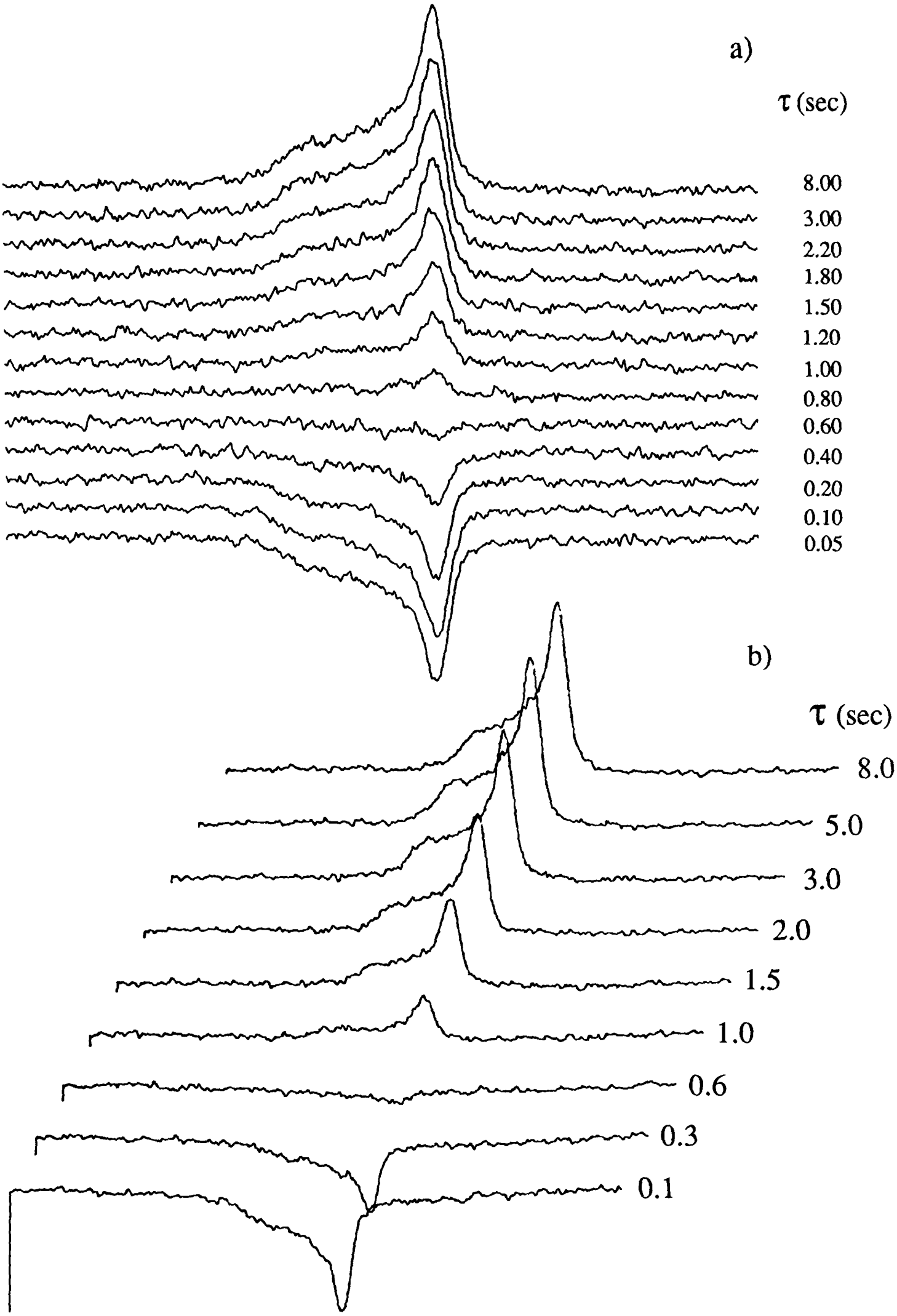


Fig.3.18.
^{31}P-NMR stack plot representations for phosphorus-31 spin-lattice (T_1) relaxation time determinations by inversion recovery for DMPC/bacterio-rhodopsin complexes of mole ratios a) 67:1; b) 95:1 at 33°C.

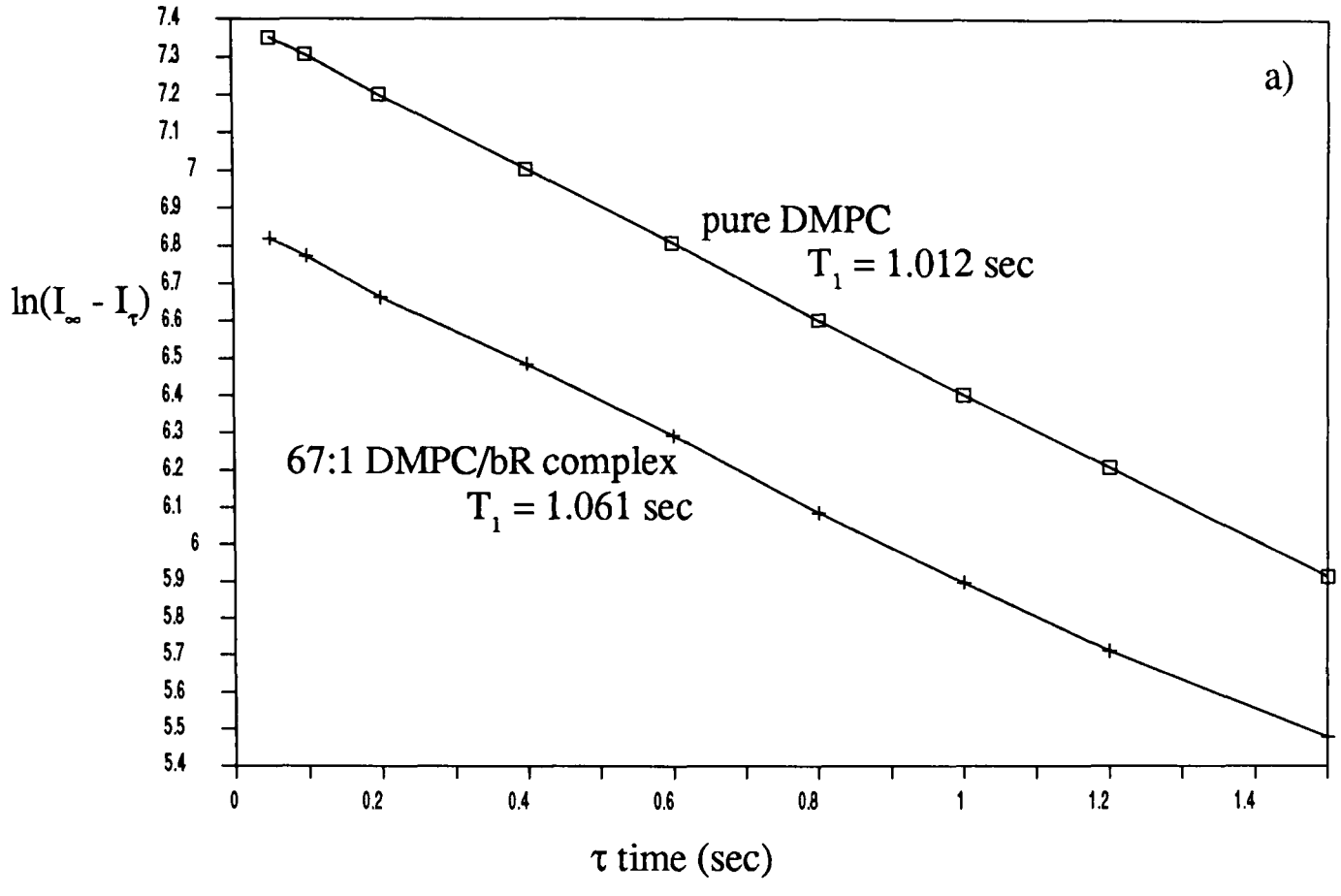


Fig.3.19. Analysis of phosphorus-31 NMR relaxation time data obtained from DMPC in protein-free bilayers and bacteriorhodospin-containing complexes by logarithmic plots;

a) spin-lattice relaxation times (T_1). Data from inversion recovery method.

b) spin-spin relaxation times (T_2). Data from Carr-Purcell spin-echo method. I is the intensity for the 90° orientation.

longer than 0.6s for both protein-free lipid and bacteriorhodopsin-containing complexes, indicating similar spin-lattice relaxation times.

Plots of loge(Io-It) vs τ time, where I is the intensity of the 90° orientation yield straight lines (Fig.3.19.a); the gradients of which equal $-1/T_1$. The straight line clearly demonstrates a single component spin-lattice relaxation time (T_1) for the 90° orientation. The phosphorus-31 T_1 values calculated for the 90° orientations are presented in Table 1. For pure lipid a value of 1.02s was obtained. Incorporation of bacteriorhodopsin increased the T_1 values by a maximum of 16% (Table 1); the most significant increase in T_1 value being observed for the highest lipid content complex. Increasing the temperature from 33°C to 45°C is seen to have little effect on the phosphorus-31 T_1 time measured for the 95:1 mole ratio DMPC/bR complex.

Table 1. ^{31}P-NMR spin-lattice relaxation times measured by the inversion recovery method for pure DMPC and DMPC/bR complexes.

complex	measured T_1 (sec)	
mole ratio	33°C	45°
pure DMPC	1.023	--
218:1	1.188	--
95:1	1.129	1.145
67:1	1.061	--

Phosphorus-31 spin-spin (T_2) relaxation times were in the order of 1ms i.e. around 1,000 times shorter than the corresponding T_1 values. Spin-spin relaxation time values calculated from the intensity of the 90° orientation (upfield) of pure DMPC and DMPC/bR complexes at 33°C are presented in Table 2. The phosphorus-31 spin-spin

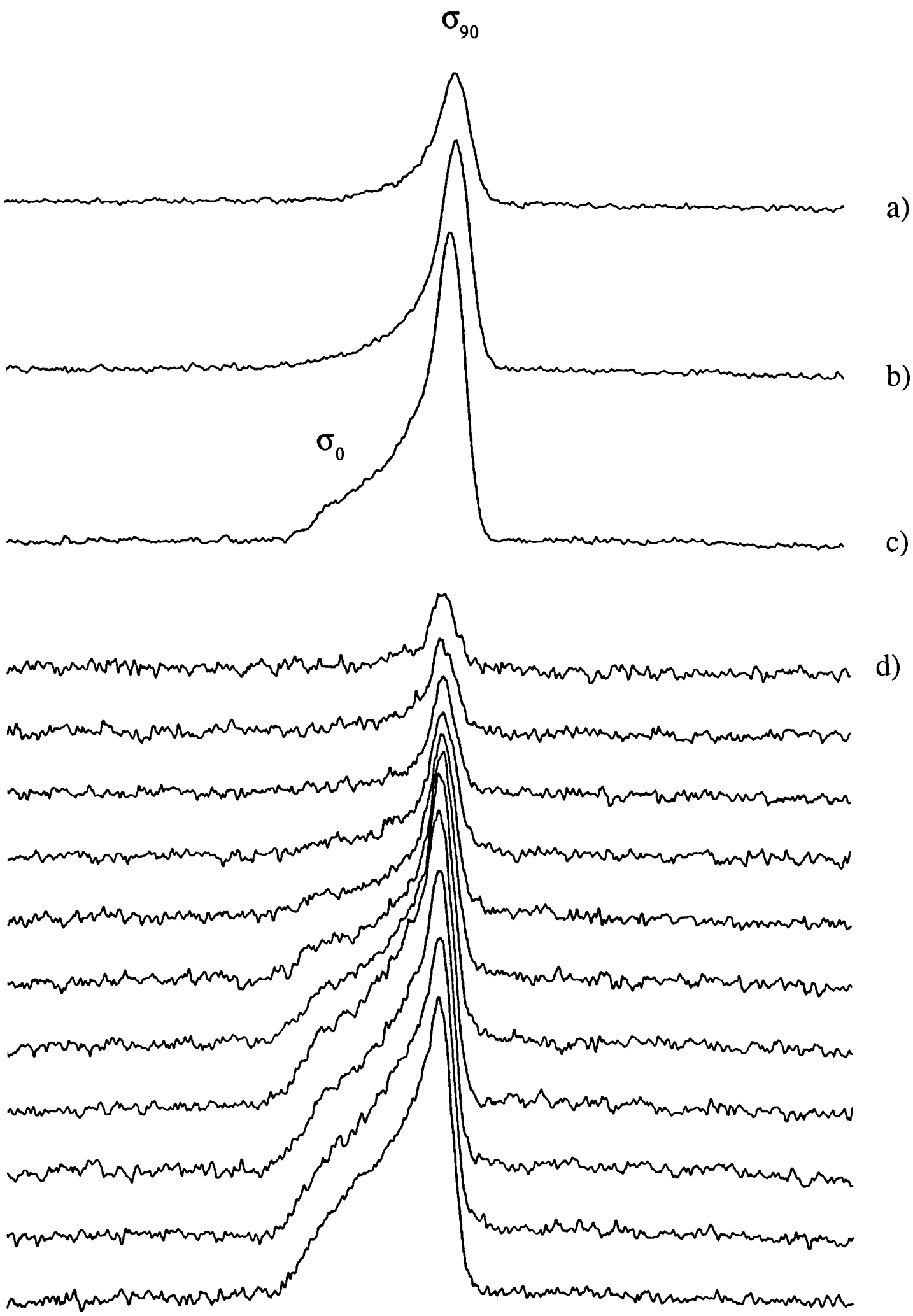


Fig.3.20. Stack plot representations for phosphorus-31 spin-spin (T_2) relaxation time determinations of protein free DMPC with τ time delays a) 0.9ms; b) 0.5ms c) 0.04ms and d) the 67:1 mol ratio DMPC/bR complex with τ time delays 0.8, 0.7, 0.6, 0.5, 0.4, 0.3, 0.2. 0.1, 0.08, 0.05 and 0.04ms (from top to bottom).

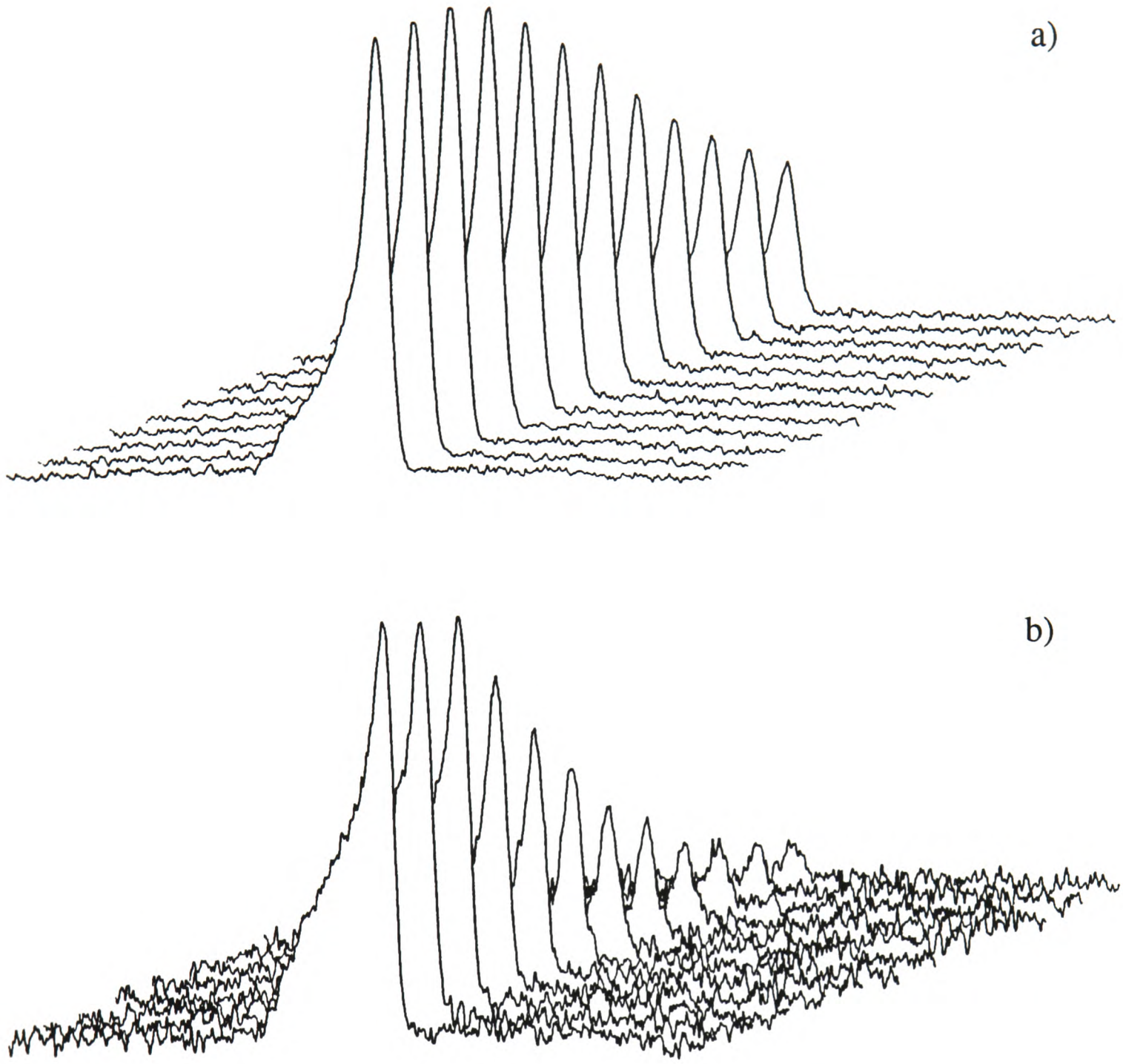


Fig.3.21. Stack plot representations for phosphorus-31 NMR spin-spin (T_2) relaxation time determinations by the Carr-Purcell spin echo method for a) protein free DMPC dispersions; b) 218:1 mole ratio DMPC/bR complex at 33°C. Identical τ values (0.04, 0.08, 0.10, 0.20, 0.30, 0.40, 0.50, 0.60, 0.70, 0.80, 0.90 and 1.00 ms; from bottom to top) were used for both experiments and the more rapid decay for the protein-containing complex is apparent.

relaxation times were found to be anisotropic for pure lipid and for all bacteriorhodopsin-containing complexes (Fig.3.20); the (downfield) intensity for the 0° orientation exhibiting a faster decay. For pure lipid intensity for the 0° orientation is clearly detectable in spectra acquired with short τ delay times (Fig.3.20.c). Applying a τ time of 0.9ms (Fig.3.20.a) is sufficient to allow all the signal from the 0° orientation to decay, while that for the 90° orientation is still clearly detectable. Spectra used for T_2 determinations for the 67:1 mole ratio DMPC/bR complex (Fig.3.20.d) demonstrated a similar spectral anisotropy in that phospholipids in the 0° orientation displayed shorter T_2 values. Good agreement was obtained between T_2 values calculated using a Nicolet curve fitting program and those calculated from least fit square methods on a LOTUS 123 program.

Table 2 Phosphorus-31 spin-spin (T_2) relaxation times determined by the Carr-Purcell spin echo method for the phosphate moiety of protein-free DMPC and DMPC/bR complexes.

complex mole ratio	spin-spin relaxation time (T_2) 33°C. (ms).	
	Nicolet program	LOTUS 123
pure DMPC	1.35	1.27
218:1	0.85	0.82
95:1	0.97	0.97
67:1	0.96	0.94

Addition of bacteriorhodopsin was found to reduce the measured T_2 relaxation times by between 29 - 37% relative to pure lipid for all complexes. The largest decrease was observed for the highest lipid-content complex (218:1 mole ratio DMPC/bR). Stack

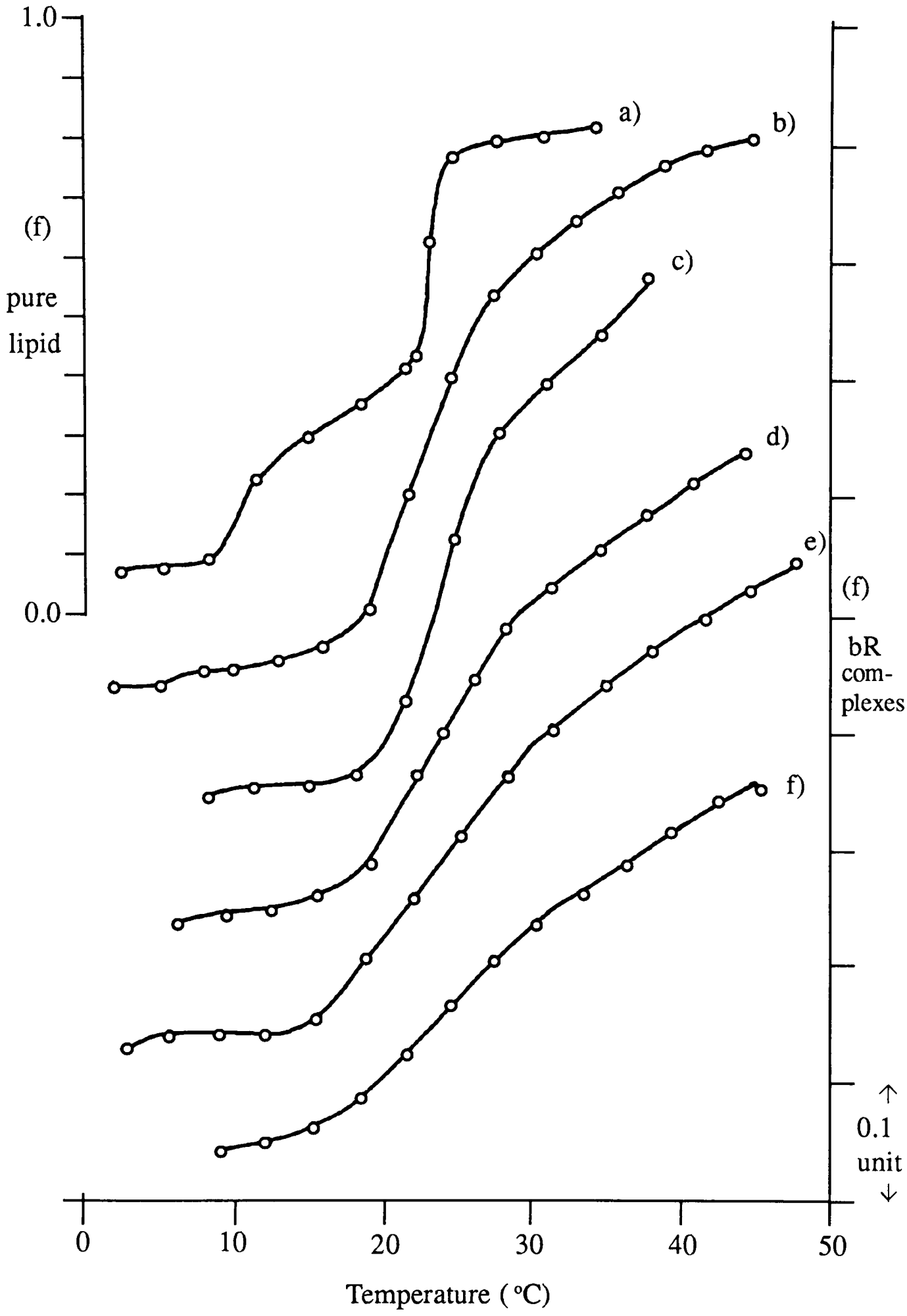


Fig.3.22. Phase transitions for DMPC/bR complexes of mole ratios; a) protein-free DMPC; b) 218:1; c) 187:1; d) 131:1; e) 95:1; f) 67:1, as determined by the TEMPO partitioning method. DMPC/bR profiles are offset by 0.1 units for clarity. The apparent partition coefficient parameter (f) scale for pure lipid is reduced by a factor of 0.5 (left scale).

plots spectra for T_2 determinations for protein-free DMPC and the 218:1 mole ratio complex at 33°C are shown in Fig.3.21. The same τ delay values were used for both experiments and the faster decay of the intensity for phospholipids in the 90° orientation in the protein containing complex is apparent. In Fig.3.19.b., plots of $\log_e I$ vs 2τ reveal straight lines, the slopes of which equal the $-1/T_2$, where I is the measured absolute intensity of the perpendicular (90°) orientation.

C). **TEMPO partitioning**; Fig.3.22 displays the calculated apparent partition coefficients (f) for partitioning (Marsh & Watts, 1982) of the spin-label TEMPO into the bilayer phase as a function of temperature for the 67:1, 95:1, 131:1, 187:1 and 218:1 mole ratio DMPC/bR complexes and protein-free DMPC dispersions. For the bacteriorhodopsin complexes, the profiles are displaced on the vertical scale by 0.1 units for clarity. The vertical scale for the protein-free DMPC partition coefficients is reduced by a factor of two. For all the protein contents investigated, the DMPC displays a main gel-to-liquid crystalline phase transition, as observed for protein-free DMPC (a). The phase transition mid-points and ranges for pure lipid and protein-containing vesicles of increasing bacteriorhodopsin content are presented in Table 3.

Table 3. Phase transition ranges and mid-points for DMPC/bR complexes of increasing protein content as determined from TEMPO partitioning data (Fig.3.22).

complex mole ratio	range of phase transition (°C)	midpoint of phase transition (°C)
pure DMPC	22 - 24	23.0
218:1	19 - 27	23.0
187:1	18 - 28	23.5
131:1	14 - 30	23.5
95:1	14 - 31	23.0
68:1	15 - 34	23.5
67:1	14 - 30	23.5

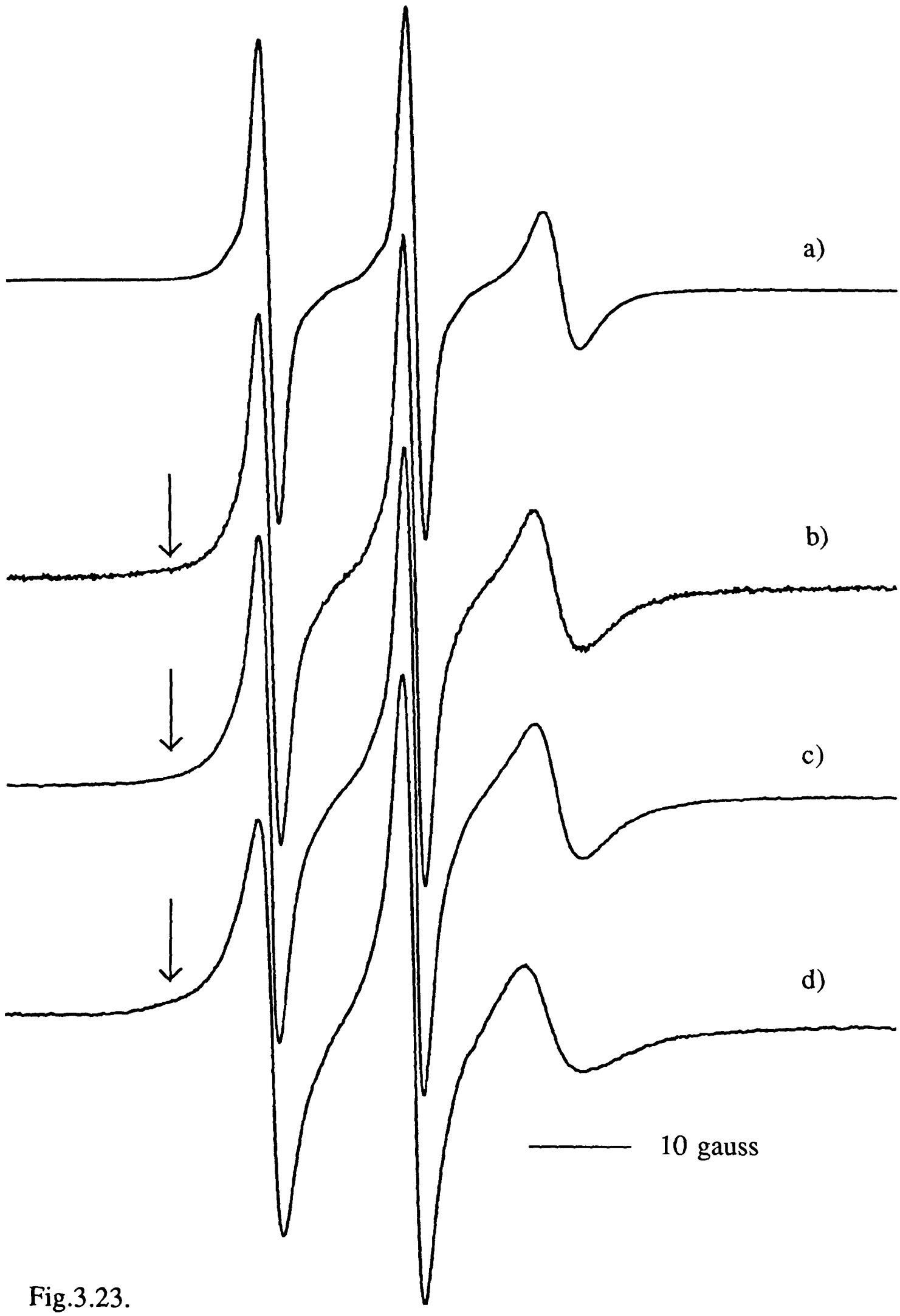


Fig.3.23.

ESR spectra of 14-PCSL in DMPC/bacteriorhodopsin complexes of mole ratios; a) protein-free DMPC; b) 187:1; c) 131:1; and d) 68:1 recorded at 41°C in 10mM Tris/HCl, pH 7.5.

Increasing the protein content of the complex, however, broadens the main phase transition with respect to that observed for pure DMPC but maintains the midpoint at 23°C +/- 0.5. Also, the presence of protein broadens out or suppresses the pre-transition observed in pure DMPC at 10°C.

D). **ESR studies using spin-labelled phospholipids**. Representative ESR spectra recorded at 41°C for 14-PCSL incorporated into DMPC/bR complexes of various protein contents and for protein-free DMPC are presented in Fig.3.23. The ESR spectra for 14-PCSL (Fig.3.23) and 14-PGSL in the protein containing vesicles are characteristic for those seen for spin-labelled fatty acids, sterol and phospholipid molecules in other lipid/protein systems (cytochrome *c* oxidase, Jost *et al.*, 1973, Knowles *et al*,. 1979 and 1981; bovine rhodopsin, Watts *et al.*, 1979 and 1982; shark rectal gland Na+-K+-ATPase and reviewed in Marsh & Watts, 1982, 1987) in that they are two component; a broad component being distinguishable in addition to the narrow fluid component, which resembles the ESR spectrum recorded for 14-PCSL in fluid protein-free lipid systems at temperatures above the phase transition (Fig.3.23.a).

The broad component is most prominent as a wing to the low field peak (arrowed). The magnitude of the broad component is seen to increase with the bacteriorhodopsin content of the vesicle and is most significant in the 68:1 mole ratio complex. The size of the broad component is also seen to increase directly with protein content in other reconstituted integral protein systems such as yeast cytochrome *c* oxidase/DMPC vesicles (Knowles *et al.*, 1979). The relationship of the proportion of the broad component to protein content and its fixed stoichiometry presented evidence that the motionally restricted spin-label component arises from spin-labelled lipid molecules that are in contact with the protein surface itself (Jost *et al.*, 1973 and Knowles *et al.*, 1979). As for other integral proteins, the presence of two distinct components in the ESR spectra, presents evidence that the exchange rate between lipid bound to the protein surface and bulk phase bilayer lipid is slow on the ESR timescale i.e. $\upsilon_{ex} < 10^8$ s^{-1}. Thus unlike ^{2}H-NMR spectra, ESR spectra provide a "snapshot" of

the proportion of boundary lipid molecules to free bilayer lipid molecules.

i) *Effect of the presence of bacteriorhodopsin on the bulk phase bilayer lipids.* The narrow fluid component observed in the ESR spectra from 14-PCSL in DMPC/bR vesicles is seen to be sensitive to the amount of protein in the vesicles; in particular the fluid component observed for 14-PCSL in the 68:1 mole ratio DMPC/bR complex (Fig.3.23.d), is clearly broadened compared to that for pure DMPC (Fig.3.23.a). For 14-PCSL in the 68:1 mole ratio DMPC/bR complex at 37°C, the fluid component resembled the ESR spectrum of 14-PCSL in protein free DMPC at 23°C i.e. in effect 1.47 mol% bacteriorhodopsin (68:1 DMPC/bR mole ratio) has a similar effect on the fluid bilayer lipids to that of reducing the temperature by 14°C. The effect of increasing the protein content on the fluid component can be quantified in terms of the changes in the measured $2A_{max}$ values and the apparent order parameter (S_{app}). Both are increased with increasing protein content of the vesicle for all temperatures above the main phase transition (Table 4). The apparent order parameter, S_{app}, is related to A_{max} by (taken from Marsh & Watts, 1982))

$$S_{app} = \quad (A_{//} - 2A_{\perp}) / A_{zz} + 2(A_{xx} + A_{yy}).\ a_o/a$$

where $A_{//}$ is equal to A_{max} as measured from the spectra (shown in Marsh & Watts, 1981), and $A_{\perp}$ is the anisotropy perpendicular to the bilayer normal and is related to A_{min} measured from the spectra by

$$A_{\perp} = A_{min} + 1.4(A_{//} - A_{min})/[A_{zz} - 0.5(A_{xx} + A_{yy})]$$

The isotropic hyperfine splitting in the bilayer is given by:

$$a = (A_{//} + 2A_{\perp})/3$$

and the isotropic hyperfine splitting constant corresponding to the single crystal

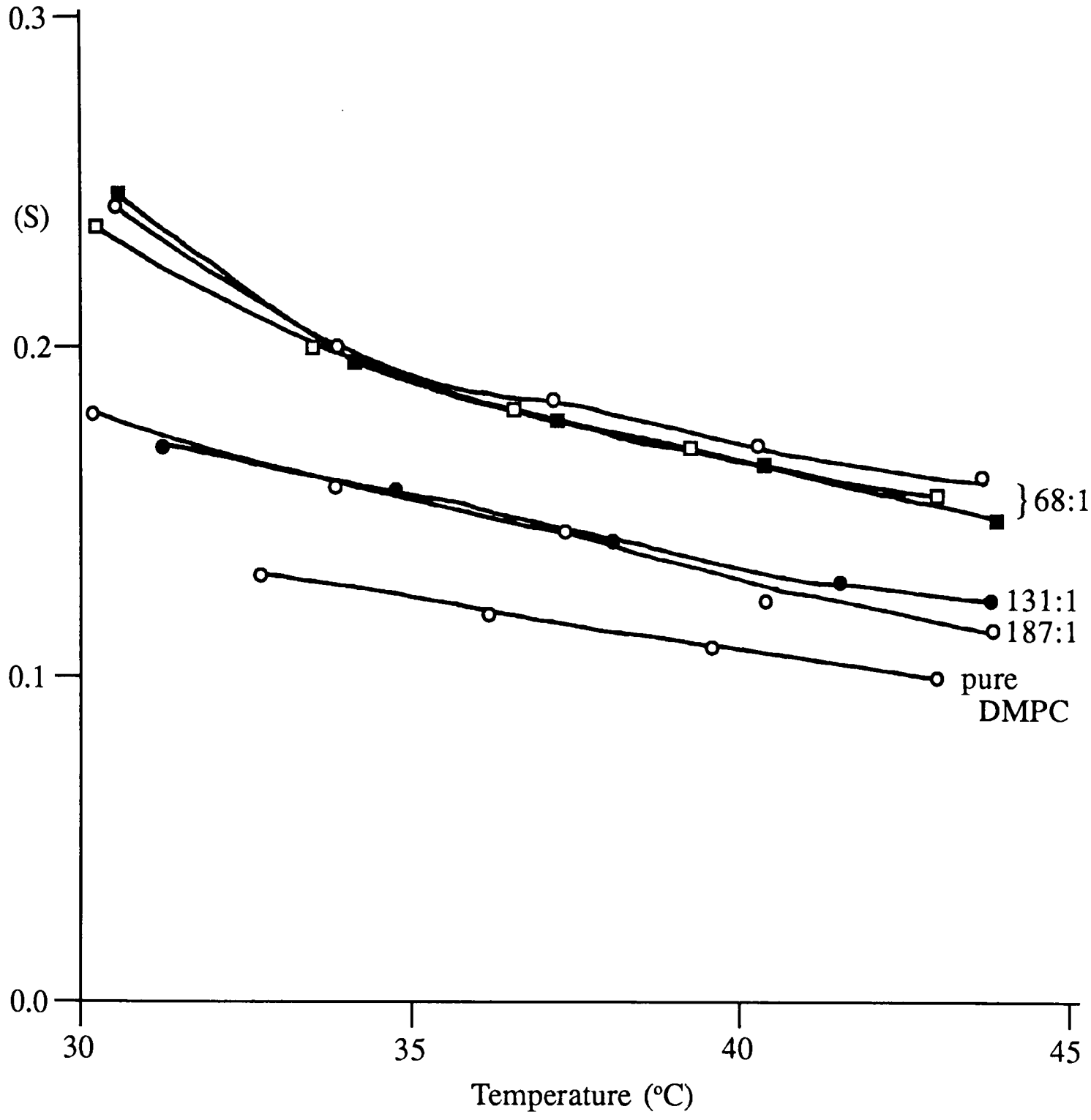


Fig.3.24.

Apparent ESR order parameters (S) calculated from fluid components of 14-phospholipid-spin labels in DMPC/bR complexes plotted as a function of temperature. All vesicles in 10mM Tris/HCl, pH 7.5, unless otherwise stated.

Key for 68:1 mole ratio DMPC/bR complex

14-PGSL □
2NaCl 14-PGSL ■
14-PCSL o

environment is: $a_o = (A_{xx} + A_{yy} + A_{zz})/3$, where A_{xx}, A_{yy} and A_{zz} are the principal values of the nitroxide hyperfine tensor measured in a single crystal host (Jost *et al.*, 1971).

Table 4. Values for $2A_{max}$ measured from the fluid components and the calculated apparent order parameters (S_{app}) for 14-PCSL in DMPC/bR complexes in 10mM Tris/HCl, pH 7.5.

	Temperature 40.5 +/-1°C	
complex	$2A_{max}$ (gauss)	S
pure DMPC	31.35	0.108
131:1	31.54	0.129
68:1	31.96	0.170

	Temperature 35.0 +/-1°C	
complex	$2A_{max}$ (gauss)	S
pure DMPC	31.52	0.119
131:1	31.89	0.156
68:1	32.18	0.195

In Fig.3.24 the calculated order parameters (S) for the fluid components of 14-PCSL in the 68:1, 131:1 and 187:1 mole ratio DMPC/bR complexes in low salt buffer (10mM Tris/HCl, pH 7.5) and also protein-free DMPC are plotted as a function of temperature. Above 35°C, the order parameters are seen to decrease with increasing temperature at a similar rate that is independent of the protein content. Also shown in Fig.3.24 are the order parameters calculated for the fluid component exhibited by 14-PGSL in the 68:1 mole ratio DMPC/bR complex in the absence and presence of 2M

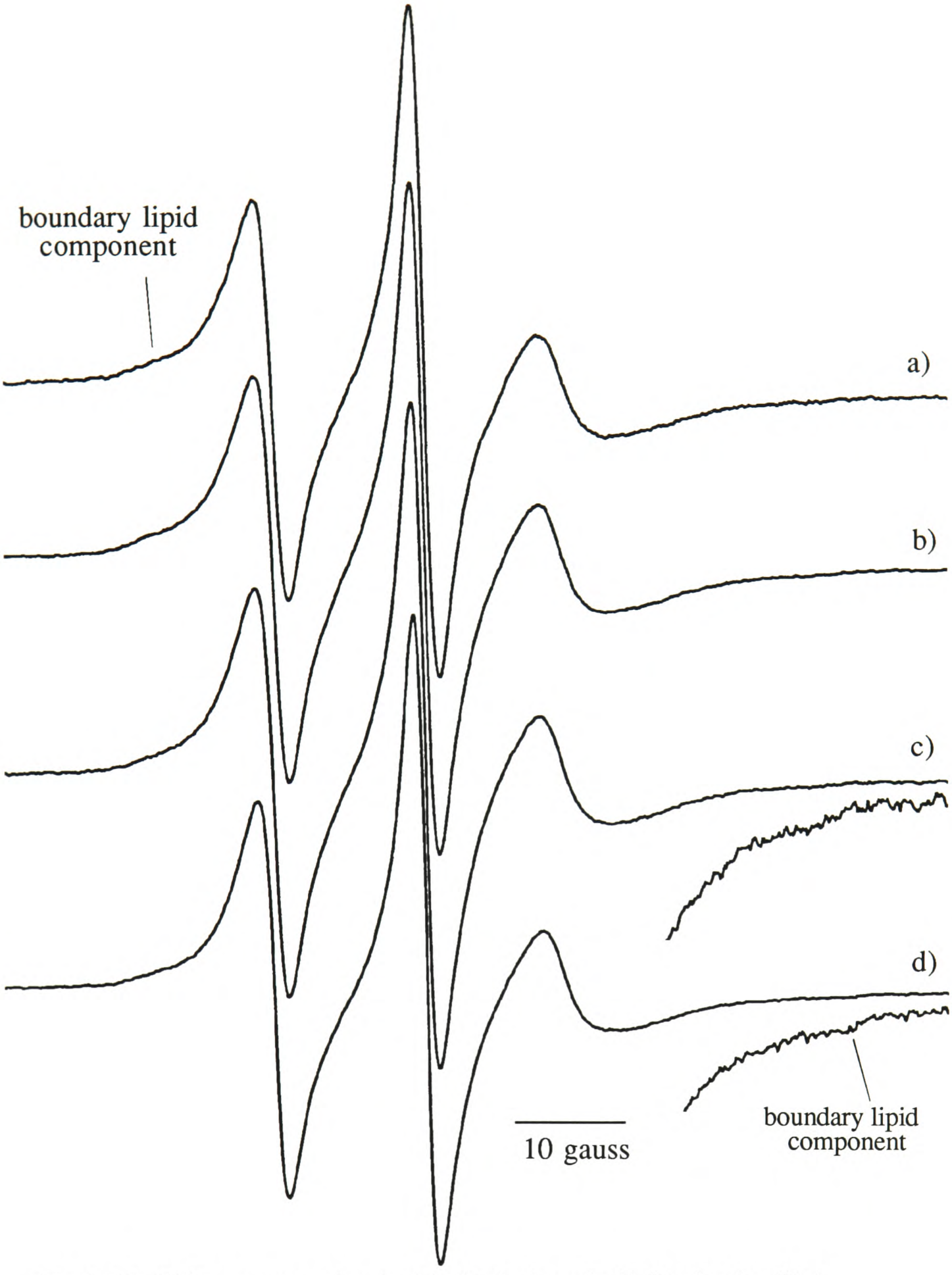


Fig.3.25. ESR spectra of spin-labelled phospholipids in the 68:1 mole ratio DMPC/bR complex at 34°C (± 1°C). Vesicles in 10mM Tris/HCl, pH 7.5 (except d).

a) 14-PCSL within one day of labelling by ethanol injection.

b) 14-PCSL three weeks after labelling by ethanol injection.

c) 14-PGSL (high field wing enlarged 16x).

d) 14-PGSL labelled vesicles in 2M NaCl, 10mM Tris/HCl, pH 7.5 (high field wing enlarged 8x).

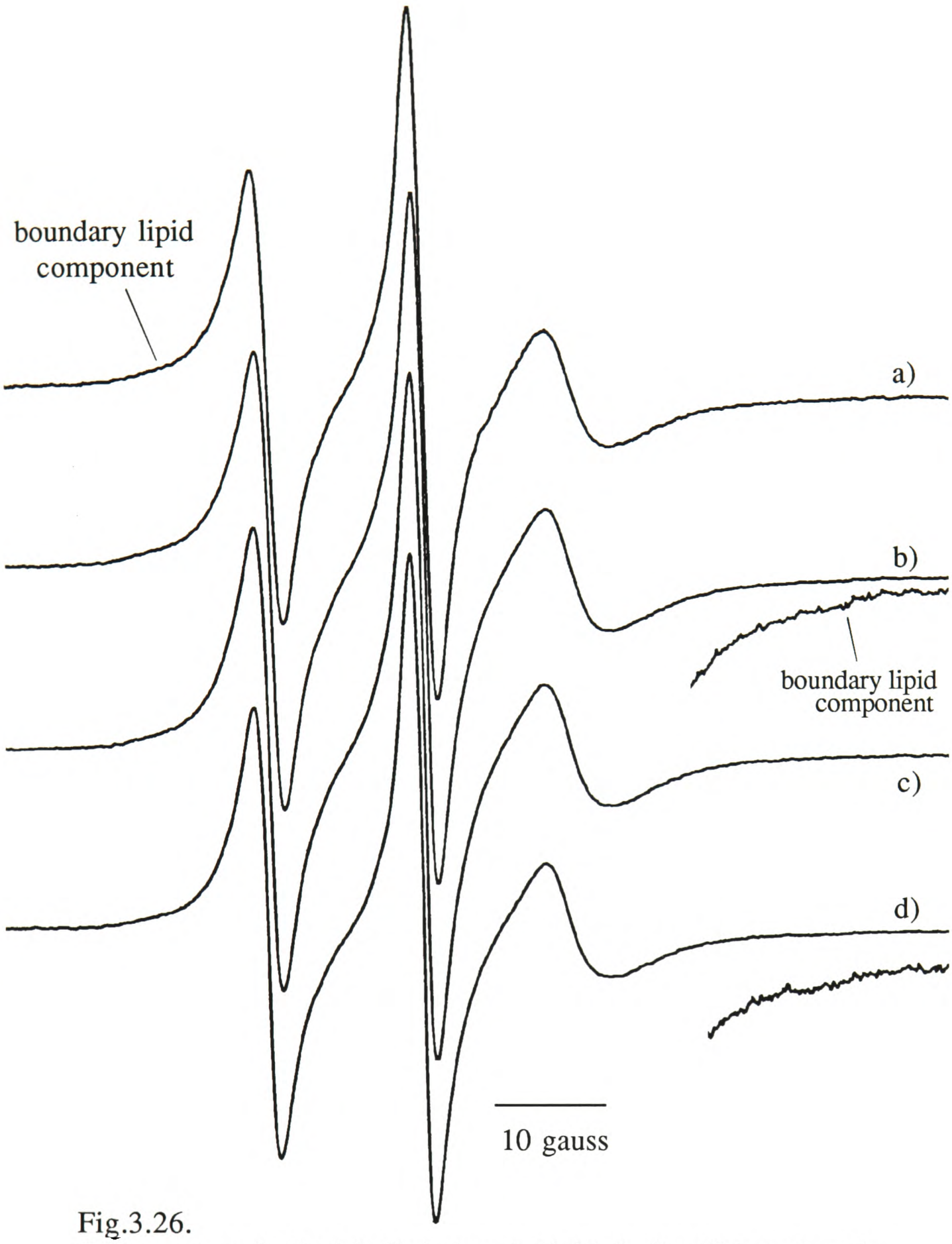


Fig.3.26.
ESR spectra of spin-labelled phospholipids in the 68:1 mole ratio DMPC/bR complex at 40°C (±1). Vesicles in 10mM Tris/HCl, pH 7.5 (except d).
a) 14-PCSL within one day of labelling by ethanol injection.
b) 14-PCSL three weeks after labelling by ethanol injection (high field wing enlarged 8x).
c) 14-PGSL
d) 14-PGSL labelled vesicles in 2M NaCl, 10mM Tris/HCl, pH 7.5 (high field wing enlarged 8x).

salt. The values calculated from the fluid component of 14-PGSL spectra recorded in the absence and presence of salt are very similar to each other and also to those calculated for 14-PCSL in the same complex. From Fig.3.24, it can be seen that for any temperature the apparent order parameter is increased by the presence of protein.

ii) *Quantitative analysis of the number of boundary lipids per protein by spectral subtraction and simulation.* Fig.3.25 and Fig.3.26 present spectra of 14-spin-labelled phospholipids in the 68:1 DMPC/bR mole ratio complex at 34°C and 41°C, respectively. It is apparent that after three weeks at 4°C, the motionally restricted component for 14-PCSL (spectrum b) becomes better defined and slightly more predominant at both temperatures as judged from the wing to the low field peak compared to in the spectra recorded within 18 hr of ethanol injection of the 14-PCSL (spectrum a). The ESR spectrum from the spin-labelled phosphatidylglycerol molecule (14-PGSL) in the 68:1 mole ratio DMPC/bR complex (Figs.3.25 and 3.26.c) appears to exhibit a motionally restricted component of similar magnitude to that of 14-PCSL (a). Furthermore for 14-PGSL, the proportion of the motionally restricted component in the ESR spectrum does not seem to be affected by the presence of 2M NaCl in the aqueous medium (spectrum d).

One problem of quantitative analysis of the magnitude of the motionally restricted component in ESR spectra of reconstituted DMPC/protein systems is that even in the presence of high protein contents, the DMPC undergoes a phase transition (as detected by TEMPO-partitioning results; Fig.3.22) which, depending on the protein content, is complete at around 30°C (Table 3). Spin-labelled lipid in patches of the bilayer below the phase transition exhibit a broad component that is indistinguishable from the motionally restricted component, arising from spin-labelled lipid in contact with the protein, itself. For this reason, ESR spectra of 14-PLSL in DMPC/bR complexes at temperatures below 33°C are not analyzed, since their motionally restricted components may be increased due to "frozen lipid" components. For natural membrane systems e.g. rod outer segment membranes, the heterogeniety of the fatty acyl chains

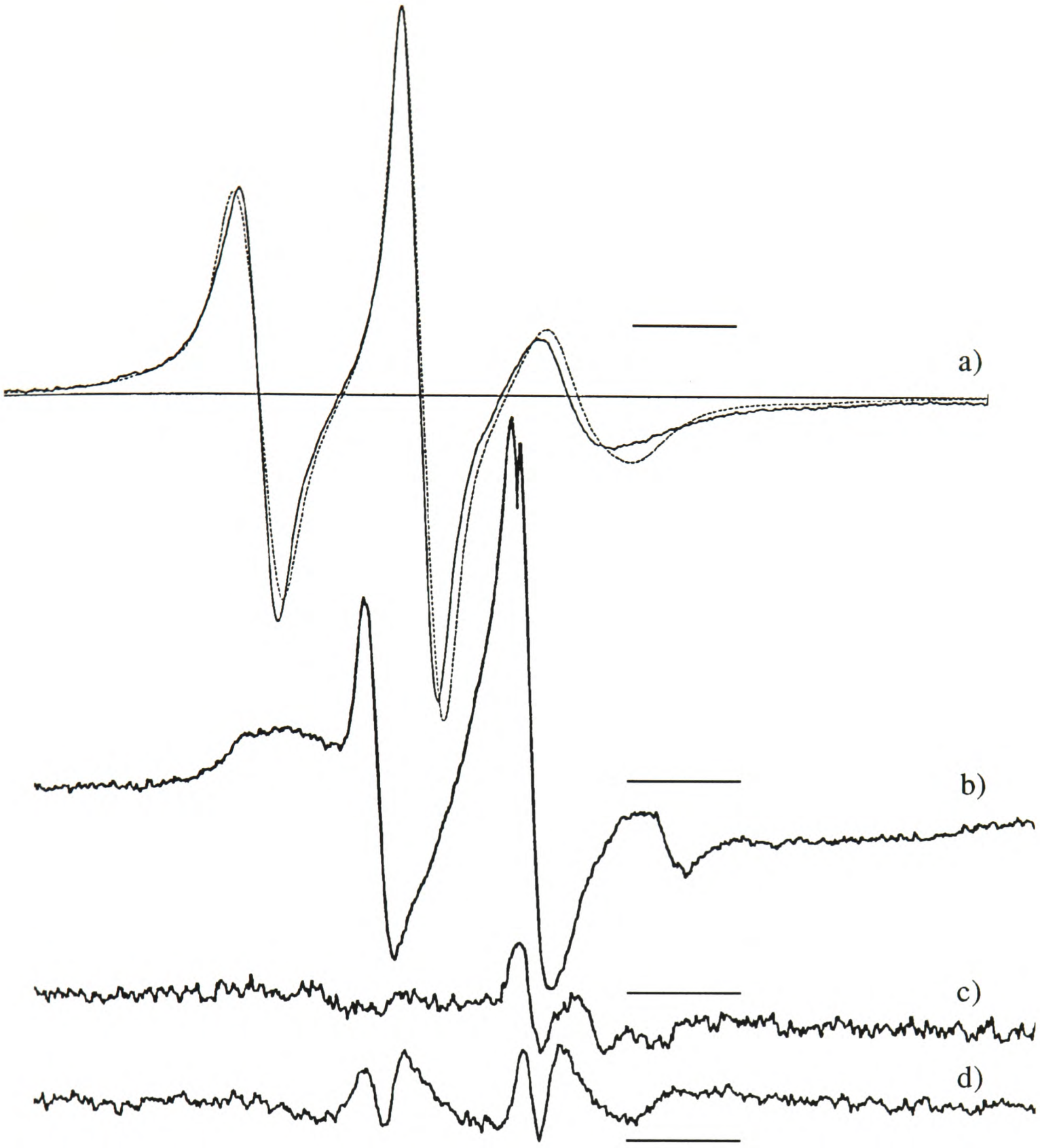


Fig.3.27. a) ESR spectrum for 14-PCSL in 68:1 mole ratio DMPC/bR complex (37°C) and simulated spectrum (dotted line) in which 26% of the spin-label was motionally restricted. The fluid component used in the simulation was the spectrum for 14-PCSL in pure DMPC at 23°C; b) ESR difference spectrum (vertically enlarged 4x) for motionally restricted component obtained by subtraction of spectrum for 14-PCSL in pure DMPC (23°C) from spectrum of 14-PCSL in 68:1 mole ratio DMPC/bR complex (34°C); c) ESR difference spectrum (vertically enlarged 8x) obtained after subtraction of spectrum for 14-PGSL in 68:1 mole ratio DMPC/bR complex (34.2°C) from that for 14-PCSL in the same complex (34.0°C); d) ESR difference spectrum (vertically enlarged 8x) obtained after subtraction of spectrum for 14-PGSL in 68:1 mole ratio DMPC/bR complex in 2M NaCl (34.2°C) from that for 14-PGSL in the same complex in absence of salt (34.2°C).

Bar = 10 gauss.

abolishes any co-operative phase transition.

The two component spectra obtained from protein/lipid systems may be resolved into constituent components by spectral subtraction methods (Knowles *et al.*, 1979) for quantitative analysis. The spectra for the 68:1 mole ratio DMPC/bR used in the subtractions were recorded at 37°C. Difference spectra for the motionally restricted spin-label component were produced by subtracting a spectrum of 14-PCSL in protein-free DMPC recorded at 23°C (as this resembled the fluid component in lineshape, linewidth and calculated order parameters; described above). The difference spectrum obtained for the motionally restricted component displayed by 14-PCSL in the 68:1 mole ratio DMPC/bR complex is shown in Fig.3.27.b. There still remains a small fluid component which could not be removed. The $2A_{max}$ value measured for this component was measured at 60 gauss which is typical for motionally restricted lipid and resembles the spectrum (not shown) obtained from 14-PCSL in pure DMPC at temperatures well below the pre-transition temperature. The broad lineshape implies that the protein presents an environment in which the lipid acyl chain motion is more restricted than in pure fluid lipid. For this reason, the broad component is referred to as the motionally restricted component.

Another method to estimate the amount of immobilised component is by spectral simulation. The ESR spectrum of 14-PCSL in the 68:1 mole ratio DMPC/bR complex at 37°C and a simulated spectrum with 0.26 mole fraction of the spin-label motionally restricted is shown in Fig.3.27.a. The fluid component used in the simulation was that from 14-PCSL in protein-free DMPC bilayers at 23°C. The proportions of the motionally restricted components in the total spin-label spectra calculated by the two methods are presented in Table 5.

The proportion of motionally restricted components calculated by the two methods are in good agreement, although the subtraction method estimates slightly higher values. This may reflect the small amount of fluid component remaining in the immobilised difference spectrum (Fig.3.27.b). By multiplying the calculated proportions of motionally restricted lipid by the total lipid/protein mole ratio, a value

for the number of boundary lipids is obtained. These are also shown in Table 5.

Table 5. Proportion of motionally restricted component (f) and number of boundary lipids calculated per 26,000Da bR monomer in ESR spectra for 68:1 mole ratio DMPC/bR complex at 37°C.

spin-labelled lipid	salt	subtraction method		simulation method	
		f	n_b	f	n_b
14-PCSL	none	0.30	20	0.26	18
14-PGSL	none	0.23	16	0.19	13
14-PGSL	2M NaCl	0.23	16	0.20	14

The motionally restricted component displayed by 14-PCSL in 68:1 mole ratio DMPC/bR vesicles at 37°C is between 26 and 30% of the total spin-label signal. From this it is calculated that each 26,000 Mr bR monomer restricts the motion of some 18 - 20 DMPC boundary lipids. For 14-PGSL, however, in 68:1 mole ratio DMPC/bR vesicles at 37°C, the proportion of boundary component determined by both spectral subtraction and simulation was found to be 7% less. This may imply a negative selection for the PG headgroup by bacteriorhodopsin in DMPC bilayers in 10mM Tris/HCl, pH 7.5. Spectral subtraction, however, of the ESR spectrum (Fig.3.25.c) of 14-PGSL in the 68:1 mole ratio complex (34°C) from that of 14-PCSL (Fig.3.25.a) in the same complex (33.6°C) produced a flat featureless baseline (Fig.3.27.c) implying little difference in the relative proportions of motionally-restricted and fluid components. Furthermore, the proportion of boundary lipids displayed by 14-PGSL is not influenced by the ionic strength of the aqueous environment. Thus, both spectral subtraction and simulation determine similar proportions of motionally-restricted

component for 14-PGSL in the 68:1 mole ratio DMPC/bR vesicles in the presence of 2M NaCl (Fig.3.26.d), to that for vesicles suspended in aqueous environments with no salt. Indeed spectral subtraction of the spectrum (Fig.3.25.c) obtained in the absence of salt at 34.2°C from the corresponding spectrum (Fig.3.25.d) in the presence of salt yielded a flat baseline (Fig.3.27.d) confirming this.

3.IV). Discussion.

The effects of bacteriorhodopsin on the DMPC main phase transition in the absence of the purple membrane lipids are similar to those obtained using DSC and fluorescence depolarisation studies in DMPC systems in which the purple membrane phospholipids were retained (Heyn *et al.*, 1981a and b). For all complexes a main gel to liquid crystalline phase transition is observed as for pure bilayers (Fig.3.22) by TEMPO-partitioning. In pure DMPC bilayers, the mid-point occurs sharply at 23.5°C. In the absence of endogenous purple membrane lipids, bacteriorhodopsin maintains the mid-point of the main transition for the supporting DMPC bilayer at 23 - 24°C for all the complexes produced (Table 3). Only lipids remote from, and thus unperturbed by the protein are capable of undergoing the phase transition. In protein/lipid systems where the protein exists in an aggregated state, lipid-lipid contacts are conserved due to protein-protein contacts being maximised. Thus lipid-lipid co-operativity can still occur, thereby retaining the main phase transition at 23 -24°C (for DMPC). Thus proteins that tend to self-associate in bilayers of lipids that undergo a well defined gel-to-liquid crystalline phase transition (e.g. DMPC) do not alter the mid-point temperature of the transition. This appears to be the case for bacteriorhodopsin. Proteins which exist in the bilayer as monomeric species (e.g. bovine rhodopsin) alter both the mid-point temperature and the width of the lipid transition (Silvius, 1982; McLheney, 1986).

TEMPO partitioning data (Table 3), however, reveals a broadening of the bilayer phase transition relative to pure DMPC with increasing bacteriorhodopsin content. Earlier fluorescence depolarisation studies show a similar qualitative effect for

DMPC/endogenous lipid/bR complexes (Heyn *et al.*, 1981b). The observed broadening of the main transition arises presumably from a decrease in the size of the lipid pools as the protein content of the vesicles increases. The range of the phase transition depends on the degree of lipid co-operativity, which in turn is influenced by the size of the lipid pool undergoing the gel-to-liquid crystalline bilayer transition (Marsh & Watts, 1982). Freeze fracture electron microscopy (Chapter 4) presents evidence that irrespective of the protein content in vesicles above the phase transition, the lipids and protein particles are randomly interspersed. Increasing the lipid content, serves to increase the size of the lipid pools and more important the number of lipids free from protein contact. Both effects enhance lipid-lipid contacts and hence the degree of co-operativity of the phase transition, resulting in a sharper phase transition as the protein content is decreased as observed in Fig.3.22.

The bilayer pre-transition observed at 10 - 12°C for pure DMPC bilayer is not evident for DMPC bilayers containing bacteriorhodopsin for any of the complexes produced. DSC results for DMPC/bR complexes with the endogenous lipids retained also reveal no pre-transition in the lipid (Heyn *et al.*, 1981b). It therefore appears that this perturbation of the lipid bilayer is an effect of the protein itself and not the purple membrane lipids, as shown by other integral proteins (McLheney, 1986).

The measured c.s.a.s obtained from broadline ^{31}P-NMR spectra for phospholipids in bilayer conformations report on the motional properties of the diester phosphate segment; in particular the amplitude of motion. Some of the possible variations obtainable in measured c.s.a.s and ^{31}P-NMR lineshapes of bilayer spectra for different lipid and protein-lipid systems are illustrated in Fig.4. of the Introduction to this work. Substantial changes in c.s.a. are not generally observed even with large external perturbations; the large increases observed in c.s.a.s for the α-phosphate moiety powder patterns from *H.halobium* purple membrane (-60.8 ppm) and red membrane (-53.5 ppm) (Fig.4. Introduction) relative to that (~-40 ppm) of protein-free PGP bilayers (Ekiel *et al.*, 1981) are extreme examples (Smith & Ekiel, 1984). In purple membrane the protein content (bacteriorhodopsin) is twice as high as the protein content

(halorhodopsin) in red membrane; purple membrane being 20% lipid (w/w) compared to 38% for red membrane (Kates, 1978). Thus, increasing the *H.halobium* integral membrane protein content in PGP bilayers acts to increase the c.s.a.. This is interpreted in terms of a reduction in the amplitude (i.e. extent of motion) and rate of motion of the lipid headgroup due to interaction with the respective proteins, bacteriorhodopsin and halorhodopsin. The very large c.s.a. for purple membrane is consistent with the lipids being ordered and motionally restricted in the two dimensional hexagonal paracrystalline lattice of the purple membrane.

The measured c.s.a. for a phospholipid system also depends on the phospholipid headgroup type. Thus for protein-free DMPC the c.s.a. is some 10 ppm larger than for DMPG (Fig.4 Introduction). This may be interpreted in terms of ionic interactions between the zwitterionic choline headgroups in DMPC ordering the phosphate moieties more than the intermolecular hydrogen bonds in DMPG. Also the negatively charged phosphoglycerol headgroups will tend to repel each other. The measured c.s.a. for phosphatidylserine (PS) is reported as being even larger than that for PC (Browning & Seelig, 1980); again consistent with rigid headgroup ordering from electrostatic interactions.

For all the DMPC/bR complexes, produced by the slow cholate removal technique, the apparent c.s.a. is smaller than that observed for pure lipid both at 33°C and 45°C. This is interpreted in terms of introduction of bacteriorhodopsin into the DMPC bilayer as causing a net disordering effect at the PC headgroup (i.e. an increased amplitude of motion of the phosphate group around the glycerol backbone) relative to that in pure PC. As shown in Fig. 3.15, incorporation of small amounts of bacteriorhodopsin (up to 0.55 mol%) cause the most significant decreases in measured c.s.a. after which further incorporation of protein effects a linear increase in the measured c.s.a. with protein content. This biphasic relationship is explained in terms of two opposing effects, the relative contributions from which depend on the protein content.

One effect is the disruption of phosphocholine headgroup order at the membrane

surface on addition of integral membrane proteins in the bilayer. As discussed above the large c.s.a. of DMPC (-52.5 ppm) compared to other phospholipids (e.g.DMPG - 42.0 ppm) implies an ordering effect on the phosphate moiety, possibly by ionic interaction with positively charged trimethyl ammonium group. Addition of an integral membrane protein (e.g. band-3, rhodopsin, SR Ca^{++}- ATPase, cytochrome *c* oxidase) will disrupt these interactions, so permitting greater amplitude of motion of the phosphocholine headgroup about the glycerol backbone. This is reflected in a decrease in the c.s.a. observed in broadline phosphorus-31 (Rajan *et al.*, 1981, Seelig *et al.*, 1981; Ryba *et al.*, 1986). This effect is observed in DMPC/bR vesicles of low protein content; 0.45 - 0.55 mol% (218:1 and 182:1 mole ratio DMPC/bR complexes). The disruption of ionic interactions between the phosphocholine moieties relative to those in pure PC, appears to be long range in that small amounts of protein cause significant effects.

On increasing the protein-content, however, a second effect predominates. This is a reduction in the amplitude of motion for the phosphate moiety. The magnitude of this effect is directly related to the bacteriorhodopsin content of the vesicle and opposes the disrupting effect imposed by small quantities of integral protein on the ionic interactions between the phosphocholine headgroup moieties. The ordering effect on the amplitude of motion of the phospholipid α-phosphate group by increasing contents of *H.halobium* integral membrane proteins (halorhodopsin & bacteriorhodopsin) is clearly demonstrated by the increase in c.s.a. observed for the phosphorus-31 NMR spectra of red and purple membranes (discussed above; Fig.4 Introduction). The reason for the reduction in amplitude of motion on increasing protein content may reflect an ionic interaction between the negatively-charged phosphate moiety and positive charges at the protein surface or alternatively may merely reflect a reduction in space available for motion due to the presence of the protein bulk.

For protein-free lipid the ^{31}P-NMR c.s.a. is insensitive to changes in temperature, implying that the amplitude of motion of the phosphate moiety of pure DMPC is not affected. The c.s.a.s measured for the DMPC phosphate moiety in the presence of

protein show a small increase in amplitude of motion for the phosphate group on warming (Fig.3.16). This may reflect the ordered phosphocholine headgroups being rendered more susceptible to thermal perturbations in the presence of integral membrane proteins.

For a spherically averaged deuterium NMR powder pattern, the magnitude of the quadrupole splitting is influenced by the amplitude of motion i.e. the ordering of the particular segment. For the choline headgroup in PC bilayers, the small quadrupole splitting (~1,100 Hz) observed for the γ-methyl groups at temperatures above the main phase transition imply only slightly hindered motion. The increase in quadrupole splitting for segments located nearer the glycerol backbone (4,380 Hz for b-CD2 and 6,040 Hz for α-CD_2 at 45°C) indicates the motional freedom becoming increasingly reduced. In agreement with ^{2}H-NMR studies (Gally *et al.*, 1975) reported on the DPPC headgroup, the angular oscillations of the choline C-α segment (Fig.3.9) in protein-free DMPC bilayers show little variation with temperature, while the C-β and C-γ (Fig.3.5) segments exhibit a more pronounced temperature dependence; increasing the temperature inducing smaller quadrupole splittings consistent with increased amplitudes of motion. Like the ^{31}P-NMR c.s.a. measured for the neighbouring phosphate group, the quadrupole splitting for the choline C-α methylene segment, is also insensitive to changes in temperature. These results were interpreted in terms of oscillations of the Cγ-Cβ region of the choline headgroup around the Cα-Cβ bond which increase as the temperature is raised; the Cα and phosphate segments remaining relatively rigid. The choline headgroup is characterised as a flexible, temperature dependent structure. Its orientation in space is not fixed, either perpendicular or parallel to the protein surface. Instead all segments undergo angular oscillations around the normal to the bilayer surface, but with increasing degrees of restriction towards the glycerol backbone (Gally *et al.*, 1975).

From the ^{2}H-NMR spectra of DMPC reconstituted with bacteriorhodopsin, it would appear that for all the protein contents studied, these motional restraints on the choline headgroup are preserved, at least to some degree. The temperature

dependencies (Fig.3.9) of the quadrupole splittings for both the α- and β-methylene segment powder patterns are seen to parallel those displayed by pure lipid although the actual quadrupole splitting values vary with protein content. For all the protein containing complexes increasing the temperature above that of the phase transition brings about a decrease in the β-methylene quadrupole splittings while those of the α-splittings appear to be insensitive to changes in temperature. The temperature-dependent decrease in the β-methylene segment quadrupole splittings observed for complexes of all protein-contents, implies an increase in amplitude of oscillation of the β-methylene segment about the Cα-Cβ bond as the temperature is increased, while the variation of the amplitude of motion of the α-methylene segment with changes in temperature appears to be unaffected by the presence of protein.

The choline γ-methyl group quadrupole splittings measured from DMPC-d_9/bR complexes were found to be particularly sensitive to vesicle size which was in turn influenced by the speed of cholate removal during the reconstitution. Indeed, DMPC-d_9 data from small vesicle complexes could easily be mis-interpreted. Thus, the marked reduction in the measured quadrupole splittings, relative to those of pure DMPC-d_9, displayed on warming the 187:1 (Fig.3.5.d) and 1,444:1 (Fig.3.5.e) mole ratio DMPC/bR complexes, produced by the fast cholate removal procedure, could have been mis-interpreted in terms of a temperature dependent dispersion of bacteriorhodopsin as was observed for band-3 in reconstituted DMPC-d_9 vesicles (Chapter 5, this work; Dempsey *et al.*, 1986). Also from analysis of results presented in Figs.3.3, 3.4 and 3.5, the DMPC-d_9 spectral lineshapes and quadrupole splittings would appear to be sensitive to the lipid/protein content of the vesicles. The trends, however, observed in Fig. 3.5 are explained in terms of differences in vesicle size. Indeed for DMPC/bR complexes with large vesicles produced by slow cholate removal, the measured quadrupole splittings for the choline γ-methyl groups are little affected by protein content and are relatively insensitive to temperature.

For small vesicles, two diffusion processes contribute to the averaging of the spectral anisotropy; rapid Brownian tumbling of the entire vesicle (characterised by the

diffusion coefficient D_t) and lateral diffusion of the lipids around the vesicle (with diffusion coefficient D_{diff}). The correlation time τc is given by the equation (Burnell *et al.*, 1980);

$$1/\tau_c = 6(D_t + D_{diff})/r^2$$

where r is radius of a vesicle and $D_t = kT/8\Pi r\eta$, where η is the viscosity of the medium. Values of τ_c calculated for vesicles of different diameters are presented in Table 6. The D_{diff} used at 303K (30°C) is 0.65 x 10^{-7} $cm^2.s^{-1}$ (Galla *et al.*, 1979). The viscosity, η, used is that for water at 303K (Handbook of Physics and Chemistry), which is 7.975 x 10^{-4} kg/cm.s. The Boltzman constant is 1.38 x 10^{-19} $kg.cm^2.s^{-1}K^{-1}$.

Table 6. Effect of vesicle diameter on the averaging of spectral anisotropy estimated for quadrupole splittings of 1,000 Hz and 4,000 Hz.

diameter (nm) of vesicle	τ_c (s)	$\tau_c^2(2\Pi.\Delta\nu_q)^2$ $\Delta\nu_q$ 1,000 Hz	$\tau_c^2(2\Pi.\Delta\nu_q)^2$ $\Delta\nu_q$ 4,000 Hz
1000	6.4 x 10^{-3}	1617	25872
400	1.0 x 10^{-3}	39	657
300	5.7 x 10^{-4}	13	209
200	2.5 x 10^{-4}	2	41
100	6.4 x 10^{-5}	0.16	2.5

Also calculated are the values for the square of the correlation time multiplied by the square of the quadrupole splitting ($\Delta\nu_q$). Two quadrupole splitting values of 1,000 Hz (approximating that of DMPC-d_9) and 4,000 Hz (approximating that of the β-methylene segment of DMPC-d_4) are considered. When the $\tau_c^2(2\Pi.\Delta\nu_q)^2$ value is two or three orders of magnitude greater than 1, there is little contribution to averaging

of the spectral anisotropy by Brownian tumbling effects; for values approaching 1, however, some effects on the spectral anisotropy are expected. For diameters such that the $\tau_c^2(2\Pi.\Delta\nu_q)^2$ value is less than 1, significant decreases in the spectral anisotropy are predicted. Thus for vesicles with diameters smaller than 300 nm the quadrupole splittings for the choline γ-methyl groups are likely to be sensitive to the rate of lateral diffusion, D_{diff} and the viscosity of the medium. The larger residual splittings of the β-methylene segments of DMPC-d_4, however, mean that contributions to spectral averaging by Brownian tumbling do not become significant until diameters of below 100 nm.

The vesicle diameters of the 187:1 (300 - 500 nm) and in particular, the 1,444:1 DMPC/bR mole ratio complexes (100 - 300 nm) produced by the fast cholate removal technique are in the range predicted (Table 6), where the DMPC-d_9 quadrupole splittings will be sensitive to vesicle tumbling. Furthermore, it is possible that the diameters determined by negative stain electron microscopy are over-estimated due to a flattening of the vesicles on drying. The vesicles diameters are on the limit where changes in the rate of lipid diffusion, D_{diff}, will effect the correlation time, τ_c, such that on passing through the main phase transition, the increase in rate of lateral diffusion (D_{diff}) of the lipids around small radii, superimposed on the rapid rate of vesicle tumbling (D_t) is sufficient to significantly reduce the residual quadrupole splittings. Indeed, the temperature dependence of the measured quadrupole splittings for the 187:1 DMPC/bR mole ratio complex (Fig.3.5) is found to reflect exactly the broadened phase transition determined by TEMPO partitioning (Fig.3.22); the increased temperature sensitivity between 18 and 28°C (with a mid-point occurring at approximately 23°C) coinciding with the broadened phase transition of the DMPC. The extreme temperature sensitivity demonstrated by the quadrupole splittings from the small vesicle 1,444:1 mole ratio complex at 24°C reflects the sharper phase transition associated with increasing lipid content of a vesicle, as observed by TEMPO-partitioning (Fig.3.22) and the smaller vesicle diameters. The DMPC-d_9 quadrupole splittings obtained from vesicles produced by the slow cholate removal technique (diameters around 1,000 nm)

will be unaffected.

In contrast, the c.s.a.s measured from the phosphorus-31 NMR spectra (Fig.3.13) are less sensitive than the corresponding deuterium-NMR γ-methyl group (DMPC-d_9) quadrupole splittings (Fig.3.4) to the differences in vesicle size obtained by the fast and slow cholate removal procedures. The spectral anisotropy (c.s.a. ~-50 ppm) for the phosphorus-31 NMR spectra at 121.4 MHz is ~6,000 Hz, and is thus less susceptible to Brownian motion tumbling than those estimated for the DMPC-d_4 β-methylene quadrupole splittings. Only the ^{31}P-NMR spectrum of the 1,444:1 mole ratio complex, with vesicles diameters between 100 nm and 300nm (and many even smaller) reveals a significant isotropic component, and a decreased c.s.a.. The spectral lineshape for the spectrum of this complex is similar to that predicted for 500nm diameter lipid vesicles (Burnell *et al.*, 1980).

The DMPC-d_9 results only provide information interpretable in terms of lipid/protein interactions if the vesicles are larger than 600 nm in diameter (i.e. vesicles produced by the slow cholate removal procedure). For smaller vesicles, increasing the temperature above the main phase transition results in a decrease in the measured quadrupole splitting that does not accurately reflect the lipid-protein interaction. From Fig.3.5, it can be seen that incorporation of small amounts of protein (0.71 mol% bacteriorhodopsin; that is 141:1 mole ratio DMPC/bR complex) reduces the quadrupole splittings for the γ-methyl groups, by ~200 Hz relative to protein-free lipid for temperatures above the main phase transition. Increasing the protein content to 1.47 mol% (68:1 mole ratio complex) is seen to increase the quadrupole splitting by ~100 Hz relative to the lower protein content complexes. This protein content mediated increase in quadrupole splitting is interpreted in terms of a reduction in the amplitude of motion of the γ-methyl segments. Similar motional restrictions are seen to be imposed by increasing protein content on the β-CD_2 methylene segment and the phosphate group.

The opposing effects of protein content on the measured quadrupole splittings for the α-methylene segment powder patterns at constant temperature compared to those

on the quadrupole splittings of the β-methylene segments (Fig.3.12) and choline γ-methyl groups and the phosphorus-31 c.s.a.s (Fig.3.15), indicate that increasing the protein content in DMPC bilayers imposes differing motional restraints on neighbouring segments within the phosphocholine headgroup. Incorporation of small amounts of protein (up to between 0.45 and 0.55 mol% bR; that is DMPC/bR mole ratios of 222:1 to 182:1) appears to enhance the amplitude of motion of the β-CD_2 methylene segment (Fig3.12) and the γ-methyl rotors about the glycerol backbone relative to that in the protein-free lipid as judged by the decrease in the quadrupole splitting. The Cα segment, however, remains unaffected, although the neighbouring phosphate group amplitude of motion is also increased judging from the decrease observed in phosphorus-31 NMR c.s.a. (Fig.3.15). Increasing the protein content further (up to 1.49 mol% bR i.e. DMPC/bR mole ratios 67:1), however, appears to have an ordering effect on the Cβ and Cγ segments as shown by the increase in their quadrupole splittings (Figs.3.12 and 3.5). This may take the form of a reduction in amplitude of oscillation about the glycerol backbone via the Cα-Cβ bond. The motion of the phosphate group is also increasingly restrained at higher protein contents (Fig.3.15), but, in apparent contradiction, the Cα segment motion appears to be increased in amplitude about the glycerol backbone, relative to pure lipid. The apparently opposing motional requirements placed on these adjacent segments may be reconciled in two ways.

First, high protein contents may serve to homogenise the motions of the α- and β-methylene segments as indicted by their increasingly similar quadrupole splittings. The magnitude of the difference between the α- and β-powder pattern quadrupole splittings at 30 and 45°C (Fig.3.12) is reduced by increasing the protein content of the vesicles. Indeed for the 67:1 mole ratio complex even at 45°C, the α- and β-powder patterns are barely resolvable (Fig.3.6). This implies that the presence of protein tends to synchronise the extent of motion of the α- and β-CD_2 methylene segments. In pure lipid the major motion within the choline headgroup is rotation of the Cγ-Cβ segment around the Cα-Cβ bond (Gally *et al.*,1975). For low protein content vesicles, this

motion around the Cα-Cβ bond is preserved, although its amplitude increases (decrease in β-quadrupole splittings), relative to that in pure lipid. Increasing the protein content may have the effect of shifting the centre of oscillation towards the phosphate group but at the same time reducing the overall amplitude of motion of the choline headgroup; in effect the amplitude of oscillation about the Cα-Cβ bond is reduced relative to low protein content complexes (increasing the β- and γ-quadrupole splittings), but motion around the phosphate-Cα linkage is increased by protein relative to pure lipid. The net result is a synchronisataion of the amplitudes of motion of the Cα and Cβ methylene segments by higher protein contents. The DMPC phosphate group, itself also experiences a protein-mediated restraint on amplitude of motion as judged by the increase in c.s.a. with protein content. This may reflect an ionic interaction between the negatively charged phosphate moiety and sites on the bacteriorhodopsin molecule that would bind PGP and PGS.

Second, the increased amount of protein surface exposed to lipid as the protein content of the vesicle increases, may impose a conformational change, perhaps at the Cα-Cβ bond, that effects the packing restraints at different regions of the choline headgroup. In particular, the conformational change may alter the torsional angle of the α-CD_2 methylene segment, such that the quadrupole splittings from the α-powder pattern are decreased. Large changes in the quadrupole splittings, however, do not necessarily imply an extensive reorganisation of the phospholipid headgroup, since the residual quadrupole splittings are rather sensitive to small variations in torsion angle (Seelig & Gally, 1976). Indeed, 50mol% cholesterol hardly effects the ^{31}P c.s.a. or the α-CD_2 methylene segment quadrupole splittings for DPPC, but reduces the β-CD_2 methylene quadrupole splitting by a factor of two (Brown & Seelig, 1978); a change in the Cα-Cβ bond torsion angle from 81° to 83.5° accounting for a two fold reduction in β-methylene quadrupole splitting. Thus, the β-methylene segment, γ-methyl groups and phosphate group appear to experience to a protein mediated restraint in amplitude of motion about the glycerol backbone as the bacteriorhodopsin content in the vesicle is increased. The α-methylene segment, however, may also experience such

an ordering, only its reorientation by the protein disguises this effect in the observed α-CD_2 methylene quadrupole splittings.

From ESR spectra of phospholipids, spin-labelled at the C-14 segment of the fatty acyl chains, it appears that high bacteriorhodopsin contents also order the acyl chain regions of the phospholipids that are not even in direct contact with the protein, itself. The fluid component of the two component ESR spectra from DMPC/bR systems resembles the ESR spectrum of fluid lipids in protein-free systems and arises from the lipid molecules that are not directly in contact with the protein surface itself. Both the $2A_{max}$ values measured, and the apparent order parameters (S) calculated for the fluid components from ESR spectra of 14-PCSL in the 68:1, 131:1, 187:1 and pure DMPC are seen to be increased by protein content at all temperatures above the main phase transition, relative to protein-free lipid. This implies that protein free lipid shells, beyond the immediate boundary lipid shell, are also perturbed by the presence of bacteriorhodopsin protein particles. Such increases in order parameter are consistent with a protein-mediated ordering, that is, a reduction in amplitude of oscillation and/or a reduction in rate of motion of the terminal regions of the fatty acyl chains. Cytochrome *c* oxidase (Knowles *et al.*, 1979) also broadens the fluid component. ESR analysis of fluid components produced by computer subtraction indicated that the influence of cytochrome *c* oxidase on the lipid fluidity extends beyond the boundary lipid shell by approximately five shells. Beyond the boundary shell at least two further shells are strongly perturbed, a third shell is less strongly perturbed and a further two or three shells may be still weakly perturbed. Similarly qualitative analysis of the fluid component of 14-SASL in rod outer segment membranes (Watts *et al.*, 1982) indicates that rhodopsin also decreases the motional rate, and or motional amplitude of the lipid chains not directly interacting with the protein. Fluorescence depolarisation studies (Rehorek *et al.*, 1985) show that bacteriorhodopsin reconstituted into DMPC (as described in Cherry *et al.*, 1978) increases the order of the bulk lipids and that long range interactions from the protein affect most lipids. In these complexes the endogenous purple membrane phospholipids were retained. At 35°C, (i.e. when all the

protein is monomeric) the order parameter measured was found to increase linearly by a factor of two on adding protein to DMPC to a 52:1 mole ratio (total phosphate/protein).

While the phosphorus-31 c.s.a. values and deuterium NMR quadrupole splitting values provide information on the amplitude of segmental motions, information on the rates of motion can only be obtained from the spin-lattice (T_1) and spin-spin (T_2) relaxation times. Such measurements were performed for the phosphate group by phosphorus-31 NMR but not for deuterium methylene segments. The 29 - 37% reduction in phosphorus-31 (T_2) spin-spin relaxation times observed on addition of bacteriorhodopsin may reflect a protein mediated decrease in the rate of mobility of the phosphate moiety. This result is consistent with those for other integral proteins. The presence of 83% (w/w) cytochrome *c* oxidase in DMPC reduced the measured spin-spin relaxation time (90° peak) from 7.4 ms to 3.1 ms at 60.7 MHz (Rajan *et al.*, 1981).

A cytochrome *c* oxidase content of 83% (w/w) (Rajan *et al.*, 1981) was found to significantly reduce the phosphorus-31 spin-lattice relaxation times (T_1) from 660ms for protein-free DMPC to 170ms (at 60.7 MHz i.e. 3.52T). The linear τ vs $\ln(I_o-I_t)$ plots (Fig.3.19) imply the whole phosphorus-31 powder pattern for DMPC to be determined by a single T_1 time both in the absence and presence of bacteriorhodopsin. Initial inspection of the ^{31}P-NMR spin-lattice relaxation times (Table 1) obtained for DMPC/bR complexes at 33°C shows them to be less sensitive to incorporation of bacteriorhodopsin than described for cytochrome *c* oxidase. This, however, may be an artifact. It is reported (Tamm & Seelig, 1983) that the ^{31}P-NMR T_1 values for pure POPC exhibits a temperature minimum at 15°C of ~1s (121.4 MHz.). Lowering the temperature to -10°C or increasing it to +40°C serves to lengthen the T_1 to ~1.5s. The presence of cyt *c* oxidase elevated the T_1 to by ~0.1s and shifted the temperature minimum to 25°C. Similarly (Seelig *et al.*, 1981) the phosphorus-31 T_1 temperature profiles for DOPC and sarcoplasmic reticulum membrane with DOPC also exhibited minima; for pure DOPC, the minimum occurred at 4°C with a relaxation time of ~1s, whereas for DOPC in sarcoplasmic reticulum, the minimum was shifted to 14°C and had a longer T_1 of ~1.2s (121.4MHz.). In view of the temperature dependence and the

protein-mediated shift in minimum, a direct comparison of the ^{31}P-NMR T_1 values obtained for different DMPC/bR complexes and protein-free DMPC at 33°C cannot be made.

Freeze fracture electron micrographs of DMPC/bR complexes (see Chapter 4) quenched from above that of the main phase transition reveal that at all protein contents the protein particles are dispersed; there being no evidence of changes in the protein aggregation state with lipid/protein content. Thus changes in the α- and β-CD_2 methylene segment quadrupole splittings (Fig.3.12) and the phosphorus-31 c.s.a.s (Fig.3.15) observed with varying the protein content may be explained in terms of a proportional increase in lipid-protein interactions at the expense of lipid-lipid interactions. The linear dependence of the quadrupole splittings for the α- and β-methylene segments with protein content at constant temperature is significant as it implies that the number of boundary lipids associated with each bacteriorhodopsin molecule is the same, irrespective of the protein content of the vesicles. This supports freeze fracture electron microscopy studies (Chapter 4) that the protein aggregation/dispersion properties are independent of lipid/protein ratio.

Quantitative analysis, in terms of a fast two-site exchange model, of the ^{2}H-NMR quadrupole splitting data plotted as a function of the protein content (Fig.3.12) allows determination of n_b, the number of boundary lipids per bacteriorhodopsin monomer. For these calculations it is postulated that the residual quadrupole splitting for lipid in direct contact with the protein, that is boundary lipid, is zero (Sixl *et al.*, 1984). The value obtained from the β-methylene splitting data was negative, although if the β-methylene quadrupole splitting of pure lipid is negative, however, then a positive value of 15 DMPC molecules would be obtained. The absolute values obtained for the number of boundary lipids per 26,000 Da bacteriorhodopsin monomer ranged from 12 (α-methylene segment data) to 15 (β-methylene segment data) being within 30% of the values obtained from analysis of ESR data.

From the spectral subtraction and simulation analysis of ESR spectra for 14-PCSL in the 68:1 mole ratio DMPC/bR complex, each 26,000Mr bacteriorhodopsin

monomer appears to be associated with between 18 and 20 DMPC boundary lipid molecules in the absence of endogenous purple membrane lipids at temperatures above the main phase transition. This value is considerably more than the 6 and 10 polar lipids reported per bR in purple membrane (Kates *et al.*, 1983 and Blaurock, 1975, respectively) and the 10 phospholipids determined by high resolution ^{31}P-NMR (Chapter 2). In purple membrane where the protein particles are tightly packed into paracrystalline arrays (Blaurock & Stoeckenius, 1971) it is likely that lipid molecules are shared between protein particles and serve to organize the protein particles into the lattice. In DMPC bilayers in the absence of purple membrane lipids, the protein particles are more dispersed (Chapter 4) and so a larger surface area is presented to lipids. Thus the number of boundary lipids observed for bR in DMPC bilayers is in keeping with a greater degree of dispersion.

Compared, however, to other protein systems studied so far, each 26,000 Da bacteriorhodopsin monomer has a relatively small number of boundary lipids. For 14-PCSL, there are effectively 55+/-5 lipids per 200,000 Da cytochrome *c* oxidase (Knowles *et al.*, 1979), 58+/-4 lipid molecules per 265,000 Da Na^+-K^+-ATPase and 24+/-3 boundary lipids per 37,000 Da bovine rhodopsin molecule (Watts *et al.*, 1979). Of some significance is that the number of boundary lipids (18 - 20) for bacteriorhodopsin in DMPC/bR vesicles is within 20% of the 22-25 displayed by rhodopsin in bovine rod outer segment membranes (Watts *et al.*, 1979) and the 22-23 reported in DMPC/rhodopsin vesicles of similar mole ratio composition (Ryba *et al.*, 1986).

Vertebrate rhodopsin solubilized in the non-ionic detergent dodecyldimethylamine oxide was shown by small-angle X-ray scattering to be a very elongated molecule (maximum length 94Å) with a diameter between 31.4 and 33.7Å (Sardet *et al.*, 1976), which is similar to the 25 x 35Å diameter dimensions for the bacteriorhodopsin molecule (Henderson & Unwin, 1975). In fact the bacteriorhodopsin density map for the seven transmembrane α-helices closely defines the transmembrane core for models of ovine rhodopsin (Findlay & Pappin, 1986). Rotational diffusion

measurements (Cone, 1972) and ^{2}H-NMR data (Ryba *et al.*, 1986) demonstrate rhodopsin to be monomeric and not to exist as an oligomer either in the dark or on bleaching (Downer, 1985). The transmembrane hydrophobic portions of the monomeric bacteriorhodopsin and rhodopsin molecules are thus likely to expose similar surface areas for interaction with lipid and hence motionally restrict similar numbers of boundary lipids. Indeed estimation of the number of boundary lipids per 26,000 Da bacteriorhodopsin monomer from the electron density map (Pates, 1978; Marsh & Watts, 1982) predicts some 26 phospholipid molecules, which is similar to the number determined for rhodopsin in rod outer segments (Watts *et al.*, 1979) and DMPC bilayers (Ryba *et al.*, 1986). Thus the number of boundary lipids determined by ESR analysis are consistent with bacteriorhodopsin existing in a monomeric state in DMPC bilayers at temperatures above 30°C. More aggregated states would tend to increase protein-protein contacts over lipid-protein contacts, so reducing the number of boundary lipids observed per protein. It is possible that the slightly smaller number of boundary lipid (20%) observed for the case of bacteriorhodopsin compared to rhodopsin is due to a small degree of protein-protein association although this may also reflect experimental error or genuine differences in the number of boundary lipids per monomer. One argument against a fully monomeric bacteriorhodopsin species at temperatures above the phase transition in DMPC bilayers in the absence of endogenous purple membrane lipids is the observed increase in the magnitude of the motionally-restricted component over a period of three weeks at 4°C. This could be interpreted in terms of the existence of oligomeric protein structures into which the spin-label lipids exchanges very slowly.

The difference spectrum (Fig.3.27.b) for the motionally restricted component displayed by 14-PCSL at 37°C in the 68:1 mole ratio DMPC/bR complex retains a small fluid component. It is reported that 16-SASL in purple membrane displays the presence of two populations of bound spin-label (Chignell & Chignell, 1975; Hoffmann, *et al.*, 1980); the more fluid of which is seen to increase relative to the immobilised component at higher temperatures. Indeed the spectrum obtained at 40°C (Hoffmann *et al.*, 1980), revealed very little motionally restricted component. The

presence of the two components were attributed to two different conformations of the bacteriorhodopsin (Hoffmann *et al*,. 1980), the relative proportions of which are dependent on the temperature. A possible explanation, therefore, for the existence of a less motionally restricted component present in the difference spectrum for the bacteriorhodopsin boundary lipid component at 37°C, presented in Fig.3.27.b, is that it represents the signal from 14-PCSL in contact with a small proportion of the bacteriorhodopsin which is in the high temperature conformation.

The two component nature of ESR spectra provides a method for investigating specificity of integral membrane proteins for particular types of phospholipid headgroups. Increased selectivity of a certain spin-labelled phospholipid headgroup over another is manifested in a larger proportion of motionally restricted component. Such studies previously have presented evidence for selectivity of cytochrome *c* oxidase (Knowles *et al.*, 1981) and Na+/K+-ATPase for cardiolipin (Watts *et al.*, 1982) and rhodopsin for phosphatidyl serine (Watts *et al.*, 1979). From the phospholipid composition of the purple membrane it would not be unreasonable to predict that bacteriorhodopsin would exert a preference for negatively charged phospholipid headgroups, in particular phosphatidylglycerols. From comparison of the motionally restricted components in spectra in Figs.3.25 and 3.26.b and c, however, this does not appear to be the case. In fact spectral subtraction and simulation analysis show the magnitude of the motionally restricted component displayed by 14-PCSL in the 68:1 mole ratio DMPC/bR complex in 10mM Tris/HCl, pH 7.5 to be 7% larger than those determined for 14-PGSL. The flat baseline, however, obtained by spectral subtraction of the spectrum for 14-PGSL from that of 14-PCSL does not support any negative selectivity for PG-headgroup. The implication is that in DMPC/bR vesicles, the monomeric bacteriorhodopsin particles certainly do not display any positive selectivity for the negatively charged PG headgroup over the zwitterionic PC headgroup.

Both the fluid and boundary lipid components (Figs.3.25 and 3.26) displayed by 14-PGSL in the 68:1 DMPC/bR mole ratio complex appear to be unaffected by the presence of 2M NaCl in the aqueous environment. The apparent order parameters for

the fluid components are virtually identical (Fig.3.24) in the presence and absence of salt. A salt induced change in the dispersion properties of the protein particles would alter the protein surface available for lipid interaction and hence the magnitude of the motionally restricted component in ESR spectra. From this it would appear that the protein dispersion properties are not influenced by ionic strength of the aqueous environment. Indeed freeze-fracture electron micrographs of a DMPC/bR complex in 2M and 4M NaCl reveal similar distributions of the 11nm diameter protein particles (Chapter 4).

Chapter 4

The effect of temperature and protein content on the dispersive properties of bacteriorhodopsin from *H.halobium* in reconstituted DMPC complexes free of endogenous purple membrane lipids: A freeze fracture electron microscopy study

4.I). Introduction

Freeze fracture electron microscopy has been used to study the aggregation behaviour for bR in exogenous phospholipid bilayers produced by a variety of methods (Cherry *et al* 1978 and 1980; Hwang & Stoeckenius, 1977; van Dijck *et al.* 1981; Lewis & Engelman, 1983). Protein aggregation appears to depend upon the lipid composition of the bilayer from studies of lipid/bR bilayers in which either up to 90% of the endogenous purple membrane lipids were removed or all endogenous lipids were retained (Hwang & Stoeckenius, 1977). The exogenous lipids used for vesicle formation included asolectin and soybean phosphatidylcholine, which have heterogeneous acyl chains. Bacteriorhodopsin, reconstituted into bilayers of the well defined homogeneous lipid, DMPC, but with all the endogenous purple membrane phospholipids still retained, has been studied by electron microscopy, X-ray diffraction and circular dichroism (Cherry *et al.*, 1978).

To date, only one freeze fracture electron microscopic study of bR in phosphatidylcholine bilayers, free of endogenous purple membrane lipids, has been reported (Lewis & Engleman, 1983). In that study, it was shown that the protein remains dispersed above the bilayer lipid phase transition temperature (T_c) in phosphatidylcholine bilayers of a variety of acyl chain lengths including dilauroyl (C12), dimyristoyl (C14), dipalmitoyl (C16) and distearoyl (C18). Only in didecanoyl (C10) phosphatidylcholine bilayers was the bacteriorhodopsin found to be extensively aggregated. However, only one lipid/protein ratio and one temperature (above the phase transition for each lipid) was examined for each chain-length lipid. For the DMPC

complex, this ratio was 278:1 (mol/mole) and complexes were quenched from 34°C.

In this chapter, DMPC/bR complexes with a wide variety of protein/lipid ratios have been studied by freeze-fracture electron microscopy. The effect of quenching dispersions from both above and below the gel to liquid crystalline phase transition temperature of DMPC in the complex is reported, as well as the solubility of bR in the complete absence of endogenous purple membrane lipids. Bacteriorhodopsin solubility appears to be dependent on lipid-protein ratio, the presence or absence of endogenous lipids, as well as the physical state of the bilayer acyl chains.

4.II). Materials and Methods

Freeze fracture electron microscopy. The different DMPC/bR complexes were studied by freeze-fracture electron microscopy after quenching from a range of temperatures from 6 to 55°C. Samples were quenched using liquid propane and the sandwich technique, in which the complexes were mounted between two plain-faced copper holders to give a quenching rate of ~10^5K.s^{-1}. To effect a lower cooling rate for the complexes when required, one of the copper holders used had a depression onto which the sample was positioned; in this situation the sample layer is thicker and the cooling rate on quenching about an order of magnitude slower (~10^4K.s^{-1}) than when using the plain faced holders (Costello *et al.*, 1982).

4.III). Results.

Representative freeze-fracture electron micrographs for the DMPC/bR complexes, entirely free of endogenous purple membrane lipids, are shown in Figs.4.1 to 4.4. The packing properties and arrangement of protein particles of bacteriorhodopsin in the DMPC bilayers appear to depend upon the temperature (T_q) from which the complex was quenched, the DMPC/bR ratio as well as the rate of freezing of the complex when quenched from above the phase transition temperature.

Freeze fracture electron micrographs of DMPC/bR complexes quenched from temperatures below the main phase transition. DMPC/bR complexes quenched from temperatures below the phase transition reveal similar features in freeze fracture



a)

b)

Fig.4.1. Freeze fracture electron micrographs of DMPC/bR complexes with all endogenous purple membrane lipids removed quenched from temperatures below the main phase transition. The DMPC/bR mole ratios of the complexes were; a) 1,444:1 (13.5°C); b) 379:1 (6°C); c) 222:1 (15°C); d) 168:1 (15.5°C); e) 141:1 (15.5°C) and f) 68:1 (15.5°C). Bar = 100 nm.

c)

d)





e)

f)

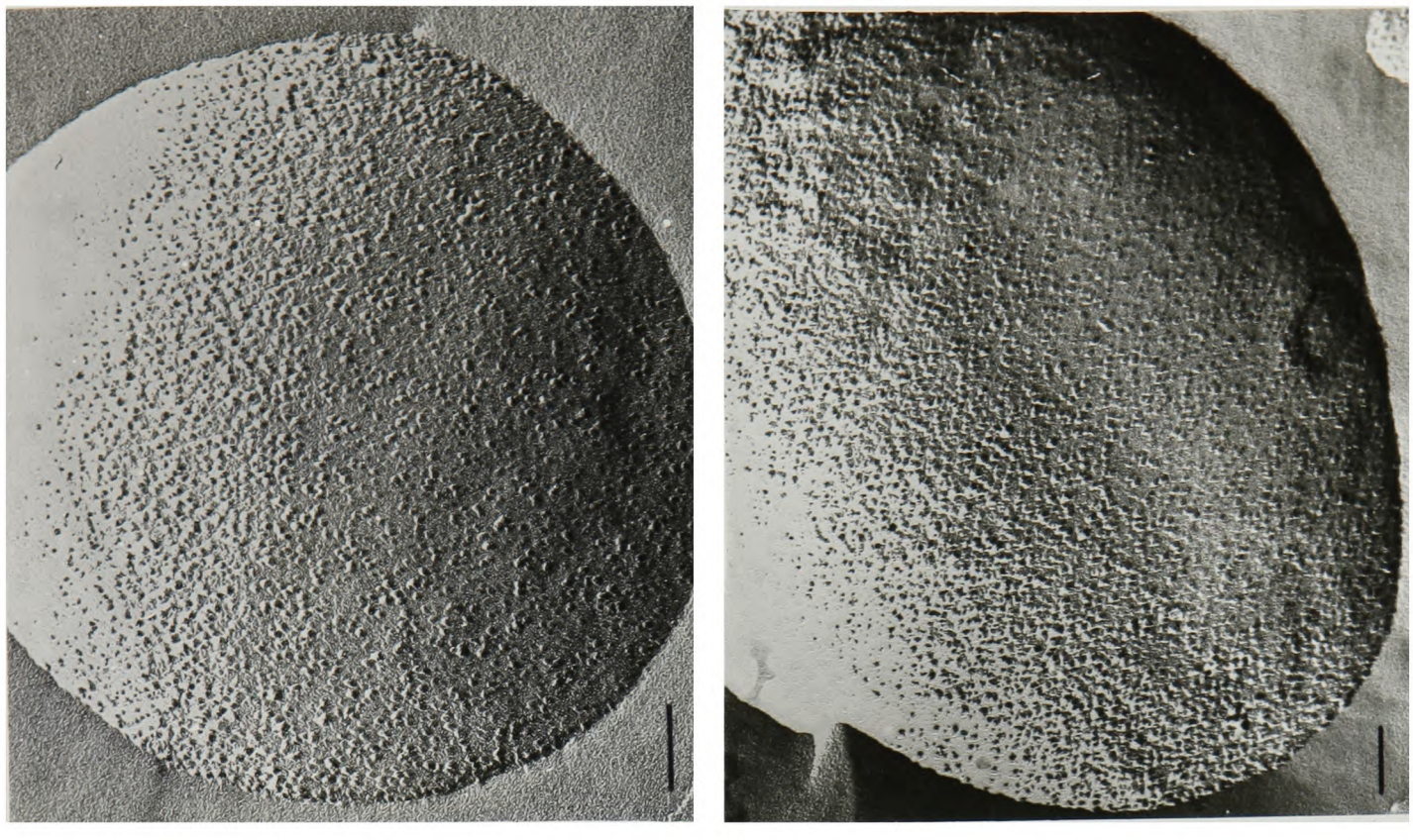




Fig.4.1. (cont.)

a)

b)



c)

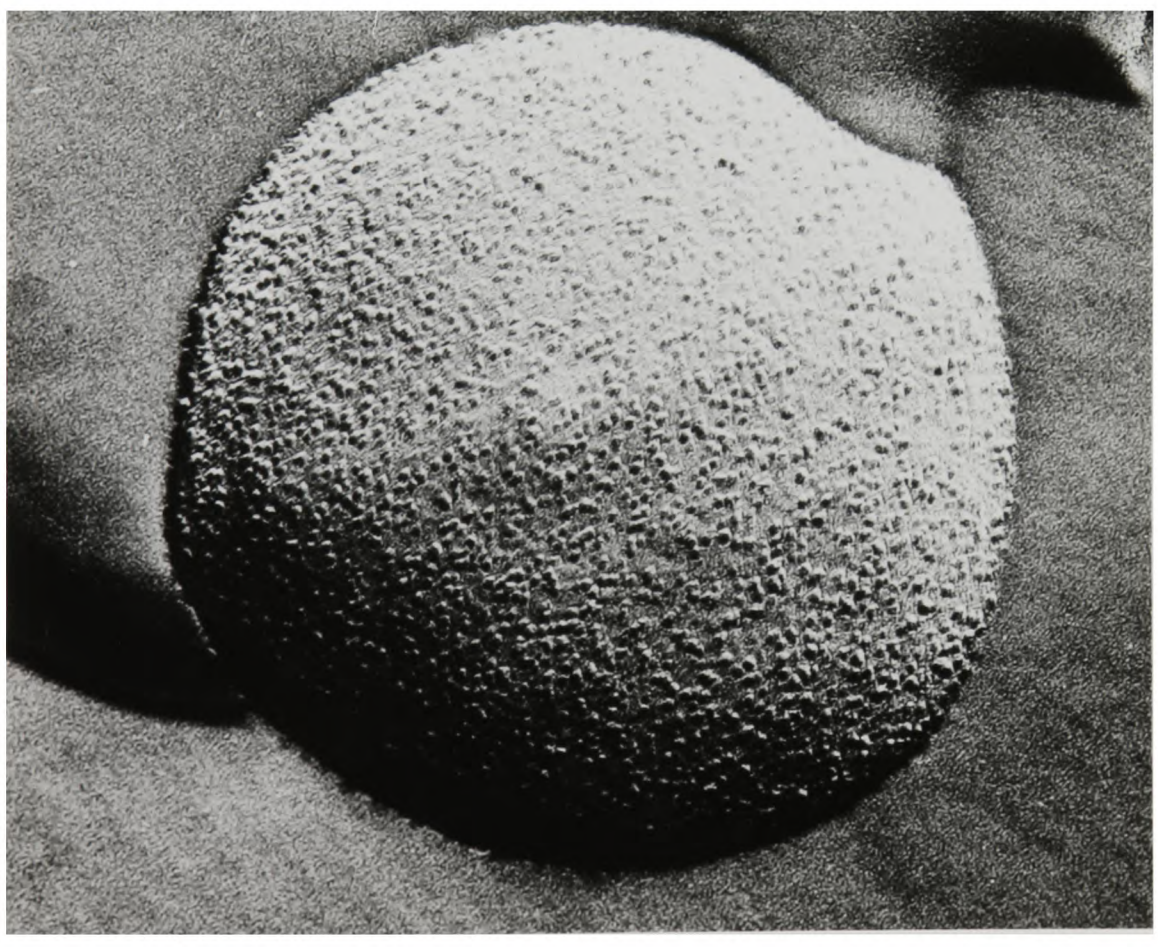
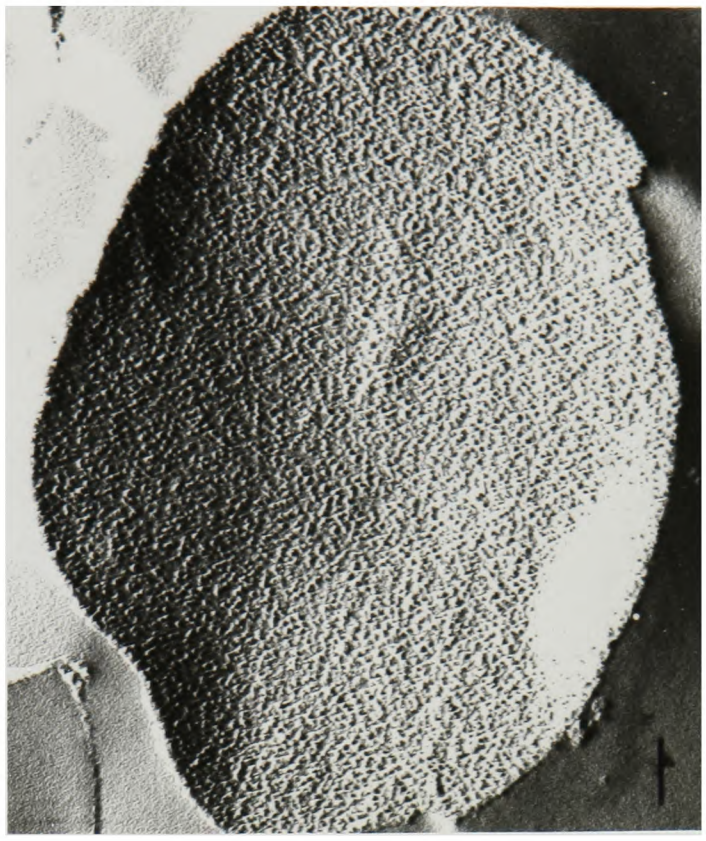


Fig. 4.2. Freeze fracture electron micrographs of DMPC/bR vesicles of mole ratios; a) 222:1; b) 182:1; c) 141:1; d) 95:1 and e) 68:1 quenched from 55°C by the fast rate of cooling technique (~10^5K.s^{-1}). Bar = 100 nm.

d)



e)

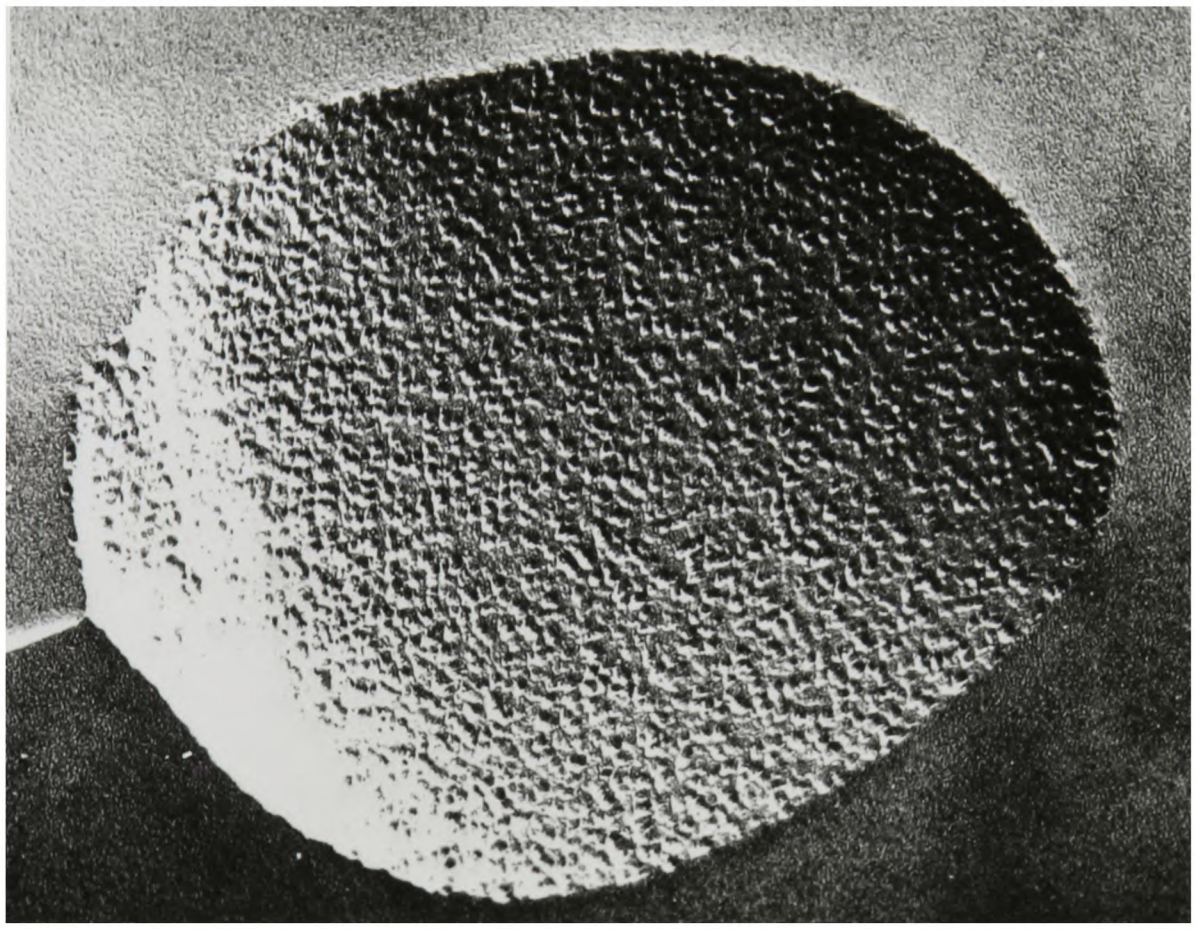


Fig. 4.2. (cont.)

electron micrographs whether they are quenched slowly (~10^4K.s^{-1}) or more quickly (~10^5K.s^{-1}), irrespective of the protein content. The lipid bilayer regions of complexes with a low protein content display ridges (Figs. 4.1a,b), similar to those observed in protein-free DMPC (Luna & McConnell, 1976) and DMPG (Watts *et al.*, 1978) bilayers when quenched from temperatures between the pre- and main bilayer phase transition temperature. The bacteriorhodopsin particles appear to be organised along the DMPC ridges (Fig. 4.1a and b) in these low protein content complexes giving linear particle arrangements.

With increasing protein content, that is less than 222:1 DMPC/bR mole ratio, the ripples are found to disappear (Figs.4.1c-f). Electron micrographs (Fig.4.1.c-e) from vesicles of intermediate protein content (222:1 to 141:1 mole ratio DMPC/bR) reveal the protein particles to be organised into one-dimensional linear arrays, which may represent the ridges in the DMPC bilayer regions. At very high protein contents (68:1 mole ratio DMPC/bR) the linear arrays of protein particles are seen to be less prominent (Fig.4.1.f) than at intermediate protein contents. Indeed, other electron micrographs (not shown) of the 68:1 mole ratio DMPC/bR complex quenched from 15.5°C displayed no distinct linear organisation of protein particles; the particles appearing more dispersed. At high protein contents, however, nearly all the bacteriorhodopsin particles, maintained contacts with neighbouring particles forming short chains (~3-5 particles) or clusters.

Freeze fracture electron microscopy of DMPC/bR complexes quenched from temperatures above the main phase transition using different quenching rates. Complexes quenched from temperatures above the phase transition using the sandwich technique with faster cooling rate (~10^5K/sec) show well dispersed and irregularly distributed protein particles in the micrographs both in vesicles of lower (Figs. 4.2a, b and c) and of higher protein contents (Fig.4.2d).

Freeze-fracture electron micrographs of DMPC/bR complexes quenched also from temperatures above the main phase transition but using the sandwich technique with a slower cooling rate (Costello *et al.*, 1982) show distinct and often regular

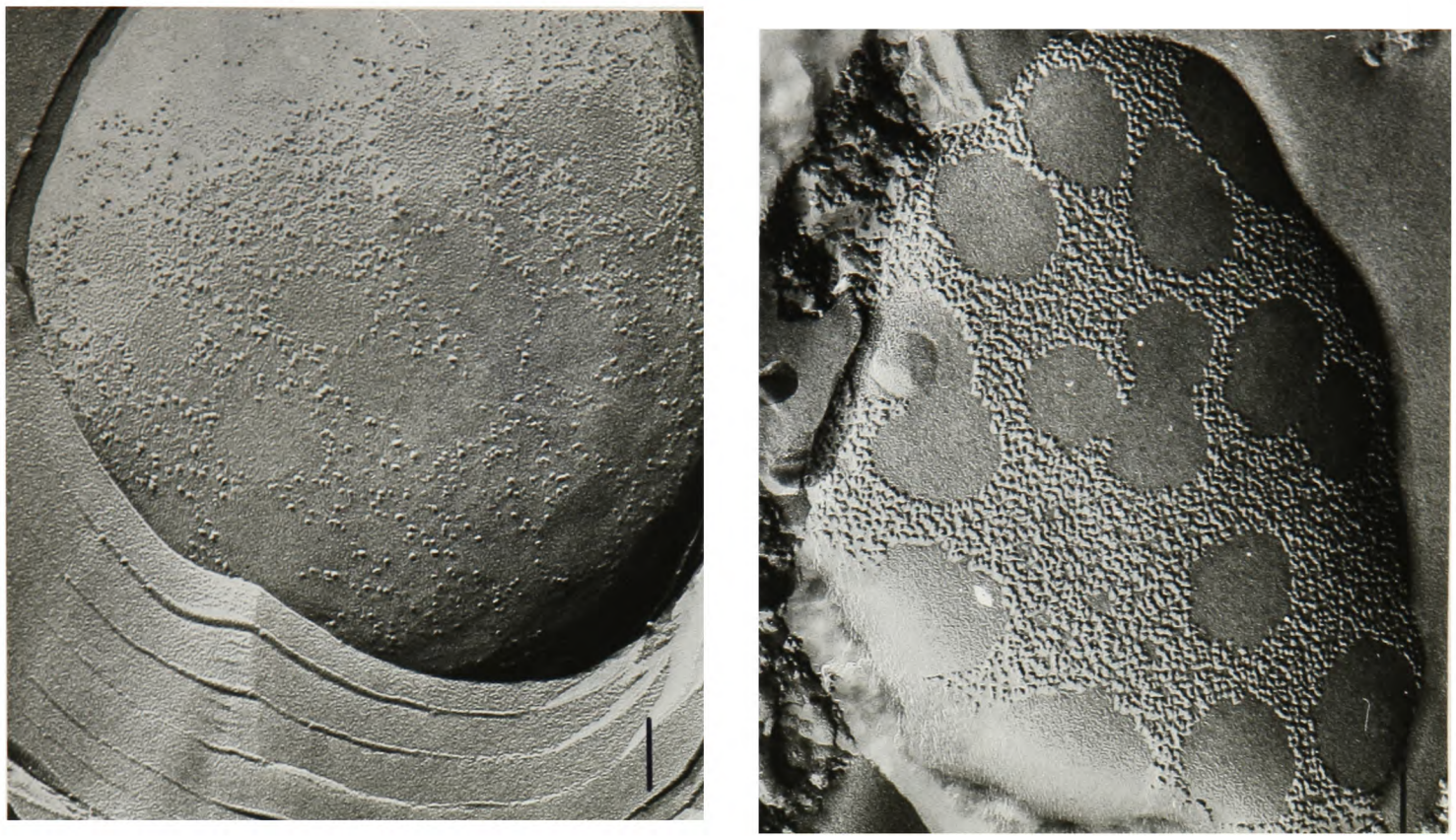
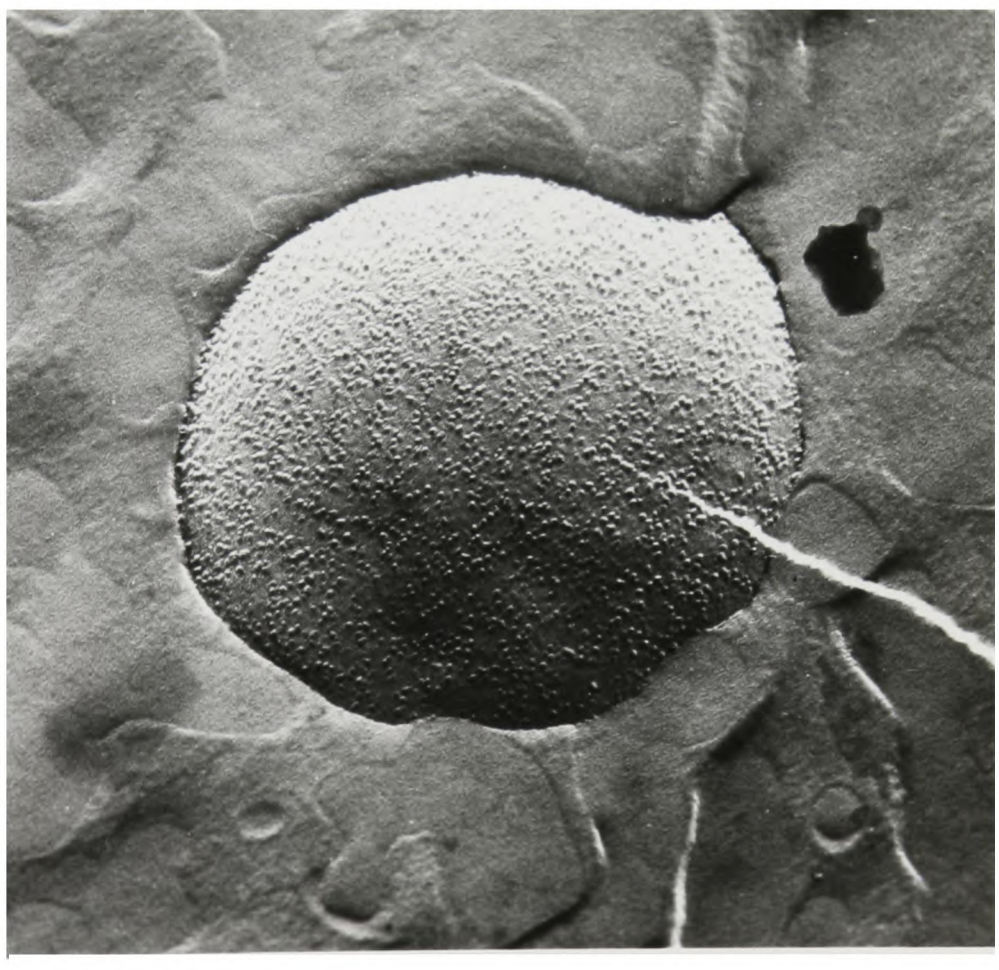


Fig.4.3. Freeze fracture electron micrographs of DMPC/bR complexes quenched by the slow cooling technique (cooling rate ~10^4K s^{-1}) from temperatures well above the completion of the main phase transition. DMPC/bR complex mole ratios; a) 1,444:1 (50°C); b) 187:1 (45°C); c) 187:1 (45°C); and d) 68:1 (55°C). Bar = 100 nm.



a)



b)

Fig.4.4. Freeze fracture electron micrographs of 168:1 mole ratio DMPC/bR complex quenched by the slow cooling method from 55°C.
Vesicles in a); 10mM Tris/HCl, pH 7.5 and b) 4M NaCl.

patterns of particle-free areas (Fig. 3). The protein particle free islands are almost circular and of varying diameters. This lateral phase segregation was more clearly observed for higher protein content vesicles e.g. the 187:1 DMPC/bR mole ratio complex (Fig. 4.3.b and c) compared to lower protein content vesicles e.g. 1,444:1 DMPC/bR mole ratio (Fig. 4.3a). It should be noted that as the protein content is increased so the sizes of the protein-free pools become smaller.

It is important to notice that in all cases, below and above T_c and at low or at high protein content of the DMPC/bR complexes in the bilayers totally free of endogenous lipid, the bacteriorhodopsin particles do not display a hexagonal packing similar to that observed in the patches of *H. halobium* purple membranes (Blaurock & Stoeckenius, 1971). In marked contrast to these observations bR aggregates display a hexagonal-like packing in DMPC/bR complexes still containing endogenous purple membrane lipids (as shown for the 21:7.6:1 mole ratio DMPC/PMPL/bR nsTP-produced complex in Fig.5.18) when quenched from below T_c (Cherry *et al.*, 1978).

Effect of high ionic strength on the dispersion properties of the bacteriorhodopsin particles. For all the electron micrographs presented above the DMPC/bR vesicles were suspended in 10mM Tris/HCl, 1mM EDTA, pH 7.5. Addition of NaCl to a concentration of 4M was seen to have little affect on the protein particle dispersion properties in a 168:1 mole ratio DMPC/bR complex at 55°C (Figs.4.4.a and b). Also the dimensions of the protein particles are not effected by the ionic strength of the aqueous environment.

4.IV). Discussion.

Freeze fracture electron microscopy is a good technique for investigating the interior of a membrane and the arrangement and distribution of particles (presumed to be proteins) within the plane of the bilayer (Branton, 1966; Meyer & Winkelmann, 1969). It has been assumed that the cytoplasmic membranes of *H. halobium* bacteria split along the interior plane (Blaurock & Stoeckenius, 1971). In the purple membrane patches the outer lamellar shows a smooth fracture face which lacks proteins, while the

inner lamellar reveals a hexagonal array of particles; the bR remaining embedded in the cytoplasmic half after fracturing. The electron micrographs presented here for DMPC/bR complexes without the endogenous purple membrane lipids also clearly reveal the presence of such particles presumed to be bR, although these particles may not be individual bacteriorhodopsin monomers, from their size (~8-10 nm diameter), but small aggregates symmetrically oriented in the DMPC bilayers. Freeze fracture electron microscopy and diffraction techniques have been used to define the polypeptide content of similar 11.9 nm diameter single membrane particles in purple membranes and it was concluded that such particles contains 9-12 bacteriorhodopsin monomers i.e. 63-84 transmembrane α-helices (Fisher and Stoeckenius, 1977).

A considerable amount of freeze fracture electron microscopic data has been published on bacteriorhodopsin containing vesicles. For example, vesicles have been produced in which 80-90% of the endogenous purple membrane lipids were removed using deoxycholate treatment followed by sucrose density gradient centrifugation. (Hwang & Stoeckenius, 1977). Electron microscopy, together with X-ray diffraction and circular dichroism revealed that the protein-associated particles did not form the regular hexagonal lattice obtained in isolated purple membrane or whole cells. When partially delipidated bacteriorhodopsin was reconstituted with total *H. halobium* lipid extract, patches of protein formed which had a highly ordered planar hexagonal lattice structure, although no preferential orientation was obtained (Hwang and Stoeckenius, 1977). Clearly this implies a role for the endogenous lipids in forming the ordered hexagonal two-dimensional patches. A link between protein orientation and particle size was suggested. In that study no temperature studies were performed and lipids of heterogeneous fatty acyl chain composition (asolectin and soybean PC) were used; DMPC used here is well defined and chemically homogeneous.

Freeze fracture results presented here of bacteriorhodopsin in DMPC vesicles with no endogenous purple membrane lipids present reveal in no cases, both below (Figs. 4.1) and above the phase transition temperature (Figs. 4.2) the regular hexagonal lattice obtained in isolated purple membrane patches (Blaurock & Stoeckenius, 1971).

Even for higher protein content vesicles, the bacteriorhodopsin particles are randomly distributed both below (Fig. 4.1.f) and above the phase transition (Fig.4.2.d). Electron micrographs taken from temperatures above the main phase transition but using a freeze fracture technique with slower cooling rate display a lateral segregation of the particles into large aggregates (Fig.4.3) and protein-free lipid pools. The protein particles in these aggregates are packed together but they are not ordered into the hexagonal two dimensional crystalline array as in the purple membrane patches (Blaurock & Stoeckenius, 1971) or in DMPC complexes (below Tc) when the endogenous purple membrane lipids are still present (Cherry *et al.*, 1978 and as shown in Fig.5.18). These results add further support to a role of the highly negatively charged headgroups in ordering the protein particles into a hexagonal lattice.

It is interesting to note that for all lipid environments so far investigated (Cherry *et al.*, 1978, 1980; Hwang & Stoeckenius, 1977; van Dijck *et al.*, 1981; Chapters 5 and 6 of this thesis) the dimensions for the bacteriorhodopsin protein particles observed by freeze fracture electron microscopy are very similar, measuring ~10nm in diameter. Freeze fracture data for the purple membrane, itself, also reveals the presence of similar particles, for which the polypeptide content was shown to be nine to twelve 26,000Da bacteriorhodopsin monomers (Fisher & Stoeckenius, 1977). Such particles were observed in DMPC bilayers with all the endogenous purple membrane lipids present (Cherry *et al.*, 1978) when quenched from temperatures at which circular dichroism and rotational diffusion studies revealed the bacteriorhodopsin to be monomeric. Also the number of boundary lipids (calculated from ESR data; Chapter 3 this thesis) per 26,000 Da bacteriorhodopsin molecule are consistent with the protein surface area for a fully monomeric species assuming similar dimensions to bovine rhodopsin (discussed in Chapter 3). To explain this apparent discrepancy between electron microscopy and biophysical studies, it was postulated (Cherry *et al.*, 1978) that local micro-aggregation occurs during the rapid freezing of the samples for electron microscopy. During the time calculated for the freezing, the lateral diffusion rate measured for integral proteins would allow for movement between distances of 10 and 100Å, so accommodating low

temperature induced local aggregation of the dispersed 26,000Da monomers into the larger particles observed in freeze fracture electron microscopy. Alternatively these particles, may not actually consist of the 9 - 12 26,000Da bR monomers, but may instead be the "monomeric" species detected by C.D. measurements. Their apparent large size may be an artifact of the freeze-fracture and etching process. Clearly the lipid environment or the absence or presence of 4M NaCl in these aqueous medium does not affect the integrity of the these 10nm diameter particles, implying (if they really are oligomeric structures) protein-protein interactions within the bilayer core to be important in packing and organising the individual 26,000Da subunits into groups of nine or twelve. In this case the role of the purple membrane lipids would appear solely to promote an ordered aggregation of these particles into the hexagonal para-crystalline lattice of purple membrane.

In conclusion, freeze-fracture electron microscopy data reveals similar bacteriorhodopsin particle distributions in DMPC bilayers at temperatures above the phase transition, irrespective of the presence or absence of endogenous purple membrane lipids. In conjunction with ESR boundary lipid analysis (Chapter 3) and C.D. results (Cherry *et al.*, 1978) it would appear that in DMPC bilayers, whether the endogenous purple membrane lipids removed or present, the bacteriorhodopsin exits as monomers at temperatures above the main phase transition temperature. Furthermore, in DMPC bilayers with all the endogenous purple membrane lipids removed, the protein dispersion properties are independent of vesicle protein content as shown by freeze-fracture electron microscopy and the linear dependence of the a- and b-methylene segment deuterium NMR quadrupole splittings on protein content (Chapter 3).

Chapter 5.

Bacteriorhodopsin/DMPC interactions in vesicles produced by nsTP mediated addition of DMPC to purple membrane.

5.I). Introduction.

In Chapter 1, a novel detergent-free method was described for producing DMPC lipo-protein complexes in order to study protein-lipid interactions. The technique used bovine non-specific transfer protein (nsTP) to promote transfer of selectively headgroup deuterated DMPC into natural membranes. Two biological membrane systems were judged as particularly suitable for this form of labelling, since they contain a major species of integral protein. In sucrose-density-gradient-purified purple membrane, the integral protein is exclusively the 26,000Da bacteriorhodopsin molecule (Oesterhelt & Stoeckenius, 1974). In erythrocyte ghosts, there are two major integral membrane proteins - band 3 and glycophorin. Another attractive feature of these two natural membrane systems is that numerous biophysical studies have been performed on band-3 (Cherry, 1979 for review; Nigg & Cherry, 1979; Dempsey *et al.*, 1986) and bacteriorhodopsin (Cherry *et al*,1977, 1978, 1980; Heyn *et al.*, 1981.a and b) relating to the dispersion/aggregation properties of these two integral membrane proteins in a variety of lipid environments.

One method used to study the aggregation states of integral membrane proteins is to measure the rotational diffusion coefficients for the protein molecules themselves. The time dependent decay of the absorption anisotropy for eosin-5-maleimide labelled band-3 in erythrocyte ghost membranes at 37°C was interpreted in terms of two different populations of band-3 with different rotational mobilities (Nigg & Cherry, 1979); one slowly rotating and the other an order of magnitude faster. The time-dependent decay of the absorption anisotropy became progressively less as the temperature is lowered from 45 to 1°C due to a change in the equilibrium between fast and slowly rotating populations of band-3. The slowly rotating species became

increasingly dominant as the temperature is reduced, implying a temperature dependent aggregation of the band-3 molecules. At higher temperatures the smallest units were demonstrated to be dimers as reaction with copper-phenathrolone which covalently links band-3 into dimers produced no change in rotational motion on either the fast or the slowly rotating components. Furthermore no change in rotational motion was observed when spectrin and actin were removed from the ghost membrane; supporting the absence of a direct association between band-3 and spectrin.

The aggregation/dispersion properties of bacteriorhodopsin reconstituted into DMPC bilayers have been extensively studied by measuring rates of rotational diffusion of the protein and also by circular dichroism studies (as reviewed in the Introduction to this thesis). In these DMPC/bR systems, all the endogenous purple membrane lipids were retained. From Chapters 3 & 4 (and references cited therein) it is apparent that removal of the endogenous purple membrane lipids considerably alters the aggregation/solubility properties of the protein in DMPC bilayers. In particular the absence of the purple membrane lipids in DMPC bilayers appears to inhibit the low-temperature crystallization of the protein-particles into the hexagonal arrays, characteristic of purple membrane. It would thus seem that the purple membrane lipids have special properties that promote the crystallization.

Some 90% of the purple membrane lipids are polar lipids while the remaining 10% are the neutral isoprenoid derived compounds (Kates, 1978). The polar lipids include the phospholipids and the glycolipid sulphate. All the polar lipids are negatively charged to varying degrees at the polar headgroup moieties. Of the phospholipids the major species is 2,3-di-O-phytanyl-*sn*-glycero-1-phosphoryl-3'-*sn*-glycerol-1'-phosphate (PGP), which accounts for 52% of the total lipid (61% of the polar lipids) and has the potential to bear three negative charges. This is a major difference to DMPC, the phosphocholine headgroup of which is zwitterionic and carries a permanent positively charged N,N,N-tri-methylammonium moiety in addition to the negative phosphate group. The purple membrane phospholipids are different from the synthetic lipid 1,2-dimyristoyl-glycero-3-phosphocholine (DMPC), not only in headgroup

composition, but also in the alkyl group chain structure. The alkyl chains of the purple membrane lipids are derived from isoprenoid units and are saturated C-16 chains with a methyl group every four carbons (Kates, 1978). Furthermore the alkyl groups are linked to the glycerol backbone by ether linkages in contrast to the ester linked acyl chains of DMPC.

Control of the packing and dispersion properties of the protein particles may be mediated through the saturated isoprenoid alkyl chains in the bilayer core or through the headgroup moieties, or both. One mechanism for packing the protein particles into the hexagonal two-dimensional array of purple membrane may involve ionic bridges between the negative charges on the polar lipid headgroups and basic residues at the protein surface. The ether linked phytanyl chains may also facilitate dispersion of the protein as monomers into DMPC bilayers above the phase transition; their branched structures matching the hydrophobic regions of the protein. In particular the methyl sidegroups could be visualized as filling crevices in the sides of the α-helices.

In Chapter 2 (this present work), high resolution ^{31}P-NMR analysis of the phospholipid composition of the complexes produced by nsTP mediated addition of exogenous DMPC revealed that between 76 and 86% of the endogenous purple membrane phospholipids are retained. These complexes therefore provide a system by which the deuterium and phosphorus-31 NMR results obtained, can be compared with those from which all the purple membrane lipids have been removed. In this chapter, ^{2}H-NMR is used to investigate to temperature dependent changes in aggregation properties of bacteriorhodopsin in DMPC systems with most of the endogenous purple membrane lipids retained. For headgroup-deuterated DMPC systems reconstituted by detergent techniques (Dempsey *et al.*, 1986) with band-3, the measured quadrupole splittings were found to decrease significantly on heating relative to those measured from the protein-free lipid dispersions. This was interpreted in terms of a reversible temperature dependent aggregation/dispersion of the band-3 trimers. In contrast the measured quadrupole splittings from DMPC/rhodopsin systems were found to be independent of temperature above the phase transition (Ryba et al., 1986), supporting

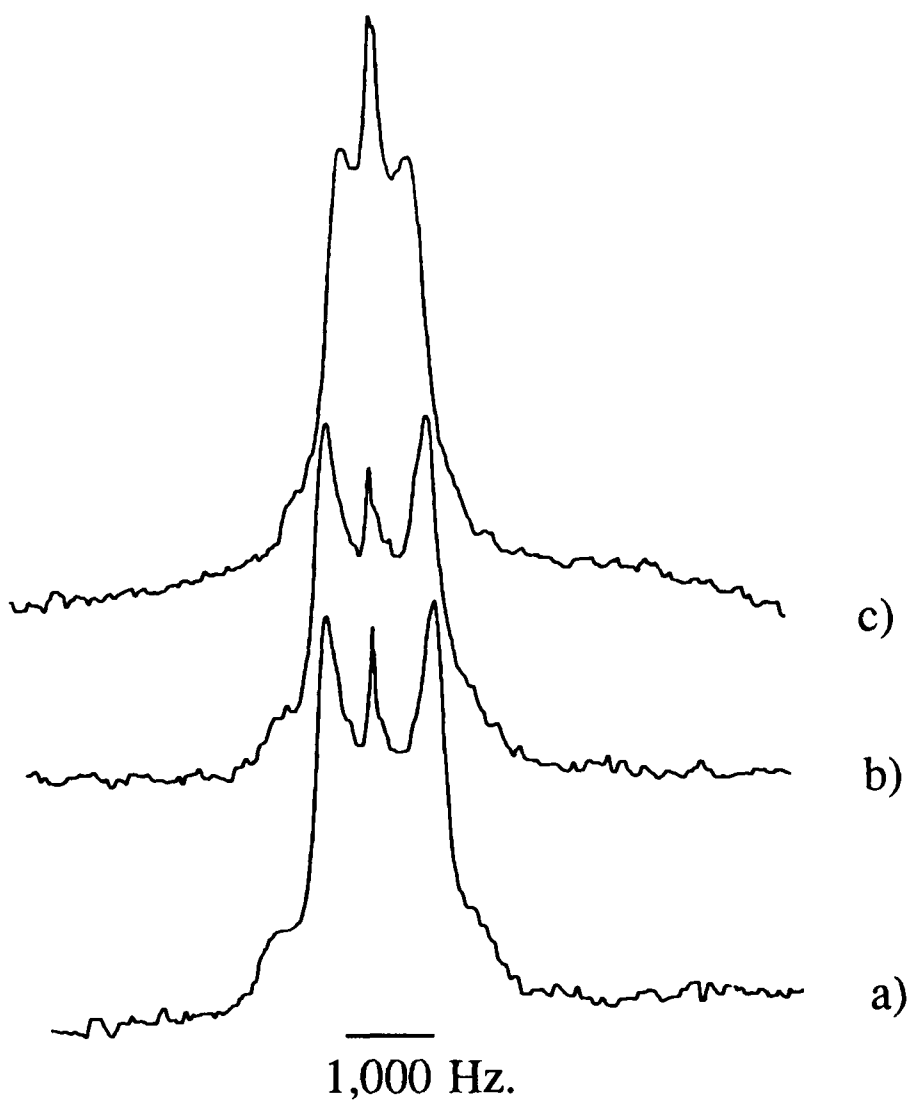


Fig.5.1. Deuterium-NMR spectra (46.1 MHz.) of DMPC-d_9 added to erythrocyte ghosts by nsTP. Spectra recorded at; a) 24°C; b) 27°C; and c) 42°C.

no temperature dependent change in aggregation state of the protein.

In addition it is of interest to contrast the lipid-protein interaction conclusions yielded from the nsTP technique, which is an entirely detergent free method, with those already published for complexes reconstituted from detergent-solubilized protein mixtures that retained the purple membrane lipids (Cherry *et al.*, 1978; Heyn *et al.*, 1981a).

5.II). Methods. Deuterated DMPC labelled purple membrane vesicles and erythrocyte ghosts were prepared as described in Chapter 1. All deuterium and phosphorus-31 NMR spectra and TEMPO data were recorded as described in Chapter 3.

5.III). Results.

A). nsTP-labelled ghosts.

i) **Deuterium NMR.** *Broadline deuterium-NMR spectra of DMPC-d_9 in erythrocyte ghosts.* Representative deuterium NMR spectra recorded at a variety of temperatures above that of the main phase transition from the choline γ-methyl CD_3 groups of DMPC-d_9 incorporated into the erythrocyte ghost lipid bilayer by nsTP are shown in Fig.5.1. At all temperatures well-resolved quadrupole splittings are displayed, although on increasing the temperature from 24 to 42°C, the spectral anisotropy is reduced. At 42°C the quadrupole splitting from the ghost powder pattern is significantly reduced in magnitude ($\Delta\nu_{q(obs)}$ = 800 Hz) compared to that of pure DMPC-d_9 ($\Delta\nu_{q(obs)}$ = 1150 Hz; taken from Dempsey *et al.*, (1986)) at a similar temperature. The spectra also show an isotropic component which may be from donor SUVs that were not removed by the sucrose density gradient.

Effect of temperature on the measured quadrupole splittings. Plotting the quadrupole splittings obtained from DMPC-d_9 in the erythrocyte ghost membranes as a function of temperature (Fig.5.2.b) reveals a significant decrease in magnitude relative to those obtained for protein-free DMPC-d_9 dispersions (Fig.5.2.a) on increasing the

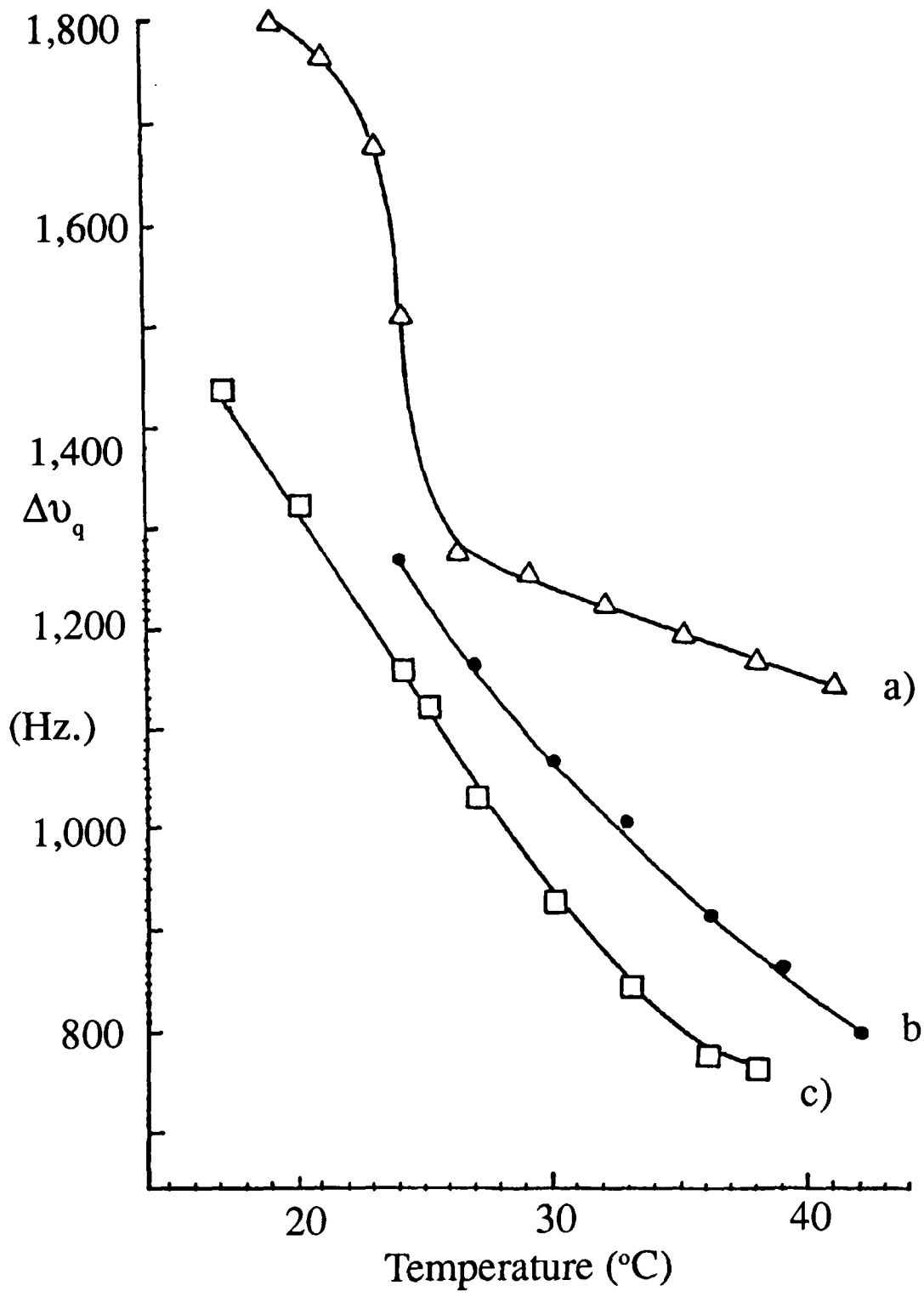


Fig.5.2. Temperature dependence of measured quadrupole splitting from DMPC-d_9 added to erythrocyte ghosts by nsTP (b), relative to those of protein-free lipid (a) and detergent reconstituted DMPC-d_9/ band-3 complex (c) of protein/lipid ratio 1:1.4 (w/w). Data for (a) and (c) taken from Dempsey *et al* ., 1986.

temperature above the phase transition. Near the phase transition of protein-free DMPC, the quadrupole splittings for the ghosts system are similar to those measured for pure lipid. On warming to higher temperatures, however, the ghost quadrupole splittings display a greater sensitivity to temperature than those for protein-free lipid. It should be noted that the temperature profile displayed by the ghosts is similar to that obtained for the quadrupole splittings of a band-3/DMPC-d_9 detergent reconstituted complex (Fig.5.2.c) of lipid-protein ratio (w/w) 1:1.4 (results taken from Dempsey *et al.*, 1986).

For the band-3/DMPC reconstituted complexes, the magnitude of the reduction observed in the measured quadrupole splittings is dependent on the protein content of the vesicle (Dempsey *et al.*, 1986). Neither the final lipid/protein ratio, the amount of DMPC incorporated, nor the phospholipid headgroup composition of the nsTP-modified ghosts was determined. Also, the band-3/DMPC detergent reconstituted vesicles do not contain spectrin or glycophorin. Thus a direct comparison cannot be made with the detergent reconstituted results.

Temperature dependence of quadrupole splittings from DMPC-d_9 in erythrocyte ghost membranes is interpreted in terms of a change in the aggregation/dispersion properties of the integral membrane proteins. The temperature dependent decrease in the observed quadrupole splittings for the band-3/DMPC reconstituted complexes was interpreted to demonstrate a reversible temperature dependent self-association of the band-3 protein particles within the plane of the bilayer (Dempsey *et al.*,1986). Lipid directly in contact with the protein surface i.e. boundary lipid, is postulated to exhibit a small quadrupole splitting of magnitude approaching zero, due to disordering of the lipid headgroup by the protein. In contrast, bilayer lipid exhibits a large well defined residual quadrupole splitting (Fig.3.4a). Assuming a fast two site exchange model for the boundary and bulk bilayer lipid species, the deuterium-NMR spectra of protein-lipid systems exhibit only a single component, which is a time-averaged spectrum of the boundary lipid and bulk bilayer lipid. Thus the effect of increasing the protein surface available for lipid interaction is to increase the contribution to the observed spectrum

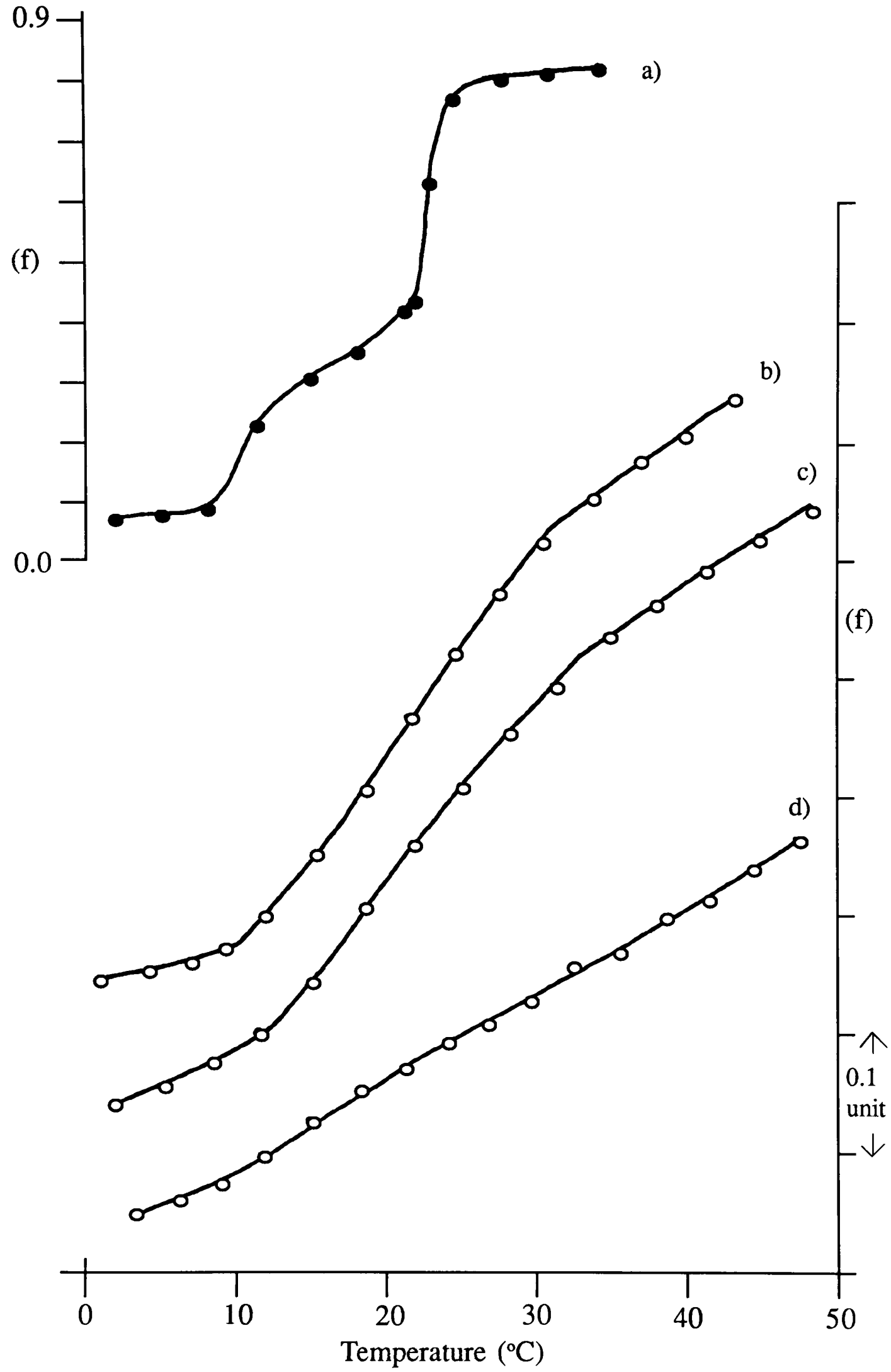


Fig.5.3. Phase transitions for nsTP-produced DMPC/purple membrane complexes as determined by TEMPO partitioning. Apparent partition coefficient scale (f) for pure DMPC (a) is half that for protein complexes of DMPC/PMPL/bR mole ratios; b) 109:7.8:1; c) 72:7.3:1; d) 21:7.6:1.

from the boundary lipid and so reduce the measured quadrupole splitting. One mechanism that would effectively expose more protein surface to lipid is dissociation of band-3 aggregates into dimers within the plane of the membrane as reported by Nigg & Cherry, (1979).

The deuterium NMR results presented in this work are interpreted to demonstrate a dispersion of the integral proteins (band-3 and glycophorin within the erythrocyte ghost bilayer on increasing the temperature.

B). nsTP-labelled purple membrane.

i) **Gel-to-liquid crystal phase transitions for nsTP-produced complexes as determined by TEMPO partitioning.** The apparent coefficients determined for the partitioning of TEMPO into the hydrophobic region of the lipid bilayer are plotted as a function of temperature (Fig.5.3) for the 109:7.8:1, 72:7.3:1 and 21:7.6:1 mole ratio DMPC/PMPL/bR complexes, produced by the nsTP method. The ranges and midpoint temperatures of the main phase transition for the higher lipid complexes are presented in Table 1.

Table 1. Data on main gel-to-liquid crystalline phase transition for nsTP-produced DMPC/PMPL/bR complexes.

DMPC/PMPL/bR	Temperature (°C).		
mole ratio	main transition	range	mid-point
109:7.8:1	11 - 31	10	21
72:7.3:1	12 - 33	11	22

The 72:7.3:1 and 109:7.8:1 mole ratio complexes exhibit detectable main gel-to-liquid crystalline transitions (Fig.5.3.b and c) which are significantly broadened when

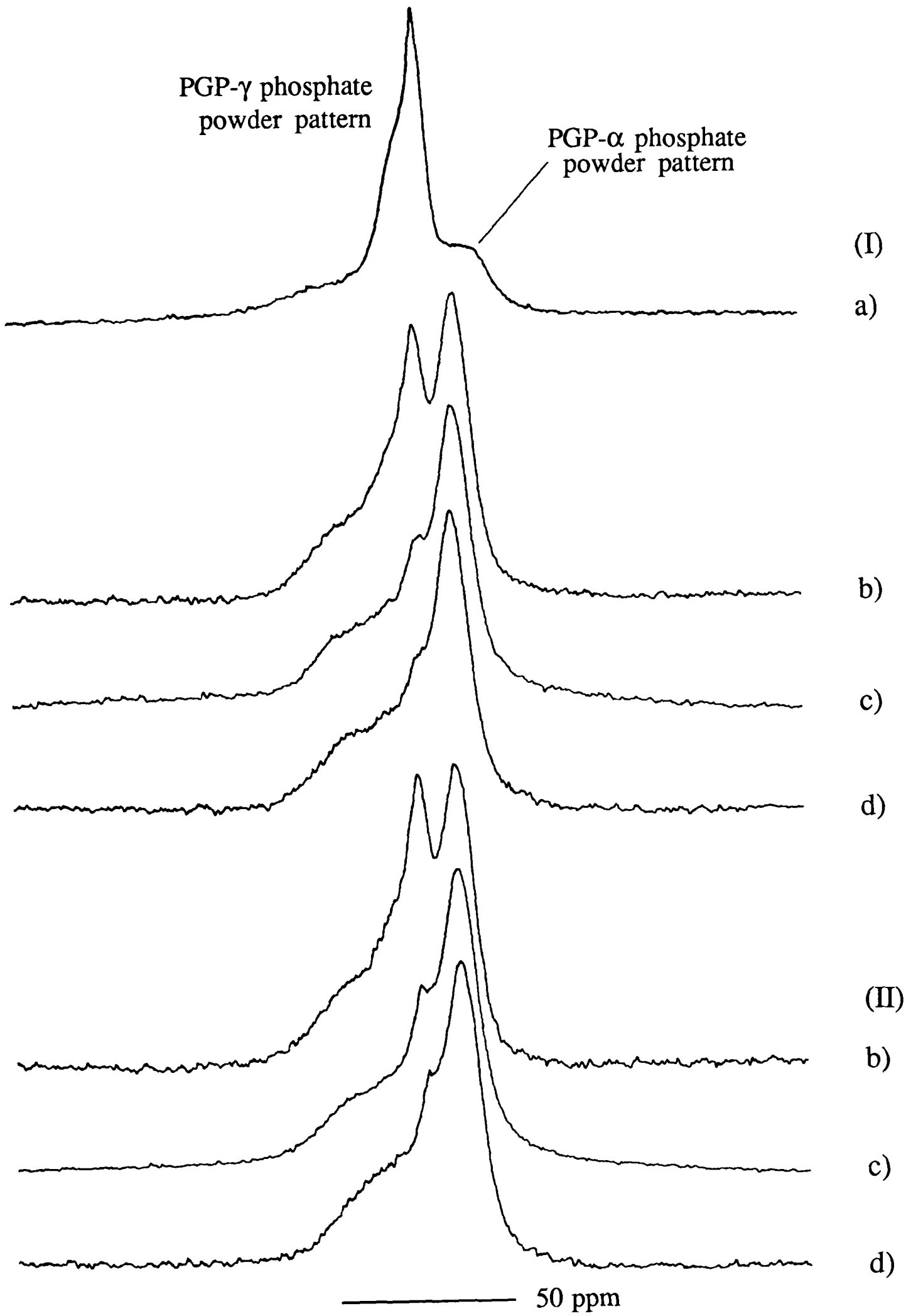


Fig.5.4.

^{31}P-NMR spectra (145.9 MHz) of purple membrane (a) and DMPC/ purple membrane complexes produced by nsTP-mediated DMPC transfer of DMPC/PMPL/bR mole ratios; b) 21:7.6:1; c) 72:7.3:1; d) 109:7.8:1; at 33°C (I) and 45°C (II). Complexes loaded into NMR tube as a pellet from 10 mM Tris/HCl, pH 7.5.

compared to the protein-free DMPC. However, the estimated midpoints for the main transitions are slightly lower than that observed for pure lipid, occurring at approximately 21°C (Table 1).

The range of the main phase transition appears to be broadened with increasing protein content. For the very high protein content 21:7.6:1 DMPC/PMPL/bR mole ratio complex, main phase transition of DMPC is broadened to such an extent, that partitioning of TEMPO into the complex increases linearly with temperature and no definable limits can be detected. For all three complexes the pre-transition observed for protein-free DMPC (Fig.5.3.a) at approximately 10°C is abolished.

ii) **Broadline phosphorus-31 NMR.** In this section broadline phosphorus-31 NMR spectra are presented for the DMPC/PMPL/bR complexes produced by the nsTP method. The effect of protein content, temperature, the viscosity of the sample in the NMR tube and the effect of saturated sodium chloride in the aqueous medium are described. Also for the high protein-content complex the spin-lattice relaxation times for both the α-phospholipid phosphates and the γ-phosphate of *H.halobium* PGP are determined.

Phosphorus-31 NMR spectra are two component but typical of phospholipids in a bilayer conformation. Representative broadline ^{31}P-NMR spectra (recorded at 145.9 MHz) for the 21:7.6:1, 72:7.3:1, and 109:7.8:1 mole ratio DMPC/PMPL/bR complexes after pelleting by centrifugation (100,000g; 30min; 15°C) from 10mM Tris/HCl, 1mM EDTA, pH 7.5, are presented in Fig.5.4, along with that of purple membrane itself (a). All samples were loaded into the NMR tube as a semi-solid pellet. The spectra demonstrate the phospholipids in the nsTP-produced complexes to be organized into bilayer structures at both 33 and 45°C. As described in the Introduction to this thesis, the α-phosphate powder pattern of purple membrane (Fig.5.4.a) demonstrates an extreme magnetic ordering, in that the intensity from the 90° orientation is significantly reduced relative to that of the 0° orientation (Seelig *et al.*, 1985). Incorporation of DMPC appears to oppose the ordering from the α-helix dipole

moments as judged from the increase in intensity of the 90° orientation, relative to that of the 0° orientation.

There is in each of the spectra from the ^{31}P-NMR spectra from nsTP-produced DMPC/bacteriorhodopsin complexes, in addition to the main bilayer component, a second distinct component that could be incorrectly to small phospholipid vesicles undergoing rapid isotropic motion (Cullis & de Kruijff, 1979; Burnell *et al.*, 1980). As shown in Fig.5.4, increasing the temperature from 33 to 45°C, enhances the resolution of this second component. The magnitude of the second component with respect to that of the main α-phosphate component, is directly proportional to the protein content of the vesicles, being very prominent in the 21:7.6:1 spectrum but almost insignificant in the 109:7.8:1 spectrum. This component, however, does not arise from time-averaging of the spectral anisotropy by rapid tumbling of small diameter vesicles, but instead represents the signal from the less motionally restricted γ-phosphate moiety of the major endogenous purple membrane phospholipid species, PGP. In purple membrane itself (Fig.5.4.a), red membrane (Fig.4 Introduction to this thesis) and pure PGP bilayers (Ekiel *et al.*, 1981), the γ-phosphate component is seen to account for a major part of the spectrum. Thus, both broadline and high resolution phosphorus-31 spectra (Chapter 2) detect the presence of the endogenous purple membrane phospholipids.

The phospholipid α-phosphate powder patterns displayed in spectra recorded at 33°C and 45°C for all protein contents are seen to be single component (Fig.5.4). This is consistent with:

a) the DMPC being incorporated into the purple membrane lipid bilayer, itself,

b) the absence of patches of bacteriorhodopsin crystallized into hexagonal purple membrane patches at high temperatures; the existence of purple membrane patches within the DMPC bilayer, would give rise to two component spectra, assuming a little exchange of the purple membrane PGP mediating the crystallisation with the bulk phase DMPC,

and c) a fast exchange between lipid in contact with the protein and bulk bilayer phase lipid.

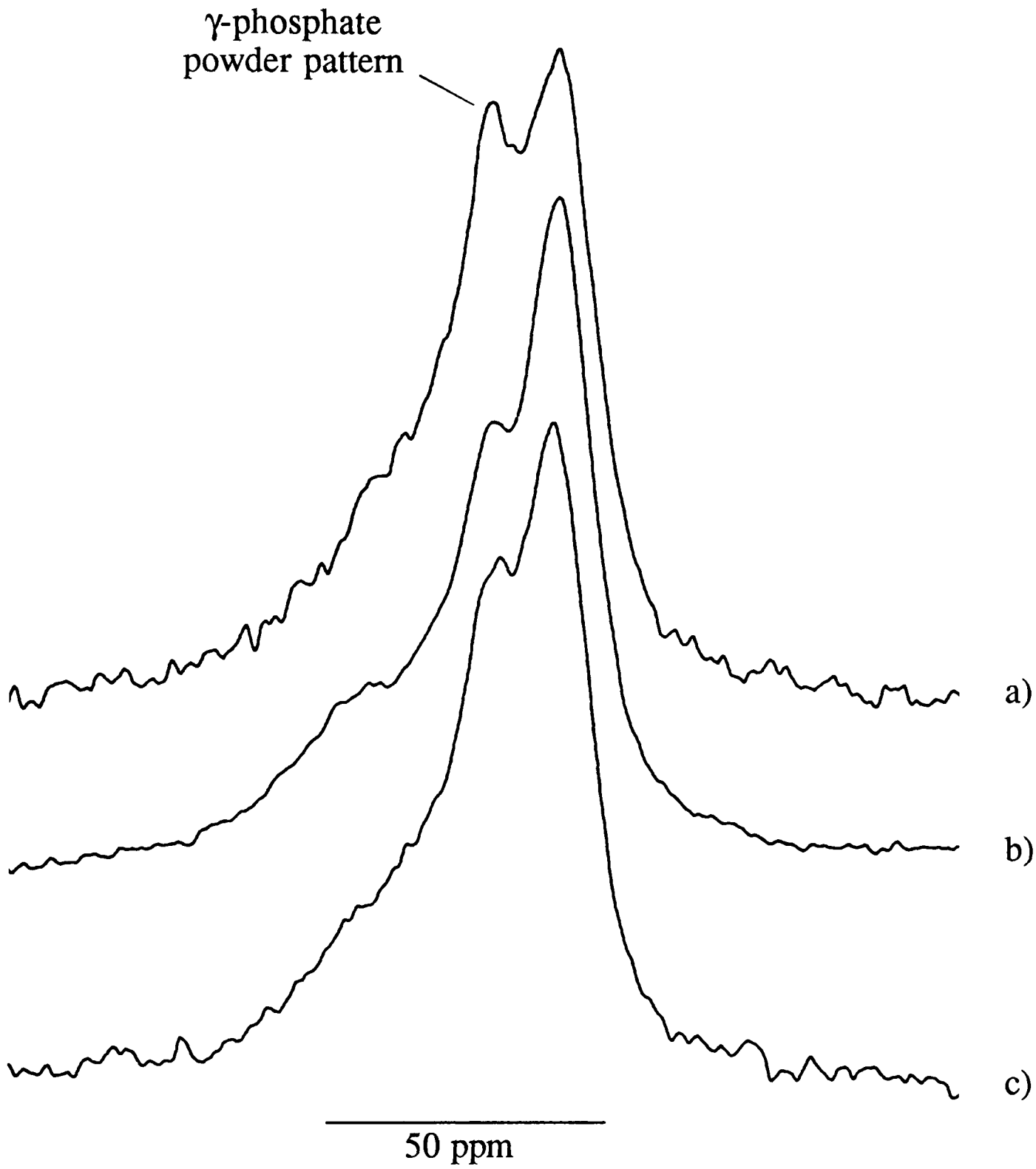


Fig.5.5. Broadline ^{31}P-NMR spectra (121.4 MHz) of nsTP-produced DMPC-d_9/purple membrane complexes of total lipid phosphate/bR mole ratios; a) 31:1, suspended in deionised water; b) 60:1, pelleted from deionised water; c) 65:1 suspended in saturated NaCl.
Spectra recorded at 33°C.

Effect of the presence of saturated NaCl in the aqueous environment on ^{31}P-NMR spectra. Fig 5.5 displays spectra (recorded at 121 MHz) for the 31:1 and 60:1 mole ratio (total lipid phosphate/bR) nsTP-produced complexes in deuterium depleted water alone and the spectrum for the 65:1 mole ratio complex suspended in saturated NaCl. The ionic strength of the aqueous environment does not appear to alter the conformational properties of the phospholipids in bacteriorhodopsin-containing bilayers.

Effect of vesicle packing on the phosphorus-31 NMR spectra. The 60:1 mole ratio sample (Fig.5.5.b) was loaded into the NMR tube as a solid pellet after centrifugation (100,000g; 30 min; 15°C), while the 31:1 (Fig.5.5.a) and 65:1 (Fig.5.5.c) mole ratio samples were suspended in 0.5cm^3 of aqueous buffer. The semi-solid pellet sample spectrum (Fig.5.5.b) displays a larger c.s.a. by ~4 ppm and a better defined bilayer lineshape in comparison to the spectra from the suspension samples. This may reflect an averaging by some degree of the spectral anisotropy by the rapid tumbling motions of small vesicles in the suspension sample. For small spherical vesicles, two diffusion processes contribute to averaging of the spectra anisotropy of broadline phosphorus-31 NMR spectra: rapid Brownian tumbling motion of the entire vesicle (characterised by the diffusion coefficient D_t) and lateral diffusion of lipids around the vesicle (with diffusion coefficient D_{diff}). The averaging of the spectral anisotropy is related to the correlation time τ_c given by the equation:-

$$1/\tau_c = 6/R^2(D_t + D_{diff})$$

where $D_t = kT/8r\Pi\eta$ and r is the radius of the vesicle and η the viscosity of the medium (Burnell *et al.*, 1980). Restriction of vesicle tumbling (D_t) due to the increased viscosity η in the solid pellet sample (Fig.5.5.b) may serve to oppose the averaging of the spectral anisotropy.

Effect of protein content on the magnitude of the phosphorus-31 c.s.a.s. The phosphorus-31 spectra presented in Fig.5.4 were all obtained from solid pellet samples and the magnitudes of the c.s.a.s measured for the 109:7.8:1, 72:7.3:1 and 21:7.6:1

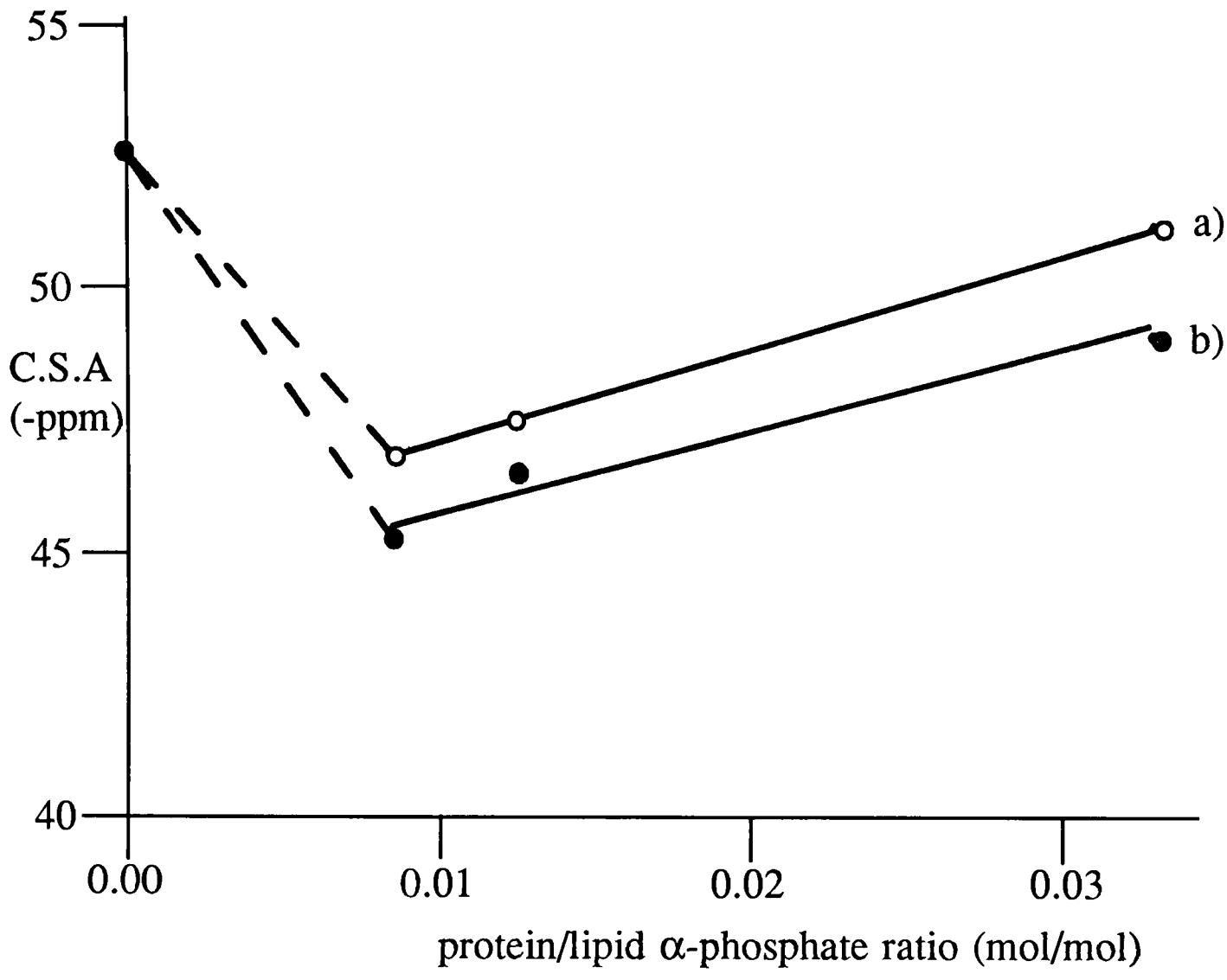


Fig.5.6.
Effect of protein content (moles bR/mole of phospholipid α-phosphate i.e. DMPC + PMPL) on the measured ^{31}P-NMR C.S.A.S for the nsTP-produced DMPC/purple membrane complexes at; a) 33°C; and b) 45°C. Samples loaded into NMR tube as a semi-solid pellet.

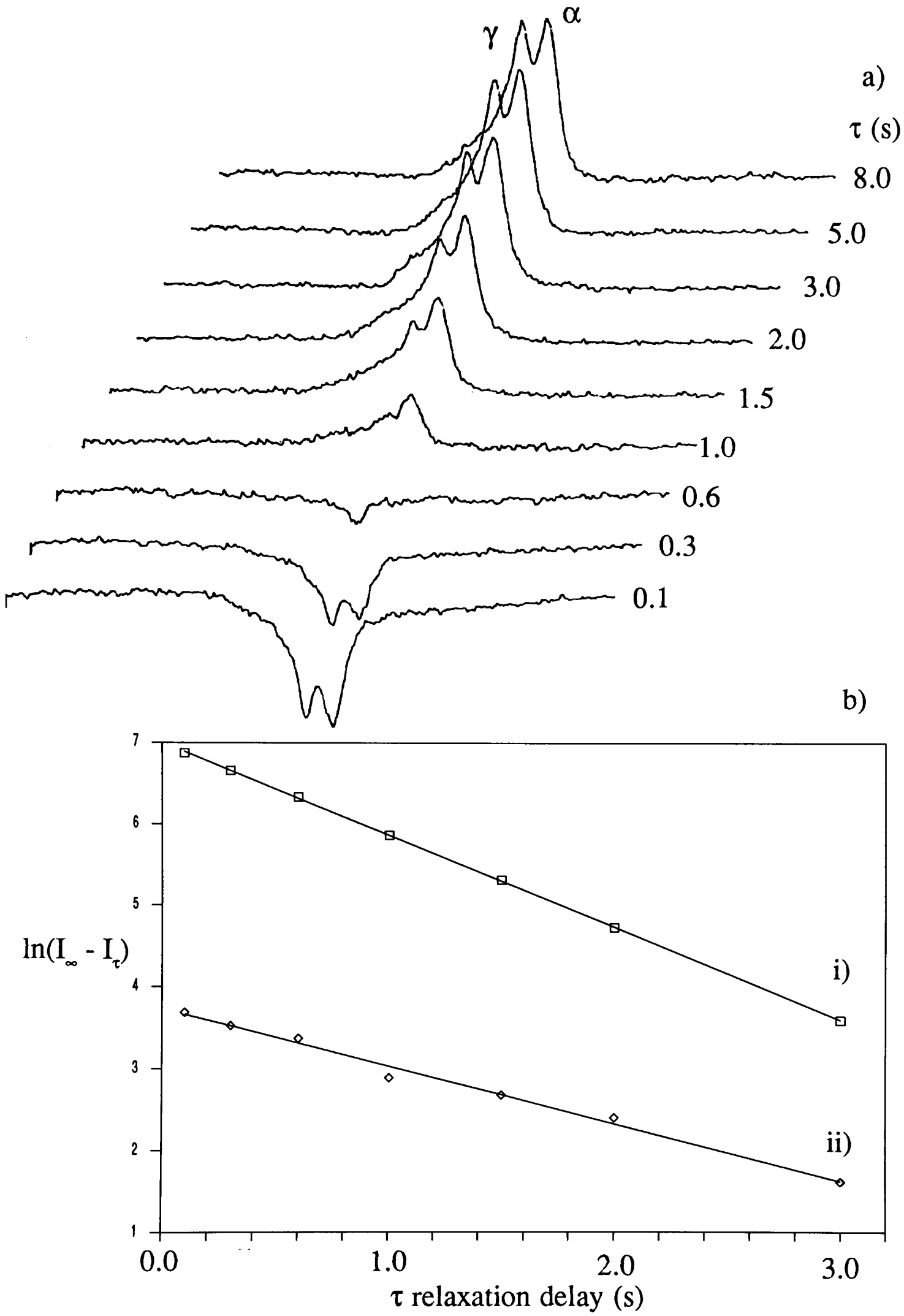


Fig.5.7. Broadline phosphorus-31 NMR spin-lattice (T_1) relaxation time determination by inversion recovery method for the 21:7.6:1 DMPC/PMPL/bR mole ratio complex at 33°C;

a) stack plot of spectra;

b) logarithmic plot of data

i) DMPC and PGP α-phosphates (T_1 = 0.88s)

ii) PGP γ-phosphate (T_1 = 1.42s)

mole ratio DMPC/PMPL/bR complexes are less than that of -52.5 ppm displayed by protein-free DMPC dispersed in buffer. This could either represent an averaging of the spectral anisotropy by residual rapid tumbling of the small vesicles produced by the nsTP method or may reflect a disruption of the ordering within the phosphocholine headgroups at the bilayer surface in protein-free lipid. The measured c.s.a.s at both 33 and 45°C are shown to exhibit a linear dependence on the vesicle protein content (Fig.5.6); increasing the lipid content of the nsTP-produced vesicle having the effect of decreasing the magnitude of the c.s.a..

Incorporation of 109 DMPC molecules per bacteriorhodopsin monomer by nsTP reduces the magnitude of the measured c.s.a. by 4.7 ppm, at 33°C, relative to that measured from the complex with only 21 DMPC molecules added per 26,000Da bR monomer. Similar trends were observed for the phosphorus-31 c.s.a.s displayed by the DMPC/bR complexes with all the endogenous purple membrane lipids removed (Chapter 3) and can be interpreted in terms of an ordering effect mediated by the protein on adjacent lipids. Alternatively the trend may reflect the increase in lipid viscosity as the protein content is increased (Cherry *et al.*, 1977).

Dynamics of the phosphate moieties in the nsTP-produced complexes. Fig.3.7.a exhibits a stack plot spin-lattice relaxation time (T_1) determination by the inversion recovery method (see Introduction) for the 21:7.6:1 DMPC/PMPL/bR mole ratio complex at 33°C. Logarithmic plots of the intensity data for the 90° orientations (Fig.3.7.b) against the τ delay time reveal straight lines which is consistent with single component T_1 values. As in the purple membrane itself (data not presented), the γ-PGP phosphorus-31 powder pattern for the 21:7.6:1 DMPC/PMPL/bR mole ratio complex has a longer spin-lattice relaxation time (1.42 s) than the lipid α-phosphate powder components (0.88 s). This implies a faster rate of segmental motion for the γ-phosphate moiety than for the more rigid backbone α-phosphate and is consistent with deuterium NMR data from DMPG-d_5 and DPPG-d_5 (Chapter 6 this thesis; Wohlgemuth *et al.*, 1980) which shows an increase in segmental amplitude of motion with increasing number of segments from the glycerol backbone. It should be noted that the α-

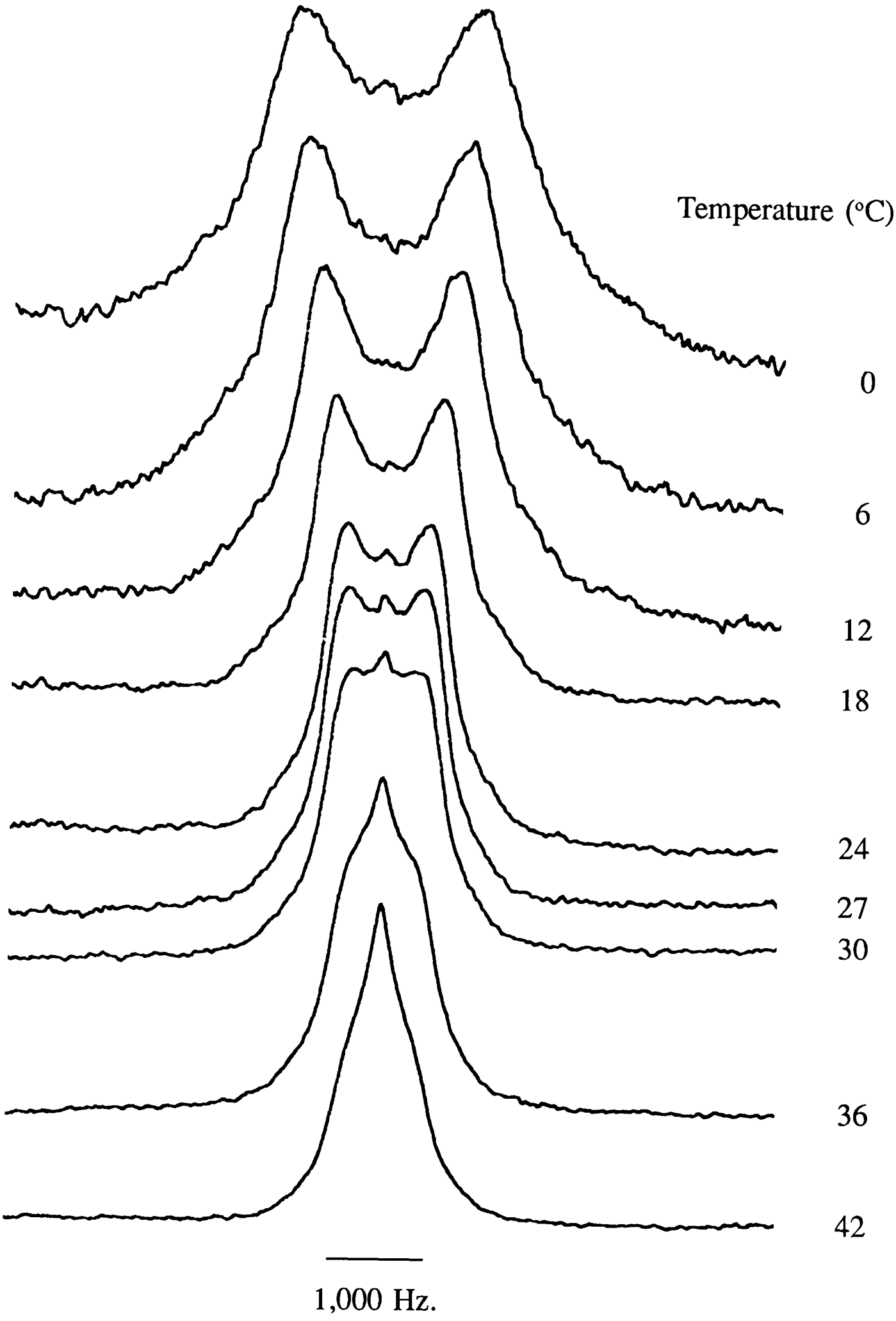


Fig.5.8. Broadline ^{2}H-NMR spectra (46.1 MHz) for the choline γ-methyl groups of DMPC in nsTP-produced DMPC-d_9/purple membrane complex (65:1 total lipid phosphate/bR mole ratio) showing the marked temperature dependence of the quadrupole splitting. Vesicles suspended in deuterium-depleted water.

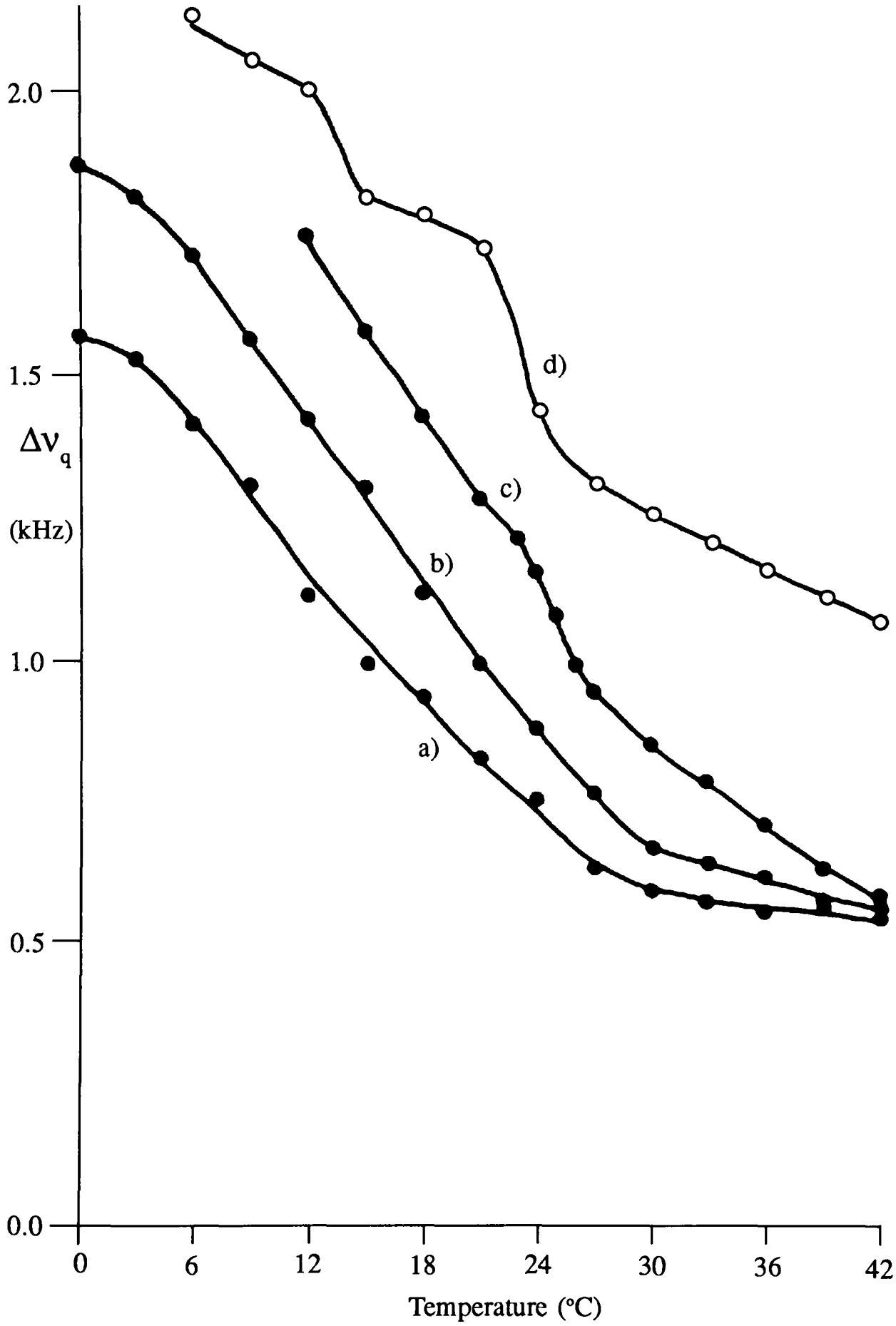


Fig.5.9. Temperature dependence of quadrupole splittings for the choline γ-methyl groups of DMPC-d_9 in the nsTP-produced complexes of total lipid phosphate/bR mole ratios; a) 31:1; b) 65:1; c) 152:1 and d) protein-free DMPC dispersions.

phosphate T_1 value for the 21:7.6:1 DMPC/PMPL/bR mole ratio complex is shorter than the value of 1.02s determined for the T_1 of protein-free DMPC (Chapter 3). This may reflect a reduced rate of molecular motion for the phosphate group in the presence of high contents of bacteriorhodopsin. Due to the heterogeneous molecular composition of the α-powder pattern (26.6 mol% being PMPL α-phosphates) in the 21:7.6:1 DMPC/PMPL/bR mole ratio complex, a direct comparison with the pure DMPC or purple membrane T_1 values is difficult to interpret.

iii) **Broadline Deuterium NMR.**

Temperature dependencies of DMPC-d_9 quadrupole splittings as a means to investigate temperature-dependent aggregation/dispersion of bacteriorhodopsin. Deuterium NMR spectra recorded at 46.1 MHz for the choline γ-methyl groups of DMPC-d_9 after incorporation into purple membrane to yield a total lipid phosphate/protein mole ratio of 65:1 are shown in Fig.5.8. At low temperatures, the spectra are broadened and characteristic of protein-free lipid below the phase transition temperature, and well defined quadrupole splittings are exhibited. On warming the magnitude of the quadrupole splitting decreases considerably, until above 30°C, they exhibit a complete collapse and a central isotropic component becomes prominent. Accurate measurement of the quadrupole splitting at higher temperatures is impossible. Above 30°C, the anisotropy from the 0 deg orientations appears to be time-averaged to the extent that intensity in this region of the spectrum is smoothed out almost beyond recognition.

The measured quadrupole splittings measured for the choline γ-methyl groups of DMPC-d_9 in complexes of total lipid phosphate/bR mole ratios ranging from 31:1 to 152:1 and for protein-free DMPC are plotted as a function of temperature in Fig.5.9. At all temperatures the measured quadrupole splittings are smaller than for pure lipid. For the bacteriorhodopsin-containing complexes, the temperature profiles reveal plateaus at low and high temperatures. Between 6 and 30°C, however, the residual quadrupole splittings decrease rapidly with increasing temperature, relative to that of pure lipid. The mid-point temperature for the collapse was found to vary with lipid content of the

vesicle. Increasing the protein content has the effect of shifting the mid-point to lower temperatures (Table 2).

Table 2. Estimated mid-point temperatures for temperature sensitivity of quadrupole splittings.

mole ratio of complex	estimated mid-point temperature (°C)
88:1	19.5
65:1	16.5
31:1	14.0

The marked temperature-dependent decreases in the residual quadrupole splittings of the choline γ-methyl groups relative to those of pure lipid could be interpreted as for the erythrocyte ghosts systems, thus presenting NMR evidence to confirm the reversible aggregation/dispersion properties of bacteriorhodopsin previously reported in detergent reconstituted systems (Cherry *et al.*, 1978; Heyn *et al.*, 1981a) with the endogenous purple membrane lipids retained. Below 6°C for a 71:1 (mole ratio) DMPC complex with all the purple membrane endogenous lipids retained, c.d. and rotational diffusion data (Heyn *et al.*, 1981a) indicate the bacteriorhodopsin to be aggregated. X-ray diffraction and freeze-fracture electron microscopy revealed the protein particles are organized into aggregates that have the same hexagonal structure as purple membrane (Cherry *et al.*, 1978). Since it would appear that the endogenous purple membrane lipids mediate this aggregation (Hwang & Stoeckenius, 1977 and Chapter 4), it could be argued that DMPC will be completely excluded from the protein rich areas and hence not exposed to protein surface. This is reflected in the large quadrupole splittings measured at low temperatures, that resemble those of protein-free

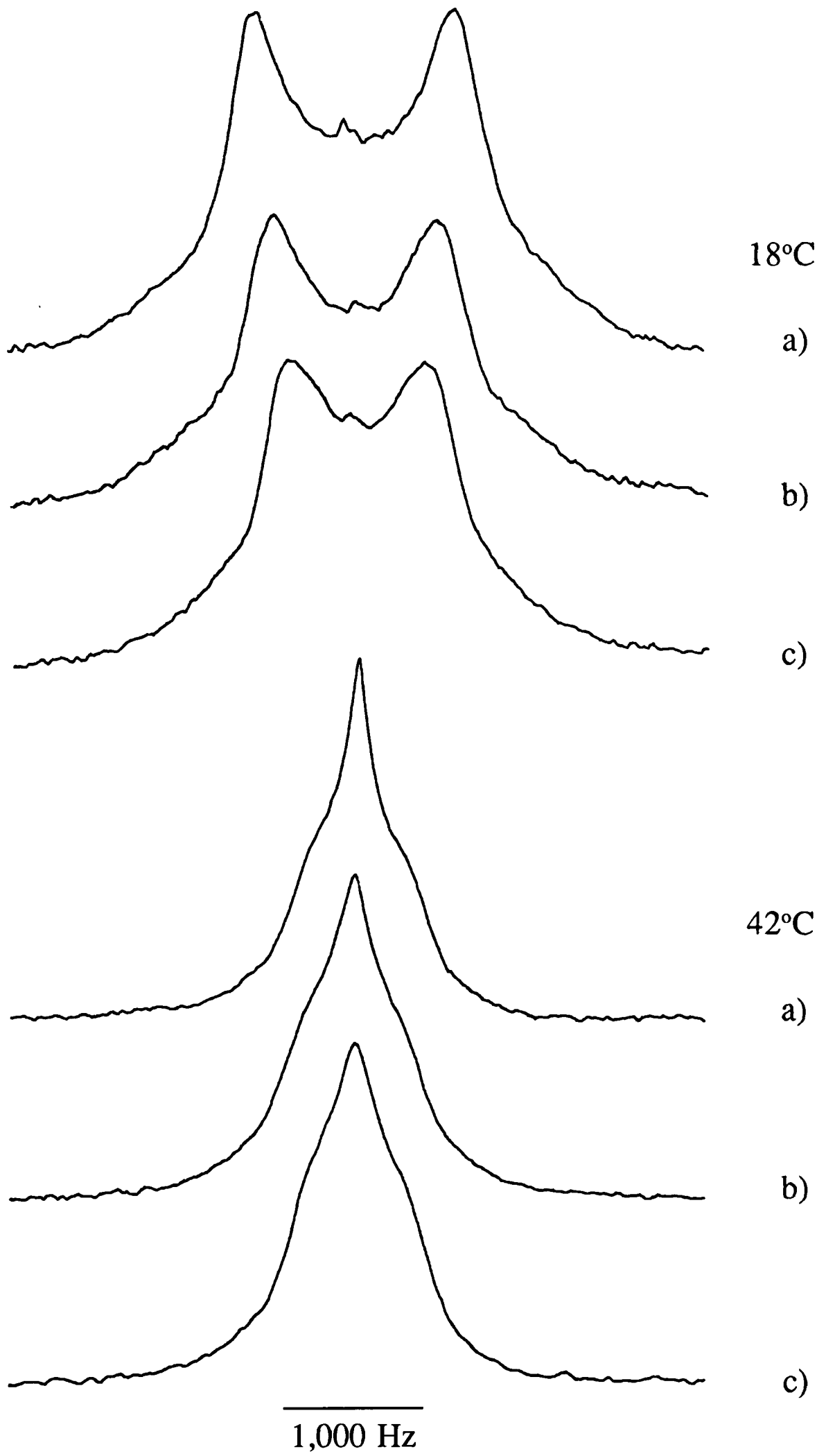


Fig.5.10. Deuterium NMR spectra (46.1 MHz) of choline γ-methyl group powder patterns from nsTP-produced DMPC-d_9/bR complexes of total lipid phosphate/bR mole ratios; a) 152:1; b) 65:1; and c) 31:1. Vesicles suspended in water alone.

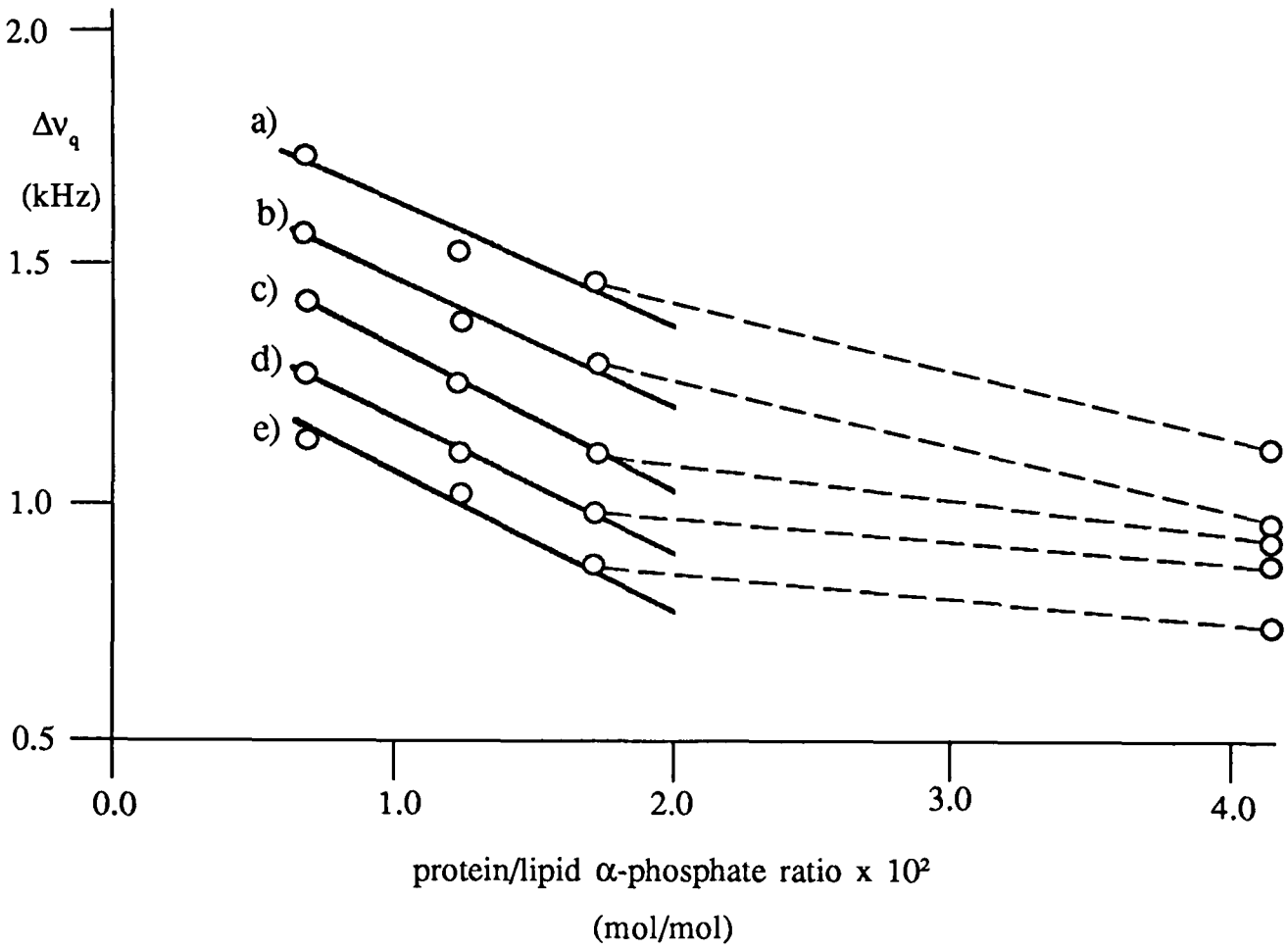


Fig.5.10.d. Deuterium NMR DMPC-d_9 quadrupole splittings measured for the 152:1, 88:1, 65:1 and 31:1 total lipid phosphate/bR mole ratio nsTP-produced complexes plotted as a function of the protein to lipid α-phosphate mole ratio at temperatures of; a) 12; b) 15; c) 18; d) 21; and e) 24°C.

lipid. As the temperature is raised so the aggregates begin to disperse. The mid-point of dissociation as determined by c.d. and protein rotational studies is 17°C for all complexes (Heyn *et al.*, 1981a). C.d. results, demonstrate the protein to be completely monomeric by 24°C in the 71:1 mole ratio complex. The increased protein surface area exposed to DMPC would account for the observed reduction in the residual quadrupole splitting of single component deuterium NMR spectra, assuming that the exchange rate between boundary lipid and free bilayer lipid is fast on the NMR time scale (i.e. ν_{ex} $>10^5$ sec^{-1}). The complete collapse of the DMPC-d_9 splittings observed for all complexes would reflect the large protein surface area presented by fully dispersed monomeric bacteriorhodopsin. Similar collapsed spectra, obtained for DMPC-d_9 reconstituted into bovine rhodopsin systems at high protein content (Ryba *et al.*, 1986), were interpreted to reflect to the monomeric nature of the protein irrespective of temperature.

Effect of protein content on the DMPC-d_9 spectra at different temperatures. Spectra for nsTP-produced DMPC-d_9/bR complexes of varying protein contents are presented in Fig.5.10 at temperatures of 18° and 42°C. At high temperatures above 36°C, the spectra and quadrupole splittings obtained for the complexes are similar and appear independent of protein-content; the spectral anisotropy of both the 90° and 0° orientations being reduced and the quadrupole splittings collapsing into a central isotropic component. At 18°C the spectra are sensitive to the protein content; the magnitude of the quadrupole splittings decreasing with increasing protein content, and the spectra appearing more broadened. Indeed at temperatures between 12 and 30°C, the quadrupole splittings are seen to be dependent on the lipid/protein ratio of the vesicle.

Stoichiometry of DMPC/bR interactions. Plots of the measured quadrupole splittings as a function of the inverse of the total lipid α-phosphate/protein ratio ($1/n_t$) for the temperatures 12 to 24°C, show that increasing the protein content reduces the measured quadrupole splitting. For the 65:1, 88:1 and 152:1 total phosphate to protein ratio complexes, the quadrupole splitting displays linear variation with $1/n_t$ at constant

temperature (Fig.5.10.d) as also seen for rhodopsin (Ryba *et al.*, 1986) and band-3 (Dempsey *et al.*, 1986) reconstituted with DMPC-d_9. At higher protein contents, however, there is a deviation from linearity and the quadrupole splittings measured for 31:1 total lipid phosphate/protein mole ratio, were found to be too large to fit the best fit line (Fig.5.10.d).

The linear dependence of the observed quadrupole splitting vs $1/n_t$ for the higher lipid content vesicles (Fig.5.10.d) suggests that the equation for a fast two site exchange model (Sixl *et al.*, 1984; Watts, 1987)):

$$\nu_{obs} = \nu_f + n_b.(\nu_b - \nu_f)/n_t$$

may be applied (derivation described in Chapter 3), where ν_b, ν_f and ν_{obs} are the quadrupole splittings for lipid in contact with protein, for lipid in protein-free lipid bilayers and that observed from a complex, respectively, and n_b is the number of boundary lipids. If a DMPC-d_9 molecule in contact with a bacteriorhodopsin molecule exhibits a quadrupole splitting of small magnitude approaching zero, i.e. $\nu_b = 0$ (Sixl *et al.*, 1984), then the number of lipids in contact with the protein, n_b, is equal to the inverse of the x-axis intercept. Best fit lines determined using the linear regression routine on LOTUS 123 for the three higher lipid content complexes (152:1, 88:1 and 65:1) at different temperatures intercepted the x-axis at values corresponding to lipid-protein ratios presented in Table 3.

Table 3. Number of boundary DMPC phospholipids determined per 26,000Da bR monomer from DMPC-d_9 quadrupole splitting data at different temperatures assuming a fast two site exchange model and a quadrupole splitting for boundary lipid of 0 Hz.

Temperature (°C)	Number of boundary lipids (n_b) per bR monomer (mol/mol)
12	13.7
15	15.1
18	18.8
21	19.1
24	19.1

From this data it is would appear that warming from 12 to 21°C, increases the number of DMPC boundary lipids from 14 per bacteriorhodopsin monomer to 19. The observed increase in the number of boundary lipids is entirely consistent with the increase in exposed protein surface area that would occur on dispersion of aggregated protein into monomers. Furthermore, the temperature for the observed increase in the number of boundary lipids coincides with the midpoint temperature (17°C) for dispersion of bR aggregates seen by C.D. and rotational diffusion studies (Cherry *et al.*, 1978; Heyn *et al.*, 1981a).

The results imply that at 24°C, the temperature at which dispersion of the aggregates is reported to be complete (Heyn *et al.*, 1981a), each monomer has 19 DMPC boundary lipids. It should be noted that this coincides with the number of boundary lipids determined by spectral subtraction of ESR data for bacteriorhodopsin in DMPC bilayers with all the endogenous purple membrane lipids removed (Chapter 3). The deviation of the experimental data from the best fit line for complexes of high

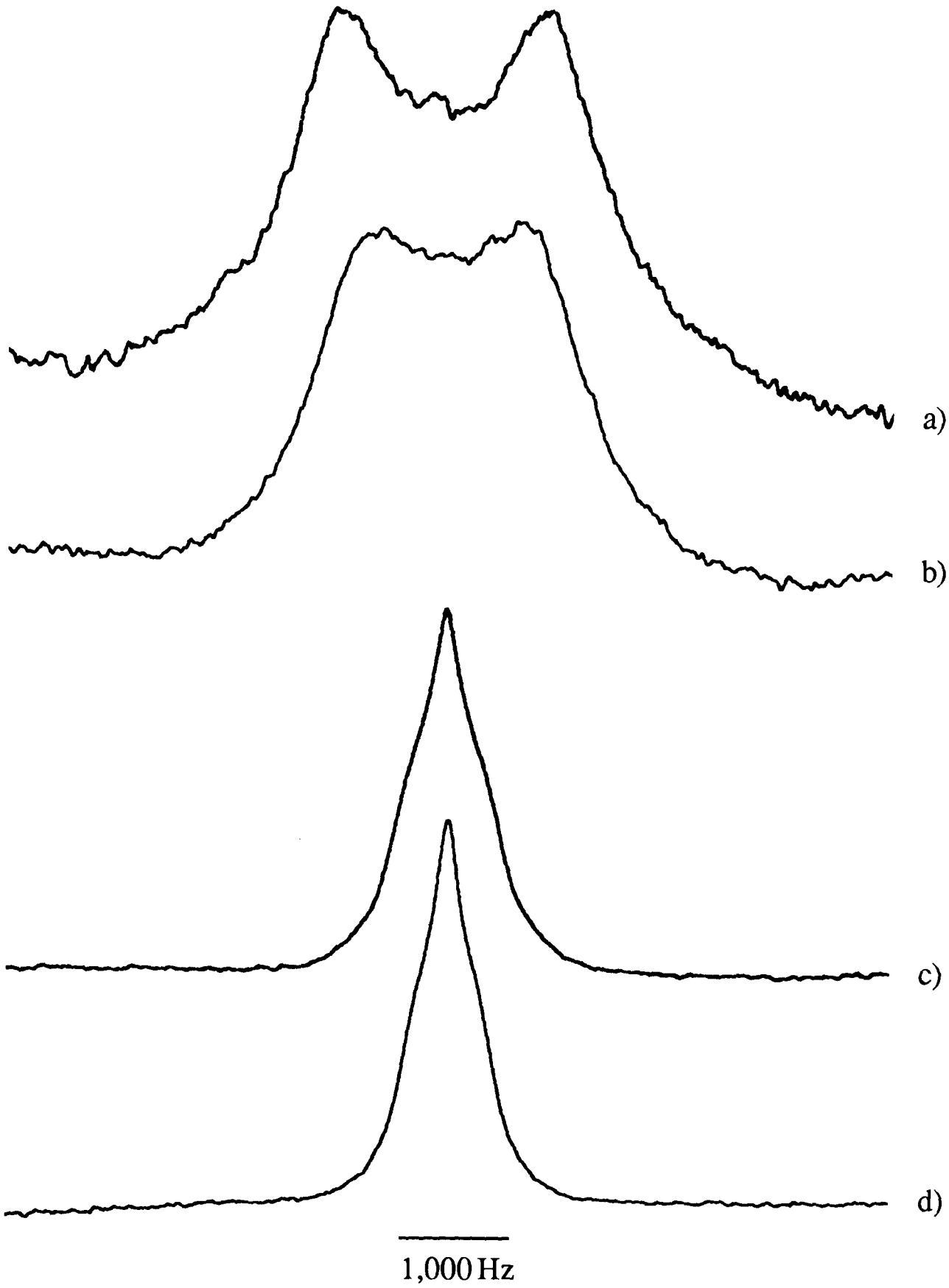


Fig.5.11. Effect of the ionic strength of the aqueous environment on the deuterium NMR spectra (46.1 MHz) recorded from the 65:1 mole ratio total lipid phosphate/bR (DMPC-d_9) complex at low and high temperatures;
a) in deuterium-depleted water alone at 0°C;
b) in saturated NaCl at 0°C;
c) in deuterium-depleted water alone at 42°C;
d) in saturated NaCl at 42°C;

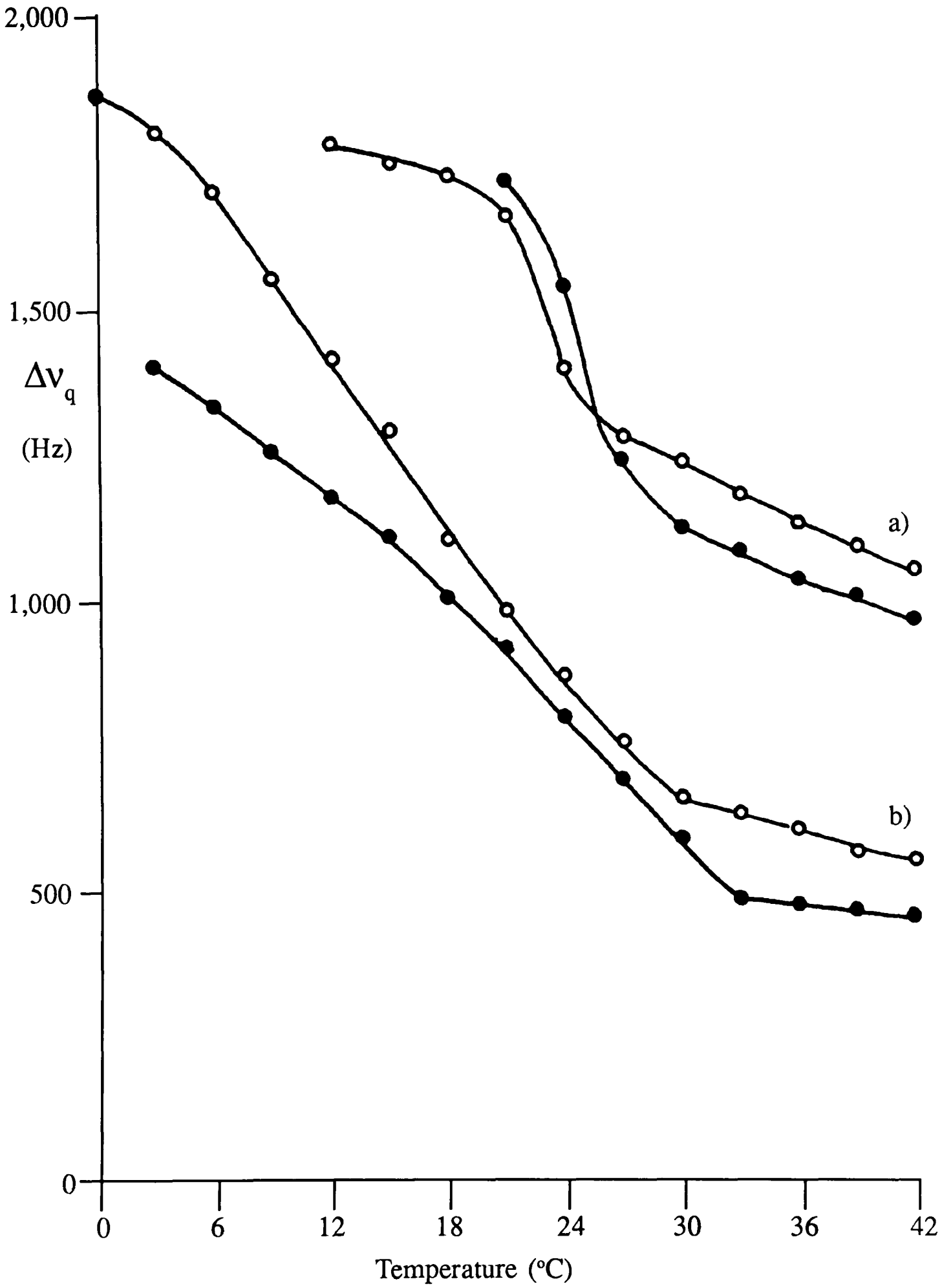


Fig.5.12. Effect of sodium chloride on the measured ^{2}H-NMR quadrupole splitting vs temperature profiles for protein-free DMPC (a) and the 65:1 total lipid phosphate/bR mole ratio nsTP-produced DMPC-d_9/purple membrane complex (b).

o pure water • saturated NaCl

protein content i.e. 31:1 total phosphate/protein mole ratio complex, can be explained in terms of incomplete solubilization to monomers at low lipid contents. Indeed it is reported that for lipid/protein ratios below 41:1, complete dispersion of aggregates does not occur above the DMPC phase transition (Heyn *et al.*, 1981a).

Effect of saturated NaCl on the deuterium NMR DMPC-d_9 data. The deuterium-NMR data described above was obtained from nsTP-produced complexes suspended in buffers of low ionic strength (water alone). In order to investigate the effects of high concentrations of sodium chloride in the aqueous environment, the 65:1 total lipid phosphate/bR mole ratio complex was resuspended in saturated NaCl. The broadline phosphorus-31 NMR spectrum (Fig.5.5.c), demonstrates that at 33°C, the lipid retains a bilayer conformation in the presence of saturated salt and the measured c.s.a. is ~-50 ppm. Deuterium NMR spectra for the 65:1 total lipid phosphate/bR mole ratio complex in saturated salt are compared with the corresponding spectra obtained in deuterium depleted water alone in Fig.5.11. As in water alone, the spectra exhibit a collapse at higher temperatures. However, below the phase transition temperature salt is seen to reduce the spectral anisotropy and quadrupole splittings are less well defined compared to spectra in salt-free environments.

The effects of salt on the measured quadrupole splittings obtained for pure lipid and the 65:1 mole ratio complex as a function of temperature are shown in Fig.5.12. Saturated sodium chloride has little effect on the values for pure lipid, although it may shift the phase transition by the order of one °C. For temperatures above 18°C, salt does not significantly alter the quadrupole splittings for the 65:1 total lipid phosphate mole ratio complex. Below this temperature, however, the magnitudes of the measured quadrupole splittings are considerably reduced compared to those measured from the complex suspended in water alone. The significant effect of sodium chloride in the aqueous environment on the low temperature quadrupole splittings from the 65:1 mole ratio complex may reflect an inability of the protein particles to crystallize into the two-dimensional hexagonal purple membrane-like structures within the plane of the bilayer; the salt may serve to suppress ionic interactions between the negatively charged

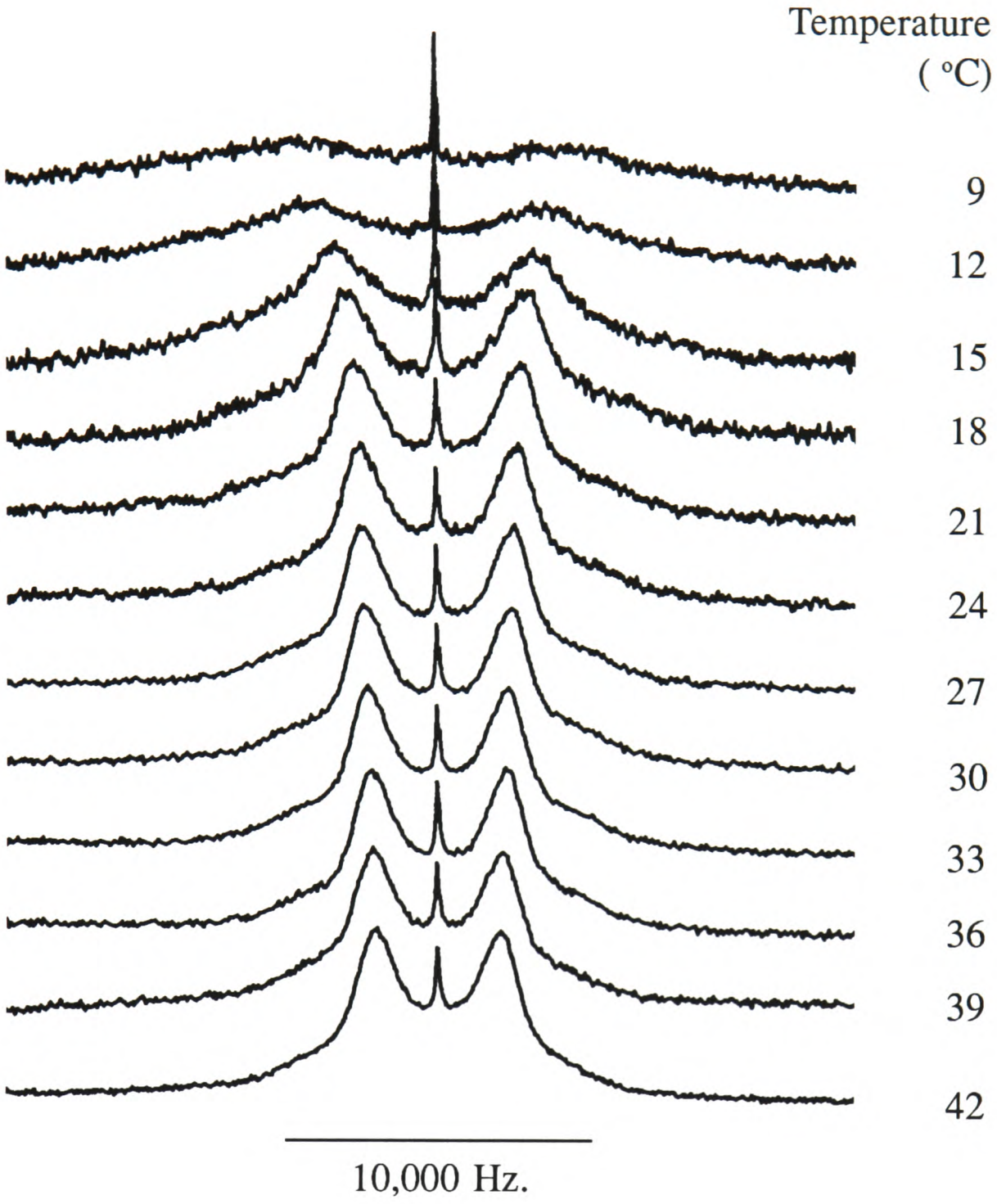


Fig.5.13. ^{2}H-NMR spectra (46.1 MHz) recorded from the 60:1 mole ratio total lipid phosphate/bR (DMPC-d_4) complex pelleted from water alone.

headgroups of PGP and PGS purple membrane lipids and positive charges on the surface of the bacteriorhodopsin molecule that are responsible for mediating crystallization of the protein particles into the hexagonal para-crystalline arrays observed in such vesicles at low temperatures in aqueous environments of lower ionic strengths (Cherry *et al.*, 1978). If this is the case, then the deuterium NMR quadrupole splittings obtained from the nsTP-produced complex in the presence of salt and plotted as a function of temperature display the DMPC undergoing a phase transition between 15 and 33°C with a mid-point around 24°C. Indeed, this agrees well with the phase transition determined for the 72:7.3:1 mole ratio DMPC/PMPL/bR complex by TEMPO partitioning (Fig.5.3).

Deuterium NMR spectra from DMPC-d_4 incorporated into purple membrane by nsTP. Fig.5.13. shows deuterium-NMR spectra obtained from DMPC-d_4 incorporated into purple membrane to give a total phospholipid phosphate/bacteriorhodopsin mole ratio of 60:1. At temperatures above 21°C, powder patterns typical of fluid lipid bilayers, with well defined quadrupole splittings are observed. Spectra were not recorded below 9°C as the powder patterns were broadened out to the extent that quadrupole splittings could not be accurately measured. One advantage of using DMPC selectively deuterated in the α- and β-methylene segments (DMPC-d_4) as opposed to in the γ-methyl groups (DMPC-d_9) is that even at high temperatures a large residual quadrupole splitting is observed (for example, 4,077 Hz at 42°C). This is consistent with an increased restriction on the amplitude of segmental motion within the choline headgroup towards the glycerol backbone (discussed in Chapter 3 this thesis; Gally *et al.*, 1975) and also with less sensitivity of the larger quadrupole splitting to Brownian motion tumbling effects of small diameter vesicles (Table 6 in Chapter 3).

Deuterium NMR spectra from an nsTP-produced DMPC-d_4-d_9/bacteriorhodopsin complex of higher DMPC content, 72:7.3:1 DMPC/PMPL/bR mole ratio (i.e. 85:1 total lipid phosphate/bR) and recorded at increasing temperatures are presented in Fig.5.14. As described previously for the nsTP-produced DMPC-d_9/bR complexes, the spectral anisotropy for the choline g-methyl powder patterns decreases significantly on

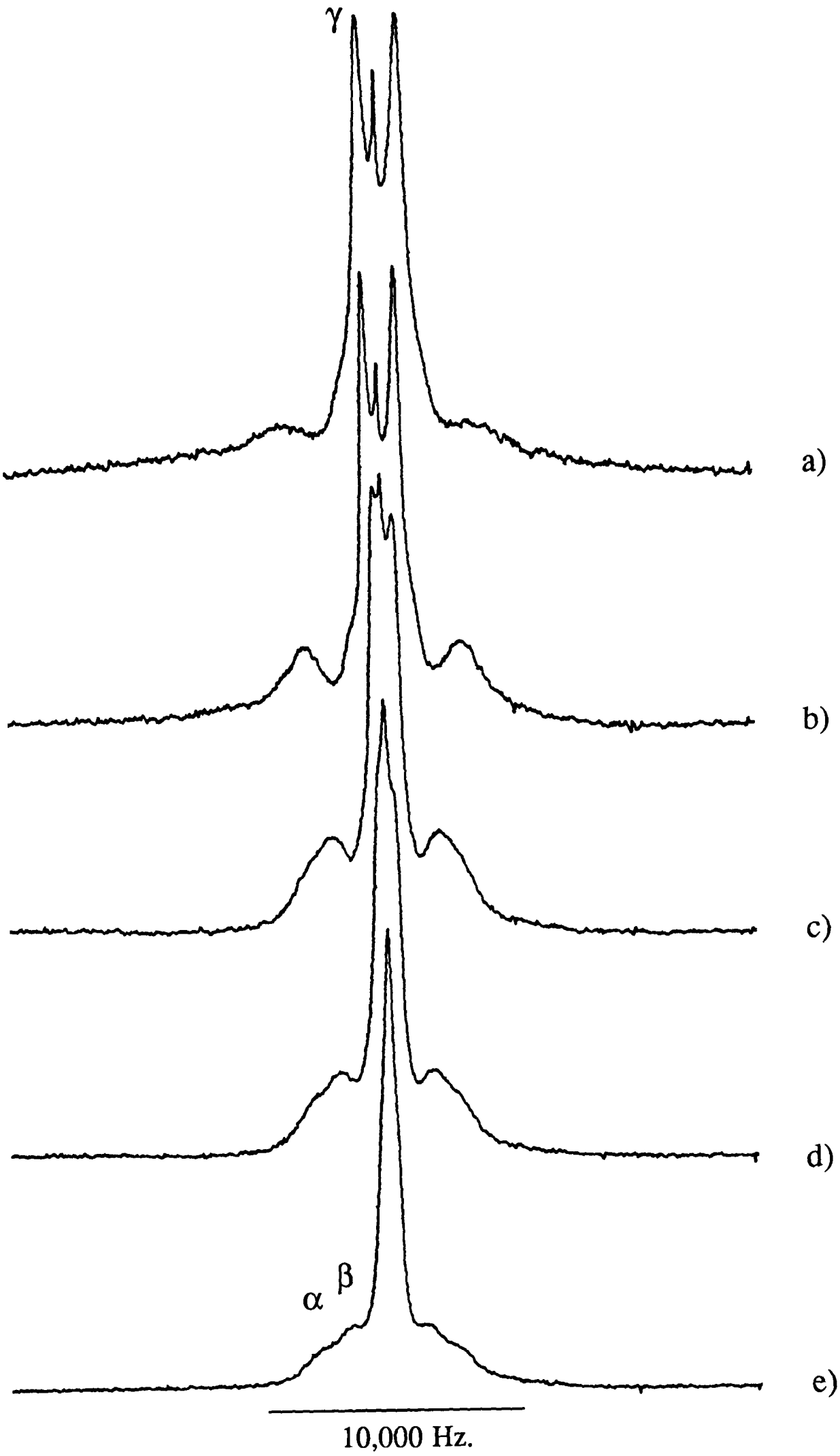


Fig.5.14. ^{2}H-NMR spectra (55.3 MHz) recorded at temperatures of; a) 9°C; b) 15°C; c) 30°C; d) 36°; and e) 45°C for the 72:7.3:1 DMPC/PMPL/bR mole ratio complex (DMPC-d_4-d_9) produced by nsTP-mediated transfer.

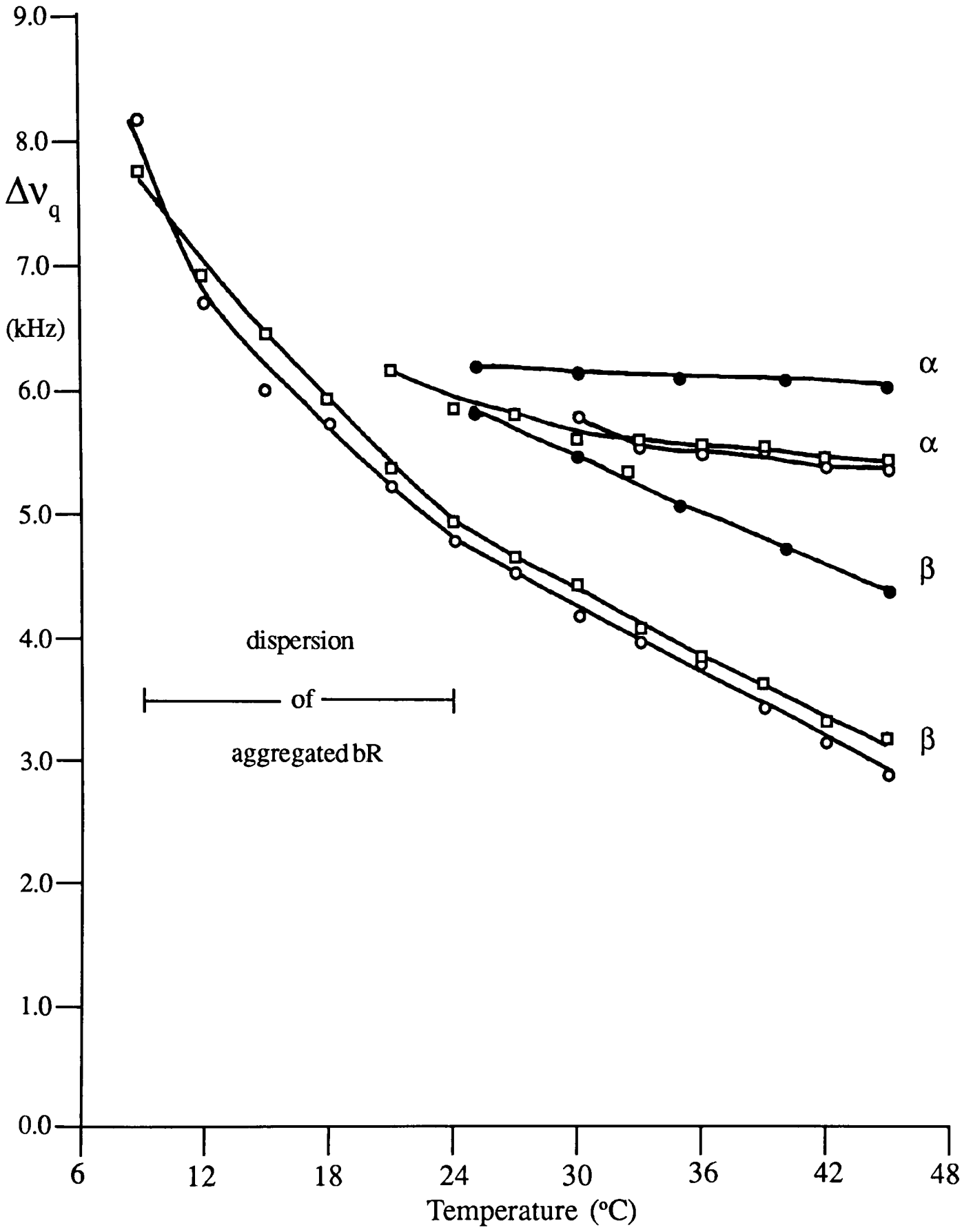


Fig.5.15. Measured ^{2}H-NMR quadrupole splittings for the α- and β-methylene segments of DMPC-d_4 plotted as a function of temperature obtained from the 72:7.3:1 and 109:7.8:1 DMPC/PMPL/bR mole ratio complexes produced by nsTP and from protein-free lipid.

- ○ 72:7.3:1 complex
- □ 109:7.8:1 complex
- ● pure DMPC

warming. At this higher lipid content, increasing the temperature to 30°C and above is seen to resolve the powder patterns from the α- and β-methylene segments (Figs.5.14.d and e).

Effect of temperature on the DMPC-d_4 quadrupole splittings. Plots of the measured quadrupole splittings for the α- and β-methylene segments in the 72:7.3:1 and 109:7.8:1 DMPC/PMPL/bR mole ratio complexes against temperature (Fig.5.15), reveal that as for protein-free lipid (Gally *et al.*, 1975), the β-methylene segment quadrupole splittings are sensitive to changes in temperature; while those for the α-methylene segment powder patterns remain relatively unaffected. Indeed, the temperature sensitivities for both the α- and β-methylene segment powder patterns from the 72:7.3:1 and 109:7.8:1 DMPC/PMPL/bR mole ratio complexes are seen to parallel those displayed by protein-free lipid over the 30 - 45°C range (Fig.5.15), although the magnitudes of the quadrupole splittings are different. This implies that at temperatures above the phase transition the temperature dependent changes in the amplitudes of segmental motion within the phosphocholine moiety are preserved relative to those in protein-free DMPC (Gally et al., 1975; and Chapter 3 of this thesis). For both the 72:7.3:1 and 109:7.8:1 DMPC/PMPL/bR mole ratio nsTP-produced complexes, the β-methylene segment quadrupole splittings are of significantly smaller magnitude relative to those of protein-free lipid. Thus at 45°C, the β-methylene segment quadrupole splitting for the 72:7.3:1 DMPC/PMPL/bR mole ratio complex is 2,890 Hz, which is 1,500 Hz smaller than that for protein-free lipid. The α-methylene segment quadrupole splittings are also reduced relative to those of protein-free lipid, although not as significantly as the β-splittings, those for the 72:7.3:1 DMPC/PMPL/bR mole ratio complex being some 670 Hz smaller at 45°C.

As also observed for the 60:1 total lipid phosphate/protein mole ratio nsTP-produced complex (data not shown), plots for the β-methylene segment quadrupole splittings measured as a function of temperature from the 72:7.3:1 and 109:7.8:1 DMPC/PMPL/bR mole ratio complexes exhibit two phases. A sharp decrease in measured quadrupole splitting is observed on warming from 9 through to 24°C, with

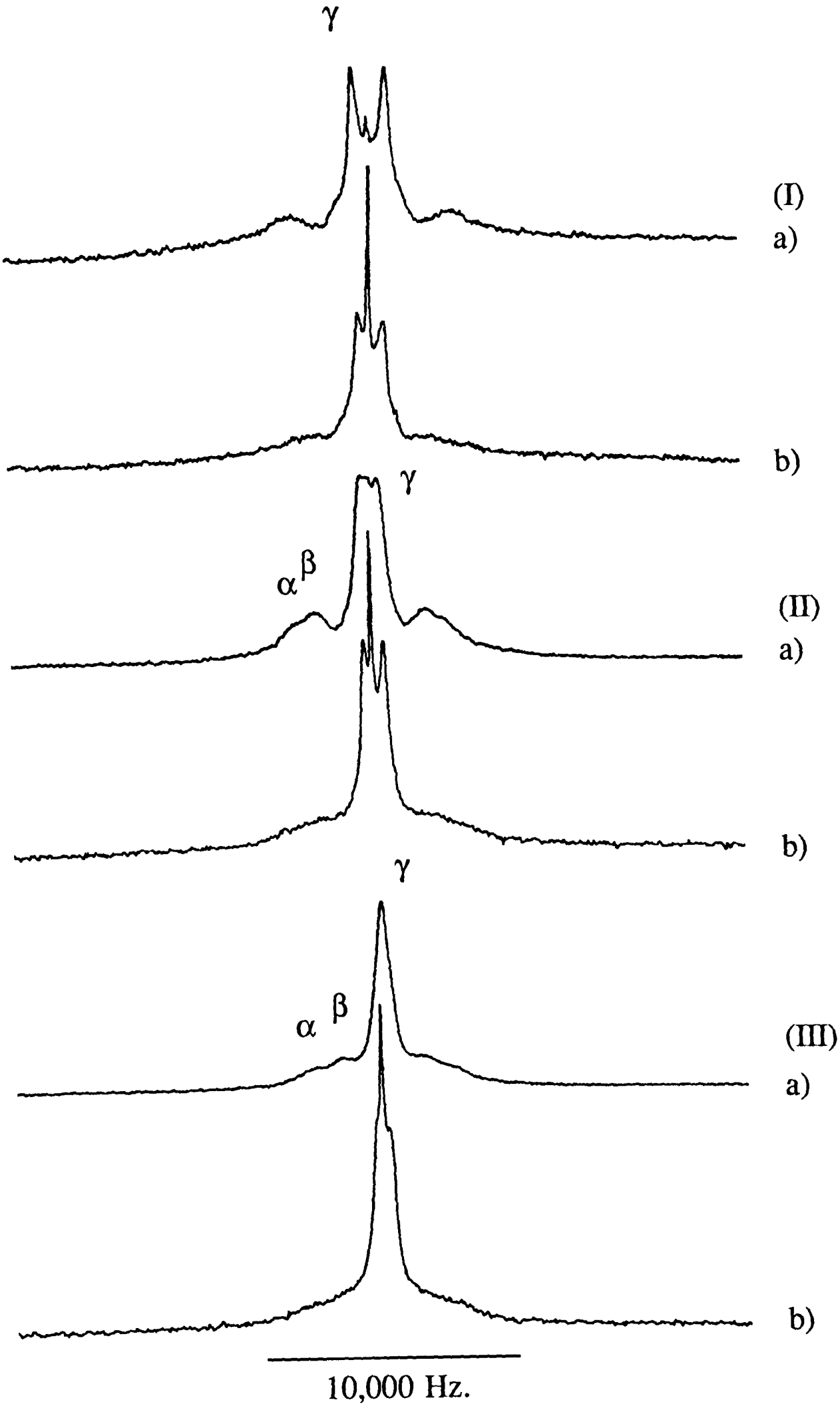


Fig.5.16. ^{2}H-NMR spectra (55.3 MHz) of DMPC-d_4-d_9/PMPL/bR complexes of mole ratios; a) 109:7.8:1 and b) 21:7.6:1 recorded at; (I) 15°C; (II) 30°C and (III) 45°C and produced by nsTP-mediated transfer.

an apparent mid-point around 17°C. This is followed by a less temperature sensitive decrease between 24 and 45°C, that parallels that observed for the β-methylene segment splitting of protein-free lipid. It should be noted that the quadrupole splitting vs temperature profiles for the β-methylene segments are significantly different to those of the choline γ-methyl groups (Fig.5.9).

Effect of bacteriorhodopsin content on the deuterium NMR spectra of DMPC-d_4 in nsTP-produced complexes. Comparing the deuterium NMR spectra obtained at high temperatures from the 60:1 total lipid phosphate/bR mole ratio (Fig.5.13) and the 85:1 total lipid phosphate/bR (72:7.3:1 DMPC/PMPL/bR) mole ratio (Fig.5.14) complexes reveals that on increasing the protein content, the resolution between the α- and β-methylene segment powder patterns is reduced. Indeed for the 60:1 total lipid phosphate/bR mole ratio complex the α- and β-methylene segment powder patterns appear to be superimposed, such that only a single powder pattern is detected. Similar effects were observed (Fig.3.11) for the detergent-produced DMPC/bR complexes in which all the endogenous purple membrane lipids were removed. The increased resolution of the component α- and β-methylene segment powder patterns observed at higher lipid contents results from a decrease in the magnitude of the quadrupole splitting displayed by the β-methylene segment powder pattern; that for the 72:7.3:1 DMPC/PMPL/bR mole ratio complex being 933 Hz smaller at 42°C than that for the 60;1 total lipid phosphate/bR mole ratio complex. Increasing the lipid content of the nsTP-produced complexes further to 123:1 total lipid phosphate/bR mole ratio (i.e. 109:7.8:1 DMPC/PMPL/bR mole ratio) results in little change in the deuterium NMR spectra in that broad α- and β-methylene segment powder patterns are resolvable at 30°C, (Fig.5.16.II.a); the resolution increasing on warming to 45°C (Fig.5.16.III.a). Also presented in Fig.5.16 are the deuterium NMR powder patterns for an nsTP-produced DMPC-d_4-d_9 complex of very low lipid content - 36:1 total lipid phosphate/bR mole ratio (phospholipid composition determined to be 21:7.6:1 DMPC/PMPL/bR in Chapter 2). At such high protein contents, however, the α- and β-methylene segment powder patterns are broadened to the extent that no quadrupole

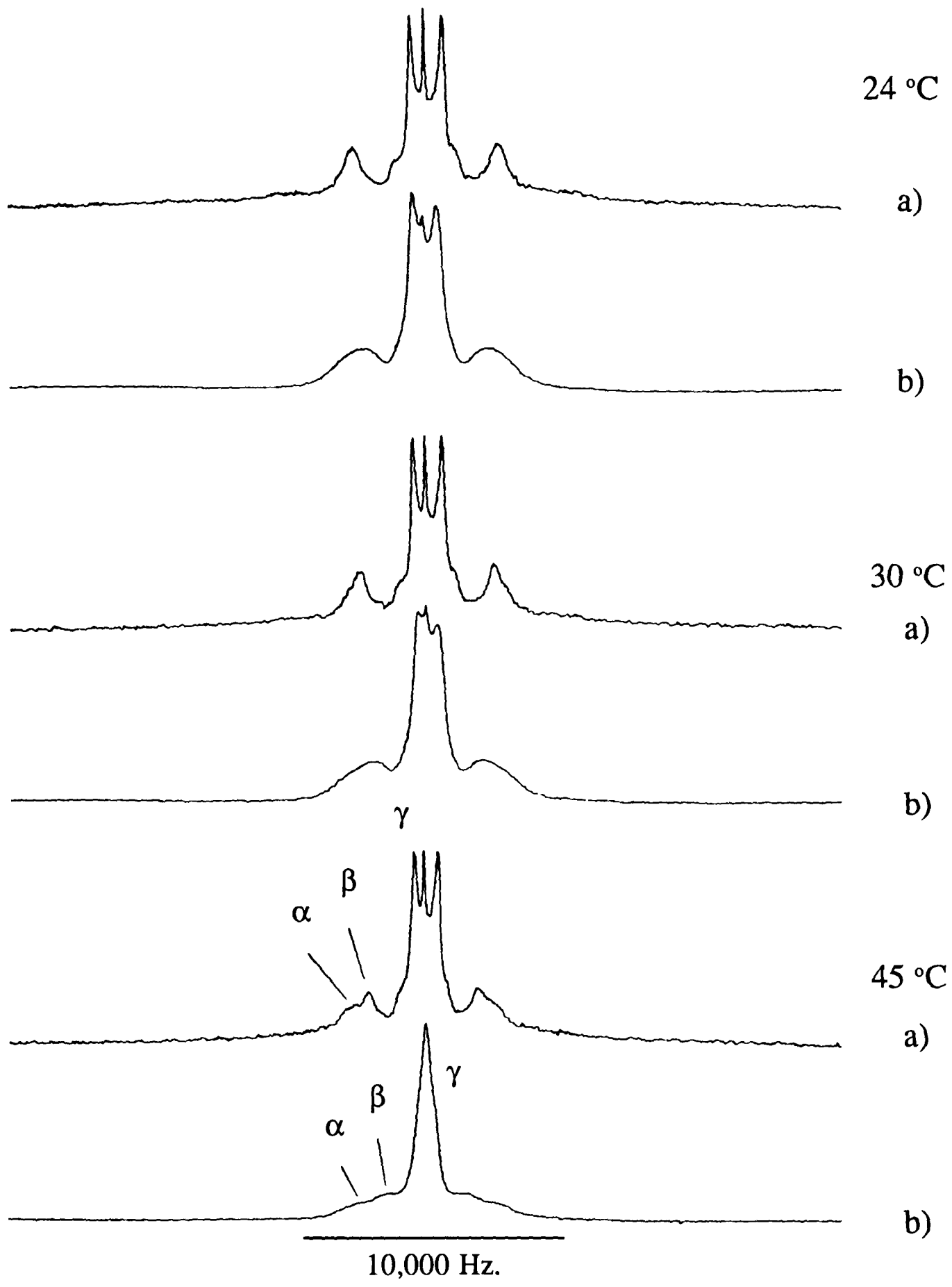


Fig.5.17. Comparison of ^{2}H-NMR spectra (55.3 MHz.) from (a) detergent-produced 95:1 mole ratio DMPC-d_4-d_9/bR complex (all endogenous purple membrane lipids removed) with those from (b) nsTP-produced 72:7.3:1 mole ratio DMPC-d_4-d_9/PMPL/bR complex at different temperatures.

splitting is measurable at either 30°C (Fig.5.16.II.b) or 45°C (Fig.5.16.III.b).

Comparison of deuterium NMR spectra from DMPC-d_4-d_9/bR complexes produced by the nsTP technique with those of similar protein contents produced by detergent techniques. The 72:7.3:1 DMPC/PMPL/bR mole ratio nsTP-produced complex is of similar protein content to the 95:1 DMPC/bR mole ratio complex produced by detergent dialysis with all the endogenous purple membrane lipids removed. Fig.5.17. compares the ^{2}H-NMR powder patterns obtained for the detergent-produced 95:1 DMPC/bR mole ratio complex, with the corresponding spectra for the 72:7.3:1 mole ratio DMPC/PMPL/bR complex. At lower temperatures, (24° and 30°C) the choline γ-methyl group deuterium powder patterns from the nsTP-produced complexes are broadened and the quadrupole splittings are of significantly smaller magnitude compared to those from the large vesicle detergent produced complexes. At higher temperatures (45°C) the γ-methyl group powder patterns for the nsTP-produced complexes have collapsed and the spectral anisotropy is almost completely time averaged in contrast to the well defined splittings exhibited in the spectra of the large detergent produced vesicles.

The powder patterns from the α- and β-methylene segments from the nsTP-produced complexes are also broadened compared to the detergent produced DMPC/bR complex. For both complexes, however, distinct α- and β-methylene segment powder patterns are resolved at 45°C. As described above increasing the protein content of the nsTP-produced vesicles (from 72:7.3:1 DMPC/PMPL/bR to 60:1 total lipid phosphate/bR mole ratios) is seen to increase the magnitude of the β-methylene segment quadrupole splittings, such that the α- and β-methylene segment powder patterns are no longer resolved. Similar effects are observed on increasing the protein-content of the detergent-produced vesicles (from DMPC/bR mole ratios of 95:1 to 67:1) with all endogenous lipids removed (Fig.3.11). Indeed the DMPC-d_4 powder pattern (Fig.5.13) from the 60:1 total phosphate/bR mole ratio nsTP-produced complex is similar to that from the 67:1 (Fig.3.6) mole ratio DMPC/bR detergent-produced complex in that component α- and β-methylene segment powder patterns are virtually

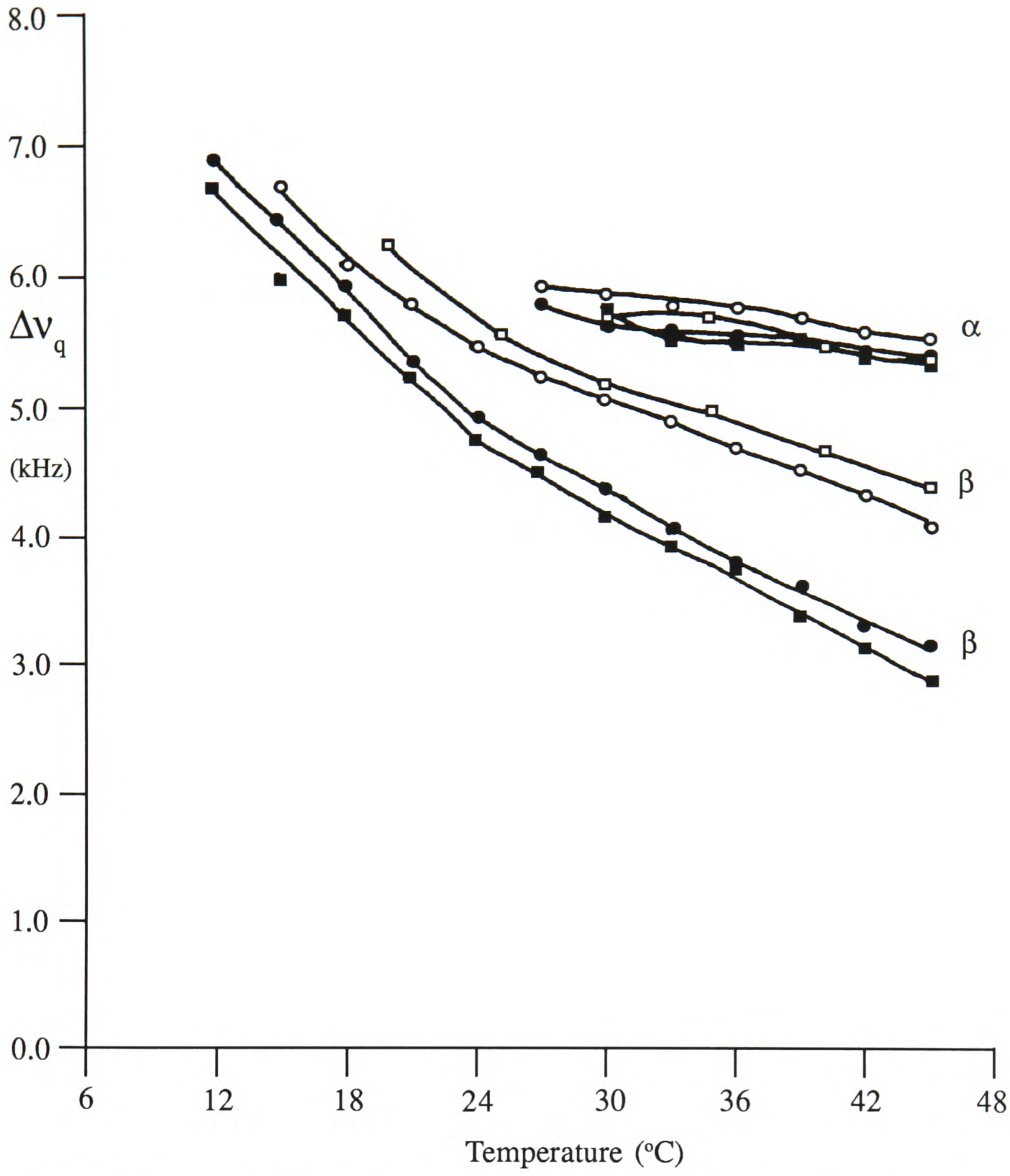


Fig.5.18. Comparison of DMPC-d_4 α- and β-methylene segment quadrupole splittings as a function of temperature measured from nsTP-produced complexes with the endogenous purple membrane lipids retained (filled data points) with those measured from detergent produced DMPC/bR complexes of similar protein content but all purple membrane lipids removed (open data points).

- ■ 72:7.3:1 DMPC/PMPL/bR nsTP-produced complex
- ● 109:7.8:1 DMPC/PMPL/bR nsTP-produced complex
- ▫ 67:1 DMPC/bR detergent-produced complex
- ○ 95:1 DMPC/bR detergent-produced complex

superimposed.

Comparison of temperature sensitivities for DMPC-d_4 quadrupole splittings in complexes produced by the two different techniques. The α- and β-methylene segment quadrupole splittings for the 72:7.3:1 and 109:7.8:1 DMPC/PMPL/bR mole ratio nsTP-produced complexes and the detergent-produced 67:1 and 95:1 DMPC/bR mole ratio complexes are plotted as a function of temperature in Fig.5.18. The temperature sensitivities of the α- and β-methylene segment quadrupole splittings are similar in both complexes; those from the α-segments being relatively unaffected by changes in temperature, while those from the β-segments display a significant reduction on warming. From this it would appear that the changes in amplitude of segmental motion experienced by the choline methylene segments on warming above the phase transition are similar irrespective of the method of vesicle production and whether the endogenous purple membrane lipids are retained. The magnitudes of the α-methylene segment quadrupole splittings appear to be similar in all four complexes and relatively unaffected by the method of vesicle production. In marked contrast, the β-methylene segment powder pattern quadrupole splittings for the nsTP-produced complexes are of significantly smaller magnitudes compared to those of the detergent-produced DMPC/bR complexes of similar lipid protein ratio with all the endogenous purple membrane lipids removed. Indeed the quadrupole splitting for the 72:7.3:1 DMPC/PMPL/bR mole ratio nsTP-produced complex is some 1,500 Hz smaller than that for the detergent produced 95:1 DMPC/bR complex at 45°C.

iv) *Freeze fracture electron microscopy.* Freeze fracture electron microscopy was performed on the 21:7.6:1 DMPC/PMPL/bR mole ratio complex quenched from two temperatures in 10mM Tris/HCl, 1mM EDTA, pH 7.5. The vesicles quenched from low temperatures (15°C) (Fig.5.19.a.) distinctly reveals the hexagonal packing arrangement characteristic of purple membrane, with protein particles arranged at angles of 120° to each other. It is tempting to speculate that the protein free patch is a pool of protein-free DMPC, although it may be an artifact of the fracture. It should be noted that the temperature (15°C) from which the vesicles were quenched is near that determined for

a)



b)



Fig.5.19. Freeze fracture electron micrographs of the 21:7.6:1 mole ratio DMPC/PMPL/bR nsTP-produced complex in 10mM Tris/HCl, 1mM EDTA, pH 7.5 quenched from; a) 15°C; and b) 55°C.

Bar = 100 nm.

the mid-point for dispersion of aggregates (Heyn *et al.*, 1981a). When quenched from higher temperatures, 55°C, (Fig.5.19.b), the ordered hexagonal paracrystalline structure is absent and the densely packed protein particles are randomly associated. At both temperatures the protein particles have diameters of around 10nm and resemble those seen in freeze-fracture electron micrographs of bacteriorhodopsin in other lipid environments (Chapters 4 and 6 this work; Hwang & Stoeckenius, 1977; Cherry *et al.*, 1978; Lewis & Engelman, 1983), including purple membrane, itself (Blaurock & Stoeckenius, 1971). The bacteriorhodopsin content of these particles has been shown to be between 9 and 12 monomers of 26,000Da (Fisher & Stoeckenius, 1977).

5.IV). Discussion.

Labelling of erythrocyte ghosts with nsTP. The most important result from the deuterium NMR data of DMPC-d_9 incorporated by nsTP into erythrocyte ghost membranes is the similar trend displayed in the temperature sensitivity of the measured quadrupole splitting (Fig.5.2.b) when compared to that of the detergent reconstituted band-3/DMPC complex (Fig.5.2.c) from Dempsey *et al.*, (1986). In both protein containing systems, the measured quadrupole splittings are significantly reduced in magnitude, relative to those measured for protein-free lipid on warming above the main phase transition of DMPC. This agreement is significant for two reasons:

a) the large size of the resealed erythrocyte ghosts, opposes the explanation that the tumbling effects of small vesicles may be responsible for the decrease in magnitude of quadrupole splittings observed in the detergent produced complexes of Dempsey *et al.*, (1986). Similar sensitivities in the magnitude of quadrupole splitting to changes in temperature are observed for the DMPC-d_9/bacteriorhodopsin complexes reconstituted by the fast cholate removal technique (Figs.3.4 and 3.5). For these complexes, however, the collapse in quadrupole splitting displayed on increasing temperature co-incides with the broadened DMPC phase transition and the decrease in the spectral anisotropy was attributed to rapid lateral diffusion around small diameters vesicles. The deuterium NMR results from the nsTP-labelled ghosts thus support the results obtained from the

detergent band-3/DMPC complexes as reflecting protein-lipid interactions rather than vesicle size artifacts.

b) the increased temperature sensitivity observed in the detergent reconstituted complexes is not due to traces of detergent remaining or some alteration in the protein thermal properties as a result of the detergent solubilization. It could be argued that detergent-treated band-3 is more prone to effects of temperature than the *in situ* protein and when present in the reconstituted DMPC bilayers, it exposes the phosphocholine moiety to perturbations in amplitude of motion that become enhanced at higher temperatures.

As with band-3 reconstituted into DMPC vesicles, the deuterium NMR data from DMPC incorporated into ghosts by nsTP is consistent with a dispersion of band-3 aggregates into dimers on warming.

Labelling of purple membrane with nsTP. The vesicles produced by addition of DMPC by nsTP to *H.halobium* purple membrane were shown (in Chapter 2) to be of homogeneous lipid/protein ratios, with some 76 - 86% of the endogenous purple membrane phospholipids retained. As demonstrated for detergent produced DMPC/bR complexes with all the endogenous purple membrane lipids retained, (Cherry *et al.*, 1978) freeze fracture electron microscopy reveals hexagonal ordering of the bacteriorhodopsin particles into aggregates in the nsTP-produced vesicles when quenched from low temperatures. Furthermore, at higher temperatures this ordered arrangement is seen to break down, implying a disruption of the forces responsible for maintaining the lattice and a dispersion of the particles.

Negative stain electron micrographs (Chapter 2) reveal the nsTP-produced DMPC/purple membrane complexes to be in the order of 150 - 350 nm diameter. In chapter 3, results for cholate produced complexes reveal that vesicles of such size cause an artifactual reduction in magnitude of the residual DMPC-d_9 quadrupole splitting above the phase transition (see Fig.3.4.c) due to averaging of the spectral anisotropy by rapid vesicle tumbling effects (discussed in Chapter 3). The vesicle size is such that at temperatures below the phase transition, the lipid lateral diffusion is sufficiently

restricted for the quadrupole splitting to be relatively unaffected by the tumbling effects of small vesicles. On warming through the phase transition, however, such motional restrictions are lifted and the increase in the rate of lipid diffusion (D_{diff}) around fast tumbling vesicles of small radii causes averaging of the spectral anisotropy resulting in a collapse of the measured quadrupole splitting. Thus, it is probable that the collapses observed in the quadrupole splittings for the choline γ-methyl group powder patterns (DMPC-d_9) from the nsTP-produced complexes on increasing the temperature are, predominantly, the result of time-averaging the spectral anisotropy by rapid tumbling of small diameter vesicles.

Indeed, comparison of the quadrupole splitting vs temperature profiles for the DMPC-d_9 data with the phase transitions determined by TEMPO-partitioning adds further support to this conclusion. Maximum sensitivity of the observed quadrupole splittings to changes in temperature is observed between 6°C and 30°C for the 65:1, 88:1 and 152:1 total lipid phosphate/bR mole ratio complexes (Fig.5.9). For all nsTP-produced complexes, including the 109:7.8:1 and 72:7.3:1 DMPC/PMPL/bR mole ratios (data not shown in Fig.5.9), the enhanced temperature sensitivity displayed by the DMPC-d_9 quadrupole splitting is seen to end at 30/33°C, which coincides with the completion of the main phase transition as detected by TEMPO partitioning for the 72:7.3:1 and 109:7.8:1 DMPC/PMPL/bR mole ratio complexes (Fig.5.3). As for the detergent-produced DMPC/bR complexes (Fig.3.5), small vesicles render the DMPC-d_9 quadrupole splitting vs temperature profiles sensitive to the beginning and end-points of the phase transitions. Thus, it is likely that the DMPC-d_9 quadrupole splittings plotted as function of temperature for the nsTP-produced complexes are reporting the main gel-to-liquid crystalline phase transition. The magnitude of the quadrupole splittings, however, is also seen to be sensitive to temperature as low as 6°C i.e. several degrees lower than beginning of the phase transition as detected by TEMPO partitioning. This implies that the observed temperature sensitivity in this temperature range may be reflecting the temperature dependent changes in dispersion/aggregation properties of the protein particles as previously reported (Heyn *et al.*, 1981a). Of some significance is

the alteration of the quadrupole splitting vs temperature profile for the 65:1 total lipid phosphate/bR (DMPC-d_9) complex in the presence of saturated salt (Fig.5.12), such that the temperature sensitivity coincides with the phase transition determined by TEMPO-partitioning for the 72:7.3:1 DMPC/PMPL/bR mole ratio complex (Fig.5.3). If salt acts to suppress low temperature aggregation, then this would support the sensitivity of the quadrupole splittings to temperature in the 6 - 12°C range in the absence of salt as reporting on changes in the aggregation state of the bacteriorhodopsin.

Thus, the DMPC-d_9 quadrupole splitting vs temperature profiles for the nsTP-produced vesicles, suspended in low salt aqueous solutions e.g. water alone or 10mM Tris/HCl, pH 7.5, report the effects of not only low temperature changes in the aggregation/dispersion properties of the protein itself, but also the main phase transition for the DMPC in the complexes. In high salt aqueous buffers, however, the low temperature aggregation of the protein particles is possibly suppressed and the quadrupole splitting profiles demonstrate only the main phase transition of the supporting DMPC bilayer.

In contrast to the DMPC-d_9 data, the temperature profiles displayed by the α- and β-methylene segment powder patterns of DMPC-d_4 incorporated into purple membrane, do not reflect the broadened phase transitions determined by TEMPO partitioning. The larger residual quadrupole splittings displayed by the α- and β-methylene segment powder patterns render the spectral anisotropy less susceptible to averaging by tumbling effects of small vesicles (Table 6 in Chapter 3). For nsTP-produced complexes with total lipid phosphate/bR mole ratios ranging from 60:1 to 123:1 (i.e. 109:7.8:1 DMPC/PMPL/bR mole ratio complex), the β-methylene quadrupole splitting vs temperature profiles reveal two distinct phases of temperature sensitivity; a sharp decrease in quadrupole splitting is observed from 9 to 24°C with a mid-point of approximately 17°C. This temperature-dependent reduction is interpreted to reflect the dispersion of hexagonal "purple membrane like"-aggregates into free monomeric bacteriorhodopsin particles. As reported previously (Heyn *et al.*, 1981a) for

similar ratio complexes, the solubilization into monomers is completed by 24°C. Above 24°C, the temperature dependences of both the α- and β-methylene quadrupole splittings are similar to those displayed by pure lipid, implying no further change in the protein aggregation state.

It would appear that at temperatures above the phase transition, the dispersion properties of bacteriorhodopsin in DMPC bilayers are unaffected by the presence or absence of the endogenous purple membrane lipids. Thus, both in the absence (Chapter 4; Lewis & Engelman, 1983) and presence (Fig.5.19; Cherry *et al.*, 1978) of the endogenous purple membrane lipids, freeze fracture electron micrographs of the bacteriorhodopsin in DMPC bilayers, quenched from temperatures above the phase transition, reveal the presence of similar sized bacteriorhodopsin particles, which are seen to be dispersed within the plane of the bilayer. Circular dichroism data (Cherry *et al.*, 1978; Heyn *et al.*, 1981a) revealed the bacteriorhodopsin to be monomeric in DMPC bilayers with all the endogenous purple membrane lipids present at temperatures above the main phase transition. The number of boundary lipids calculated from ESR data for bR in DMPC bilayers with all the purple membrane lipids removed is also consistent with a monomeric species (Chapter 3). Furthermore, both the phosphorus-31 NMR c.s.a.s and the deuterium NMR quadrupole splittings for the β-methylene segments are seen to increase in magnitude with protein content for both the nsTP-produced complexes, with endogenous purple membrane lipids retained, and the detergent-produced DMPC/bR complexes with all the endogenous purple membrane lipids removed. These results are interpreted to reflect reductions in the amplitudes of segmental motion within the phosphocholine moiety on incorporation of monomeric bacteriorhodopsin in the DMPC bilayer. Thus at temperatures above the phase transition, it would appear that bR is monomeric in DMPC bilayers irrespective of the presence of endogenous purple membrane lipids.

In apparent contradiction, however, the deuterium NMR spectra from complexes produced by the two techniques, although of similar protein contents, are significantly different (Fig.5.17) at temperatures above 24°C. The broadening of the α- and β-

methylene segment powder patterns and the significant reductions in the magnitude of the β-methylene segment quadrupole splittings observed above 24°C in the spectra of nsTP-produced complexes compared to the detergent-produced complexes may be explained by:

a) larger inhomogenieties in protein content within the individual nsTP-produced vesicles. This is unlikely since linear sucrose density gradient centrifugation revealed single sharp bands (Chapter 2) consistent with vesicles of homogeneous protein contents.

b) effect of the negative charged headgroups of the remaining endogenous purple membrane phospholipids on the amplitudes of motion of the choline segments. Increasing the mole fraction of the negatively charged phospholipid, DMPG, in DMPC bilayers reduces the magnitudes of the choline γ-methyl quadrupole splittings (Sixl & Watts, 1982). 50 mol% DMPG reduces the β-methylene segment quadrupole splittings by over fivefold and doubles the magnitude of the splitting for the α-methylene segment. Contributions from this effect are likely to be minor in view of the small proportions of purple membrane PGP relative to the DMPC.

c) reflect perturbations within the detergent produced DMPC/bR vesicles from using detergents to solubilize the purple membrane.

d) differences in vesicle sizes. The diameters measured for the DMPC/bR vesicles produced by the slow cholate removal procedure are large enough (1,000 - 1,500 nm) so that the residual spectral anisotropy from the α- and β-methylene powder patterns is not reduced by vesicle tumbling effects (Table 6 in Chapter 3 this thesis; Burnell *et al.*, 1980). According to the conclusions from Table 6 of Chapter 3, the larger diameter nsTP-produced vesicles (diameter 300 nm) are not small enough to significantly effect the spectral anisotropies of the β-methylene segment powder patterns, assuming a quadrupole splitting of 4,000 Hz. For the smaller vesicles (diameters of 100 nm), however, Brownian tumbling is likely to effect to some extent the spectral anisotopy. It should also be noted that the actual vesicle sizes measured by negative stain electron microscopy may be an over-estimation due to a flattening of the spherical liposomes

during the staining technique. Furthermore, the conclusions made from the calculations in Table 6 (Chapter 3), differ slightly with previous work, where it is reported from simulations (Burnell *et al.*, 1980) that even vesicle diameters as large as 500 nm are small enough to significantly effect the lineshape and c.s.a. of phosphorus-31 NMR spectra using a "real" c.s.a. of 3,550 Hz, which is similar to the 4,000 Hz used in the calculation for Table 6 (Chapter 3). Indeed the phosphorus-31 c.s.a.s and lineshapes obtained for the nsTP-produced complexes appear to be sensitive to whether the sample is a semi-solid pellet or a liquid suspension. In the pellet form, the Brownian tumbling of the vesicles is likely to be more restricted due to the increased viscosity of the medium.

In conclusion, it is most likely that small vesicle size is responsible for the collapse of the choline γ-methyl powder patterns at high temperatures and that the powder patterns from the β-methylene segments are also effected although to a lesser extent. The broadening of the α- and β-methylene segment powder patterns, particularly for the 21:7.6:1 mole ratio DMPC/PMPL/bR complex, for which the vesicles are between 100 and 200 nm in diameter possibly reflects the range of vesicle sizes; the smaller ones causing more averaging of the residual spectral anisotropy than the larger diameter vesicles.

Chapter 6.

Studies of bacteriorhodopsin dispersion properties in the synthetic phospholipid DMPG, with all endogenous purple membrane lipids removed.

6.I). Introduction

From the previous three chapters and past publications, it is clear that the phospholipid environment plays a role in controlling the packing properties and solubility of the protein particles within the plane of the bilayer. The endogenous purple membrane lipids, although present at mole ratios of between only seven and twelve per bacteriorhodopsin monomer (Kates *et al.*, 1983), appear to be particularly important in this respect. In DMPC and DPPC bilayers at low temperatures, the presence of the endogenous purple membrane lipids appears to mediate the organization of protein particles into the hexagonal para-crystalline two-dimensional array, characteristic of purple membrane (Cherry *et al.*, 1978 & Chapter 5). However, at temperatures above the main phase transition of the saturated lipids in PC/bR complexes, the dispersion properties appear to be less dependent on the presence of the purple membrane lipids; the protein probably being monomeric irrespective of whether they are present or removed (Cherry *et al.*, 1978 & Heyn *et al.*, 1981a; Chapter 3).

The purple membrane lipids comprise an unusual assortment of polar and non-polar lipids (Kates, 1978 & Kates, *et al.*, 1983). The polar lipids include the phospholipids and the glycolipid sulphates. The major phospholipid (PGP) is unusual in having the potential to bear three negative charges at the phosphoglycerolphosphate headgroup moiety. Indeed all the *H.halobium* polar lipid species are negatively charged to varying degrees. This is a major difference to DMPC, the choline headgroup of which is zwitterionic, carrying a permanently positively charged N,N,N-trimethylammonium moiety in addition to the negatively charged phosphate group.

Control of the packing and dispersion properties of the protein particles may be mediated through the saturated isoprenoid alkyl chains in the bilayer core or through

the headgroup moieties or both. One mechanism for packing of the protein particles into the hexagonal two-dimensional array of purple membrane may involve ionic interactions between the negative charges on the PGP headgroup and basic residues at the protein surface. *H.halobium* grow in conditions of saturated salt and thus the significance of ionic interactions at the membrane surface in arranging the protein particles may be reduced. ^{2}H-NMR results, however, presented in Chapter 5 imply that the presence of high concentrations of NaCl in the aqueous medium may suppress the low temperature-induced aggregation of bacteriorhodopsin in DMPC bilayers with most of the purple membrane phospholipids present, thus providing evidence in support of ionic interactions as an important mechansim for organizing protein packing.

Phosphatidylglycerol (PG) is one of the major phospholipid classes occurring in higher plants, algae and bacteria. Furthermore, 2,3-O-diphytanoyl-PG is reported to be present in the purple membrane itself (Kates *et al.*, 1978 & Chapter 2), although it only accounts for 5%(w/w) of the polar lipids (4.5% total lipid). Unlike PC, it has a negatively charged headgroup with a pK_a between 2.8 and 5.0 depending on the ionic strength (Sacre & Tocanne, 1977, Watts *et al.*, 1978 and Chapter 7 of this thesis).

In this chapter the packing and dispersion properties of bacteriorhodopsin in DMPG bilayers, with all endogenous purple membrane lipids removed, is studied to determine whether replacement of the zwitterionic phosphocholine group with the negatively charged phosphoglycerol moiety is sufficient to organize the protein particles into hexagonal arrays at temperatures below the phase transition. Also it is of interest to investigate the solubility properties of bacteriorhodopsin in DMPG bilayers at temperatures above the phase transition and in particular, whether the 10nm diameter bacteriorhodopsin particles are still observed in freeze-fracture elctron micrographs. Additional information on the solubility properties of bR in DMPG bilayers above the phase transition temperature is obtained by determining the number of boundary lipids per bacteriorhodopsin monomer by ESR and comparing this result with those obtained for DMPC bilayers.

For the work presented here, the DMPG used was selectively deuterated at the α-

, β- and γ-carbons of the glycerol headgroup moiety (as shown in Fig.3.1.b; Chapter 3 of this thesis). The α- and γ-segments both have two deuterons, while the β-carbon has a single deuteron. Thus effects of the bacteriorhodopsin on the conformation and motion of the glycerol headgroup can be studied by broadline deuterium and phosphorus-31-NMR at a variety of temperatures and compared to pure lipid.

Phosphatidylglycerols have two glycerol moieties, of which the β-carbons (C-2) are chiral centres. In *H.cutirubrum* PGP, PGS and PG, which are identical to *H.halobium* polar lipids (Kates *et al.*, 1983), both the glycerol moieties C-2 carbons are in the *sn* configuration (Kates, 1978), while the DMPG-d_5 used here has the *sn* configuration at the backbone glycerol moiety, but is racemic at the headgroup glycerol. The effects of this on the protein packing properties and whether any selectivity is exhibited for the *sn-sn* diastereomer is not known.

6.II). Materials and Methods.

Deuterated DMPG-d_5, selectively labelled in its headgroup was synthesized from deuterated glycerol-d_5 using 2,3-O-isopropylideneglycerol as an intermediate as described by Harlos & Eibl (1980). A single DMPG-d_5/bacteriorhodopsin complex was prepared as for the DMPC/bR complexes with all the endogenous purple membrane lipids removed (as described in Chapter 1). The synthetic DMPG-d_5 was rather insoluble in the cholate buffer even at 45°C. To overcome this problem, the non-ionic detergent octyl-β,D- glucopyranoside was added to a final concentration of 100mM and the mixture repeatedly tip-sonicated until all milkiness was removed. Reconstitution by dialysis was mediated by the slow cholate removal procedure (see Chapter 1) in order to facilitate large vesicle formation. After vesicles had formed (5 days) dialysis was continued for one week changing the buffer and Amberlite XAD-2 beads (BDH) twice a day. The vesicles were maintained in 150mM NaCl, 100 mM Tris/HCl, 1mM EDTA, pH 7.6 and NMR was performed in this buffer using deuterium depleted water. Vesicles were purified on a linear 15 - 45% sucrose gradient made from the above buffer; (200,000g; Beckman SW40 rotor; 4 hr; 4°C). For broadline-NMR

studies the vesicles were pelleted (40,000g; 20 min; 15°) into clear plastic centrifuge tube inserts and the supernatant removed. The centrifuge tube containing a solid pellet was clipped to size, sealed with a cork and placed in a 10mm NMR tube. This served to concentrate the vesicles into a solid mass and so reduce the effects of vesicle tumbling on the NMR spectra by increasing the viscosity of the medium (discussed in Chapter 5). Pure DMPG-d_5 was found to be prone to forming small vesicles on suspension in excess aqueous buffer as judged from the isotropic NMR signals obtained. In order to overcome this problem, a minimal amount of buffer (150mM NaCl, 100mM Tris/HCl, 1mM EDTA, pH 7.6) just sufficient to hydrate the lipid was added to the lipid.

Protein/lipid ratio analysis was performed using the modified Lowry method (Markwell *et al.*, 1981) and the phosphate method (Rouser *et al.*, 1970). Calculated protein concentrations were decreased by 20% to account for the error in the Lowry determination for bacteriorhodopsin (Rehorek & Heyn, 1979). Since the presence of Tris buffer is known to effect the Lowry determination, the complex was washed three times in 150mM NaCl before the analyses were undertaken. TEMPO partitioning, ESR and deuterium- and phosphorus-31 NMR measurements were performed as described in Chapter 3.

NMR and freeze fracture electron microscopy experiments were also performed on the protein sample in 1mM EDTA, pH 7.6 in the absence of salt. Vesicles were washed three times in 1mM EDTA, pH 7.6 (100,000g; 30min; 15°C) and then loaded onto a sucrose density gradient in order to separate any pure lipid that may be released from the vesicles by the change in ionic strength. The sample was prepared for NMR studies as described above.

Freeze-fracture electron microscopy was performed on vesicles in 150mM NaCl, 100mM Tris/HCl, 1mM EDTA, pH 7.6 and quenched in liquid Freon (-90°C) after incubation for 5m at two temperatures; 6°C (below the lipid phase transition) and 45°C (above the lipid phase transition). Freeze fracture electron microscopy was also performed on vesicles in 1mM EDTA, pH 7.6 in the absence of salt, quenched after incubation at 6°C.

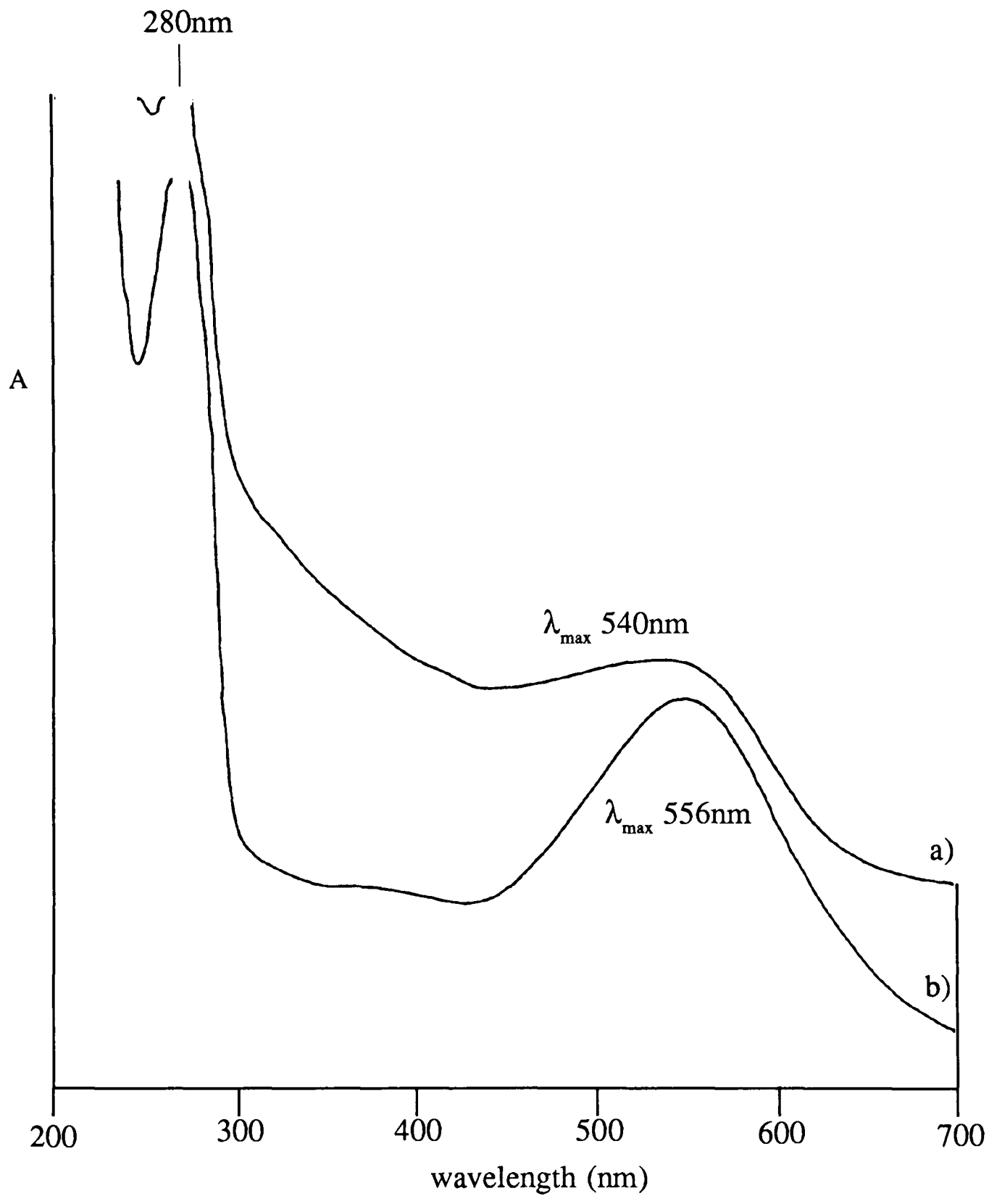


Fig.6.1. UV/vis absorption spectra of bacteriorhodopsin in DMPG bilayers suspended in aqueous media of different ionic strengths; a) 150mM NaCl, 100mM Tris/HCl, 1mM EDTA, pH 7.6 and b) after washing three times in 1mM EDTA, pH 7.5.
A is relative absorption

The DMPG/bR complex was labelled with 14-PGSL using ethanol injection as described by Watts *et al.*, (1979). Free spin-label was removed by washing twice in 150mM NaCl, 100mM Tris/HCl, 1mM EDTA, pH 7.6 (100,000g; 30min; 15°C) and then a linear 15 - 45% sucrose density gradient (250,000g; 12hr; 4°C)

6.III). Results.

One DMPG-d_5/bR complex from which all the endogenous purple membrane phospholipids have been removed was produced with a lipid/protein mole ratio of 71(±6):1. This corresponded to 1.4 mol% bacteriorhodopsin. Sucrose density gradient centrifugation (150mM NaCl, 100mM Tris/HCl, 1mM EDTA, pH 7.6), yielded a single sharp band (2mm width) implying a homogeneous protein content in the vesicles.

After removing the salt by washing in 1mM EDTA pH 7.5, density gradient centrifugation again revealed a single band and no free lipid was observed at the low density end of the gradient. Lipid:protein analysis revealed a DMPG/bR mole ratio of 62:1, confirming that little change in the complex stoichiometry occurred on removing the salt.

Visible absorption spectra. In the presence of salt at pH 7.6, the retinal chromophore of the bacteriorhodopsin in DMPG vesicles exhibited a distinct reddish hue in contrast to bacteriorhodopsin in DMPC vesicles. The UV/vis absorption spectrum (Fig.6.1.a) for the vesicles (against a salt blank) showed the retinal chromophore to exhibit an apparent A_{max} of 543nm. The retinal absorbance is superimposed on the Rayliegh scattering from the large DMPG vesicles, which increases at shorter wavelengths. The UV/vis absorption spectrum of DMPG/bR vesicles depends upon the ionic strength of the buffer (Fig.6.1.). Thus, after three washes in 1mM EDTA, pH 7.6, i.e. with no salt present, the reddish hue is replaced by the purple colour characteristic to purple membrane; the apparent A_{max} for the retinal chromophore shifting to 556nm. Furthermore, the suspension of vesicles looses its opaqueness and becomes clear. Indeed the UV/vis spectrum (Fig.6.1.b) of the vesicles in 1mM EDTA alone is very similar to that obtained from purple membrane (Oesterhelt & Stoeckenius, 1974) in that there is little contribution from the Rayliegh scattering.

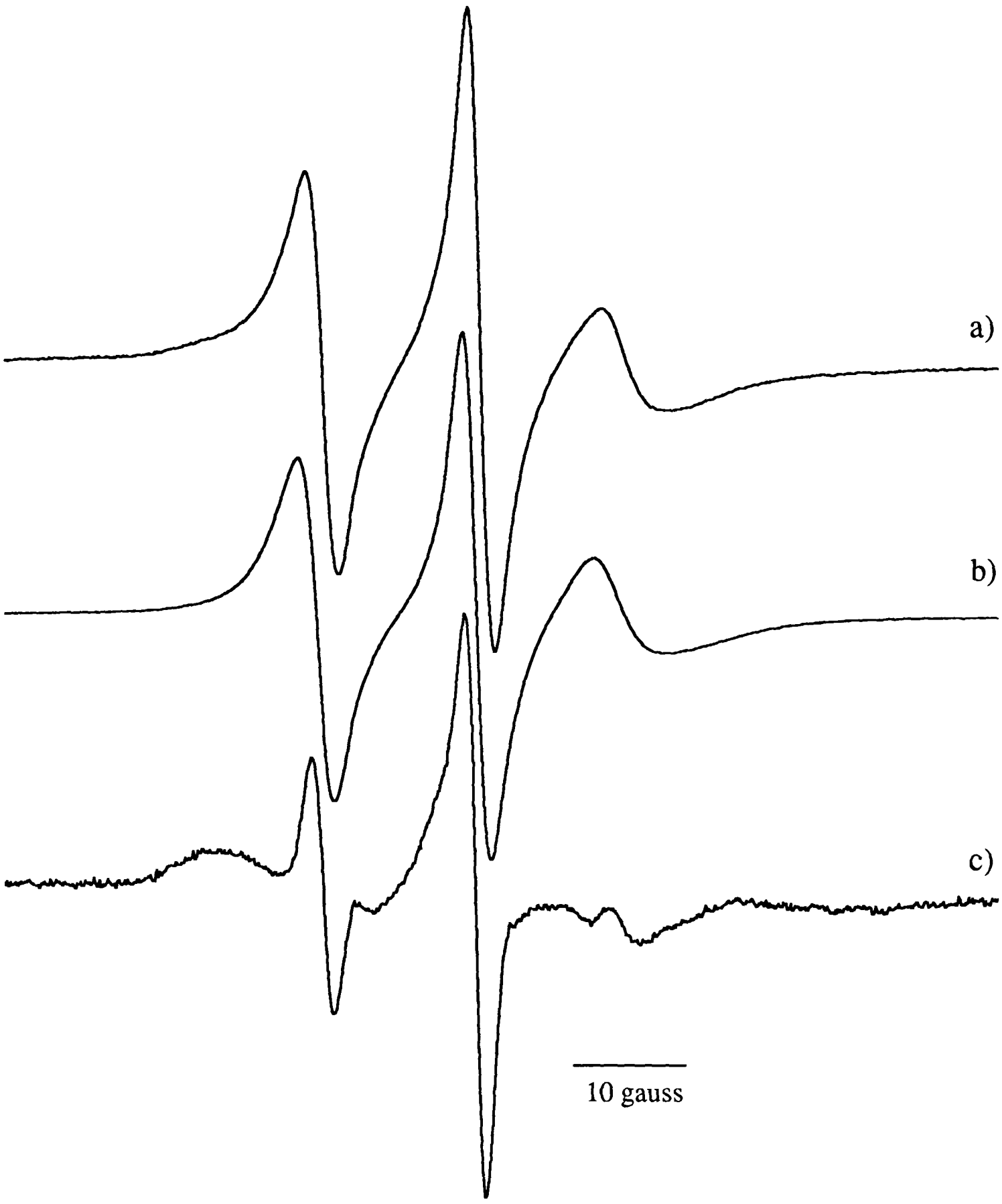


Fig.6.2. ESR spectral subtractions to determine the proportion of motionally restricted component displayed by 14-PGSL in DMPG/bR vesicles (mole ratio 71:1) at 35°C.

a) ESR spectrum of 14-PGSL in DMPG/bR complex (mole ratio 71:1). Vesicles in 150mM NaCl, 10mM Tris/HCl, 1mM EDTA, pH 7.5 at 35.3°C.

b) ESR spectrum of 14-PCSL in protein-free DMPC at 23°C; used as fluid component

c) difference spectrum of motionally restricted component produced by subtracting the fluid component spectrum (b) from (a).

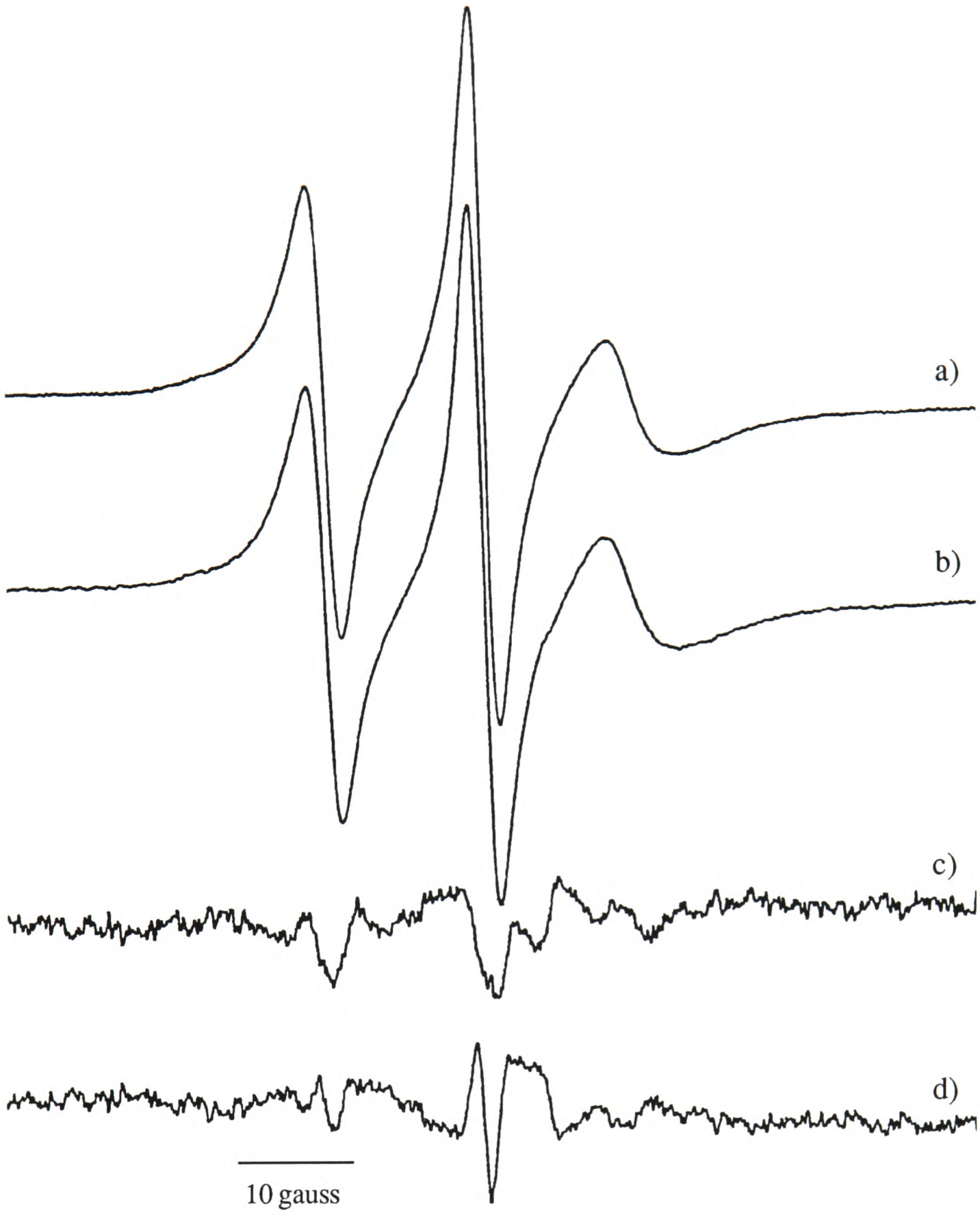


Fig. 6.3. Comparison of magnitudes of ESR motionally restricted components for bR in DMPC and DMPG bilayers at similar protein contents.

a) 14-PGSL in DMPG/bR complex (mole ratio 71:1). Vesicles in 150mM NaCl, 10mM Tris/HCl, 1mM EDTA, pH 7.5 at 35.3°C.

b) 14-PCSL in DMPC/bR complex (mole ratio 68:1). Vesicles in 10mM Tris/HCl, pH 7.4 at 37.2°C.

c) difference spectrum (vertically enlarged 8 fold) of spectrum (b) subtracted from (a).

d) difference spectrum (vertically enlarged 8 fold) of spectrum (a) subtracted from (b)

These observations are consistent with the decrease in vesicle size on removing the NaCl component from the buffer that is observed by freeze fracture electron microscopy (discussed below).

Spin-labelled phospholipid ESR results. The ESR spectrum of 14-PGSL in the 71:1 mole ratio DMPG/bR complex at 35.2°C is shown in Fig.6.2.a. For all temperatures between 29 and 42°C the spectra are two component, consisting of a motionally restricted spin-label component and a more fluid component that is characteristic of protein-free lipids. The spectrum of the motionally broadened component (Fig.6.2.c) was obtained by subtracting the fluid component (14-PCSL in protein-free DMPC at 23°C) shown in Fig.6.2.b from the spectrum of 14-PGSL in the DMPG/bR complex (Fig.6.2.a). The difference spectrum shown in Fig.6.2.c in addition to the motionally broadened component, reveals a trace of fluid component which was not removed by the subtraction procedure. The motionally restricted difference spectrum, with a measured A_{max} of approximately 59 gauss, was determined to account for 30% of the total spin-label spectrum. The lipid/protein mole ratio (71:1) of the DMPG/bR complex is very similar to that of the 68:1 mole ratio DMPC/bR complex described in Chapter 3. In both complexes all the endogenous purple membrane phospholipids have been removed. Comparison of these two systems thus provides an insight into the effect of changing the headgroup from a zwitterionic phosphocholine to a negatively charged phosphoglycerol moiety on the dispersion properties of bacteriorhodopsin in dimyristoyl phospholipid bilayers. At 36°C (±1°C), the motionally broadened component displayed by 14-PGSL in the 71:1 mole ratio DMPG/bR vesicles (Fig.6.3.a) is similar to that displayed by 14-PCSL in the 68:1 mole ratio DMPC/bR vesicles (Fig.6.3.b) in that spectral subtraction showed both to account for 30% of the total spin-label signal. By spectral simulation the proportion of motionally restricted component in the ESR spectrum of 14-PGSL in the DMPG/bR complex was found to be 25% of the total spin-label; in good agreement with the 26% determined for 14-PCSL in the DMPC/bR complex (Fig.3.27.a). Indeed spectral subtraction of the spectrum of 14-PGSL in the DMPG/bR complex from that of 14-

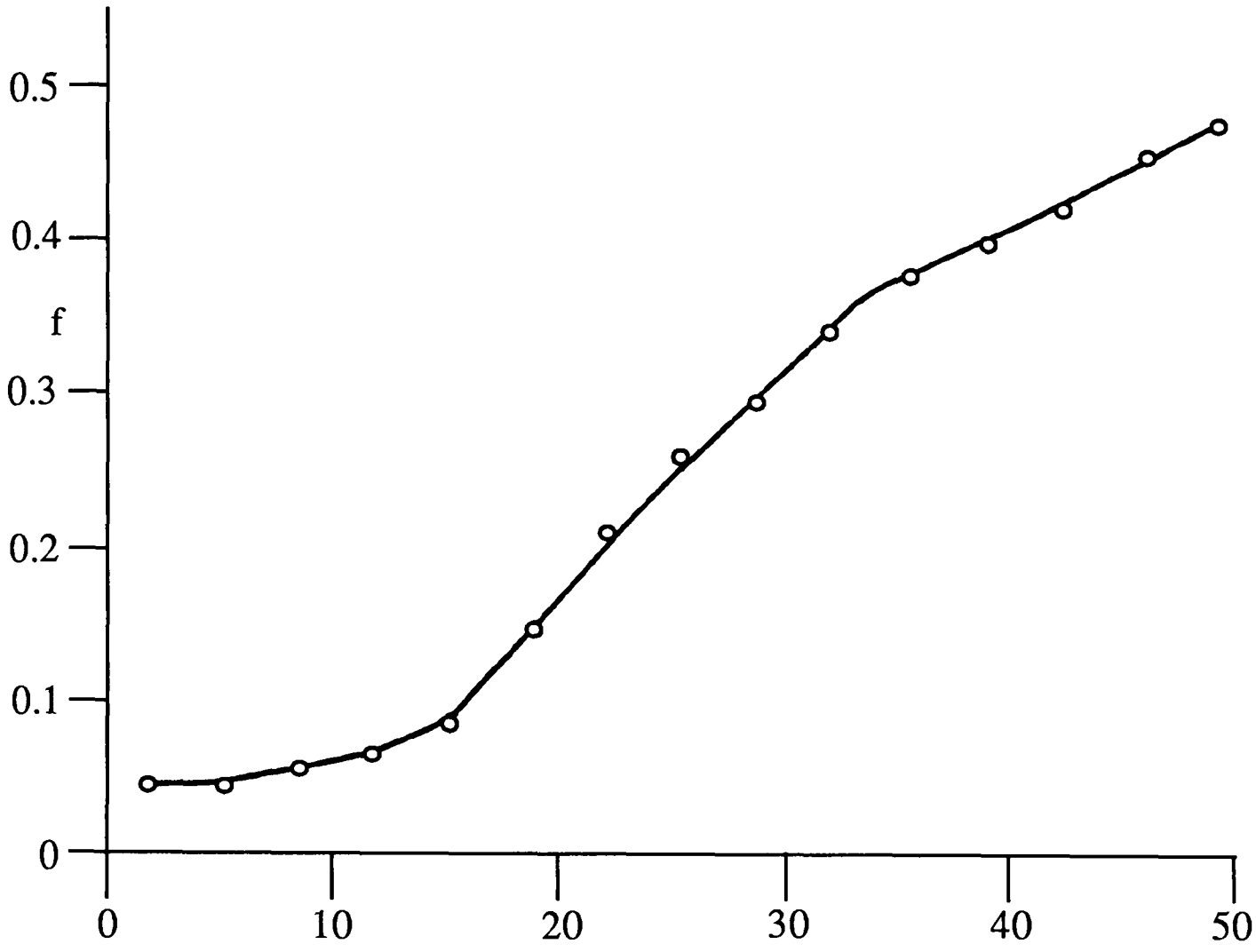


Fig.6.4. The phase transition for DMPG (as determined by TEMPO partitioning) is broadened in 71:1 mole ratio DMPG/bR vesicles though the mid-point is retained at 23°C. Vesicles in 150mM NaCl, 100mM Tris/HCl, 1mM EDTA, pH 7.6.

f is the apparent partition coefficient for the TEMPO spin-label determined from the peak heights (Marsh & Watts, 1982).

PCSL in the DMPC/bR complex and *vice versa* produced flat baselines (Figs.6.3.c and d). This presents evidence that the number of boundary lipids and hence the exposed protein surface areas are similar if not identical in both the 71:1 mole ratio DMPG/bR and the 68:1 mole ratio DMPC/bR complexes. Furthermore the apparent order parameters calculated for the fluid components of 14-PGSL in 71:1 mole ratio DMPG/bR complex (as described in Chapter 3) are increased relative to those of protein-free lipid by a similar degree to those determined for 14-PCSL and 14-PGSL in the 68:1 mole ratio DMPC/bR complex (Fig.3.25), implying similar protein-mediated perturbations on the lipid shells beyond the immediate boundary shell in both DMPC and DMPG systems. Determination of the magnitudes of the motionally restricted components by spectral subtraction (Figs.6.2 and 3.27) imply that in both DMPG and DMPC bilayers with lipid/protein molar ratios of 68:1 and 71:1, respectively, at 36(±1)°C, some 30% of the lipid is boundary lipid. Thus spectral simulation and subtraction analysis of ESR data demonstrate each 26,000 Da protein monomer appears to be associated with a boundary shell of 18 - 21 phospholipid molecules when reconstituted into either DMPC or DMPG bilayers at 36 (±1)°C. The spin-labelled phospholipid ESR data presents evidence that in the absence of the purple membrane phospholipids, the dispersion properties of bacteriorhodopsin in dimyristoyl phospholipid bilayers above the phase transition are the same irrespective of whether the phospholipid headgroup net charge is zero or one negative.

Effect of bacteriorhodopsin on the main gel-to-liquid crystalline phase transition. For DMPG lipid systems, the actual phase transition mid-point is dependent on the pH of the medium. At pH values well above the pK_a for the lipid phosphate group (pK_a is between pH 3 and 5 depending on the ionic strength; Sacre & Tocanne, 1977; Watts *et al.*, 1978; and Chapter 7 of this thesis), the phase transition is at 23 - 24°C for DMPG (Watts *et al.*, 1978). On titrating the aqueous medium pH to below the pK_a, however, the temperature for the phase transition increases to 45°C. All the experiments described in this chapter on the 71:1 mole ratio DMPG/bR complex were performed at pH 7.6, at which the phase transition for protein free DMPG is similar to that of DMPC

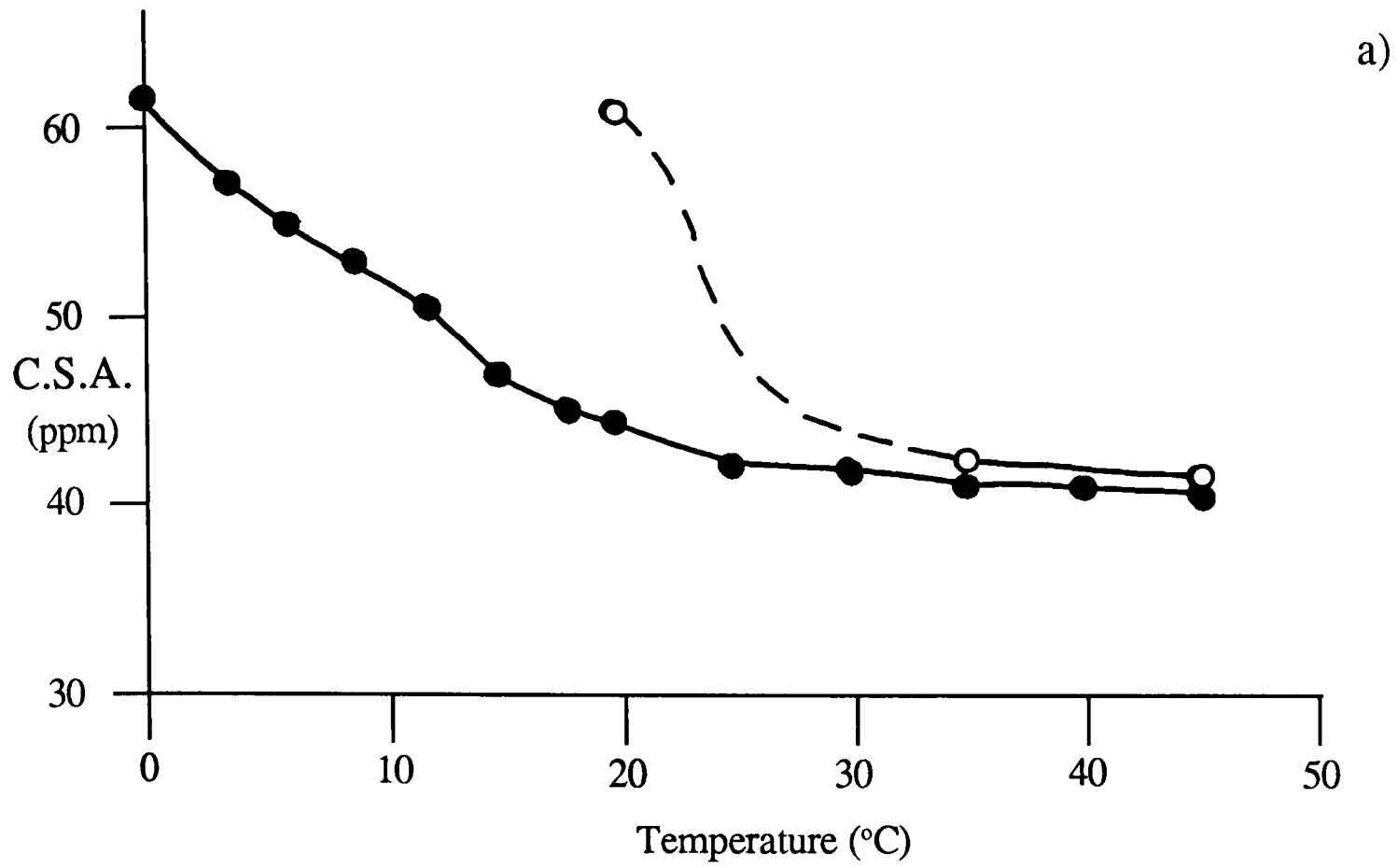


Fig. 6.5. Chemical shift anisotropies (C.S.A.) measured for protein-free DMPG bilayers (open) and for the 71:1 mole ratio DMPG/bR complex (filled) plotted as a function of temperature (a). Vesicles in 150mM NaCl, 100mM Tris/HCl, 1mM EDTA, pH 7.6.
^{31}P-NMR spectra (145.9 MHz) of DMPG/bR bilayers (71:1 mole ratio) with all endogenous purple membrane lipids removed at b) 0°C; c) 15°C; and d) 30°C.

bilayers; i.e. sharp and cooperative at 23°C (Watts *et al.*, 1978). The main phase transition for DMPG in the presence of bacteriorhodopsin (DMPG/bR mole ratio 71:1) is significantly broadened, compared to protein-free DMPG lipid systems, as measured by TEMPO partitioning (Fig.6.4.) and shows the main phase transition to begin at 14°C and end at approximately 33°C, with a midpoint at 23°C.

Effect of bacteriorhodopsin on broadline phosphorus-31 NMR spectra at different temperatures. The ^{31}P-NMR spectra of bilayers of protein-free DMPG at temperatures above the main phase transition (Fig.4.d; Introduction to this thesis) and DPPG (Wohlgemuth *et al.*, 1980) are characterised by typical fluid bilayer powder patterns (Seelig, 1978) with the measured c.s.a.s for both pure lipid systems being ~-42 ppm. Representative ^{31}P-NMR spectra (Fig.6.5.b.c and d) show that the DMPG phospholipids are also arranged in a bilayer conformation at all temperatures, between 0 and 45°C, in the 71:1 mole ratio DMPG/bacteriorhodopsin complex.

The chemical shift anisotropies measured from the phosphorus-31 NMR spectra of protein-free DMPG and the 71:1 mole ratio DMPG/bR complex are plotted as a function of temperature in Fig.6.5.a. On cooling through the phase transition temperature, the measured c.s.a. displayed in the phosphorus-31 NMR spectrum of protein-free DMPG is found to increase significantly to -61 ppm at 20°C (spectrum not shown). Similar observations were also reported for protein-free DPPG (Wohlgemuth *et al.*, 1980). Above 35°C, the measured c.s.a.s for the bacteriorhodopsin-containing complex are very similar to those observed for the protein-free DMPG system. However, a significant difference in measured c.s.a.s from the protein-free and bacteriorhodopsin-containing bilayers is observed at lower temperatures. Indeed, at 20°C, while the pure DMPG system displays a measured c.s.a. of -61 ppm, that measured for the protein-containing system at the same temperature is -44.3 ppm; i.e. the presence of bacteriorhodopsin (1 bR per 71 lipids) reduces the c.s.a. by some 17 ppm at 20°C. For the bacteriorhodopsin-containing complex, a c.s.a. value of -61 ppm is not attained until 0°C. The temperature profile displayed in Fig.6.5.a reveals a decrease in measured c.s.a. by 17 ppm for the bacteriorhodopsin-containing complex on

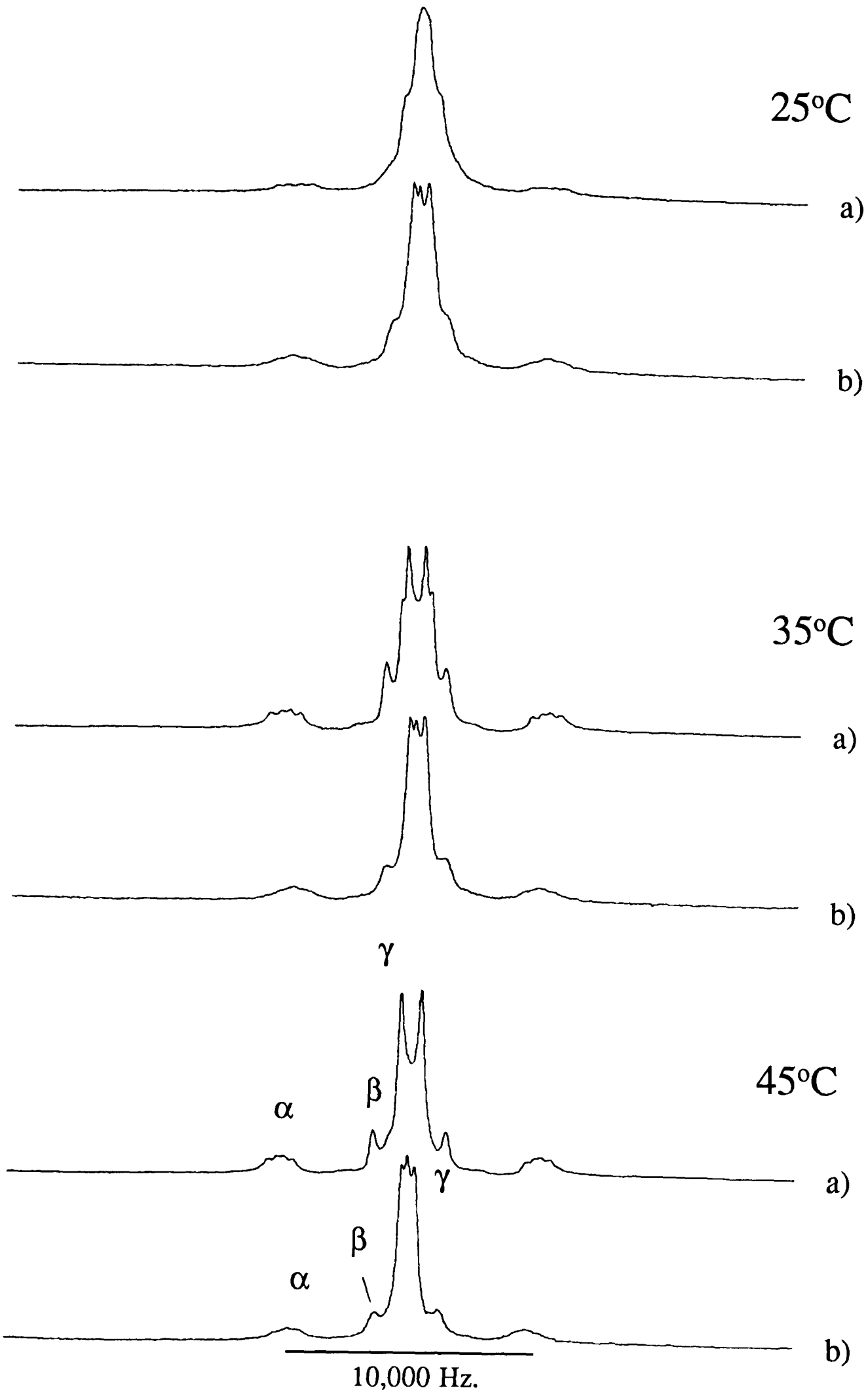


Fig.6.6. Comparison of ^{2}H-NMR spectra (55.3 MHz.) from DMPG-d_5 in a) pure lipid and b) 71:1 (mole ratio) DMPG/bR complex. Both samples as pellet from 150mM NaCl, 100mM Tris/HCl, 1mM EDTA, pH 7.6.

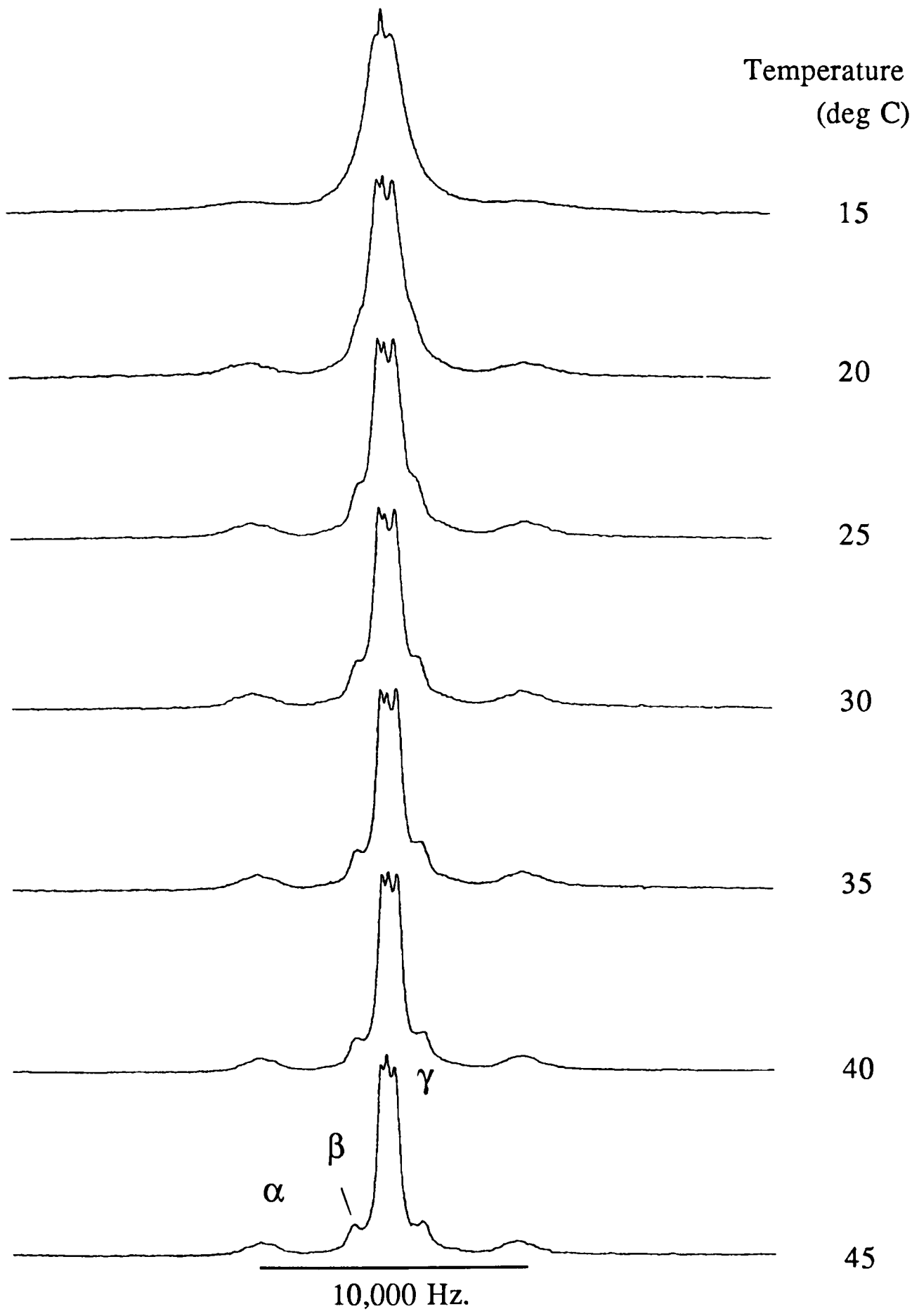


Fig.6.7. Temperature dependence of ^{2}H-NMR spectra (55.3 MHz.) obtained from DMPG-d_5/bR complex (mole ratio 71:1 with all endogenous purple membrane lipids removed). Vesicles in 150mM NaCl, 100mM Tris/HCl, 1mM EDTA, pH 7.6.

warming from 0°C to 20°C. Above 25°C, however, the c.s.a. remains insensitive to changes in temperature.

Effect of bacteriorhodopsin on broadline deuterium NMR spectra at different temperatures. ^{2}H-NMR spectra from the DMPG-d_5/bR complex (71:1 mole ratio) are displayed together with the corresponding spectra from protein-free lipid in Fig.6.6 and spectra for DMPG-d_5 bilayers with protein recorded from temperatures of 15 to 45°C are shown in Fig.6.7. For temperatures above the main phase transition, the spectra of DMPG-d_5 in both protein-free and protein-containing bilayers clearly display three major powder patterns, corresponding to those from the α-, β- and γ-segment deuterons of the glycerol headgroup (Wohlgemuth *et al.*, 1980). By comparing deuterium NMR spectra from various deuterated DPPGs (e.g. β-DPPG-d_1 and α-DPPG-d_2), Wohlgemuth *et al.*, (1980) were able to unambiguously assign the powder patterns of DPPG-d_5.

At 45°C, the measured quadrupole splittings for the protein-free DMPG-d_5 bilayers are 2,932Hz for the β-splittings and 815Hz for the γ-powder pattern. For the spectra of protein-free DMPG-d_5 bilayers, the broad α-powder pattern is seen to consist of four superimposed powder patterns of slightly different quadrupole splitting, ranging from 9,454Hz. to 11,401Hz at 45°C, which are very similar to those previously reported for DPPG (Wohlgemuth *et al.*, 1980). Furthermore for pure DMPG at 30 and 35°C, the two deuterons in the γ-segment of DMPG-d_5 also appear to be magnetically inequivalent and display two distinct powder patterns of different quadrupole splittings.

Well-resolved, single component deuterium NMR spectra, characteristic of random dispersions of fluid lipid bilayers are observed from the bacteriorhodopsin-containing bilayers at temperatures above 35°C. The presence of bacteriorhodopsin, however, is seen to broaden the deuterium NMR powder patterns relative to those of pure lipid bilayers. In particular the β-segment powder pattern is less well resolved at higher temperatures than for the protein-free DMPG bilayers (Fig.6.6). The broadening effect of the protein on the α-powder patterns abolishes the resolution of the four component powder patterns seen in the pure lipid spectra; similarly the two splittings

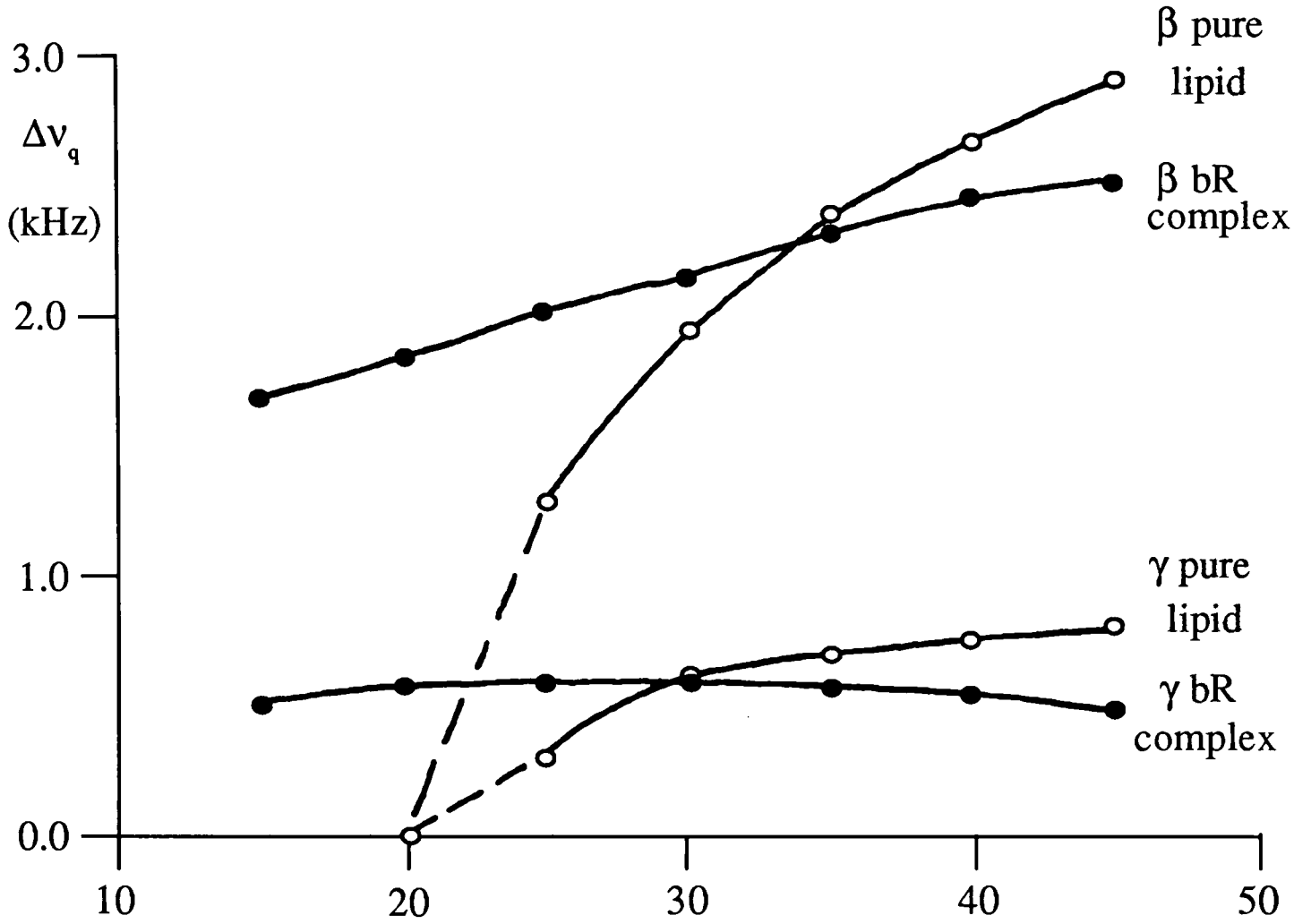


Fig.6.8. Deuterium-NMR quadrupole splittings ($\Delta\nu_q$) for the β- and γ-segment powder patterns of DMPG-d_5 in protein free bilayers and reconstituted with bacteriorhodopsin (DMPG/bR mole ratio 71:1) plotted as a function of temperature. Vesicles in 150mM NaCl, 100mM Tris/HCl, 1mM EDTA, pH 7.6.

for the γ-deuterons are not resolved in the presence of protein at 35°C.

The most significant differences between spectra from pure DMPG bilayers and those of the 71:1 mole ratio DMPG/bR complex is observed at lower temperatures (Fig.6.6). Below 25°C, the α-, β- and γ-segment powder patterns displayed in spectra of the protein-free lipid bilayers collapse into a single broad featureless spectrum. The presence of protein, however, suppresses this collapse to some extent and well-defined quadrupole splittings for the γ-segment powder pattern are resolved down to 15°C (Fig.6.7).

The measured quadrupole splittings for the β- and γ-powder patterns for both protein-free DMPG bilayers and the 71:1 mole ratio DMPG/bR complex are plotted as a function of temperature (Fig.6.8). As noted for protein-free DPPG-d_5 (Wohlgemuth *et al.*, 1980) the apparent quadrupole splitting for the β-segment deuteron of protein-free DMPG-d_5 increases with temperature. The increase is seen to be particularly significant on warming through the phase transition temperature; indeed below 25°C, the α-, β- and γ-splittings are collapsed for the pure lipid. The quadrupole splittings measured between 15 to 45°C, from the bacteriorhodopsin complex also increase with temperature, although in contrast to the pure lipid bilayers, they exhibit a close to linear and less steep temperature dependence. A similar temperature dependent increase is observed for the γ-segment splittings in the protein-free DMPG-d_5, although in the presence of protein the quadrupole splittings decrease above 30°C. At 25°C, both the β- and γ-segment quadrupole splittings are increased by the presence of bacteriorhodopsin relative to those of pure lipid. The presence of bacteriorhodopsin at 45°C, however, reduces the measured quadrupole splittings for all three powder patterns.

Effect of bacteriorhodopsin on the dynamic properties of the glycerol headgroup. ^{2}H-NMR spin-lattice (T_1) relaxation time measurements were determined by the inversion recovery method at 30 and 45°C for both protein-free DMPG-d_5 and the 71:1 mole ratio DMPG/bR complex in 150mM NaCl, 100mM Tris/HCl, pH 7.6 (Fig.6.9). The values obtained are presented in Table 1.

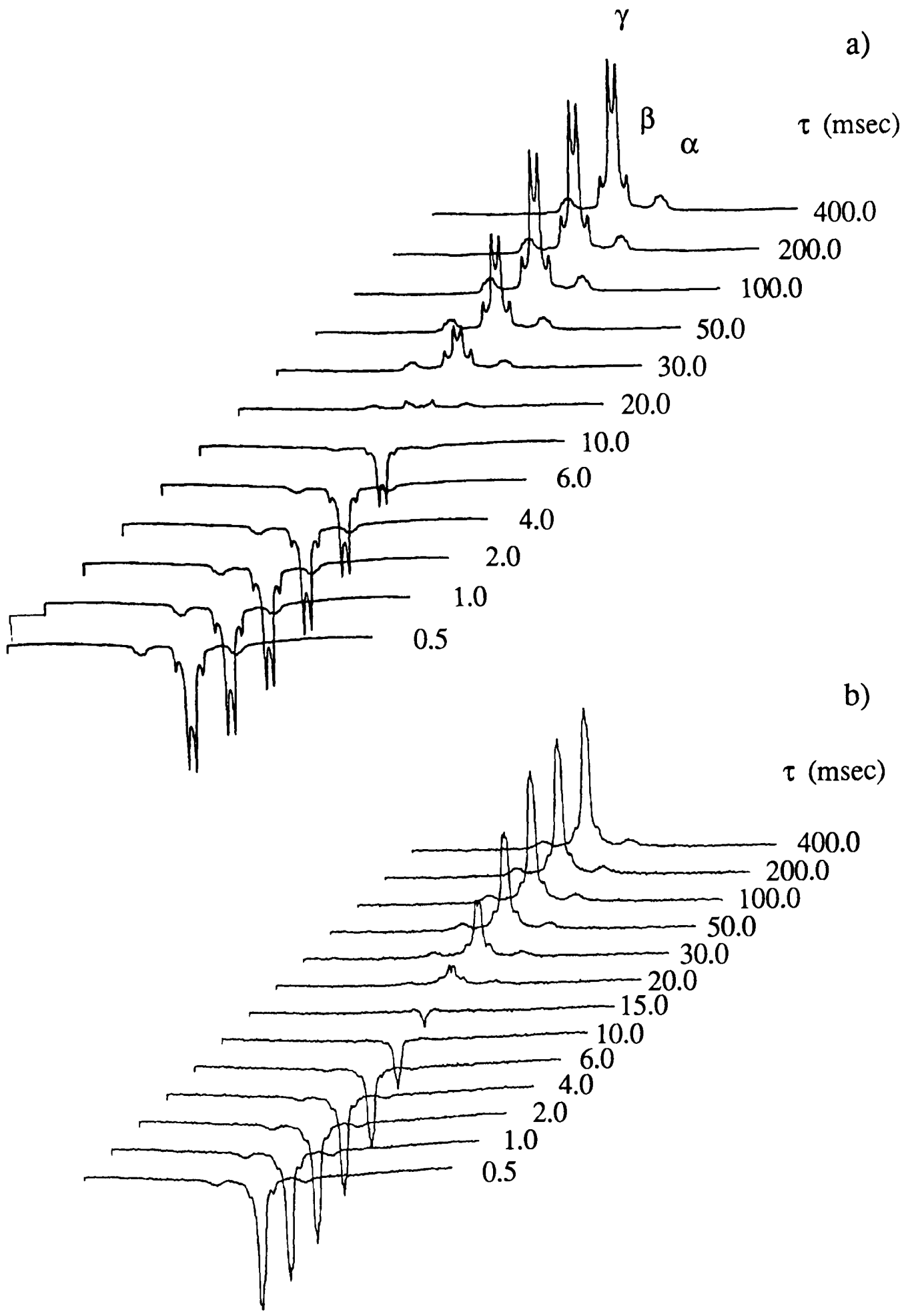


Fig. 6.9. ^{2}H-NMR (55.3 MHz.) longitudinal relaxation time (T_1) determinations using the inversion recovery method for DMPG-d_5 in protein-free bilayers (a) and with bacteriorhodopsin (b) (DMPG/bR mole ratio 71:1) at 45°C. Vesicles in 150mM NaCl, 100mM Tris/HCl, 1mM EDTA, pH 7.6.

Table 1. Deuterium-NMR spin-lattice relaxation times (T_1) measured (in ms) for the β- and γ-segments of DMPG-d_5 in protein-free bilayers and reconstituted in the 71:1 mole ratio DMPG/bR complex.

segment position	temperature (°C)	protein-free lipid	71:1 DMPG/bR complex
β	30	14.4	n.d.
β	45	20.0	17.8
γ	30	16.4	13.7
γ	45	29.0	24.0

It is apparent that for both protein-free lipid and the bR complex the effect of increasing the temperature is to almost double the spin-lattice (T_1) relaxation time for the γ-deuterons. This temperature dependent increase in T_1 value is also observed for the β-segment deuterons (although to a lesser extent) in the protein-free lipid system and is consistent with an increased rate of segmental motion on warming. At 45°C, the T_1 values measured for the γ-deuterons in both protein-free and bR-containing bilayers are longer than those for the corresponding β-deuterons. As the number of C-C single bonds between a segment and the phospholipid α-phosphate moiety increase, so the rate of segmental motion increases. Thus the overall dynamic properties (i.e. relative rates of segmental motion) and the temperature dependence of the rates of motion of the individual segments within the glycerol headgroup at the surface of DMPG bilayers are preserved in the presence of bacteriorhodopsin. The T_1 values, however, obtained for the bacteriorhodopsin-containing complexes were found to be slightly shorter than the corresponding values obtained for the protein-free DMPG bilayers, although the changes were not as significant as those observed for pure lipid on changing the

Fig.6.10.

Freeze fracture electron micrographs of DMPG/bR complex (ヲ) :1 mole ratio) in 150mM NaCl, 100mM Tris/HCl, 1mM EDTA, pH 7.6. Vesicles were quenched from 6°C. Bar = 1μm.

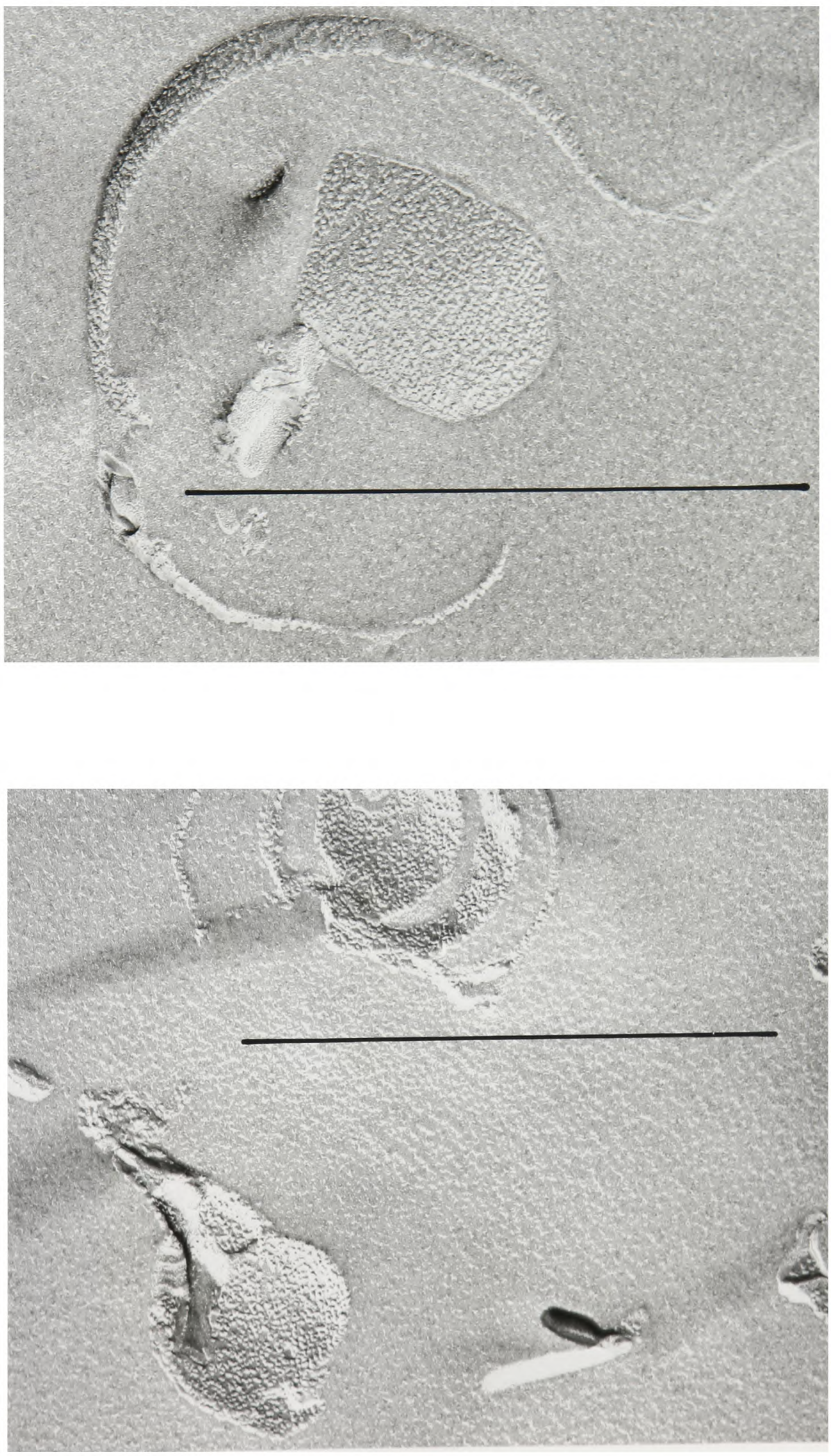
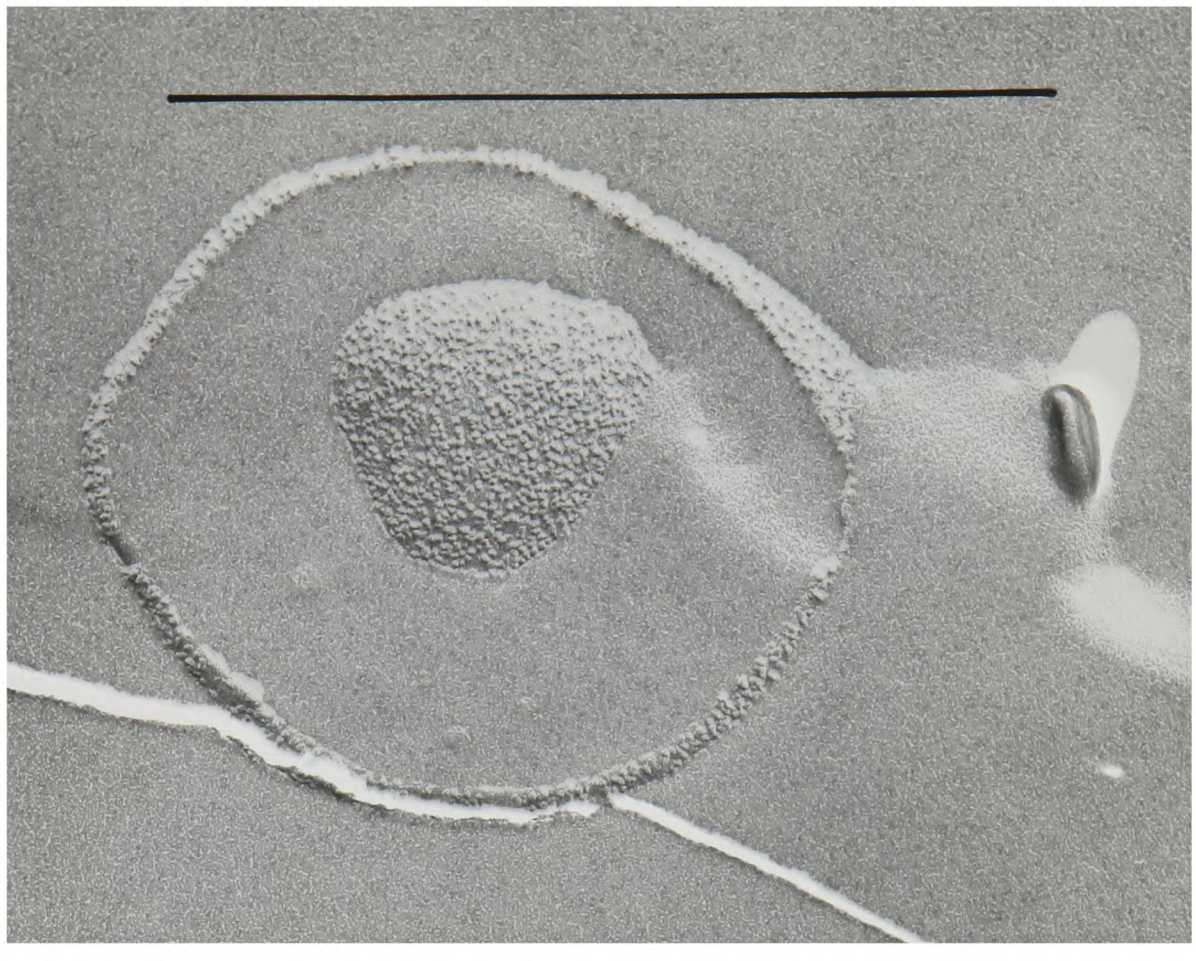


Fig.6.10 (cont.)



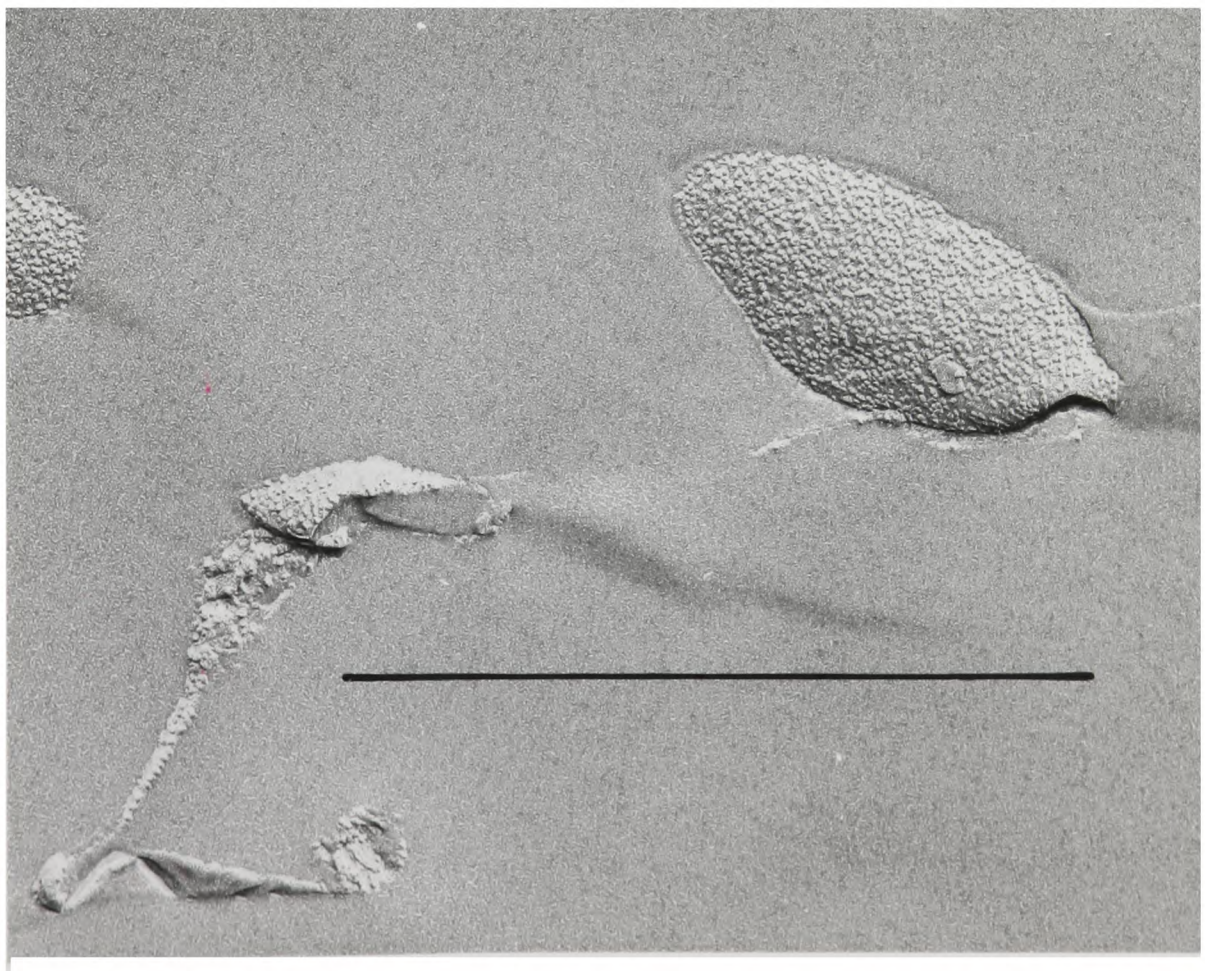


Fig.6.11.

Freeze fracture electron micrographs of DMPG/bR complex (7/ :1 mole ratio) in 150mM NaCl, 100mM Tris/HCl, 1mM EDTA, pH 7.6. Vesicles were quenched from 45°C. Bar = 1μm.

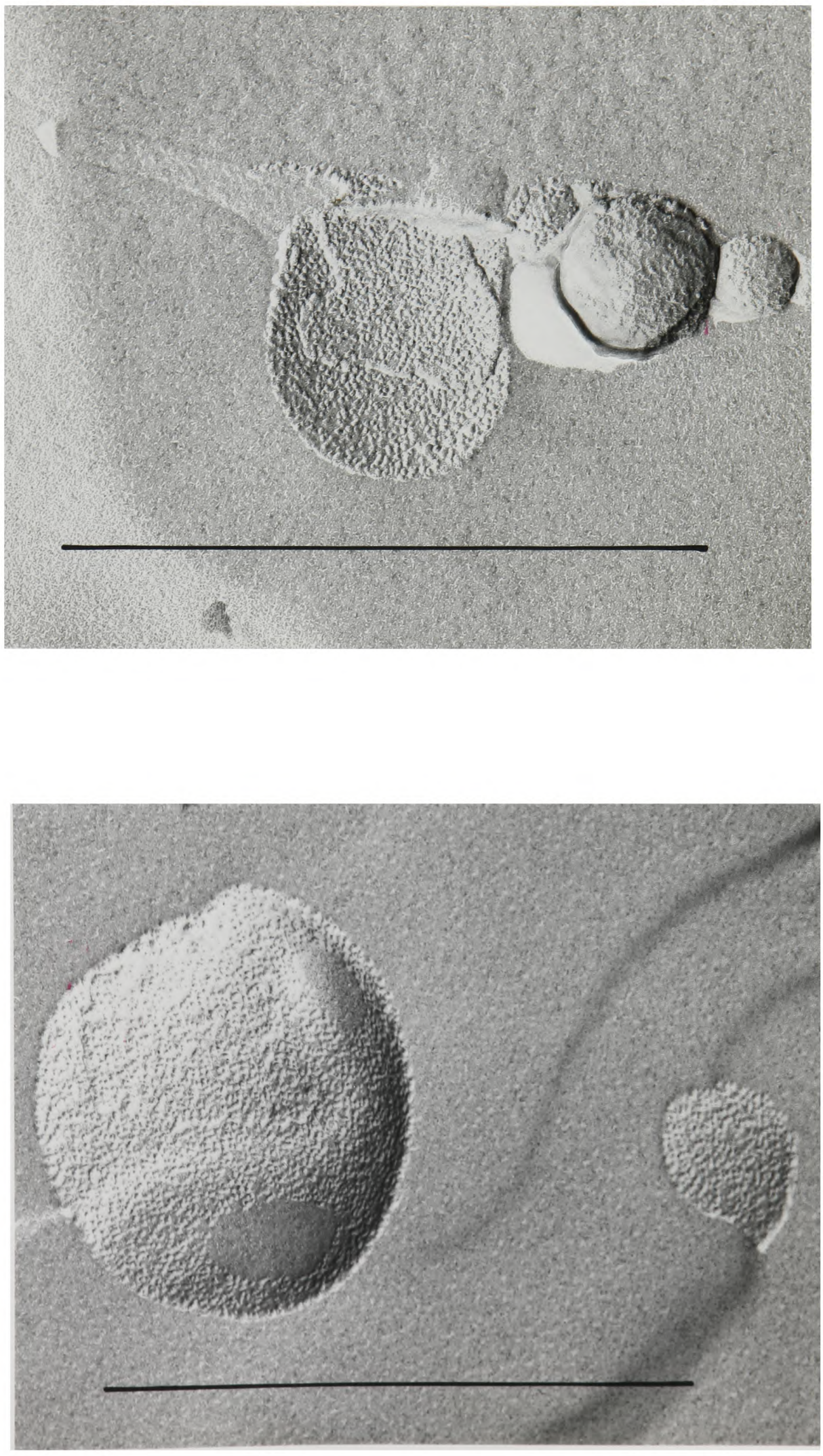
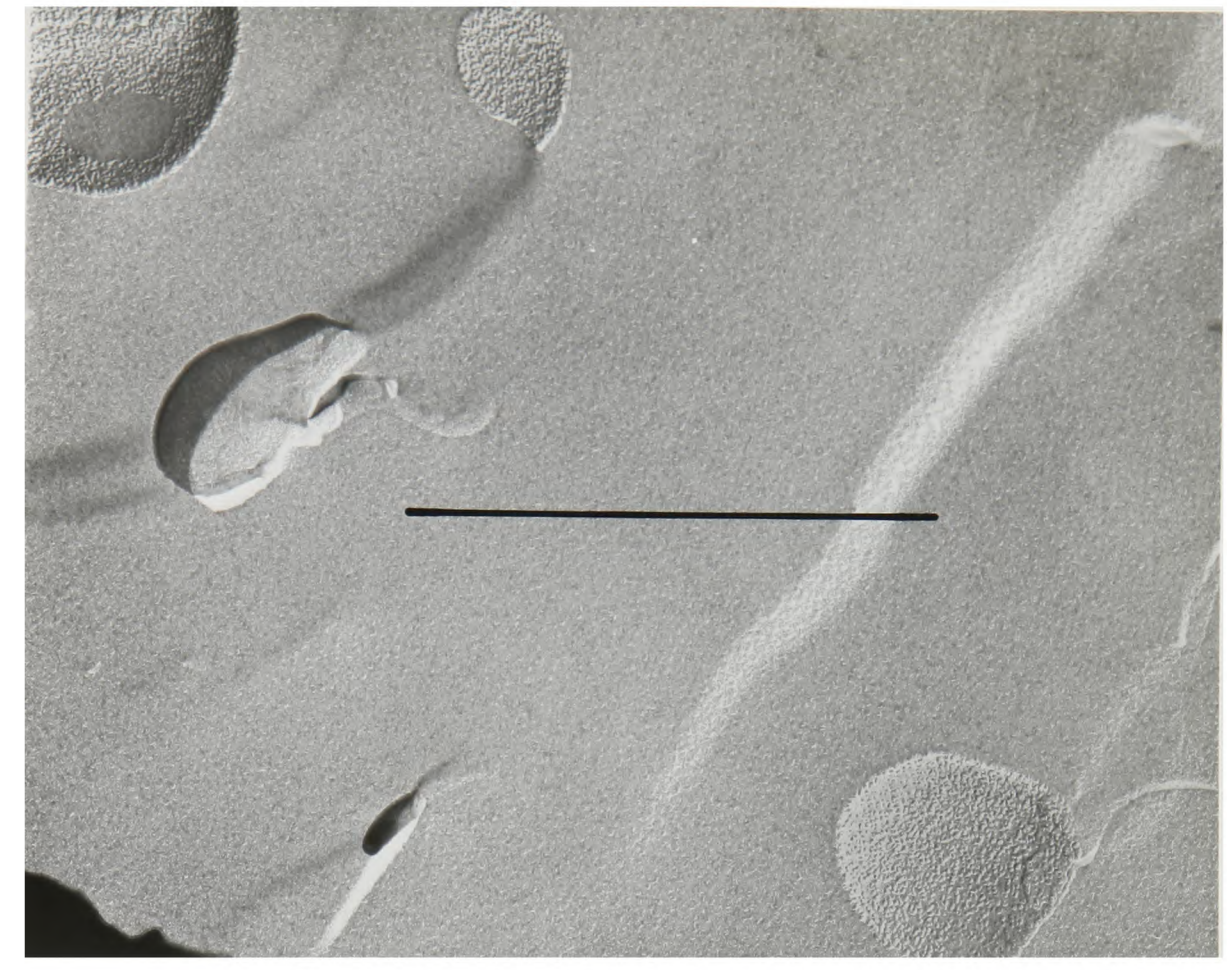


Fig.6.11 (cont.)



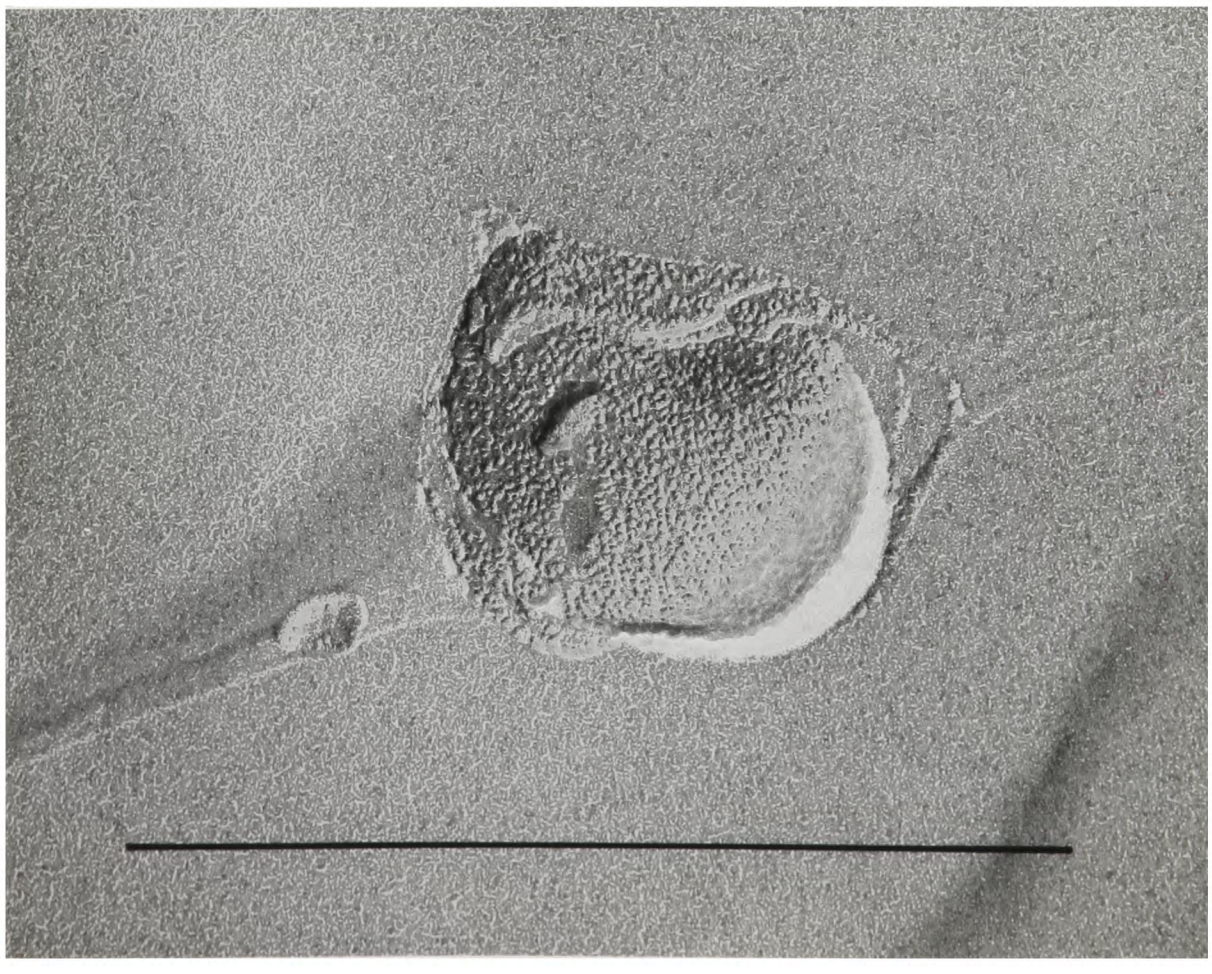


Fig.6.12.

Freeze fracture electron micrographs of DMPG/bR complex (ग१ :1 mole ratio) in 1mM EDTA, pH 7.6. Vesicles were quenched from 6°C. Bar = 200nm.

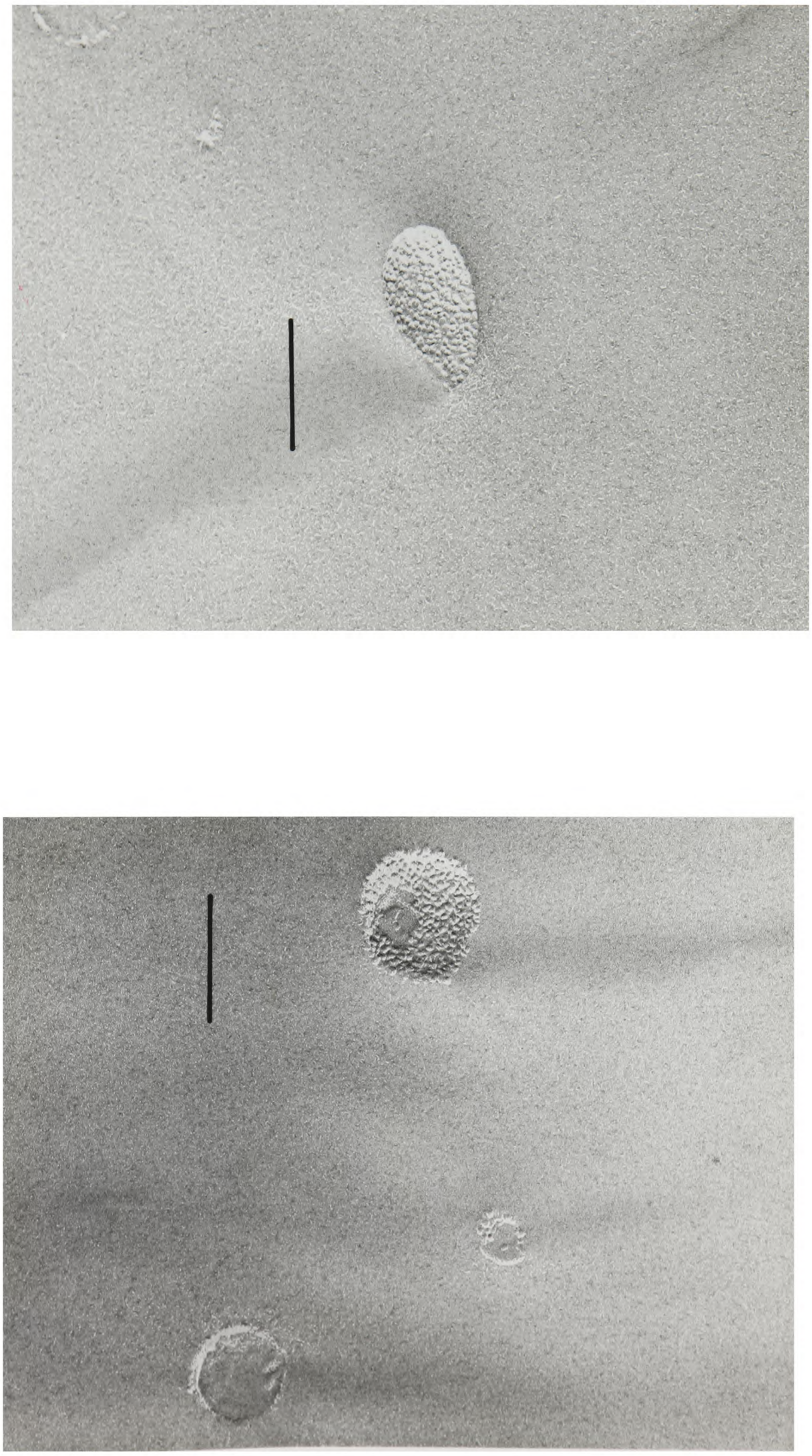
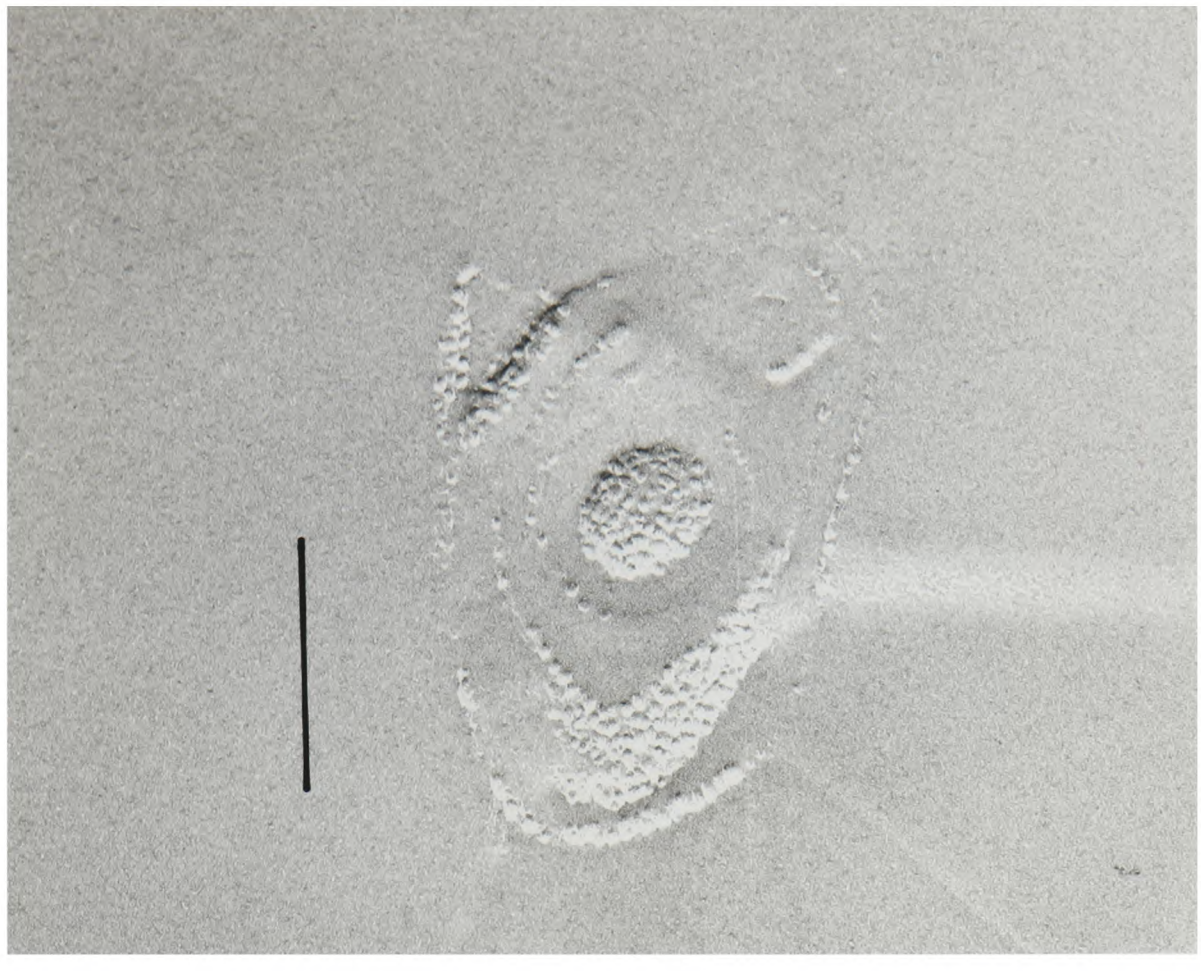


Fig.6.12 (cont.)



temperature from 45 to 30°C. The presence of a bulky integral membrane protein in the bilayer appears to hinder the rate of motion of the glycerol headgroup segments at the membrane surface.

Effect of lowering the ionic strength of the aqueous environment on solid state NMR spectra. The absence of salt in the buffer was found to little affect the deuterium and phosphorus-31 NMR spectra obtained form the protein complex, although the vesicle size is significantly reduced (below). The ^{31}P-NMR spectrum obtained at 35°C, was typical of that for phospholipids in a bilayer arrangement, displaying a measured c.s.a. of -41 ppm. At 45°C, the β- splittings were found to be very similar (within 4%), while the γ-splitting was found to be decreased from 504Hz to 332Hz on removal of the salt. The small residual γ-splitting of DMPG-d_5 renders this splitting most susceptible to the tumbling effects of small vesicles (see Table 6; Chapter 3).

Freeze fracture electron microscopy. Freeze fracture electron microscopy of the DMPG/bR complex in 150mM NaCl, 100mM Tris/HCl, 1mM EDTA, pH 7.6 quenched from temperatures of 6°C and 45°C (Figs.6.10 and 6.11, respectively) reveal large vesicles, some of which are clearly multilamellar structures. The outer bilayer membranes are between 700 and 1000nm in diameter, while the inner membranes are smaller at 300 to 500nm (diameter). As for the DMPC/bR complexes the fracture faces display numerous intra-membranous particles that are presumed to be bacteriorhodopsin particles. The diameters for these particles are in the order of 10nm and resemble those seen in all other bacteriorhodopsin/lipid systems so far studied (Chapters 4 and 5 of this thesis; Hwang & Stoeckenius, 1977; Cherry *et al.*, 1978; van Dijck *et al.*, 1981; Lewis & Engelman, 1983). When quenched from 6°C, all the protein particles exhibit a high degree of self-association, being arranged into small clumps or linear arrays. Very few particles, if any, are seen to exist free from contact with other particles. The protein particle aggregates are randomly interspersed with lipid pools. No extensive aggregates, however, are observed that display the hexagonal packing arrangement characteristic of bR in the purple membrane (Blaurock & Stoeckenius, 1971) or in DPPC bilayers below the phase transition with all endogenous

purple membrane lipids retained (Cherry *et al.*,1978). On quenching from 45°C, again no hexagonal crystalline packing arrangement is observed although there appears to be greater lateral segregation of protein particles than at 6°C; indeed some vesicles display large protein free patches with dimensions up to 100nm by 200nm; that are similar to those seen for DMPC/bR vesicles (Fig.4.3) quenched by the slow rate of cooling technique (~10^4 K.s^{-1}). Other vesicles, however, reveal well dispersed protein particles.

In Fig.6.12, freeze fracture electron micrographs of the DMPG/bR complex quenched from 6°C in 1mM EDTA alone are shown. It would appear that removal of the salt from the buffer effects a significant reduction in vesicle diameter. Some vesicles were very small with diameters of 100-150nm. There are still some multilamellar structures with outer bilayers of 400-500nm diameter. As in 150mM NaCl, the protein particles are highly self-associated into aggregates although no purple membrane structure is apparent.

6.IV). Discussion.

The reddish hue observed from the retinal chromophore of bR in DMPG vesicles suspended in 150mM NaCl at pH 7.6 indicates the beginning of a large shift in apparent A_{max} that is observed as the pH is increased to 10.5. (spectrum not shown). At pH 10.5, the sample is unrecognizable as bacteriorhodopsin, displaying a pinkish/orange colour (apparent A_{max} 500nm). UV/vis spectrophotometry and freeze fracture electron microscopy results indicate that DMPG/bR vesicles larger than 700nm in diameter are only stable in solutions containing salt. Removal of the salt causes the large vesicles to fragment into smaller vesicles, although the protein/lipid ratio appears to be conserved.

The large vesicle sizes displayed by freeze fracture electron microscopy are typical for the slow cholate removal technique (Chapter 2). As for other bacteriorhodopsin/lipid bilayers and in purple membrane itself, intramembraneous particles of approximately 10nm in diameter are observed that are presumed to be bacteriorhodopsin. When quenched from 6°C, in aqueous medium containing 150mM

NaCl, there was no evidence in the freeze fracture electron micrographs for the organization of the protein particles into the hexagonal structures observed for purple membrane. In view of the effect of salt on the low temperature aggregation of bacteriorhodopsin in nsTP-produced complexes (Fig.5.12), it could be argued that the presence of 150mM NaCl in the aqueous medium would suppress the ionic interactions between PG headgroups and positive charges on the protein surface responsible for mediating the crystallization. However, formation of hexagonal structures was also not observed in the absence of NaCl at low temperatures, even though removing the salt resulted in a uv/vis absorption spectrum more similar to that for purple membrane itself (Oesterhelt & Stoeckenius, 1974). Clearly, a single negatively-charged phosphoglycerol headgroup in combination with myristoyl chains is not sufficient to promote crystallization of bacteriorhodopsin into hexagonally ordered aggregates below the phase transition. This is not altogether surprising in view of the varied assortment of H.halobium membrane polar and non-polar lipids (Kates, 1978). It is possible that multiple negative charges per phospholipid headgroup, as in PGP and PGS, are important in a multivalent binding of the protein particles into the lattice. Also the phytanyl chains and squalenes in the hydrophobic core of the bilayer may play a role.

At low temperatures a supporting DMPG lipid bilayer appears to promote lateral phase separation into small aggregates of protein, containing around 6 protein particles and small protein-free lipid pools. Some linear arrays of protein particles (about 4-5 particles are also seen). These clusters are much more prominent in the DMPG complex, than observed the similar protein content 68:1 mole ratio DMPC/bR complex. Thus, DMPC at low temperatures (15.5°C) appears to promote organization of the delipidated bR particles into prominent linear arrays (Fig.4.1.f) or more evenly dispersed particles. It would appear that the presence of negatively charged headgroups at the surface of DMPG bilayers, although not able to promote formation of the hexagonally ordered aggregates (similar to those observed in the purple membrane) is, however, sufficient to mediate a greater degree of aggregation of the protein particles within the plane of the bilayer at temperatures below the phase transition than the

zwitterionic phosphocholine headgroups of DMPC bilayers. Thus the positively-charged N,N,N-trimethylammonium moiety of PC may oppose protein aggregation in the complete absence of the endogenous purple membrane lipids.

There are, however, clear similarities displayed by delipidated bacteriorhodopsin in DMPC bilayers (Chapter 3) and in DMPG bilayers. In both systems, freeze fracture electron microscopy reveals the presence of particles ~10nm in diameter. If these particles do indeed represent oligomeric particles (Fisher & Stoeckenius, 1977), then it would appear that protein-protein interactions are important in their formation and maintainance as they are observed in all lipid environments so far studied, irrespective of the net surface charge of the bilayer or whether the endogenous purple membrane lipids are present (Hwang & Stoeckenius, 1977; Cherry *et al.*, 1978; van Dijck, 1981; Lewis & Engelman, 1983) and, furthermore, in DMPC bilayers (Fig.4.4) their integrity is preserved in both low salt aqueous media and in the presence of 4M NaCl. As discussed in Chapter 3, however, it is possible that the presence of these oligomeric structures is an artifact of the freezing or etching process. Consitstent with this, is the observation of similar sized protein-particles in freeze-fracture electron micrographs of rhodopsin (Olive *et al.*, 1978), which is also shown to be monomeric by biophysical techniques (Cone, 1972). Alternatively, it is proposed (Cherry *et al.*, 1978) that these oligomeric structures are formed during the freezing process itself; lateral diffusion rates of the bacteriorhodopsin monomers within the lipid bilayer being fast enough to allow formation of these 11nm particles from monomers within close proximity of each other on quenching.

Furthermore in both DMPC and DMPG bilayers in the absence of the endogenous purple membrane phospholipids, each 26,000 Da bacteriorhodopsin monomer displays the same number of boundary lipids, that is between 18 - 21 phospholipids as determined by quantitative analysis of ESR data. This number of boundary lipids is consistent with the bacteriorhodopsin particles existing in a more dispersed state, possibly completely monomeric, than in purple membrane, itself; protein/lipid interactions being increased at the expense of protein-protein contacts. As discussed in

Chapter 3, the number of boundary lipids observed for bacteriorhodopsin reconstituted into DMPC and DMPG bilayers, free of endogenous purple membrane lipids, is similar to for rhodopsin (Ryba, 1986; Watts *et al.*, 1979). This is inconsistent with the aggregation of some nine to twelve 26,000 M_r bR monomers into the 11nm diameter particles observed in freeze-fracture electron microscopy. It would appear that in both DMPG and DMPC bilayers free of endogenous purple membrane lipids, that the number of boundary lipids directly in contact with each bacteriorhodopsin monomer is somewhat greater than in purple membrane, and similar to that expected for fully monomeric protein (Marsh & Watts, 1982).

Another similarity between bacteriorhodopsin reconstituted into DMPG and DMPC bilayers is the effect on the main phase transitions for the myristoyl chains; bacteriorhodopsin broadening out the transition. Even, however, at the relatively high bR contents used (68:1 mole ratio DMPC/bR and 71:1 DMPG/bR) the phase transition midpoint is retained at 23°C.

Above the phase transition, the ^{2}H-NMR spectra of protein-free DMPG-d_5 obtained are very similar to those presented by Wohlgemuth *et al.*, (1980) for DPPG-d_5. In common with other headgroup lipids e.g. PC (Gally *et al.*, 1975) the further the deuterium from the α-phosphate group, the smaller the residual quadrupole splitting implying greater restriction of motional freedom the closer the segment is located to the glycerol backbone. The spin-lattice (T_1) relaxation times determined for the β- and γ-segments support increased rate of segmental motion with increasing distance from the glycerol backbone. Similar dynamic properties were demonstrated for segments in the choline headgroup using ^{13}C-NMR spin-lattice relaxation times (Levine, *et al.*, 1971). The observed increase in the quadrupole splitting for the β- and γ-segments with temperature is unusual since an increase in temperature is expected to lead to a greater amplitude of motion and thus a smaller quadrupole splitting as observed for DMPC (Chapter 3; Gally *et al.*, 1975). Wohlgemuth *et al.*, (1980) have suggested that the increase in quadrupole splitting reflects a small change in the torsion angle of the C-D bond such that its average orientation moves away from the magic angle to which it is

already close. The presence of two quadrupole splittings from a single CD_2 group is the exception rather than the rule, although the α-methylene CD_2 headgroup segment of PC (Fig.3.10) (Gally *et al.*, 1975; Brown and Seelig, 1978) and PE (Browning and Seelig, 1980) do display two distinct powder patterns. Wohlgemuth *et al.*, (1980) presented conclusive evidence that the two quadrupole splittings displayed by the DMPG α-methylene segment are due to the two deuterons experiencing small motional inequivalence and not due to a slow conformational equilibrium between two headgroup structures. The presence of two of the three separate powder patterns from the α-deuterons in DPPG with racemic headgroup glycerol is attributed to magnetic inequivalence of the two deuterium atoms at the α-carbon in the 3,3'-DPPG optical isomer (Wohlgemuth *et al.*, 1980). Thus DPPG in which a single deuteron was stereospecifically introduced to the α-methylene segment gave a single quadrupole splitting corresponding exactly to one of the two from α-DMPG-d_2. The 3,1'- DPPG optical isomer was found to give a single quadrupole splitting.

At temperatures corresponding to the completion of the phase transition for the DMPG in the protein-complex (34°C), the ^{2}H-NMR quadrupole splittings are seen to be little affected by the presence of protein; on warming to higher temperatures (45°C), the values for the α-, β-, and γ-splittings are slightly less than those observed for protein-free lipid. This implies that the presence of bacteriorhodopsin induces only small structural distortions of the glycerol headgroup above the phase transition. Similar effects were observed for the binding of the cationic peptide polymyxin B to DMPG membranes (Sixl & Watts, 1985). Myelin basic protein at 35°C was found to reduce the quadrupole splittings (Sixl *et al.*, 1984) with increasing protein content. As observed for DMPC/bR systems the individual quadrupole splittings from the two α-methylene segment deuterons and those of the γ-CD_2 segment are no longer resolvable due to a protein-mediated T_2 relaxation broadening effect.

Deuterium-NMR relaxation rates, $R_1 = 1/T_1$, are dominated essentially by the rate of reorientation (i.e. rate of motion) of the segment involved and depend only slightly on the ordering for small degrees of anisotropic motion (Brown *et al.*, 1979). Thus

increases in the measured T_1 times for both the β- and γ-segments observed on increasing the temperature, imply a greater rate of motion at higher temperatures. At 45°C, the T_1 values obtained from the γ-segment is longer than that for the β-segment. These results are consistent with faster rates of motion for the γ-segment than the β-segment in both protein-free lipid and the bacteriorhodopsin complex. The presence of bacteriorhodopsin in the DMPG bilayer, however, serves to reduce the rates of segmental motion within the glycerol headgroup at the membrane surface relative to protein-free lipid as judged by the decrease in T_1 values. Similar results were also observed for T_1 values measured in the presence of myelin basic protein in DMPG (Sixl *et al.*, 1984). The temperature dependency of the dynamics for the γ-segment is preserved in the presence of protein as are the relative rates of segmental motion within the glycerol segment itself.

The ^{31}P-NMR spectra obtained from the 71:1 DMPG/bR complex do not exhibit a broad component in addition to the fluid bilayer lipid signal. It has been suggested (Yeagle, 1982, 1984; Albert & Yeagle, 1983) that intrinsic membrane proteins are able to cause motional restriction or immobilisation of lipids on the phosphorus-31 NMR time scale of anisotropic averaging leading to broad ^{31}P-NMR spectral components or to a reduction of the lipid intensity due to the presence of an unobserved broad component. Phosphorus-31 spectra obtained from rod outer segments and sarcoplasmic reticulum membranes (containing Ca^{++}-ATPase) were reported to consist of only a narrow component (Ellena *et al.*, 1986) indicating that most or all of the phospholipids are in a liquid crystalline phase at 22°C. If the DMPG were ordering the bR particles into the hexagonal paracrystalline lattice of purple membrane, then two possible effects on the phosphorus-31 powder patterns might be expected.;

First, if the timescale for exchange of lipids between the fluid phase and those trapped in the paracrystalline lattice were slow on the NMR time scale of averaging of the ^{31}P- or ^{2}H-anisotropy i.e. less than 10,000 exchanges per second, then two component spectra would be observed; one component corresponding to fluid DMPG (csa ~-40ppm) and a second component, similar to the phosphorus-31 NMR spectrum

for purple membrane itself (Fig.4 Introduction), from lipid trapped in the protein lattice (with a c.s.a. of approximately -60ppm).

Second, if the timescale for exchange of lipids between the bulk bilayer phase and any purple membrane like domain were fast i.e. greater than 10,000 exchanges per second, then a single component phosphorus spectrum would be observed, but with a c.s.a. larger than that observed for pure lipid. This is also not observed.

Above the phase transition, the ^{31}P-NMR c.s.a. of DMPG is virtually unaffected by the presence of bacteriorhodopsin. This contrasts with the phosphorus-31 c.s.a.s measured from *H.halobium* natural membranes (Fig.4 Introduction), which contain PG related phospholipids but much higher protein contents; namely purple membrane (csa for PGP-α phosphate -60.7ppm i.e. 19ppm larger than for pure PGP) and red membrane (c.s.a. for PGP-α phosphate -53.5 ppm i.e. 13 ppm larger than pure PGP). In these two membranes, the increase in c.s.a. relative to pure lipid is related to the protein content. It is interesting to note that the c.s.a. measured for purple membrane at 33°C, is of similar magnitude to that for DMPG below the phase transition. The extreme ordering of the PGP molecules in the paracrystalline purple membrane lattice is responsible for the large c.s.a..

The bacteriorhodopsin content (1.4 mol%) in the DMPG bilayers of the DMPG/bR complex studied in this chapter, may be insufficient to produce a significant effect on the phosphorus-31 c.s.a.. Indeed for the similar protein content 67:1 mole ratio DMPC/bR complex (Fig.3.14.a) the phosphorus-31 c.s.a. reported is very similar to that for protein-free DMPC.

From the broadline phosphorus-31 spectra, the presence of a relatively high bacteriorhodopsin content (1.4 mol%) in DMPG bilayers below the phase transition is seen to reduce the ordering of the phospholipid headgroup at low temperatures when compared with protein-free bilayers. Protein-free DMPG at pH 7.6, is in the gel phase at 20°C. The increased motional restraints and reduction in amplitude of motion are reflected in the large c.s.a. obtained for pure DMPG at 20°C of -61ppm. On warming protein-free DMPG or DPPG through the phase transition, the measured c.s.a. is

sharply reduced (Wohlgemuth *et al.*, 1980) to -41ppm. The change observed, however, in the phosphorus-31 c.s.a.s measured for the bacteriorhodopsin-containing bilayers over the 15 to 30°C range is much less significant. Similar trends are displayed by the ^{2}H-NMR measured quadrupole splittings for the α-, β- and γ-deuterons on the glycerol headgroup (Fig.6.8). While the quadrupole splittings measured for protein-free DMPG bilayers collapse sharply on cooling below the main phase transition, the values obtained in the presence of protein are relatively unaffected over the 15 to 30°C temperature range.

TEMPO-partitioning data (Fig.6.4), however, reveals little change in partition coefficient between 0 and 14°C. In contrast, the measured phosphorus-31 c.s.a. displays a 24% change over this temperature range. The high sensitivity to changes in temperature observed in the measured ^{31}P-NMR c.s.a.s at temperatures below 15°C is thus unlikely to be due to the phase transition and could be interpreted in terms of a change in the aggregation state of the protein below the DMPG phase transition; this may reflect the association of protein particles into small aggregates and lipid free pools observed by freeze fracture electron microscopy in complexes quenched from 6°C (Fig.6.10). Deuterium NMR spectra were not collected below 15°C, but in agreement with the phosphorus-31 NMR data (Fig.6.5), did not exhibit the marked temperature dependence observed for pure lipid over the 15 to 45°C temperature range (Fig.6.8).

Chapter 7

Membrane electrostatics - effect of lipid headgroup composition and ionic strength on the retinal chromophore properties of bacteriorhodopsin.

7.I) Introduction.

From chapters 3,4,5 and 6 of this thesis, it appears that interactions between the lipid headgroups and bacteriorhodopsin surface charges may influence packing properties of the protein. Evidence will be presented in this chapter, that the lipid composition of the supporting bilayer, in conjunction with the aqueous environment solute properties also influences the spectroscopic properties of the retinal chromophore.

The spectroscopic property of the retinal chromophore that is investigated in this chapter is the shift in A_{max} to longer wavelengths that occurs on acidifying the aqueous medium below pH 3.2 (Edgerton *et al.*, 1980; Moore *et al.*, 1978). It is reported (Szundi and Stoeckenius, 1987) that purple membrane (A_{max}=568nm) can be converted reversibly to blue membrane (A_{max}=605nm) by either acid titration or deionization. These authors demonstrated that removing 75% of the purple membrane lipids prevented the blue shift induced by deionization but not the shift induced by acidification. The pK_a for the purple to blue transition of native purple membrane was between pH 3 and 4; while for the partially delipidated bacteriorhodopsin it was shifted to pH 1.4. The two states of the membrane (purple or blue) probably reflect two conformations of the protein, which are controlled by titration of acid groups at the surface of the membrane. Indeed the spectral distribution and temperature dependence of the blue species suggest that it may be closely related to the photocycle intermediate O (Moore *et al.*, 1978; Mowery *et al.*, 1979). The purple colour, however, returns on further acidification of the aqueous medium (Szundi & Stoeckenius, 1987).

Due to the rigidity of the paracrystalline bacteriorhodopsin lattice, purple

membrane itself cannot form vesicles. One problem with titrating purple membrane to low pH values is that the particles aggregate considerably, so making visible absorption spectroscopy difficult. This has been successfully overcome in the Stoeckenius group by incorporating the protein into 7.5% polyacrylamide gels. Another method (adopted here) of reducing aggregation is to produce sealed phospholipid vesicles. This also offers the advantage of being able to control the phospholipid environment and hence study the effect of different phospholipid headgroups on the chromophore properties of the protein. In this chapter, the pK_as for the purple to blue shift of the retinal chromophore are determined for bacteriorhodopsin in different lipid headgroup environments. For some bacteriorhodopsin complexes the effect on the apparent pK_a for the purple to blue shift of varying the ionic strength of the aqueous medium is also investigated.

Also in this chapter, the pH titration properties of the phosphate groups in PC and PG bilayers are investigated. The phosphate diester moiety of phospholipids has a single ionizable oxygen, the actual pK_a of which is dependent on the nature of the phospholipid headgroup. The variation of lipid phase transition temperature with pH is one method that has been used to determine pK_as of phospholipid headgroups. Reduction of the membrane surface charge by protonation of the phosphate alters the packing properties of the headgroup (Tocanne, *et al.*, 1974; Sacre & Tocanne, 1977) and raises the phase transition temperature (Cullis & de Kruijff, 1976; Watts *et al.*, 1978). Thus, a pK_a of less than 2 for phosphatidylcholines and ~9.5 for the second ionisation of phosphatidic acid was demonstrated (Trauble & Eibl, 1974). The pK_a value for PA was found to be reduced to ~8 by 0.5M NaCl. A pK_a value of 2.9 (150 mM KCl) (Watts *et al.* 1978) and between 3.1 and 3.5 (150mM NaCl) (van Dijck *et al.* 1978) was obtained for DMPG using TEMPO partitioning and DSC respectively. Monitoring changes in the bilayer surface area with pH gave pK_a values for PG bilayers between 3.0 and 5.5 depending on the ionic strength (Sacre & Tocanne, 1977).

Another method, used in this chapter, is to record the change, relative to pH, in the chemical shift of the phosphate resonance measured from high resolution ^{31}P-NMR

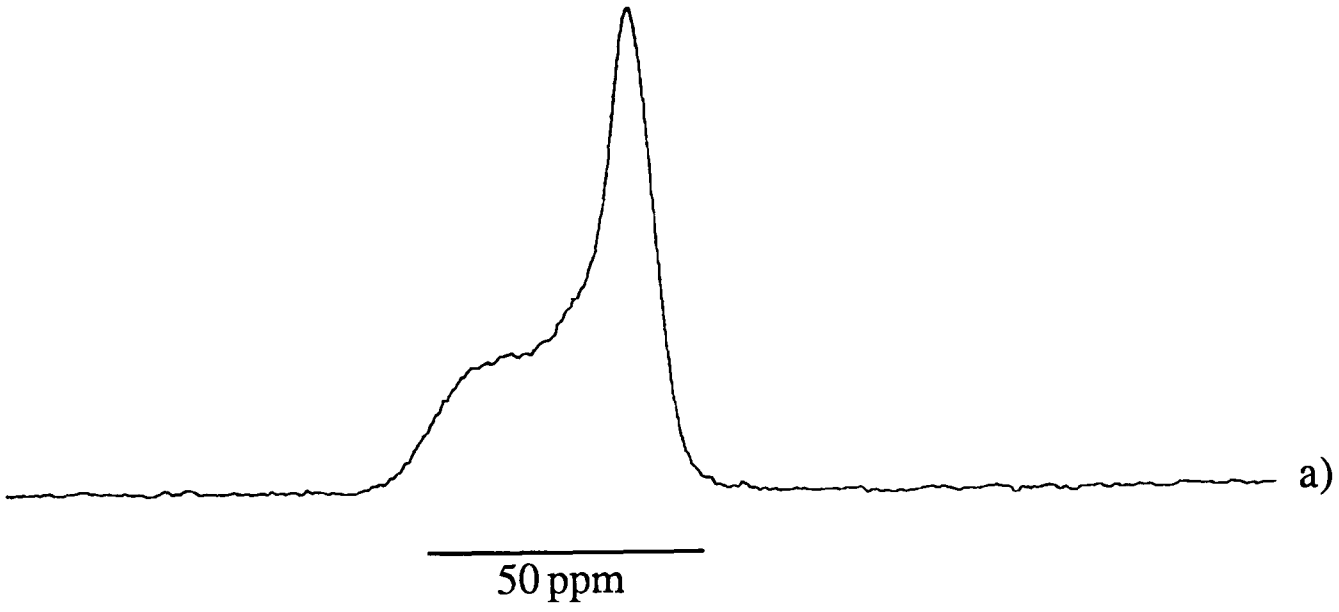


Fig.7.1. ^{31}P-NMR spectra (145 MHz) of phospholipids in aqueous solutions; a) broadline spectrum of DMPG extended bilayers in 150mM NaCl, 100mM Tris/HCl, 1mM EDTA, pH 7.5, 35°C; b) high resolution spectrum of DMPG SUVs produced by tip sonication in 5mM EDTA, pH 7.6, 50°C; and c) high resolution spectrum of binary DMPG/DMPC (1:1 mol/mol) SUVs in 5mM EDTA, pH 7.3, 50°C.

spectra of sonicated phospholipid bilayers. When DMPC or DMPG are dispersed in aqueous solutions large multilamellar vesicles with extended bilayers structures are formed. Such structures display a typical bilayer powder pattern (Fig 7.1.a) by ^{31}P-NMR and direct pH titration of the phosphate group in bilayer spectra is impossible. On tip sonicating, however, the large bilayer structures are fragmented into small unilamellar vesicles (SUVs). The rapid rate of Brownian motion tumbling of these small diameter vesicles is sufficient to completely time-average the anisotropy of the phosphorus nucleus, with the result that a sharp isotropic ^{31}P-NMR signal (Fig 7.1.b) is observed (Burnell *et al.*, 1980). This technique allows a direct estimation of the apparent pK_a of the phospholipid while in the "bilayer-like" conformation of an SUV by NMR. Using this technique, Koter, *et al.*, (1978) obtained a pK_a value for the second ionisation of phosphatidic acid which agreed with that determined by phase transition methods (Trauble and Eibl, 1974). In a recent paper, van Paridon *et al.*, (1986) determined the pK_a values of the monoester phosphate moieties of phosphatidyl inositol-4-phosphate and -4,5-bisphosphate to be 6.2, 6.6 and 7.7, respectively by ^{31}P-NMR of sonicated vesicles.

Furthermore due to the different hydrogen bonding capabilities (Henderson *et al.*, 1974) and chemical environments of the phosphate groups in DMPC and DMPG, the respective ^{31}P-NMR resonances of these phospholipids in detergent micelles or SUVs have different chemical shifts (Fig 7.1.c). Thus, at pH 7.3, the DMPC signal is well resolved from the DMPG phosphorus-31 resonance. This allows determination of the individual pK_as for the PG and PC phosphate moieties while in a binary mixture. This is a unique advantage of the technique over other methods (e.g.TEMPO partitioning; Watts *et al.*, 1978 and DSC; van DijcK *et al.*, 1978) that use changes in phase transition temperature or methods that use changes in mean molecular area (Sacre & Tocanne, 1977) to determine a pK_a.

In this chapter, high resolution ^{31}P-NMR of sonicated phospholipid small unilamellar vesicles (SUVs) is used to investigate the pK_a properties of the PG and PC phosphate moieties in single and binary lipid bilayers in aqueous media of different

ionic strengths. By altering the NaCl concentration of the aqueous environment, the effects of ionic strength on the apparent pK_as is investigated. The pK_as obtained for the phosphate groups of different phospholipids are seen to correlate with those obtained for the purple to blue shift of bacteriorhodopsin in similar lipid environments, further substantiating the conclusion of Szundi & Stoeckenius, (1987) that the lipid surface charge is significant in effecting the purple to blue shift of the retinal chromophore.

II) Materials and Methods.

1,2-dimyristoyl-*sn*-glycero-3-phosphocholine (DMPC), Mr 678 and 1,2-dimyristoyl-*s*n-glycero-3-phospho-*rac*-glycerol (ammonium salt) (DMPG) Mr 683.9 were purchased from Sigma Chemical Co..

For the single lipid systems, the phospholipid was resuspended in the appropriate buffer and tip sonicated until the milky suspension became clear. During sonication the sample was maintained at 45°C using a water jacket connected to a water bath. The DMPG samples at low pH were sonicated at pH 8.0 before lowering the pH and then resonicating. All samples were maintained at 50°C between sonication and loading into the NMR spectrometer. For measurements below pH 3.5, afresh lipid sample was used for each pH point.

For the binary systems, the desired weights of DMPC (49.8mg) and DMPG (50.2mg) to provide a molar ratio of 1:1, were dissolved in chloroform/methanol and thoroughly mixed. Solvent was removed by nitrogen and then under high vacuum (10^{-2} Torr; 15 hr). The lipid mixture was resuspended in the appropriate buffer (5mM EDTA, pH 7.4 or 200mM NaCl, 5mM EDTA, pH 7.4) at 45°C. Before sonication the sample temperature was allowed to equilibrate to 45°C in order for the DMPG to be above its phase transition temperature even at low pH. The pH was adjusted before sonication.

All buffers were made with D_2O to make use of the deuterium lock on the NMR spectrometer. For the systems in 200mM salt the pH was adjusted using HCl diluted in 200mM salt solution; otherwise HCl diluted with deionized water was used. Before each pH measurement, the pH meter was linearly calibrated on standard buffers

obtained from BDH.

High resolution ^{31}P-NMR spectroscopy was performed on an Oxford Instruments (8.4 T) magnet with a Nicolet 1180 computer. Samples were locked and shimmed on the internal D_2O and spun at 25Hz. For the pure lipid systems, spectra were collected at 145.9 MHz into 4K points (2K real and 2K imaginary) using a sweep width of 6,000 Hz and a recycle time of 1.34 s. All pure lipid spectra were recorded at 50°C, since below the pK_a, the phase transition of DMPG increases to 45°C (Watts *et al.*, 1978; van Dijck *et al.*, 1978). A line-broadening of 2Hz was applied using exponential multiplication. Chemical shifts were measured relative to MDP contained in a coaxial insert.

Visible absorption spectra of the retinal chromophore were recorded on a Perkin-Elmer Lambda 3 UV/vis spectrophotometer scanning between 700 and 400nm at a rate of 120 nm min^{-1}. All samples were at room temperature. A thermocouple placed in the sample curvette after measurement revealed a temperature of 26°C +/-1. 50µl of bacteriorhodopsin complex pellet (in 10mM Tris/HCl, 1mM EDTA, pH 7.5) was added to 2cm^3 of appropriate aqueous medium; either deionized water, 100mM NaCl or 200mM NaCl. The pH was lowered with HCl diluted in the appropriate buffer. Three minutes was allowed for the sample to equilibrate and the pH was recorded immediately after obtaining the spectrum. For comparison of spectroscopic data from the same complex, the aqueous buffer in which the vesicles were suspended was used as a reference blank. The A_{max} obtained was thus an apparent A_{max} value for the retinal chromophore; being shifted to shorter wavelengths by the superimposition on the background Rayliegh scattering from the vesicles. When directly comparing the spectroscopic data obtained for the retinal chromophore in different bacteriorhodopsin complexes it was important to remove the effects of background Rayliegh scattering which may differ between complexes produced by different techniques. For these measurements, a sample of the vesicles on which the experiment was to be performed was bleached in 1M hydroxylamine, pH 7.4, 35°C for 1hr and used as the reference sample. The A_{max} value obtained was thus the actual A_{max} of the retinal chromophore.

7.III). Results.

A) ^{31}P-NMR determination of apparent pK_as for synthetic phospholipids (DMPC and DMPG) in the bilayer environment of small unilamellar vesicles in aqueous detergent-free media.

i) *single lipid systems.*

Effect of ionic strength on the titration properties of DMPG in small unilamellar vesicles. A ^{31}P-NMR spectrum of DMPG (NH_4^+ salt) SUVs in 5mM EDTA, pH 7.6 (Fig.7.1.b) shows a single sharp resonance 17.057 ppm upfield from the MDP resonance. As the pH is lowered below 4.3, the phosphorus-31 NMR resonance for DMPG SUVs is resolved into two distinct peaks (as shown for the binary lipid spectra in Fig.7.4), demonstrating the existence of two phospholipid environments that are in slow exchange on the ^{31}P-NMR time scale. At pH 3.8, the resolution between the peaks is 45 Hz. To obtain well resolved two component NMR spectra the exchange rate has to be slower than $3\Pi(\nu_A - \nu_B)$ (see Introduction Fig.5), where ν_A is the chemical shift of a phospholipid in one environment and ν_B the chemical shift from the other environment. The exchange rate of phospholipids between these two environments is therefore less than 400 s^{-1}. The chemical shifts measured for the two DMPG peaks relative to external MDP are plotted as a function of pH in Fig.7.2.a. The NMR signals for the two environments are resolved on changing the pH because their respective lipids exhibit differing sensitivities to pH and titrate with different pK_as; the low field resonance exhibiting a pK_a between a half and one pH unit lower than the upfield resonance. Below pH 2, resolution of the low-field resonance became difficult. Decreasing the pH of the aqueous medium from 7.6 to 1.4 shifts the upfield DMPG resonance 1.17 ppm upfield. Between pH 4 and 5, the phosphorus-31 chemical shift measured for the upfield DMPG resonance relative to MDP is very sensitive to pH. Below pH 4, however, the sensitivity of the upfield resonance to changing pH is seen to decrease although the titration is not complete. This may be due to the logarithmic increase in Cl^- anion concentration (from the HCl used to lower the pH). Thus at pH 3, the [Cl^-] from the added HCl is 1mM but at pH 2 it is increased to 10mM. Since the

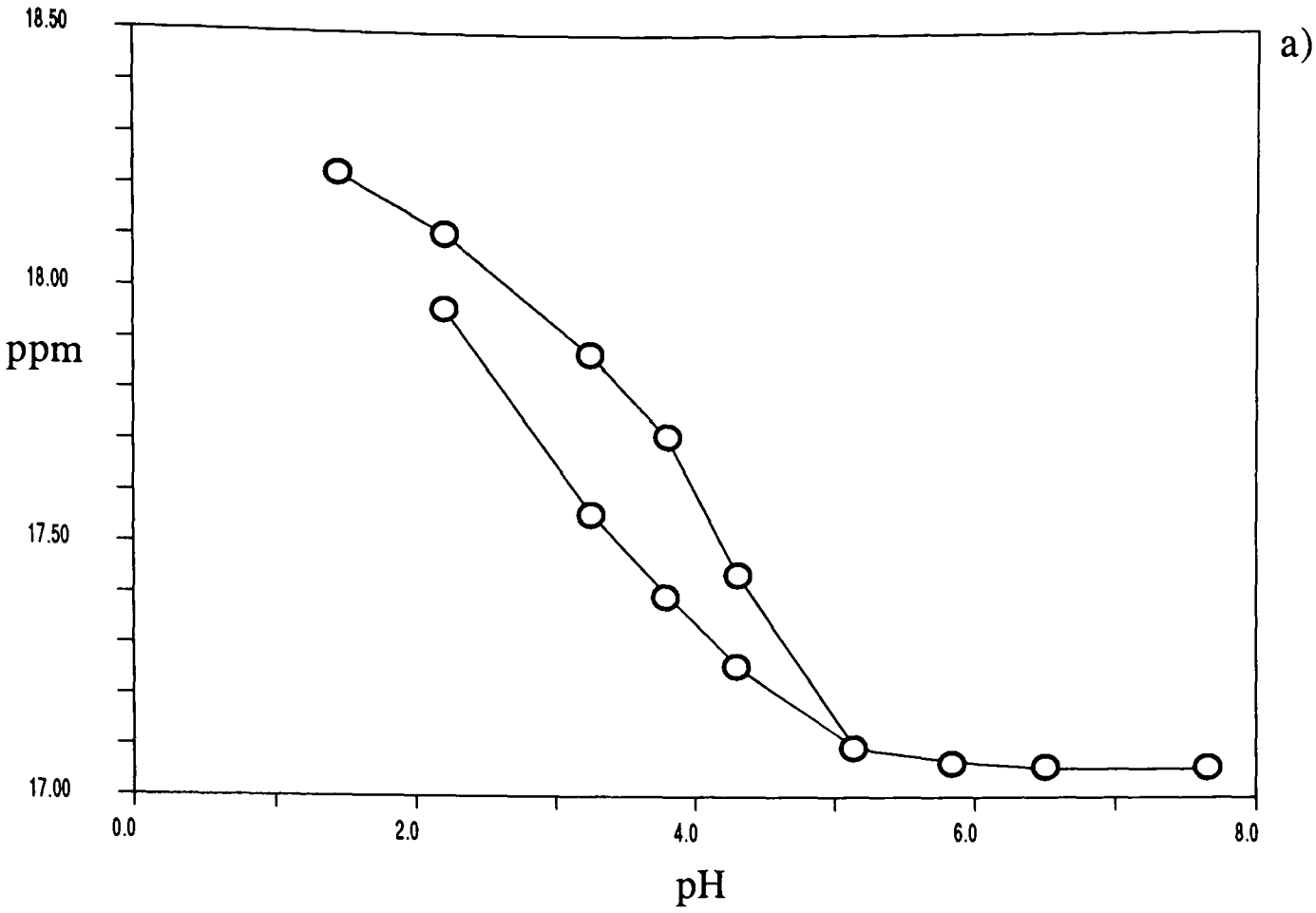


Fig.7.2. Chemical shifts measured from high resolution ^{31}P-NMR spectra of single lipid SUVs plotted as a function of pH; a) DMPG in 5mM EDTA (ppm relative to MDP); b) DMPG in 100mM sodium citrate; and c) DMPC in 120mM NaCl, 5mM EDTA (ppm relative to MDP).

c)

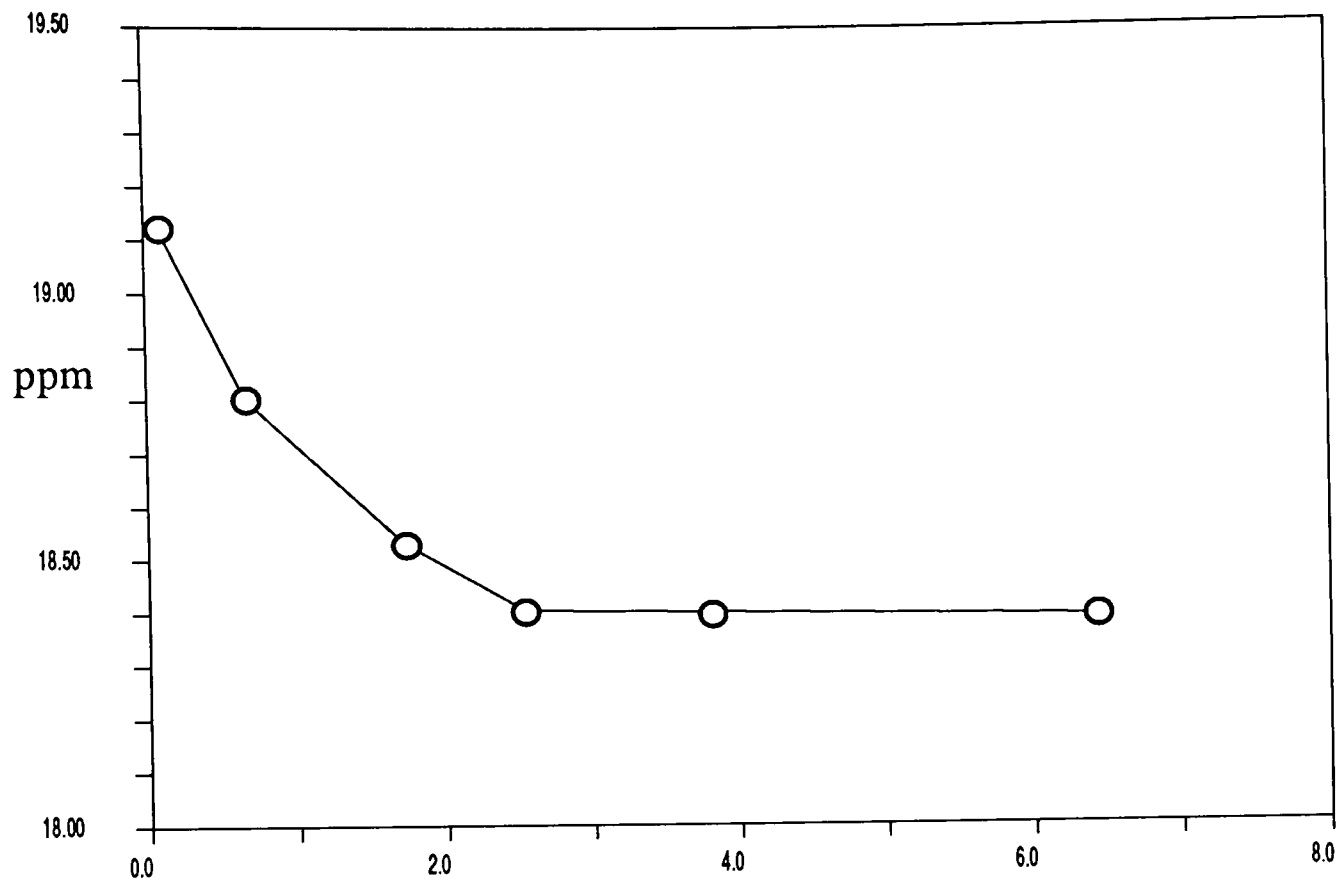


Fig.7.2. (cont.)

EDTA concentration is only 5mM, this increase in anion concentration is significant and may serve to change the effective local pH at the membrane surface with respect to the pH of the bulk aqueous phase, which is what is measured by the pH meter. Thus, the NMR titration (Fig.7.2.a) may be monitoring alteration of the phosphate proton binding due to a salt dependent change in the effective pH at the membrane surface at pH values below 3. Sacre & Tocanne, (1977) demonstrate the effect of ionic strength on the apparent pK_a to be most significant up to salt concentrations of 100mM, with significant changes on increasing the NaCl concentration from 1mM to 10mM. Thus the pH scale in Fig.7.2.a may not be a linear reflection of the pH experienced by the phosphate group at the membrane surface, rendering precise calculation of the apparent pK_a difficult. The apparent pK_a estimated from the beginning and end points of the titration and the sharp phase is pH 4.0.

To alleviate the problem of salt induced changes in effective local H^+ ion concentrations at the membrane surface during the titration, the pH titration for the phosphorus-31 chemical shift of DMPG SUVs was repeated in buffer of higher ionic strength with a Na^+ ion concentration of 300mM (100mM trisodium citrate/ 100mM Tris/HCl). As in low salt aqueous solutions, lowering the pH through the pK_a separated the PG phosphorus-31 signal into two distinct resonances. The plot of phosphorus-31 chemical shift for the upfield resonance of the pair as a function of pH (Fig.7.2.b.) reveals well defined end-points and a sharp titration with a pK_a of 2.8. (The chemical shifts plotted in Fig.7.2.b. are relative to the MDP resonance that was folded back into the spectrum due to the sweep width being set too low; the ppm scale in Fig.7.2.b merely displaying the shift experienced by the phosphate resonance). A total upfield shift in resonance of 1.07 ppm was measured on reducing the pH from 8.0 to 0.6. The increase in acid counterion concentration in reducing the pH from 2 to 1 is 90mM, which is not significant compared to the 300mM Na^+ ion concentration already present in the aqueous medium, since the apparent pK_a is little affected in solutions containing more than 100mM salt. (Trauble & Eibl, 1974; Sacre & Tocanne, 1977).

Titration of DMPC small unilamellar vesicles. A ^{31}P-NMR spectrum (Fig.7.3.c)

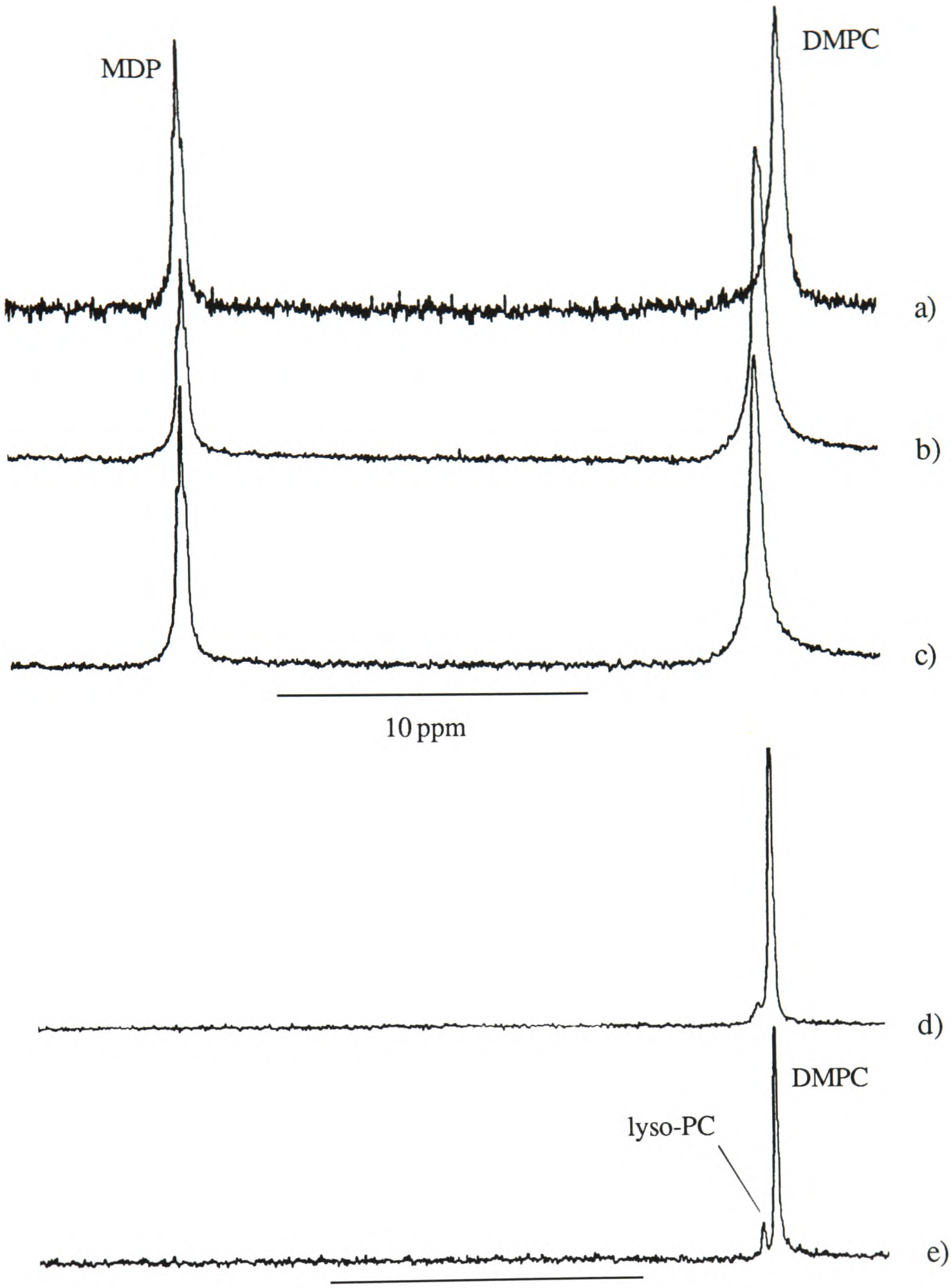


Fig.7.3. High resolution ^{31}P-NMR spectra (145.9 MHz.) of DMPC SUVs in 120mM NaCl, 1mM EDTA (50°C) at; a) pH 0.10; b) pH 2.54; and c) pH 6.44. Spectra were not proton decoupled. To determine the extent of hydrolysis of DMPC to lyso-PC during the NMR experiments at low pH, high resolution ^{31}P-NMR spectra were recorded of DMPC SUVs solubilized in 4% SDS, 500mM Tris/HCl, pH 7.5 immediately after the NMR measurements were made at d) pH 0.66; and e) pH 0.10.

of DMPC SUVs at pH 6.44 displayed a single resonance 18.392 ppm upfield from that of MDP. pH titration of the chemical shift displayed by the phosphorus-31 NMR resonance of DMPC SUVs in aqueous solutions at high ionic strength (120mM NaCl, 5mM EDTA) revealed an apparent pK_a value for the phosphocholine headgroup some 2 to 3 pH units lower than that of phosphoglycerol. Unlike PG bilayers, the PC SUV phosphorus-31 signal was not resolved into two resonances on titration (Fig.7.3.a). On lowering the pH from 6.4 to 0.1 the PC resonance shifts 0.73 ppm upfield. It would appear, however, that the titration is not complete by pH 0.10 (Fig.7.2.c). The very low pK_a of the PC phosphate precluded its accurate determination, which would require NMR measurements at pH values well below pH 0. From data in Fig.7.2.c and assuming a similar upfield shift on completion of titration to that observed for DMPG, an approximate pKa of 0.5 - 1.0 was estimated.

Determination of the extent of phospholipid hydrolysis during the NMR measurements at low pH points. The titration of the DMPC SUVs was continued down to a pH of 0.1, which is approaching a hydrogen ion concentration of 1M. Ester linkages (e.g. those linking the fatty acyl chains to the glycerol backbone in phospholipids) are susceptible to hydrolysis in acid solutions particularly at high temperatures. When titrating phospholipid samples to low pH at 50°C it is important to quantify the extent to which the DMPC hydrolyses to lyso-PC during the experiment. Indeed Koter *et al.*, (1978) did not perform measurements at pH values below 4 or above 9 to avoid lipid hydrolysis. For the NMR experiments reported here, a fresh phospholipid sample was used for each low pH point. The degree of PC degradation after the NMR experiment was determined by TLC or by high resolution ^{31}P-NMR. For TLC the samples used for the pH 2.15, 0.9, 0.67 and 0.52 points were readjusted to pH 8.0 after the NMR experiment and the lipid extracted in 2:1 $CHCl_3$/MeOH. TLC in $CHCl_3$/MeOH/NH_3 (65:35:5; v/v) showed traces of lyso-PC for samples at pH 0.67 and 0.52. The level of lyso-PC was judged to be less than 5% of the total lipid. Samples from pH 2.15 and 0.9 revealed no trace of lyso-PC. To determine the extent of phospholipid hydrolysis using high resolution ^{31}P-NMR, the sample was solubilized in

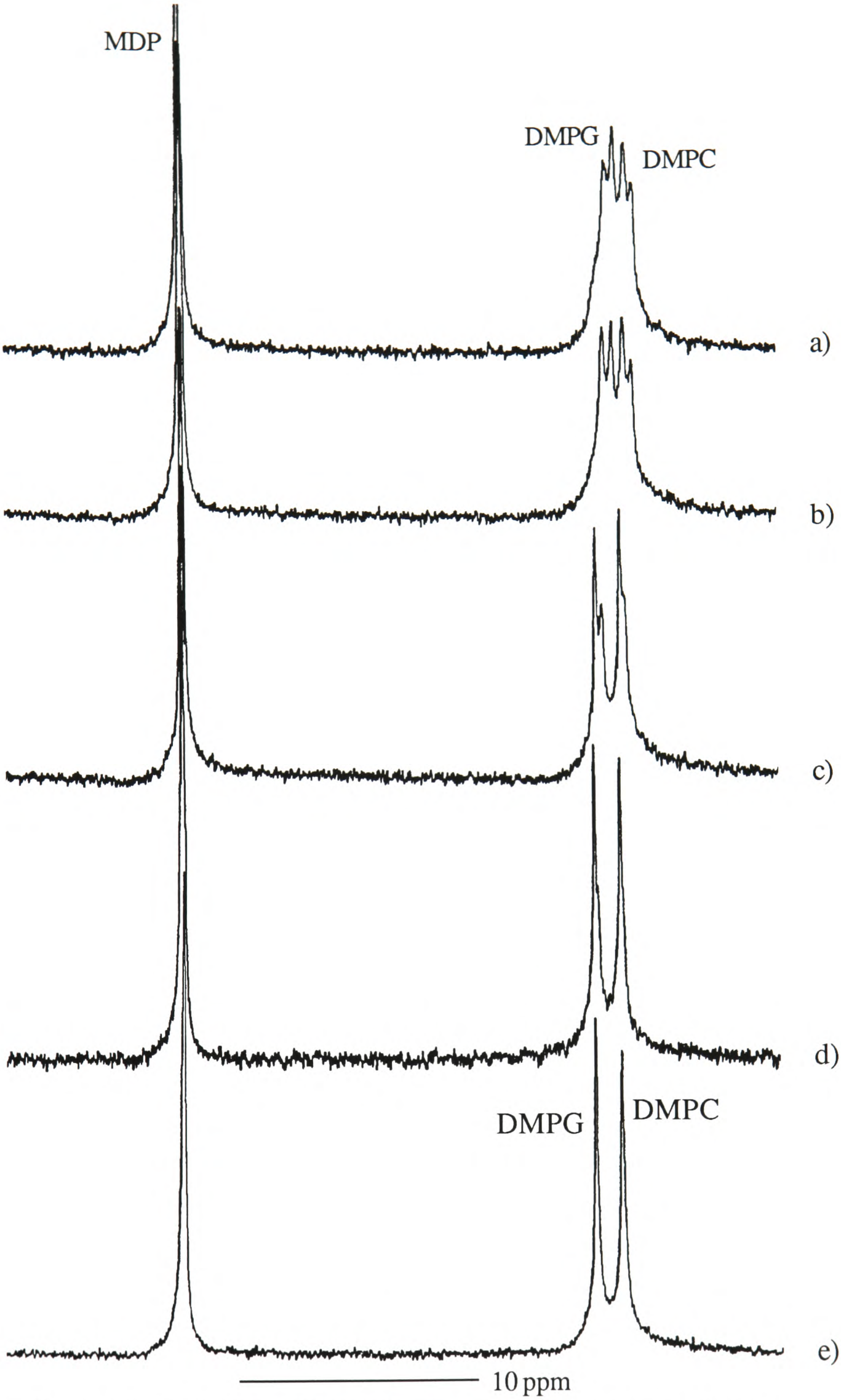


Fig.7.4. High resolution ^{31}P-NMR spectra (145.9 MHz.) of binary DMPG/DMPC (1:1 mol/mol) SUVs in low salt buffer (5mM EDTA, 50°C) at; a) pH 2.9; b) pH 3.2; c) pH 4.6; d) pH 5.4; and e) pH 7.3.

4% SDS, 500mM Tris/HCl, pH 7.5. High resolution ^{31}P-NMR resolves lyso-PC from DMPC (Henderson *et al.*, 1974). Using NMR to assess the amount of lyso-PC formed may be more effective than $CHCl_3$/MeOH extraction as not all the lyso-PC may partition into the organic solvent. For a sample at pH 0.65, ^{31}P-NMR revealed that less than 5% of the DMPC had hydrolysed to lyso-PC (Fig.7.3.d), while for a sample at pH 0.1 (Fig.7.3.e), 13.6% of the lipid was hydrolysed after the NMR experiment at 50°C, as judged from the resonance line-heights. It would appear that, providing a fresh lipid sample is used for each low pH point, titration down to pH 1.0 (but not below 1.0) is acceptable.

ii) *Binary lipid systems*. For two phospholipid species to be studied in mixed lipid systems by high resolution ^{31}P-NMR, the chemical shifts of their phosphate groups must be significantly different to allow resolution. Good chemical shift resolution is particularly important at pH values below the pK_a of the phosphate, where the resonances broaden significantly. In this respect DMPC is a good choice as the phosphate resonance lies well upfield of other phospholipids (Henderson *et al.* 1974). Fig. 7.1.c shows the noise decoupled ^{31}P-NMR spectrum of a 1:1 (mol/mol) binary mixture of DMPG/DMPC sonicated into SUVs in 5mM EDTA, pH 7.3 with external MDP. The phosphorus-31 NMR resonances from the DMPC and DMPG are separated by 1.083 ppm. The DMPG resonance is 17.121 ppm upfield from the MDP peak, while the DMPC resonance is at 18.204 ppm. The phosphorus-31 resonances from 1:1 (mol/mol) binary DMPG/DMPC SUVs were titrated in aqueous media of high and low salt content. In both ionic environments, the PG and PC resonances are resolved into two signals on titrating through the respective pK_as (Fig.7.4). The chemical shifts for the DMPG resonances and DMPC resonances in both ionic environments are plotted against pH in Fig.7.5.

Effect of the presence of PG on the properties of the PC headgroup as determined by high resolution ^{31}P-NMR. Incorporating DMPG into DMPC bilayers has three effects on the PC headgroup phosphate moiety as judged from the phosphorus-31 NMR data, while the properties of the PG headgroup phosphate appear virtually independent

of the presence of PC.

Firstly, at neutral pH values in high ionic strength media, the PC resonance is shifted 0.22 ppm downfield relative to its resonance position in pure DMPC bilayers. In contrast, the PG resonance chemical shift is virtually unaffected by the presence of DMPC, shifting only 0.065ppm upfield. The downfield shift of the PC phosphate in DMPG bilayers may be due to the increased potential for hydrogen bonding of the phosphate oxygens with the hydroxyl protons of the PG glycerol headgroup.

Second, the PC resonance is clearly resolved into two peaks at low pH values (Fig.7.4), when present in DMPG bilayers, whereas no such splitting was observed in pure DMPC bilayers (Fig.7.3.a). In aqueous solutions of low ionic strength, the splitting of the DMPG phosphorus-31 signal is clearly detectable at pH 5.4 (Fig.7.4.d), while the DMPC is just beginning to split. The resolution of each resonance into component peaks in low salt media is maximum at pH 3.2 (Fig.7.4.b) - the chemical shift resolution of pairs of signals is 0.4ppm (58 Hz) for DMPG and 0.35ppm (51 Hz) for DMPC.

Third, the pK_as of the PC phosphate in the two environments are elevated to higher pH values when mixed with DMPG; in low salt aqueous media, the pK_as for the two DMPC peaks were estimated to be 3.9 and ~2.5, i.e. some 3 and 1.5 pH units higher than the value of pH ~ 1 obtained for the phosphocholine moiety in pure PC bilayers in 10mM Tris/HCl, 5mM EDTA (data not presented). In contrast, the PG phosphate titration remains relatively unaffected by the presence of PC compared to that observed in pure DMPG bilayers.

Effect of salt in the aqueous medium on the phospholipid titration properties. The pH titration data presented in Fig.7.5 demonstrates the effect of the presence of salt in the aqueous buffer medium on the titration of the PG and PC headgroup phosphates. Increasing the ionic strength to 200mM NaCl has two effects. First, although the peaks split into two, the resolution is much lower than the resolution observed in low ionic strength solutions. Second, and most significant, the presence of salt lowers the apparent pK_as by up to 1.5 pH units. The estimated pK_as are presented in Table 1.

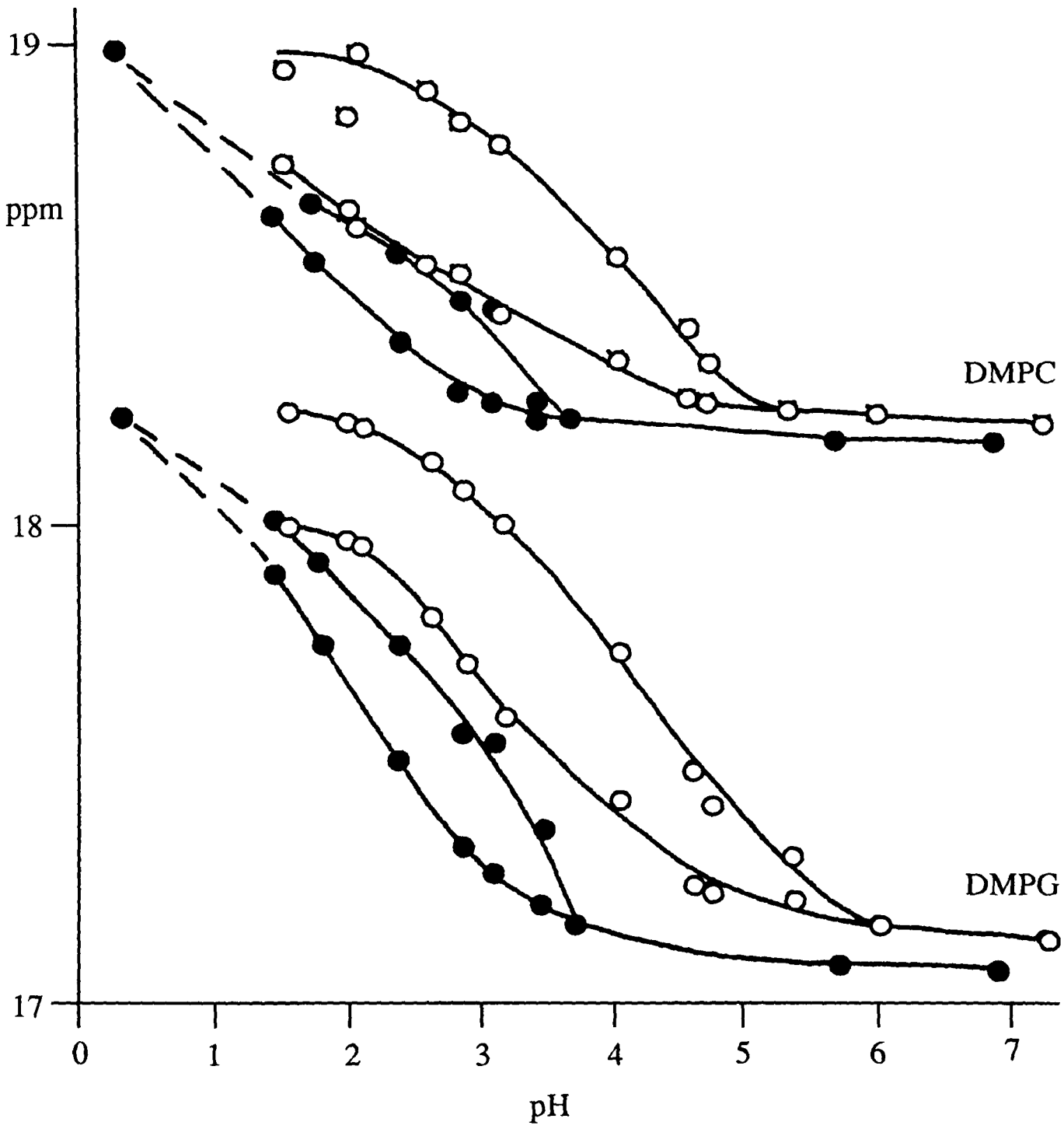


Fig.7.5. Effect of ionic strength on the apparent pK_as of the PG and PC headgroup phosphates in DMPG/DMPC 1:1 (mol/mol) binary mixtures. Chemical shifts, relative to external MDP, were measured from high resolution ^{31}P-NMR spectra of DMPG/DMPC SUVs at 50°C.

○ 5mM EDTA only

● 200mM NaCl, 5mM EDTA

Table 1. Effect of high ionic strength aqueous medium on the titration properties of DMPC and DMPG in binary mixtures.

ionic strength	pH at which titration begins	pKa for lowfield resonance	pKa for upfield resonance
	DMPG phosphate		
low	5.75	3.5	4.2
high	3.5	2.0	2.7
	DMPC phosphate		
low	4.7	~2.5	3.9
high	3.5	~1.75	~2.5

B) Membrane electrostatics and chromophore properties of the protein.

i) *Bacteriorhodopsin in detergent-produced DMPC/bR systems with all the endogenous purple membrane lipids removed.* The retinal chromophore of bacteriorhodopsin in DMPC/bR vesicles (mole ratio 67:1) with all the endogenous purple membrane lipids removed displays an A_{max} of 562nm at pH 7.8 (Fig.7.6.d) using hydroxylamine bleached vesicles as a reference blank. The hydroxylamine bleached vesicles show increased Rayleigh scattering as the wavelength shortens (Fig.7.6.e). On lowering the pH to 2.4 (Fig.7.6.c), the chromophore absorption broadens while the A_{max} shifts to the shorter wavelength of 555nm. On titrating below pH 2.4, the A_{max} is shifted sharply by 26nm to the longer wavelength of 581nm at pH 1.6 (Fig.7.6.b). This together with broadening imparts a bluish grey tinge on the complex. In Fig.7.7, the shift in measured A_{max} is plotted as a function of pH. The pK_a for the purple to blue shift is pH 1.8 (Fig.7.7). Further acidification does not generate the full blue colour characteristic of acidified purple membrane (A_{max} 600nm); indeed on reducing the pH

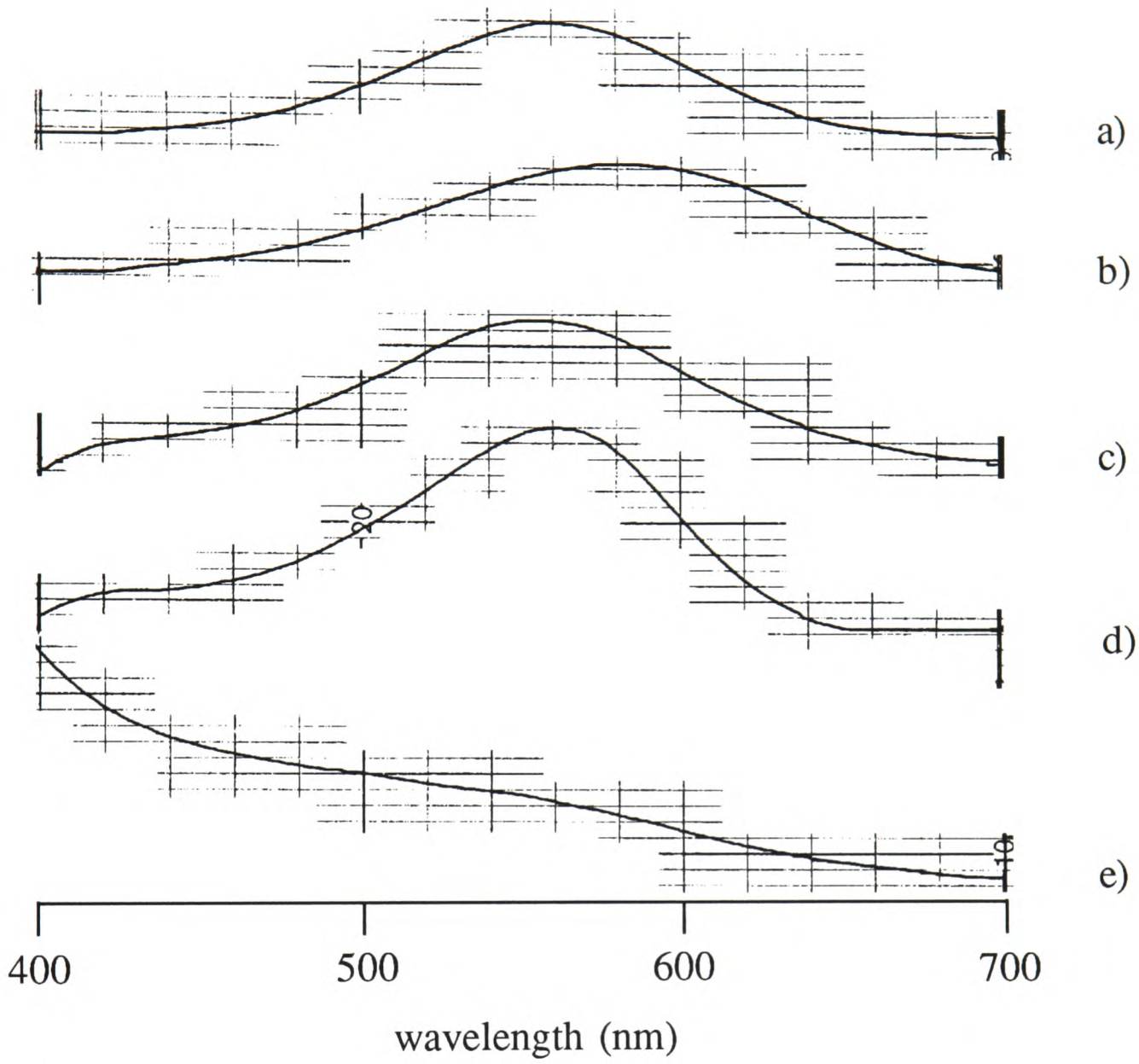


Fig.7.6. Visible absorption spectra of retinal chromophore of bacteriorhodopsin in the 67:1 (mol/mol) DMPC/bR complex (all endogenous purple membrane lipids removed) at; a) pH 0.9; b) pH 1.6; c) pH 2.4; and d) pH 7.8. Hydroxylamine bleached vesicles (spectrum shown in (e)) were used as a reference. Vesicles in deionised water at 25°C.

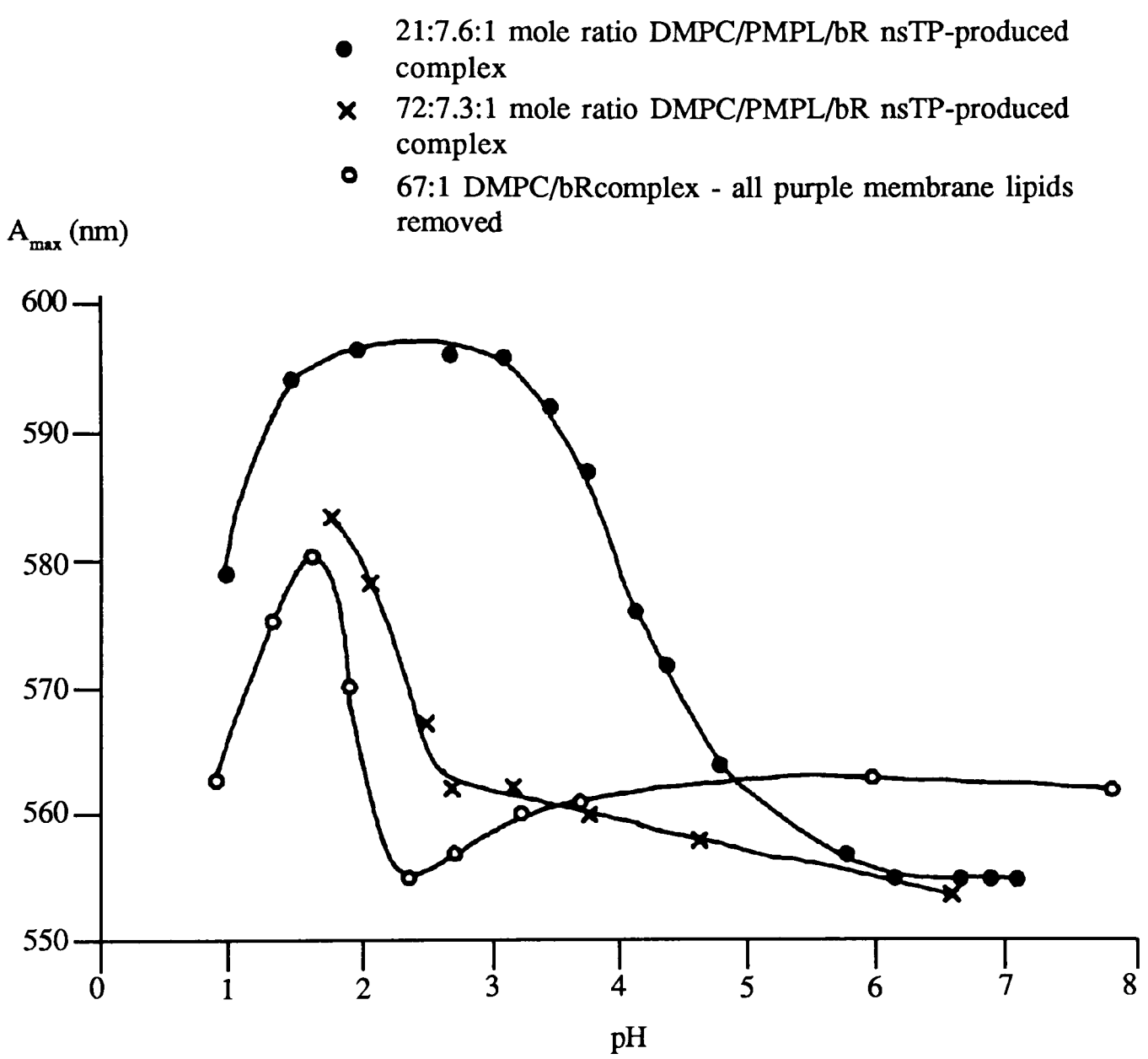


Fig.7.7. Titration of observed A_{max} for bacteriorhodopsin complexes in deionised water at room temperature against pH. The spectra from which the A_{max} values were measured were recorded against a hydroxylamine-bleached vesicles blank.

to 0.9, the A_{max} shifts back to 562 nm (Fig.7.6.a), thus regenerating the purple colour. The low pH blue to purple colour shift titrates with a pK_a of 1.4 (Fig.7.7). It seems that protonation of the group(s) (pK_a = 1.4) responsible for this low pH blue to purple shift overrides the effect of the group (pK_a 1.8) responsible for the purple to blue shift such that the full blue colour (A_{max} 600nm) is not obtained. If in the absence of the low pH blue to purple shift, a full blue colour could be generated, then the pKa estimated for the group responsible for the purple to blue shift would be lower than pH 1.8, perhaps similar to that of the PC phosphate group.

ii) *Bacteriorhodopsin in nsTP-produced complexes with most of the purple membrane lipids retained.* The A_{max} for the bacteriorhodopsin chromophore in the 72:7.3:1 mole ratio DMPC/PMPL/bR nsTP-produced complex (measured against hydroxylamine bleached vesicles) exhibits similar titration properties in deionized water (Fig.7.7) to the 67:1 mole ratio DMPC/bR complex, except that the pK_a for the purple to blue shift is at the slightly higher pH of 2.2. In contrast the chromophore for bR in the 21:7.6:1 mole ratio DMPC/PMPL/bR nsTP-produced vesicles displays an A_{max} of 596-599nm between pH 3.2 and 1.5 generating the full blue colour of acidified purple membrane. Furthermore, the pK_a for the purple to blue shift for the chromophore in the 21:7.6:1 mole ratio DMPC/PMPL/bR nsTP-produced vesicles in deionized water is significantly higher than for the 72:7.3:1 DMPC/PMPL/bR and 67:1 DMPC/bR mole ratio complexes, with a pH of 4.2; the full blue colour with an A_{max} of 596-599nm being attained at pH 3. Between the pH values of 3 and 1.5 the A_{max} measured from vesicles against a hydroxylamine bleach vesicle reference appears relatively independent of acidity (Fig.7.7). On titrating below pH 1.5, however, the A_{max} is shifts to the shorter wavelength of 575nm with a pK_a of around 1.4.

iii) *Effect of salt in the aqueous medium on the chromophore titration properties for the high protein content nsTP-produced complex.* In the presence of 200mM NaCl, the 21:7.6:1 mole ratio DMPC/PMPL/bR complex displays a purple to blue shift of similar magnitude to the complex in the absence of salt, with an Amax of 587-590nm being displayed at pH 2.15. Absorption spectra for the vesicles in 200mM NaCl at three

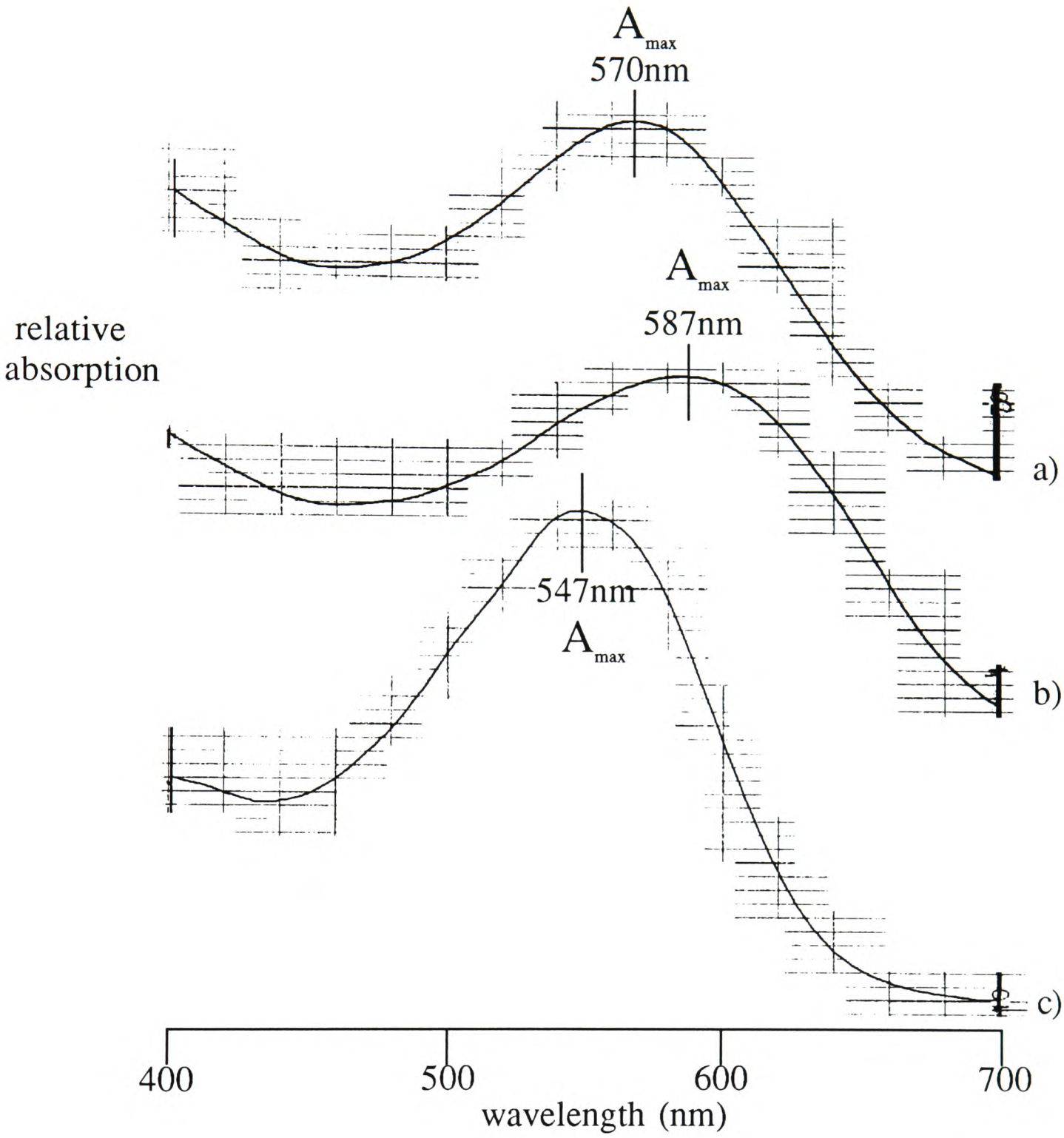


Fig.7.8. Visible absorption spectra of the retinal chromophore of bacteriorhodopsin in the 21:7.6:1 mole ratio DMPC/PMPL/bR complex (200mM NaCl, 1mM Tris/HCl) showing purple to blue shift on lowering the pH; a) pH 0.85; b) pH 2.15; and c) pH 6.00. Spectra were recorded against 200mM NaCl reference sample.

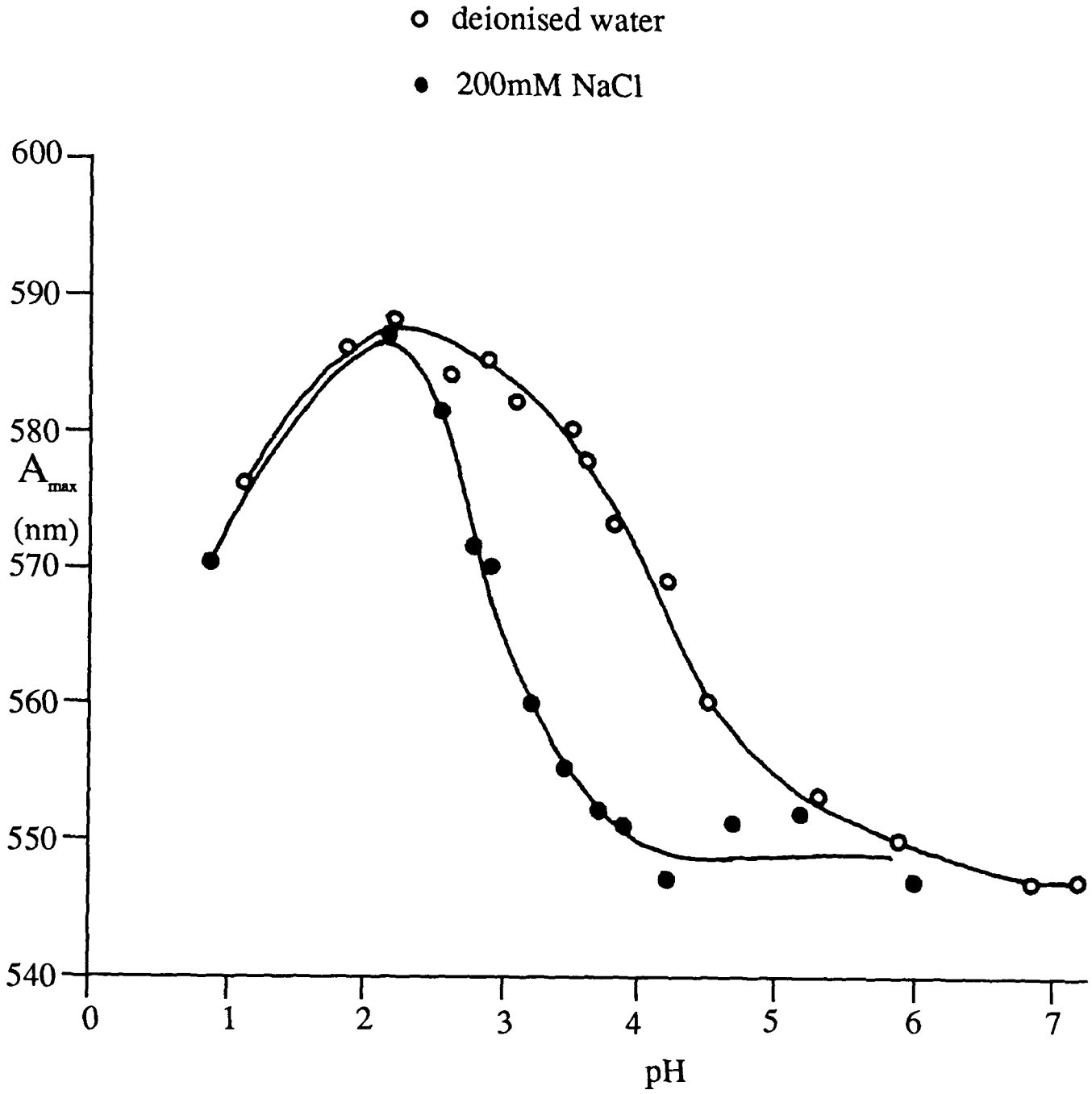


Fig.7.9. pH titration of A_{max} for bacteriorhodopsin chromophore absorption in 21:7.6:1 DMPC/PMPL/bR nsTP-produced complex in the presence and absence of salt. Increasing the ionic strength is seen to lower the pK_a by one pH unit for the purple to blue shift. Spectra from which A_{max} values were measured were recorded against a buffer blank at 25°C.

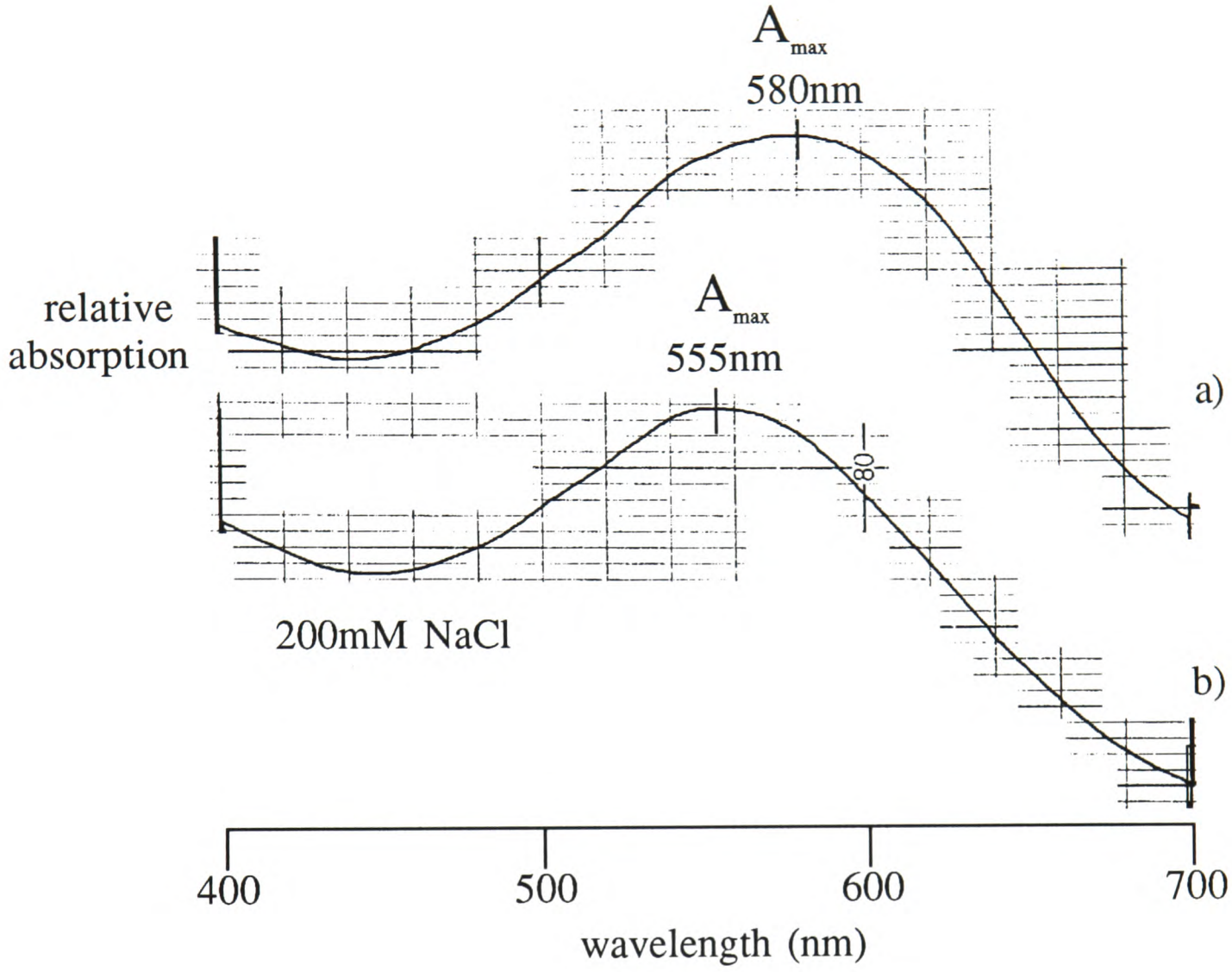


Fig.7.10. Visible absorption spectra of the retinal chromophore in bacteriorhodopsin in the 21:7.6:1 mole ratio DMPC/PMPL/bR nsTP-produced complex at pH 3.5 (25°C) in; a) deionised water; and b) 200mM NaCl. Spectra were recorded against a buffer reference.

pH values against a buffer blank reference are shown in Fig.7.8. The result of using a buffer for a reference blank instead of the appropriate hydroxylamine bleached vesicles is to shift the apparent A_{max} by 10nm to shorter wavelengths. This is due to the increased Rayleigh scattering by the vesicles as the wavelength approaches 400nm (Fig.7.6). Thus, plotting the apparent A_{max} values obtained for the 21:7.6:1 DMPC/PMPL/bR mole ratio vesicles in deionized water against a buffer blank as a function of pH (Fig.7.9), reveals a pK_a of pH 4.2, which is identical to that determined using hydroxylamine bleached vesicles as reference (Fig.7.7) except that the apparent A_{max} for the blue form was 588nm instead of 598nm. The pK_a, however, for the purple to blue shift in solutions of high ionic strength (200mM NaCl) is pH 2.95 (Fig.7.9), which is more than one pH unit lower than observed in low ionic strength solutions (deionized water). Furthermore, in the presence of salt the full blue colour (A_{max} 588nm) is not attained until pH 2.15. Increasing the ionic strength with NaCl serves to suppress the purple to blue shift to lower pH values. This is demonstrated by the absorption spectra presented in Fig.7.10. Both were recorded at very similar pH values. In the absence of salt at pH 3.5 the 21:7.6:1 mole ratio DMPC/PMPL/bR complex is distinctly blue with an A_{max} of 580nm. Adding salt to a concentration of 200mM regenerates the purple colour with an A_{max} of 555nm. As in the absence of salt, titrating below pH 2 in the presence of salt results in a shift in the apparent A_{max} to shorter wavelengths (570nm at pH 0.85; spectrum shown in Fig.7.8.a), thus regenerating the purple colour. From the titration curves presented in Fig.7.9, it would appear that the pK_a for this low pH blue to purple shift is independent of the ionic strength of the aqueous medium. In aqueous solutions of 100mM NaCl, similar titration data for the 21:7.6:1 mole ratio DMPC/PMPL/bR complex was obtained as for the 200mM NaCl; the apparent pK_a for the purple to blue shift being measured at pH 2.85.

iv) *Bacteriorhodopsin in detergent produced DMPG bilayers with all the endogenous purple membrane lipids removed.* Incorporating delipidated bacteriorhodopsin into DMPG bilayers distinctly alters the A_{max} vs pH titration properties compared to delipidated bR in DMPC bilayers. As with DMPC/bR

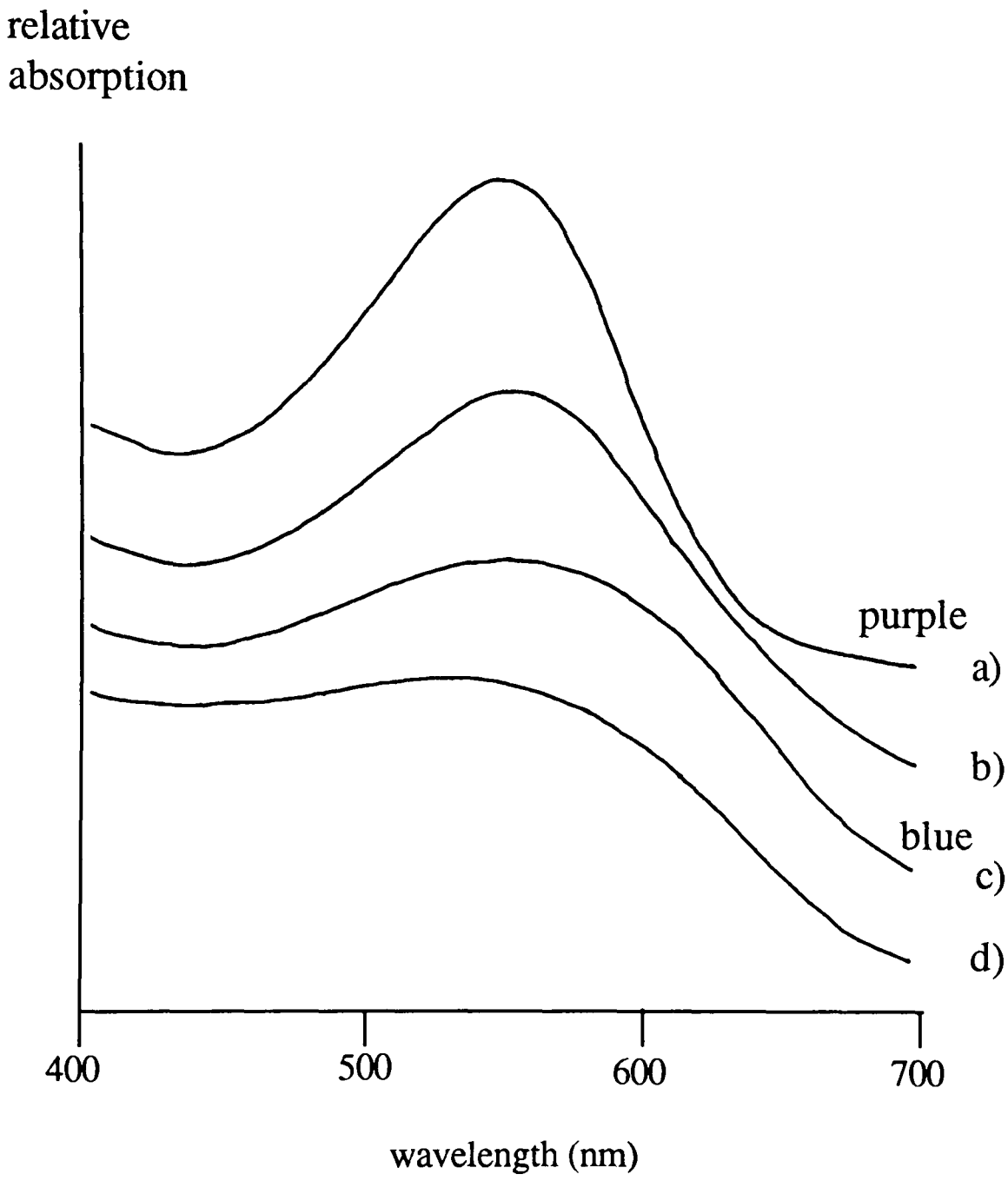


Fig.7.11. Visible absorption spectra of the retinal chromophore in bacteriorhodopsin in DMPG/bR vesicles (71:1 mole ratio) in 0.25mM EDTA at; a) pH 7.6; b) pH 5.8; c) pH 4.5; and d) pH 3.4. Spectra were recorded against a water reference.

complexes, lowering the pH of the aqueous medium of the 71:1 mole ratio DMPG/bR complex causes a broadening of the absorption spectrum (Fig.7.11). A blue colour, however, was obtained at a higher pH value - pH 4.5 (Fig.7.11.c)- than for the 67:1 mole ratio DMPC/bR complex - pH 1.6 (Fig.7.6.b). On further acidification, the blue colour was replaced by a greyish brown colour at pH 3.4 and 2.8. This was due to increased broadening of the retinal absorption (Fig.7.11.d). Addition of NaOH restored the purple colour. The development of a blue colour at pH 4.5 correlates with the protonation of the PG phosphate observed by high resolution ^{31}P-NMR titrations (see above).

7.IV) Discussion.

The difference in the apparent pK_as of DMPG and DMPC determined by ^{31}P-NMR agree with those determined by DSC (Trauble & Eibl, 1974; van Dijck *et al.*, 1978) and reflect the differing electrostatic environments experienced at the membrane surfaces. The choline headgroup of DMPC is zwitterionic; the phosphate bears a negative charge and the N,N,N-trimethyl ammonium group a permanent positive charge. Clearly strong electrostatic interactions can occur between these groups on neighbouring molecules. Protonating the phosphate group not only breaks these interactions but would also result in a net positive charge at the membrane surface. The phosphoglycerol headgroup of DMPG at pH 7 bears a single net negative charge, and in DMPG bilayers there exists a high negative charge density at the membrane surface. Consequently the phosphate headgroup of DMPG is much more readily protonated than DMPC phosphate, since protonation suppresses the negative charge and does not disrupt salt bridges. The elevation of the phase transition temperature of protonated DMPG (van Dijck *et al.*, 1978; Watts *et al.*, 1978) is due to a reduction in the mean molecular surface area of the PG molecules resulting in the requirement of more thermal energy to promote trans-gauche isomerisations in the acyl chains. Large expansions of films of PG were demonstrated (Tocanne *et al.*, 1974) at the air water interface on raising the subphase pH from 2 to 6, due to the increased mean molecular

area for the PG molecules on raising the pH above the pK_a of the PG phosphate (pH 4.5). Plotting the change in area per molecule against pH at constant surface pressure yielded titration curves (Sacre & Tocanne, 1977). The expansion is mainly due to the repulsive coulombic forces which develop in the film between adjacent negative charges as the PG phosphates become ionised.

The resolution of the phospholipid resonances into pairs of resonances that is observed for pure DMPG and DMPC/DMPG binary mixtures during protonation of the phosphate arises from different properties of phospholipids in the two leaflets of the bilayer. The rate of lipid flip-flop (that is the exchange of phospholipids from one leaflet of the bilayer to the other) is extremely slow, being in the order of days (Housley & Stanley, 1982). As calculated above the exchange rate would have to be greater than 400 s^{-1} before single component ^{31}P-NMR resonances were observed. It is established that the high radius of curvature of the SUV membrane imposes different packing properties on the headgroup regions of phospholipids in the outer leaflet compared to those in the inner leaflet; the lipid headgroups in the inner leaflet being much more tightly packed. Such packing constraints provide different surface charge densities and hydrogen-bonding environments and hence account for the observed differences in pK_as. The appearance of two resonances thus confirms that the sonicated lipid systems were bilayer rather than micellar structures. Berden *et al.* (1975) observed two peaks in ^{31}P-NMR spectra for sonicated egg lecithin vesicles in 25mM Tris/HCl, pH 7.6 at 25°C. The separation of ~0.13 ppm was found to decrease with increasing temperature which is consistent with the lack of resolution of signals from inner and outer leaflets of DMPC and DMPG bilayers at 50°C at neutral pH values. ^{31}P-NMR spectra of DPPC/sphingomyelin SUVs (Berden *et al.*, 1975) revealed that each phospholipid resonance was resolved into two at pH 7.2 and 50°C. Addition of the paramagnetic ion, Co^{++}, to concentrations of 4mM, selectively broadened out the resonance from the low field peaks, confirming the assignment of this resonance to phospholipids in the outer leaflet.

In pure DMPG systems (Fig.7.2.a) and DMPC/DMPG mixtures (Fig7.5) it is

apparent that the upfield component corresponding to the phospholipids in the inner leaflet (Berden *et al.*, 1975) titrate with higher pK_as; that is the phosphate groups of lipids in the inner leaflet of the SUV bilayer are more readily protonated. In view of the more compact headgroup packing in the inner leaflet imposed by the SUV architecture and the resulting higher negative charge density this is not surprising. Thus protonation of the negatively charged phosphate moiety of a phospholipid in the inner leaflet not only reduces the coulombic repulsive forces between neighbouring phosphoglycerol headgroups, but also decreases the mean molecular area (from 62Å^2 to 52Å^2 per PG molecule; Scare & Tocanne, 1977) so relieving the tight packing at the surface.

At neutral pH values the ratio of lipid in the outer leaflet to that in the inner leaflet varies from 1.9:1 for lecithin vesicles to 2.3:1 for PC/PS (1/1) mixtures (Berden *et al.*, 1975). This ratio is due to the high radius of curvature of the vesicle which requires more lipid to be present in the outer leaflet. From Fig.7.4 and spectra of pure DMPG SUVs it is apparent that as the pH is lowered so there is an increase in the intensity of the upfield peak (representing phospholipids in the inner leaflet) relative to the low field peak. The implication is that there is a net transfer of protonated lipid form the outer leaflet to the inner leaflet. The electrically neutral protonated PG molecules of smaller mean molecular area are clearly better suited to conditions in the inner leaflet with its high radius of curvature, tight packing constraints and high charge density than the ionised PG species. Thus the increase in upfield peak intensity may reflect a redistribution of charged and uncharged lipids across the bilayer in SUVs in solutions of different pH values. Net transfer of protonated phospholipids into the inner leaflet would require some change in the SUV structure; perhaps involving fusion with neighbouring SUVs. The larger vesicles obtained would account for the observed broadening in the resonances (Fig.7.4) at low pH values. The apparent intensity changes, however, could be due to differential pH-induced broadening from reduction in the phosphate mobility on protonation, which shortens the spin-spin (T_2) relaxation time. In view of the decrease in molecular area, this is quite plausible. Alternatively differential changes in the spin-lattice (T_1) relaxation times for phospholipids in the two

leaflets may lead to a selective saturation of the lowfield resonance; particularly as the recycle time of (1.34 s) used in similar to the T_1 values determined for phospholipids in SDS micelles (Fig.2.13).

The presence of the acidic phospholipid PG in PC bilayers, clearly modifies the electrostatic properties of the PC phosphate moiety relative to those in pure PC SUVs. The downfield shift in the PC resonance is consistent with enhanced hydrogen bonding (Henderson *et al.*, 1974) probably to hydroxyl groups on the PG glycerol moiety. The net negative charge at the membrane surface provided by the PG facilitates the protonation of the PC phosphate moiety. The PG phosphate, however, does not appear to be influenced by the positively charged N,N,N-tri-methyl ammonium group of the phosphocholine as judged from the chemical shift. A strong ionic interaction between the positive charge on the PC and the PG phosphate would be reflected in an upfield shift in PG resonance and a suppression of protonation of the PG phosphate, which is not observed.

The increase in ionic strength of the aqueous environment from 5mM EDTA to 200mM NaCl, decreases the apparent pK_a as determined by high resolution ^{31}P-NMR (Figs 7.2 and 7.5) of acidic phospholipids by at least one pH unit. For DMPG lipids in the inner leaflet of single lipid or binary PG/PC SUVs suspended in aqueous media of high ionic strength (300mM Na^+ ion concentrations), the pK_a determined by high resolution ^{31}P-NMR titration is around pH 2.8. Watts *et al.*, (1978) reported a pK_a value of 2.9 in 150mM NaCl by measuring the effect of pH on the phase transition temperature as determined by TEMPO-partitioning. van Dijck *et al.*, 1978 obtained values of between pH 3 and 3.5 for PG in 150mM NaCl by DSC. In aqueous media of lower ionic strength, however, the pK_a for protonation of DMPG in single lipid or binary DMPG/DMPC mixtures is elevated by at least one pH unit to approximately pH 4.0 (Fig.7.2 and 7.5). Trauble & Eibl (1974) demonstrated a similar effect on the second ionisation of phosphatidic acid. Sacre & Tocanne (1977) demonstrated that salt reduces the pK_a values for DLPG by up to two pH units; obtaining apparent pK_as of pH 5.0 for 1mM Na^+, pH 3.9 for 10mM Na^+ and 3.1 for 100mM Na^+ concentrations. For

the PC single lipid systems the observation of similar pK_as in low salt and high salt aqueous media is meaningless as at pH 1, the acid counterion (Cl^-) concentration is already 100mM. In the PG/PC binary lipid bilayers, the apparent pK_a for the PC phosphate is significantly reduced by the presence of salt. Salt suppresses the apparent pK_a because of the counterion effect on charged surfaces, acting to displace H^+ bound to the surface charges. Thus at low ionic strength solutions the H^+ ion concentration at the charged bilayer surface will be greater than in higher ionic strength solutions and so the local pH is lower than the bulk pH measured by the pH meter. Thus at low ionic strengths, the phosphate groups at the membrane surface will become protonated at pH values that are apparently higher than in the presence of salt. On increasing the ionic strength of the medium, however, the H^+ ions are displaced from the bilayer surface by the charged ions and the pH at the membrane surface becomes closer to that of the bulk pH measured by the pH electrode.

The pH titrations of the A_{max} for the 67:1 mole ratio DMPC/bR complex and the 21:7.6:1 and 72:7.3:1 DMPC/PMPL/bR mole ratio complexes presented in Fig.7.7 were performed under identical conditions; the corresponding hydroxylamine bleached bR vesicles being used as a reference blank to compensate for the differing effects of Rayliegh scattering from the large cholate produced vesicles and the smaller nsTP-produced vesicles. The only variable is the lipid composition of the bacteriorhodopsin vesicles. This implies that the pK_a for the purple to blue shift is either directly or indirectly determined by the phospholipid environment of protein. In the 21:7.6:1 DMPC/PMPL/bR mole ratio vesicles the proportion of PGP is relatively high (26.5 mol%). From the high resolution ^{31}P-NMR studies of pure lipid SUVs presented above it appears that the pK_a of the PG phosphate moiety is unaffected by up to 50mol% PC. It is likely that the pK_as for the PGP α-phosphate and the first ionisation of the PGP γ-phosphate in the 21:7.6:1 DMPC/PMPL/bR mole ratio complex in deionized water are similar to that displayed by DMPG in DMPG/DMPC binary mixes (Fig.7.5.a) in low salt aqueous medium; that is approximately pH 4.2. Titration of the PGP-γ resonance in sonicated 21:7.6:1 mole ratio DMPC/PMPL/bR vesicles by high resolution ^{31}P-NMR

was not performed to confirm this. It is thus significant that the pK_a for the purple to blue shift displayed by the 21:7.6:1 mole ratio vesicles is also at pH 4.2 (Fig.7.7).

Furthermore delipidated bacteriorhodopsin reconstituted into DMPG bilayers displays a blue colour at pH 4.5 in deionized water. The corresponding pK_a for pure DMPG in 5mM Tris/HCl is approximately pH 4, while in 1mM NaCl it is reported to be at pH 5.0 (Sacre & Tocannne, 1977). In the 67:1 mole ratio DMPC/bR vesicles, the only phospholipid present is DMPC, which as shown by high resolution ^{31}P-NMR has a pK_a of pH 1 or below. The pK_a for the purple to blue shift displayed by these vesicles is also low and if it were not for the low pH induced blue to purple shift the full blue (A_{max} 600nm) might be reached. In this case the pK_a for the extrapolated titration would be closer to that of DMPC.

In the 72:7.3:1 mole ratio DMPC/PMPL/bR nsTP produced complex, the PGP is significantly diluted (less than 10mol%), such that its protonation may not have a significant effect on the protein. This would imply that the purple to blue shift is sensitive to an average pK_a of the phospholipids. It should be noted that different aggregation states may exist for the protein in the two nsTP-produced complexes at 25°C and that this will profoundly effect the local concentration of PGP around the bacteriorhodopsin. Thus, in the 72:7.3:1 mole ratio DMPC/PMPL/bR complex at 25°C the bacteriorhodopsin is fully dispersed, whereas in the higher protein content 21:7.6:1 DMPC/PMPL/bR mole ratio vesicles at 25°C full solubilization may not be achieved (Heyn *et al.*, 1981a; Cherry *et al.*, 1978). In the aggregated hexagonal patches the bacteriorhodopsin molecules will probably be associated entirely with PGP lipids, since these have been demonstrated to mediate the crystallization. Thus in the 21:7.6:1 DMPC/PMPL/bR mole ratio complex, the local concentration of PGP around the protein molecules may be much higher than implied by the DMPC/PMPL/bR ratio. In contrast dispersion of the bacteriorhodopsin molecules exposes the proteins to the bulk DMPC (Chapter 5 of this thesis). Thus differences in aggregation may be significant in explaining the different chromophore titration properties of the 72:7.3:1 and 21:7.6:1 mole ratio complexes. Attempts to record spectra for the 72:7.3:1 DMPC/PMPL/bR

mole ratio complex at low temperatures, where the protein will be aggregated proved unsuccessful. In the pure DMPG bilayers, the aggregation state is not significant, since all the lipid is PG.

Further evidence for the pK_a of the lipid phosphate as determining the pK_a for the purple to blue shift, is the effect of salt on the pK_a of the purple-to-blue shift in the 21:7.6:1 vesicles (Fig.7.9). In high ionic strength solutions, the pK_a (pH 2.95) for the purple to blue shift is identical to that determined for PG in SUVs by high resolution ^{31}P-NMR (Fig.7.2.b). This implies that the group responsible for controlling the chromophore purple-to-blue shift is at the membrane surface and experiences similar salt dependent changes in local pH to the phosphate moiety in PG bilayers. Thus, the ionization state of phospholipid phosphate groups appears to control conformation of the protein, which in turns determines the spectral properties.

In contrast the pK_a for the group effecting the low-pH induced blue to purple shift remains at pH 1.4 and appears unaffected by the lipid environment composition for the 67:1 and 21:7.6:1 mole ratio complexes. Furthermore as shown in Fig.7.9 for the 21:7.6:1 mole ratio DMPC/PMPL/bR complex, the titration properties of this group are also unaffected by the ionic strength of the aqueous medium.

In conclusion, pH titration of the retinal chromophore A_{max} observed by visible spectrophotometry implicates at least two titratable groups involved in maintaining the chromophore properties of bacteriorhodopsin. One controls the purple to blue shift on lowering the pH. It is effected directly by the phospholipid headgroup environment itself and also by the ionic strength of the aqueous medium. Indeed there is a correlation between the pK_a of the phospholipid environment, determined by high resolution ^{31}P-NMR of model systems and the pK_a of the purple to blue shift. Such features indicate the responsible group as being the phosphate moiety of the membrane phospholipids. The second brings about the blue to purple shift on titrating to below pH 2.0. The pK_a for this shift is independent of the phospholipid environment and the ionic strength of the surrounding aqueous medium. This points to the responsible group being within the protein itself and sequestered away from the aqueous environment. Such a group could

be a carboxyl group near the retinal chromophore itself.

References

Albert,A. & Yeagle,P.L., (1983) *P.N.A.S.* U.S.A. **80**, 7188 - 7191.

Barrow,K.D., Collins,J.G., Rogers,P.L. & Smith,G.M. (1983) *Biochim. Biophys. Acta.*,. **753**, 324-330

Bayley,S.T. and Morton,R.A. (1978) *Crit. Rev. Microbiol.*, **6**, 151.

Berden,J.A, Barker,R.W. & Radda,G.K., (1975) *Biochim. Biophys. Acta.* **375**, 186 - 208

Blaurock,A.E.. (1975) *J.Mol.Biol.*, **93**, 139

Blaurock, A. E. & Stoeckenius, W. (1971). *Nature New Biol.*, **233**, 152-155.

Bloc,M.C., Hellingwerf,K.J., Kaptein,R. and de Kruijff,B. (1978) *Biochim. Biophys. Acta.* **514**, 178 - 184.

Bloj,B. and Zilversmit,D.B. (1983) *Methods in Enzymology*, **98**, 574-581

Bridgen,J. & Walker,I.D. (1976) *Biochemistry*, **15**, 792 - 798.

Brown,M.F. & Seelig,J. (1978) *Biochemistry*, **17**, p381-384

Brown,M.F., Seelig,J. & Haberlen,U. (1979) *J.Chem.Phys.* **70**, p5045-5053

Browning & Seelig,J. (1980) *Biochemistry*, **19**, p1262-1270

Burnell,E.E., Cullis,P.R. and de Kruijff,B. (1980) *Biochim. Biophys. Acta.* **603**, 63 - 69

Carey,M.C. & Small,D.M. (1972) *Arch. Intern. Med.*, **130**, 506

Cherry, R. J. (1979). *Biochim. Biophys. Acta.*, **559**, 289-327.

Cherry,R.J., Muller,U. & Schneider,G. (1977) *FEBS Letts.* **80**, 465 - 469.

Cherry,R.J., Muller,U., Henderson,R., and Heyn,M.P. (1978) *J.Mol.Biol.*, **121**, 283-298

Cherry,R.J. & Godfey,R.E., (1981) *Biophys.J.* **36**, 257 - 276.

Cherry,R.J., Godfrey,R.E. & Peters,R. (1982) *Biochem. Soc. Trans.*, **10**, 342 - 343.

Chignell,C.F. and Chignell,D.A. (1975) *Biochem. Biophys. Res. Commun.*, **62**, 136 - 143

Cohn,M. and Hughes,T.R. (1960) *J. Biol. Chem.*, **235**, p3250-3253

Cone,R.A. (1972) *Nat. New Biol.* **236**, 39 - 43.

Crain,R.C. and Zilversmit,D.B. (1980a) *Biochemistry.* **19**, 1433- 1439

Crain,R.C. & Zilversmit,D.B. (1980b) *Biochim. Biophys. Acta.* **620**, 37-48

Cullis,P.R. & de Kruijff,B. (1976) *Biochim. Biophys. Acta.* **436**, 523 - 540.

Cullis,P.R. & de Kruijff,B. (1979) *Biochim. Biophys. Acta.* **559**, 339 - 420.

Davis,J.H. (1983) *Biochim. Biophys. Acta.* **737**, 117 - 171

Dempsey, C.E., Ryba,N.J.P. and Watts,A. (1986) *Biochemistry.* **25**, 2180- 2187

Dencher,N.A. & Heyn,M.P. (1978) *FEBS Letters*, **96**, 322-326

Dencher,N.A. and Heyn,M.P. (1979) *FEBS Letters*, **108**, 307

Dencher,N.A. and Heyn,M.P. (1983) *Methods in Enzymology*, **88**, 5-10

Dodge,J.T., Mitchell,C. and Hanahan,D.J. (1963) *Arch. Biochem. Biophys.* **100**, 119-130

Downer,N.W. (1985) *Biophys.J.* **47**, 285-293

Downer,N.W. & Cone,R.A. (1985) *Biophys. J.* **47** 277-284.

van Dijck,P.W.M., de Kruijff B., Verkleij,A.J., van Deenen,L.L.M., & de Gier,J., (1978), *Biochim. Biophys. Acta.*, **512**, 84 - 96.

van Dijck,P.,W.,M., Nicolay, K., Levinssen-Bijvelt, J., van Dam, K. & Kaptein, R. (1981). *Eur. J. Biochem.*, **117**, 639-645.

East,J.M. & Lee,A.K. (1982) *Biochemistry.*, **21**, 4144-4151

Edgerton,M.E., Moore,T.A., & Greenwood,C., (1980) *Biochem.J.*, **189**, 413 - 420.

Ekiel,I.H., Marsh,D., Smallbone,B.W., Kates,M. and Smith,I.C.P. (1981) *Biochem. Biophys. Res. Commun.* **100**, 105 - 110

Ellena,J.F., Pates,R.D. & Brown,M.F. (1986) *Biochemistry*, Vol **25**, 3,742 - 3751.

Engelman,D.M., Henderson,R., McLachlan,A.D. & Wallace,B.A. (1980) *P.N.A.S.* U.S.A., Vol **17**, 2023 - 2027.

Findlay,J.C.B. and Pappin,D.J.C. (1986) *Biochemical J.* **238**, 625-642.

Fisher, K. A. & Stoeckenius, W. (1977). *Science*, **197**, 72-74.

Fretten,P.M., Morris,S.J., Watts,A. & Marsh,D. (1980) *Biochim. Biophys. Acta.*, **247** - 259

Gadian,D.G., Radda,G.K., Richards,R.E., & Seeley,P.J. (1979). In *Biological Applications of magentic resonance.* (ed. R.G.Shulman), p. 463. Academic Press, New York.

Gadian,D.G., (1982) *Nuclear Magnetic Resonance and its application to living systems.* Clarendon Press, Oxford.

Galla,H.J., Hartmann,W., Theilen,V. & Sackmann,E. (1979) *J.Memb.Biol.* **48**, 215 - 236.

Gally,H.U., Neiderberger,W. & Seelig,J. (1975) *Biochemistry*, **19**, p3647-3652

Glonek,T., Kopp,S.J., Kot,E. Pettegrew J.W. Harrison W.H. and Cohen M.M. (1982) *Journal of Neurochemistry*, 39, p1210-1219.

Goni,F.M., Pons, M. and Chapman,D. (1982) *2nd European Bioenergetics Conference* 433-434.

Griffin,R.G., (1981) *Meth. Enzymol.* **72**, 108 - 173.

Harlos,K. & Eible,H. (1980) *Biochemistry*, **19**, 895-899

Helenius,A., McCaslin,D.R., Fries,E. and Tanford,C. (1979) *Methods in Enzymology*, **LVI**, 734-749

Helmkamp,G.M. (1980) *Biochem. Biophys. Res. Commun.*, **97**, 1091-1096

Henderson,R., (1975) *J.Mol.Biol.* **93**, 123 - 138.

Henderson, R. & Unwin, N. (1975) *Nature*, **257**, 28-32.

Henderson, T.O., Glonek,T., and Myers,T.C. (1974) *Biochemistry*, Vol **13**, p623-628.

Heyn,M.P., Bauer,P.J. & Dencher,N.A. (1975) *Biochem. Biophys. Res. Commun.* **67**, 879 - 903.

Heyn, M. P. & Cherry, R. J. & Dencher, N. A. (1981a). *Biochemistry.*, **20**, 840-849.

Heyn, M. P., Blume, A. Rehorek, M. & Dencher, N. A. (1981b) *Biochemistry*, **20**, 7109-7115.

Heyn,M.P. & Dencher,N.A. (1983) *Methods in Enzymology*, Vol **88**, 31-35

Hoffmann,W., Clark,A.D., Turner,M., Wyard,S., & Chapman,D., (1980), *Biochim. Biophys. Acta.*, **598**, 178 - 183.

Huang, K. S., Bayley, H. & Khorana, H. G. (1980). *P.N.A.S.* **77**, 323-327.

Hwang, S. B. & Stoeckenius, W. (1977). *J. Membrane Biol.*, **33**, 325-350.

Israelachivili, J. N., Marcelja, S. & Horn, R. G. (1980). *Qu. Rev. Biophysics.*, **13**, 121-200.

Jost,P.C., Libertini,L.J., Hebert,V.C., & Griffith,H.O. (1971), *J.Mol.Biol.*, **59**, 77 - 98.

Jost,P.C., Griffith,O.H., Capaldi,R.A. & Vanderkooi,G. (1973) *P.N.A.S.* U.S.A., **70**, 480 - 484

Kang,S.Y., Gutowsky,H.S., Hsung,H.C., Jacobs,R., King,T.E., Rice,D & Oldfield,E. (1979) *Biochemistry*, **18**, 3257 - 3267.

Kates,M. (1978) *Prog. Chem. Fats other Lipids* **15**, 304-342

Kates,M., Kushwaha,S.C., & Sprott,G.D. (1983) *Methods in Enzymology*, Vol **88**, 98-

Kistler, J., Strand, R. M., Klymkowsky, M. W. Labancette, R. & Fairclough, R. H. (1982). *Biophys. J.*, **30**

Knowles,P.F., Watts,A. and Marsh,D. (1979) *Biochemistry*, **18**, 4480 - 4487

Knowles,P.F., Watts,A. and Marsh,D., (1981) *Biochemistry*, **20**, 5888 - 5894

Koter,M. de Kruijff,B. & van Deenen,L.L.M., (1978) *Biochim. Biophys. Acta.*, **514**, 255 - 263.

Kushwaha,S.C., Kates,M. and Martin,W.G. (1975) *Can.J.Biochem*, **53**, 284

Kushwaha,S.C., Kates,M., and Stoeckenius,W. (1976) *Biochim. Biophys. Acta.*, **426**, 703-710

Lind,C., Hojeberg,B. and Khorana,H.G. (1981) *J.Biol.Chem.*, **256**, 8298-8305

London, E. and Feigenson, G.W. (1979) *Journal of Lipid Research*, **20**, 408-412.

London,E. and Khorana,H.G. (1982) *J.Biol.Chem.*, **257**, 7003- 7011

Levine,Y.K., Birdsall,N.J.M., Lee,A.G., & Metcallfe,J.C., (1972) *Biochemistry*, **11**, 1416 - 1421.

Lewis, B.A. & Engelman, D.M. (1983) *Journal of Molecular Biology*, **166**, 203-210.

Markwell, M.A., Haas, S.M., Tolbert, N.E. & Bieber, L.L. (1981) *Methods in Enzymology*, **72**, 296-303.

Marsh, D. & Watts, A. (1981). Ch. 5 In:- "*Liposomes, from Physical Structure to Therapeutics Action*" (G. G. Knight, ed.) Elsevier, Amsterdam.

Marsh,D. & Watts,A. (1982) Chp 2 in:- *Lipid-Protein Interactions*, Vol 2, Jost,P.C. & Griffith,H.O. ed. (John Wiley & sons).

Marsh,D. & Watts,A. (1987) *Advances in Membrane Fluidity* (Aloia,R.C., ed) Alan R.

Liss, Inc., New York, Vol 2.

Marsh,D., Watts,A., Pates,R.D., Uhl,L.R. Knowles,P.F. and Esmann,M. (1982) *Biophys.J.*, **37**, 265 -

Maubrey-Gaud,S., (1981) Chp 5 in:- "*Liposomes, from Physical Structure to Therapeutics Action*" (G. G. Knight, ed.) Elsevier, Amsterdam.

McLheney, R.N. (1986). *Biochim. Biophys. Acta*, **864**, 361-421.

Moore,T.A., Edgerton,M.E., Parr,G., Grenwood,C., & Perham,R.N. (1978) *Biochem.J.*, **171**, 469 - 476.

Mogelson,S., Wilson,G.E., Sobel,B.E. (1980) *Biochim. Biophys. Acta.*, **619** p680-688.

van Paridon,P.A., de Kruijff,B., Ouwerkerk,R. & Wirtz,K.W.A., (1986) *Biochim. Biophys. Acta.*, 877, 216 - 219.

Petri,W.A. & Wagner,R.R. (1979) *Journal Biol. Chem.*, Vol **254**, 4313-4316

Oesterhelt, D. & Stoeckenius, W. (1974). *Meth. in Enzymology*, **31**, 667-678.

Olive,J., Benedetti,E.L. van Breugal,P.J.G.M., Daemen,F.J.M. & Bonting,S.L. (1978) *Biochim. Biophys. Acta.* **509**, 129 - 135.

Ovchinnikov,Y., Adbulaev,N., Feigira,M., Kiselev,A., & Lobanov,N. (1979) *FEBS Letts*, **100**, 219 - 224.

Rajan,S., Kang,S.Y., Gutowsky,H.S. & Oldfield,E. (1981) *J.Biol.Chem*, **256**, 1160-1166

Racker,E. & Stoeckenius,W. (1974) *J.Biol.Chem.* **249**, 662 - 663.

Rehorek,M., & Heyn,M.P.. (1979) *Biochemistry.*, **18**, 4977-4983.

Rehorek,M., Dencher,N.A., & Heyn,M.P., (1985) *Biochemistry*, **24**, 5980 - 88.

Reynolds,J.A., (1982) Chpater 5 in:- *Lipid-Protein Interactions*, 2 (Jost,P.C. & Griffith,H.O. ed) John Wiley & sons.

Reynolds.J.A. and Stoeckenius,W. (1979) *P.N.A.S.* U.S.A., **74**, 2803 - 2804.

Rice,D.M., Hsung,J.C., King,T.E., & Oldfield,E. (1979a) *Biochemistry*, **18**, 5885-5892.

Rice,D.M., Meadows,M.D., Scheinman,A.O., Goni,F.M., Gomez- Fernandez,J.C., Moscarello,M.A., Chapman, D. & Oldfield,E. (1979b) *Biochemistry*, **18**, 5893-5903

Rouser, G., Fleischer, S. & Yamamoto, A. (1970). *Lipids*, **5**, 494-496.

Ryba,N.J.P., Dempsey,C.E. and Watts,A. (1986) *Biochem.* **25**, 4818 - 4825.

Ryba,N.J.P. (1986) D.Phil thesis, Oxford University

Sacre,H.M. & Tocanne,J.F. (1977) *Chem. Phys. Lipids*, **18**, p334-354

Sardet,C., Tardieu,A. & Luzzati,V. (1976) *J.Mol.Biol.* **105**, 383 - 407.

Seelig,J., (1977) *Q.Rev. Biophys.*, **10**, 353-418

Seelig,J., (1978) *Biochim. Biophys. Acta.*, **515**, 105-141

Seelig,J. & Gally,H.U. (1976) *Biochemistry*, **15**, 5199-

Seelig,J., Tamm,L., Hymel,L., Fleischer,S. (1981) *Biochemistry*, **20**, 3922-3932

Seelig,A. & Seelig,J. (1980) *Quart. Rev. Biophys.* **13**, 19 - 61.

Seelig, A. & Seelig, J. (1985). *Biochim. Biophys. Acta.*, **815**, 153-158.

Seelig,J., Borle,F., & Cross,T.A., (1985), *Biochim. Biophys. Acta.*, **814**, 195-198.

Silvius, J. (1982) in *"Lipid-Protein Interactions"* 2 (Jost, P.C. & Griffith, O.H. ed.) Wiley Interscience, New York.

Sixl,F., Brophy,P.J. and Watts,A. (1984) *Biochemistry*, **23**, 2032 - 2039.

Sixl,F. & Watts,A. (1982) *Biochemistry*, **21**, 6446 - 6452.

Sixl,F. & Watts,A. (1983) *P.N.A.S.* (U.S.A.) **80**, 1613 - 1615.

Sixl,F. & Watts,A. (1985) *Biochemistry*, Vol **24**, 7906 - 7910

Smith,I.C.P. and Ekiel,I.H. (1984) Chpt 15 pp 447 - 475 in *Phosphorus-31 NMR*, Gorenstein,D.G. (ed.)

Spudich,E.N. and Spudich,J.L. (1983) *Methods in Enzymology*, Vol **88**, 213-216

Sotirhos, N. Herslof, B. and Kenne,L. (1986) *Journal of Lipid Research*, **27** p386-392.

Tamm,L. & Seelig,J., (1983) *Biochemistry*, **22**, 1474-1483

Tocanne,J.F., Ververgaert,P.H.J.Th., Verkley,A.J., van Deenen,L.L.M., (1974) *Chem. Phys. Lipids*, **12**, 201-219.

Trauble,H. & Eibl, (1974) *P.N.A.S.* (U.S.A.), **71**, 214 - 219.

Unwin,P.N.T. & Henderson,P., (1975) *J.Mol.Biol.*, **94**, 425 - 440.

Unwin, P.N.T. & Zampighi, (1980) *Nature*, **283**, 544-549

Warren,G.B., Toon,P.A., Birdsall,N.J.M., Lee,A.G. and Metcalfe,J.C. (1974) *P.N.A.S.* U.S.A., Vol **71**, 622-626

Watts,A. (1981) Nature, 294, 512

Watts, A., Harlos, K., Maschke, W. & Marsh, W. (1978). *Biochim. Biophys. Acta.*, **510**, 63-74

Watts,A., Volotovski,I. and Marsh,D., (1979) *Biochemistry*, **18**, 5006 - 5013.

Watts,A. Volotovski,I.D., Pates,R.D. and Marsh,D. (1982) *Biophys. J.*, **37**, 94 -

Wildenauer,D. & Khorana,G.H. (1977) *Biochim. Biophys. Acta.*, **466**, 315-324

Wirtz,K.W.A., Devaux,P.F. & Bienvenue,A. (1980) *Biochemistry.*, **19**, 3395-3399

Wohlgemuth,R., Waespe-Sarcevic,N. & Seelig,J. (1980) *Biochemistry*, **19**, p3,315-3,321

Yeagle,P.L. (1982) *Biophys.J.* Vol **37**, 227 - 239.

Yeagle,P.L. (1984) *J.Membr. Biol.* **78**, 201 - 210.

Zilversmit,D.B. (1983) *Methods in Enzymology*, **98**, 565-573